HYDROTHERMAL LIQUEFACTION OF BIOMASS AND PROCESS INTENSIFICATION

by

Jie Yang

Submitted in partial fulfilment of the requirements
for the degree of Doctor of Philosophy

at

Dalhousie University
Halifax, Nova Scotia
July 2019

TABLE OF CONTENT

LIST OF TABLES

LIST OF FIGURES

ABSTRACT

Hydrothermal liquefaction (HTL) is considered as a promising thermochemical conversion technology for biomass valorization and crude bio-oil (biocrude) production. However, moving this technology towards commercialization still faces several technical challenges, some of which were partially addressed in this thesis. This project started with evaluating the influence of biocrude recovery methods/solvents on the yield and physicochemical properties of biocrude, and the solvent extraction/filtration with dichloromethane was determined to be a favorable protocol for biocrude recovery. This was followed by the development of prediction models for the yield of HTL products using biomass model components and statistical mixture design, which offered advanced models for predicting HTL product yield as functions of feedstock composition and process variables. The chemical interaction in co-liquefying biomass model components was also explored to better understand the HTL product formation pathways. A variety of actual biomass feedstocks were hydrothermally co-liquefied, and the significance of observed co-liquefaction effect were statistically examined for the first time. The influence of mixing ratio, temperature and their interaction on co-liquefaction effect were evaluated as well. A process intensification technique, microwave irradiation, was applied in HTL of spent coffee grounds, and it was proved to be technically feasible. To gain more insights of heating method's influence on HTL products formation, HTL of biomass model components and their mixtures were carried out under microwave irradiation and conventional heating. Heating methods did not substantially alter the model components' interaction, and only slight and/or negligible influence on the chemical composition of obtained biocrudes were observed. The obtained results from this project contributed to new knowledge body in HTL research and advanced the biomass HTL technique from downstream processing methods, product yield prediction, product formation pathways, co-liquefaction of biomass and process intensification perspectives.

LIST OF ABBREVIATIONS USED

HTL	Hydrothermal liquefaction
SR	Solid residue
AqP	Aqueous phase
ANOVA	Analysis of variance
Adj R^2	Adjusted R^2
SCG	Spent coffee grounds
CCD	Central composite design
DCM	dichloromethane
THF	tetrahydrofuran
DKP	Diketopiperazine
TIC	Total ion chromatography
RSM	Response surface methodology
PCA	Principle component analysis
CI	Confidence interval
PI	Prediction interval
CE	Co-liquefaction effect
SE	Synergistic effect
AE	Antagonistic effect
MW-HTL	Microwave-assisted hydrothermal liquefaction

ACKNOWLEDGEMENTS

I would like to thank and express my sincere and deep appreciation to my supervisor, Dr. Quan (Sophia) He, for her continuous support, professional guidance, persistent encouragement and inspiration throughout my PhD study. My gratitude extends to my committee members, Dr. Haibo Niu and Dr. Kenneth Corscadden, for their support and advices, and this thesis would not be possible without their commitment.

Special thanks go to Dr. Tess Astatkie for his suggestions on experiments design and assistance on the data analysis, as well as to Mandi Wilson for her continuous inspiration and encouragement. I also would like to thank Dr. Peter Havard for having the teaching opportunities, and Linxi Yang for her guidance on the reactor operations, and Ningning Zhou, Jianan Lin and Ruoxiao Shi for their assistance on experiment conductions.

I also want to take this opportunity to thank Chris Nelson, Scott Read, Paula Colicchio, Yougui Chen and other faculty members and staff as well for their persistent help and suggestions. I would like to acknowledge the financial support from National Science and Engineering Research Council (NSERC) Discovery, Canada.

I am also grateful to all my friends, especially Jiankun Dai, Yue Guo and Qi Liu, for their support and encouragement. Last but not least, I would like to thank Xiaomei Zhong, my parents and all my families for their unconditional love, support and encouragement.

Chapter 1: Introduction

1.1 Background

Crude oil, naturally occurring from the composted organic materials, has been a major source providing inexpensive liquid fuels and a variety of chemicals since the 19th century. With increasing global industrialization and modernization, the crude oil reserve is rapidly declining due to over-exploitation and extensive usage by human activities. A delayed consciousness on the natural resource protection, combined with the associated environment problems has given our society a wake-up call. It is therefore imperative to develop renewable, economical and environmentally-friendly energy source alternatives for a sustainable production of fuels and chemicals (Demirbas, 2009; Huber et al., 2006).

Biofuels, the fuels derived from biomass, are currently the only sustainable carbon source for the production of liquid fuels that are compatible to the exiting transportation infrastructure (Shahir et al., 2014). Biofuels are carbon-neutral and can generate significantly less greenhouse gases in comparison with fossil fuels, if efficient production processes are designed and employed (Nigam and Singh, 2011). Many attempts have been made to grow energy crops for biofuels production, such as oil seeds for biodiesel production or/and corn/sugarcane for bioethanol production (Naik et al., 2010). However, growing energy crops unavoidably impacts food and feed supplies. Efforts are therefore re-orientated to use low value biomass such as agricultural and forestry waste/residues, food processing wastes and municipal solid wastes, which are widely available biomass resources and do not compete with the land and water source used for food crops cultivation (Huang and Yuan, 2015; Yang et al., 2016b).

Processing low value biomass into energy products is challenging using conventional biological methods such as fermentation or digestion due to their relatively long processing time and low product yield (Goyal et al., 2008; Naik et al., 2010). Currently developed thermochemical conversion technologies include direct combustion, gasification, and pyrolysis/hydrothermal liquefaction, which can readily convert biomass into heat, syngas, and crude bio-oil respectively. However, biomass generally contains a high water content, and thus an energy intensive pre-drying process is required prior to combustion, gasification or pyrolysis (Goyal et al., 2008). Hydrothermal liquefaction (HTL) is an emerging technology which can convert biomass into crude bio-oil in water medium at moderate to high temperature (250–350 °C) and high pressure (5-25 MPa). It stands out as a promising technology as it does not require preliminary drying processes

(Peterson et al., 2008). Additionally, more than 50 % of oxygen in the biomass can be removed, resulting in the bio-crude oil with a higher heating value from 30 MJ/kg to 40 MJ/kg (Pavlovič et al., 2013; Tekin et al., 2014).

During the past decades, many research efforts have been devoted to different aspects of biocrude production from HTL of biomass. The effect of process variables on HTL products distribution has been mostly investigated, and the optimization of process variables for maximizing biocrude yield was commonly conducted using response surface methodology (RSM). For instance, Zhu et al. (2018) used RSM to study the influence of reaction temperature, time, feedstock concentration and catalyst dosage on the biocrude yield from HTL of barley straw, and found that a maximum biocrude yield (38.7 wt.%) was obtained at 304.8 °C, 15.5 min, 18% feedstock concentration and 11.7% potassium carbonate as catalyst. As the yield/quality of biocrude were also highly associated with feedstock's biochemical composition, a variety of feedstocks that have different biochemical compositions have been evaluated for HTL biocrude production. In general, the studied feedstocks can be classified into seven categories: (1) agricultural waste and residues, (2) forest residues, (3) food processing wastes, (4) livestock waste, (5) algae, (6) sewage and municipal solid waste, and (7) plastic waste. More detailed information on the yield/quality of biocrudes generated from these feedstocks can be found in Yang et al. (2019). The influence of organic solvent addition (e.g., water vs. water-ethanol co-solvent) on biocrude's yield/quality has been primarily explored by Dr. Xu's group. Water-ethanol co-solvent was reported to give a higher biocrude yield (by 15-20%) than pure water (Cheng et al., 2010), but the use of organic solvent to some degree, diminishes the advantages of HTL of using water as a economical, green and sustainable reaction medium. A few attempts have been made to explore the feasibility of continuous HTL for biocrude production by Elliott, Rosendahl and their coworkers to improve process productivity. The progresses in developing continuous process were summarized in Elliott et al. (2015). Rosendahl and his coworkers developed a novel strategy to improve the pumpability of wood slurries in continuous HTL system by co-liquefying them with brown seaweed or microalgae (Sintamarean et al., 2017). Other research efforts include the catalytic upgrading of biocrude (Galadima and Muraza, 2018), re-use of the aqueous phase as a processing medium (Hu et al., 2017), and digestion/gasification of aqueous phase (Yang et al., 2018) etc. The life-cycle assessment and techno-economic analysis on biofuels production from HTL of forest residues were recently conducted by Nie and Bi, (2018a) and Nie and Bi, (2018b)

respectively, and suggested that HTL of biomass for transportation biofuels production is a promising route even though more technology advancements are required to reduce the production cost.

Despite considerable efforts and progresses that have been made, there are still some knowledge gaps in the development of biomass liquefaction. For instance, very limited research focuses on the biocrude recovery process, which might highly impact the yield/physicochemical properties of the resulting biocrude. There is also a lack of broadly applicable mathematical models for the predication of HTL products yield. The understanding on the products formation pathways in the process of HTL of biomass is very limited, which greatly hinders the optimization of process. Hydrothermal co-liquefaction of different biomass is considered to be advantageous over HTL of single feedstock due to low logistics costs associated with feedstock collection and transportation, and the potential co-liquefaction effect that might enhance biocrude yield. However, not all claimed co-liquefaction effects are statistically significant and sometimes confusing and conflicting results were reported even for the same feedstock combination. In addition, the influence of feedstock mixing ratio and reaction temperature on co-liquefaction effect has not been statistically assessed yet. HTL of biomass uses water as the processing medium, offering a possibility to use microwave irradiation to heat the reaction mixture, and ideally to intensify the HTL process. Unfortunately, the feasibility of microwave-assisted HTL has been rarely investigated, and it would be interesting to compare the conventional heating with microwave heating in terms of product yield/physicochemical properties.

In this thesis, the above-mentioned challenges will be addressed. The outcomes from this research will help optimize HTL process, gain insights into liquefaction mechanism, reduce processing costs, and thus accelerate the commercialization of this promising technology.

1.2 Research objectives

The main goal of this project is to fill the existing knowledge gaps and advance the research of HTL of biomass. The specific objectives are as follows:

(1) To assess the influence of HTL downstream processing methods on the yield and physicochemical properties of biocrude

(2) To develop the prediction model for HTL product yield and explore biocrude formation pathways by hydrothermally liquefying representative biomass model components (cellulose, hemicellulose, lignin, protein and lipid)

(3) To develop more advanced models for HTL product yield *via* a mixture design of biomass model components coupled with process variables

(4) To statistically determine the significance of co-liquefaction effect on product yield (either synergistic, antagonistic or additive), and to study the influence of feedstock mixing ratio on co-liquefaction effect

(5) To investigate the impact of temperature on co-liquefaction effect, and to further assess whether the temperature effect depends on the level of mixing ratio

(6) To evaluate the feasibility of HTL of spent coffee grounds under microwave irradiation

(7) To study the influence of heating methods (microwave irradiation vs. conventional heating) on HTL of biomass model components

1.3 Thesis organization

Chapter 2 presents a literature review on the fundamentals of HTL, inconsistency of HTL downstream processing methods, prediction model development for HTL product yield, hydrothermal co-liquefaction studies, and microwave-assisted biocrude production. Chapter 3 provides an investigation on the impact of downstream processing methods on the yield and physicochemical properties of HTL biocrude, with the aim to find out a favourable HTL downstream process method. HTL of biomass model components for product yield prediction and reaction pathways exploration are included in Chapter 4. Chapter 5 illustrates the development of more advanced prediction models for HTL product yield *via* a mixture design of biomass model components coupled with process variables. Chapter 6 presents the statistical determination on the significance of co-liquefaction effect from hydrothermal co-liquefaction of a variety of biomass. Chapter 7 investigates the temperature influence on the co-liquefaction effect, and further assesses whether the temperature effect depends on the level of mixing ratio of feedstocks. Chapter 8 provides an evaluation on the feasibility of microwave-assisted HTL of spent coffee grounds, and Chapter 9 further explores the effect of heating method on HTL of biomass model components.

Chapter 10 provides the overall conclusions of this project and the recommendations for the future work.

Chapter 2: Literature Review

Copyright permission:

Part of this chapter has been published in Applied Energy 250 (2019) 926-945. The copyright has been obtained from Elsevier and co-authors.

Contribution statement:

I was responsible for part of data summary, interpretation and manuscript preparation.

2.1 Fundamentals of hydrothermal liquefaction (HTL)

HTL is a thermochemical process in which biomass is decomposed and transformed to gas, liquid and solid fractions in sub- or super-critical water and sometimes in the presence of organic solvents and/or catalysts (Elliott, 2007). The typical processing temperature ranges from 270 °C to 370 °, while the pressure is between 4-22 MPa. When the temperature and pressure are close to the critical point (374 °C, 22 MPa), the properties of water change significantly, including density, dielectric constant, permittivity and polarity etc. Water, being highly compressed, is still in a liquid state but has a relatively higher ionic product (hydroxyl OH^- and hydronium H^+) and lower dielectric constant than that at ambient condition (Peterson et al., 2008). The hydrogen bonds of water become weaker, and the solubility of non-polar organic compounds increases. The water ions in such condition can facilitate the decomposition of biopolymers in biomass to further form liquid (bio-crude oil and water-soluble product), gaseous and solid fractions.

In HTL processes, the target product is liquid bio-crude oil, and the objective of HTL is to obtain high yield and high quality biocrude. Different from petroleum, biocrude oil is a complex mixture of oxygenated compounds with a wide range of molar mass. Its quality can be characterized by its higher heating values (HHV), viscosity, density, acidity, O/C or H/C ratios and chemical compositions etc. Depending on downstream application of biocrude, specific chemical composition and properties might be favored.

Considerable research has built a good understanding on the influence of HTL process variables, including reaction temperature, time, feedstock concentration, solvent type and catalyst loading. However, the knowledge for underlying reaction pathways of HTL products formation is still not well understood. Biomass have large variations in their main components such as protein,

lipid and carbohydrates (hemicellulose, cellulose and lignin). The degradation profile of each component differs from one another, and the interactions among these components during HTL process could occur, making the HTL reaction pathways as a complex network and almost impossible to be interpreted explicitly (Gollakota et al., 2018; Déniel et al., 2017a). The generally accepted reaction pathways are summarized and described as follows: 1) biomass organic molecules decompose/de-polymerize to monomer/unit structures, such as monosaccharaides, amino acids, fatty acids *via* hydrolysis/pyrolysis; 2) The monomers produced can either remain at the same state or be further decomposed/degraded into smaller fragments (e.g., glucose, organic acids, phenolics and nitrogen-containing compounds) *via* dehydration, deamination and decarboxylation etc.; and 3) These reaction intermediates are further rearranged through cyclization, condensation and repolymerization etc. to form crude bio-oil, water-soluble product, gaseous product and solid residue (Déniel et al., 2016; Peterson et al., 2008; Toor et al., 2011).

2.2 Downstream processing methods

Many efforts have been centering around investigating the effects of operation parameters on the yield/quality of biocrude (Akhtar and Amin, 2011). In these studies, different downstream processing procedures were applied to recover biocrude including separation methods, solvents used, and extraction conditions etc. as illustrated in Table 2.1. Different recovery procedures can cause significant variations on the yield and physicochemical properties of the resulting biocrude, making the literature results less comparable even for the same feedstock liquified under similar conditions, and thus hinder facilitating process optimization and better understanding of reaction mechanisms under HTL conditions.

Filtration, followed by solvent dissolving was commonly used to collect biocrude (Zhu et al., 2015; Yang et al., 2016b); Soxhlet extraction was also applied to recover the biocrude from product mixtures after HTL conversion (Chen et al., 2014a, 2014b); and ultrasound-assisted extraction was used in some studies (Zhang et al., 2013). Unfortunately, there is no literature available that investigates the influence of extraction methods on the yield/physicochemical properties of HTL biocrude. Apart from the extraction method, organic solvents for extraction vary widely from one study to another (Nazari et al., 2015; Wu et al., 2017). Very limited research has studied the effects of using different recovery solvents on the yield and properties of biocrude. Valdez et al. (2011) conducted the first research, examining the solvents' influence on the yields of bioproduct

fractions in a liquefaction of microalgae, *Nannochloropsis sp*. They found that the amount of fatty acids in the crude bio-oil were highly dependent on the solvents used, and the polar solvents garnered more fatty acids than non-polar solvents. Organic solvents used in their study included hexane, cyclohexane, hexadecane, decane, methoxycyclopentane, chloroform and dichloromethane, of which had similar dielectric constants (low to moderate). The solvent's dielectric constant is closely related to its polarity, and has proven to be an influential factor for the extraction efficiency in many fields such as food science (Singh et al., 2014) and the pharmaceutical industry (Azwanida, 2015). It is therefore necessary to use solvents with a broader dielectric constant range (low to high) to thoroughly study the impact of extraction solvents on the yield and physicochemical properties of HTL biocrude.

Table 2.1 Various downstream processing procedures used to recover crude bio-oil after hydrothermal liquefaction (HTL) conversion.

Feedstock	Downstream extraction method	Extraction solvent	Solvent evaporation	References
microalgae and swine manure	Soxhlet extraction	toluene	room temperature for 24 h within fume hood	Chen et al. (2014a)
microalgae	ultrasound-assisted, 30 mins	acetone	under atmosphere at 75 °C for 12 h	Zhang et al. (2013)
microalgae	vigorously shake, 30 mins	acetone	unavailable details	Toor et al. (2013)
barley straw	centrifuge	acetone	rotary vacuum under 60 °C and 556 mbar	Zhu et al. (2015)
microalgae	filtration	DCM	rotary vacuum at 40 °C, unknown pressure	Zhang et al. (2017)
microalgae	filtration	chloroform	rotary vacuum at 40 °C, unknown pressure	Zou et al. (2010)
microalgae and model compounds	filtration	DCM	unavailable details	Sheng et al. (2018)
microalgae and model compounds	centrifuge then filtration	DCM	nitrogen gas purging for 8 h	(Biller et al. (2016)
microalgae and model compounds	centrifuge	DCM	nitrogen gas purging for 1.5 h	Teri et al. (2014)
woody biomass	filtration	acetone	rotary vacuum at 50 °C, unknown pressure	Nazari et al. (2015)

Note: DCM= dichloromethane

2.3 HTL product yield prediction

Since the HTL product yield is largely influenced by the process variables such as temperature, reaction time, mass loading and catalyst concentration etc., many researchers have attempted to use HTL process variables as input to develop the prediction models for HTL product yield. Response Surface Methodology (RSM), especially face-centered composite design and general central composite design are most frequently used. In addition to the prediction purpose, the use of RSM allows to investigate the main effect of each process variable and even the interaction effect among process variables on the final HTL product yield, as well as to obtain the optimal HTL conditions when jointly maximizing the yield of desirable product (such as biocrude yield) and minimizing unfavorable product yield.

For instance, Gan and Yuan, (2013) used RSM to achieve the optimal reaction settings for hydrothermal conversion of corncobs, and the predicted biocrude yield from the developed models was in close agreement with the one from validation experiment. Hardi et al. (2017) recently applied a face centered central composite design of temperature, time and feedstock concentration to predict the yield of products obtained from HTL of sawdust and the properties of products. Zhu et al. (2018b) used RSM to optimize the HTL of barley straw and reported that a maximum biocrude yield of 38.7 wt.% was obtained at 304.8 °C, 15.5 min, 18% biomass loading and 11.7% K_2CO_3. Nazari et al. (2017) implemented RSM to predict the biocrude yield from co-liquefaction of sludge and sawdust, and a maximum biocrude yield of 33.7 wt.% was obtained at optimum operating conditions of 310 °C, 10 min, and 10 wt.% mass concentration.

Although incorporating HTL process variables as input of model works well to predict HTL product yield, it is limited to a specific feedstock used in the study. The HTL product yield also strongly depends on the feedstock's biochemical composition. Thus, a few attempts have been made to develop prediction models based on feedstock biochemical composition, which allows the estimation of HTL product yield for various types of feedstock. Biller and Ross, (2011) for the first time used biomass model compounds to develop a linear prediction model for HTL biocrude yield *via* 'compound additive' approach as shown in Table 2.2. This model accurately predicted the biocrude yield for some microalgae species (*Chlorella* and *Nannochloropsis*), however, it did not work well for several other species such as cyanobacterial, *Spirulina* and *Porphyridium*. Teri et al. (2014b) presented a quantitative linear model for biocrude yield prediction assuming that

model compounds lipid, polysaccharide and protein reacted independently. They also incorporated three interaction terms into this linear model by studying the liquefaction of binary mixtures of model components, and found that the model containing interaction terms was less accurate for biocrude yield prediction than the linear model.

Leow et al. (2015) used a number of microalgae species with a wide range of compositions (23-59% lipid, 58-18% protein, 12-22% carbohydrates) to develop a linear prediction model for biocrude yield, and stated that this newly developed model was more accurate in predicting biocrude yield than previous additive models derived from model compounds. From the same research group, Li et al. (2017) conducted HTL of 24 batches of microalgae with significantly different biochemical compositions, and established prediction models for various responses such as biocrude yield, solid residue yield, C,H, and N content in biocrude, HHV of biocrude, total organic carbon and total nitrogen in aqueous phase. Hietala et al. (2017) also examined the feasibility of using microalgae species with varied biochemical compositions for the prediction of biocrude yield/properties while considering the microalgae species identity as an additional factor in their models. Sheng et al. (2018b) used soya protein, castor oil and glucose as model compounds to develop a prediction model as well, which included model terms accounting for cross-interactions between model components. They compared the model prediction accuracy with that of Biller and Ross, (2011), Teri et al. (2014b) and Leow et al. (2015) and concluded that this newly developed model provided more accurate prediction than the previous models.

Déniel et al. (2017b) for the first time incorporated biomass model compounds with statistical mixture design (simplex-lattice with augmentation) to develop a prediction model for HTL biocrude yield, solid residue (SR) yield, aqueous phase (AqP) yield and gas yield. They also suggested that biomass biopolymers (such as protein, cellulose, lignin and lipid) should be used as model compounds to develop prediction model instead of using their respective monomers (amino acid, glucose, guaiacol and fatty acid). Lu et al. (2018) utilized five model components (soy protein, xylose, cellulose, lignin and soybean oil) and carried out HTL of individual and binary mixtures at 350 °C for 30 min. They developed the mathematical models for predicting biocrude yield, higher heating value and C, H, and N content of biocrude when taking the interactions among studied model components into considerations; and the newly developed models made good predictions for most cases.

Overall, the research efforts on statistical modeling of HTL product yield were firstly made to use RSM and process variables as inputs, followed by the development of prediction models that were based on feedstock biochemical composition. These developed statistical models allow a quick estimation of HTL product yield to evaluate the potential of various biomass.

Table 2.2 The prediction models for biocrude and solid residue (SR) yield from hydrothermal liquefaction of various biomass and the corresponding model compounds used.

Literature	Raw materials				Reaction conditions
Biller and Ross, (2011)	Albumin, soya protein, asparagine, glutamine (X_P, wt.% daf)	Glucose, starch (X_C, wt.% daf)	Sunflower oil (X_L, wt.% daf)		model components; 350 °C, 60 min
	Biocrude yield (wt% daf) = $0.18*X_P + 0.06*X_C + 0.8*X_L$				
Teri et al. (2014b)	Soya protein (X_P, wt.%)	Cornstarch (X_C, wt.%)	Sunflower oil (X_L, wt.%)		model components
	Biocrude yield (wt.%) = $33.4*X_P + 5.8*X_C + 95.1*X_L - 1.9*X_PX_C + 27.1*X_PX_L - 1.6*X_CX_L$				300 °C, 20 min
	Biocrude yield (wt.%) = $33.7*X_P + 12.2*X_C + 93.8*X_L + 40.2*X_PX_C - 20.5*X_PX_L - 0.3*X_CX_L$				350 °C, 60 min
	Albumin (X_P, wt.%)	Cellulose (X_C, wt.%)	Castor oil (X_L, wt.%)		model components
	Biocrude yield (wt.%) = $31.6*X_P + 6.1*X_C + 94.9*X_L + 3.8*X_PX_C + 35.9*X_PX_L - 21.2*X_CX_L$				300 °C, 20 min
	Biocrude yield (wt.%) = $34.0*X_P + 11.9*X_C + 85.2*X_L + 33.6*X_PX_C - 2.4*X_PX_L + 10.2*X_CX_L$				350 °C, 60 min
Leow et al. (2015)	*Nannochloropsis oculate* protein (X_P, % dw)	*Nannochloropsis oculate* carbohydrate (X_C, % dw)	*Nannochloropsis oculate* lipid (X_L, % dw)		microalgae (*Nannochloropsis oculate*) with different biochemical compositions; 300 °C, 30 min
	Biocrude yield (% dw) = $0.42*X_P + 0.17*X_C + 0.97*X_L$			R^2=0.99924; R^2 (*adj*)=0.85616	
Li et al. (2017)	microalgae protein (X_P, % dw)	microalgae carbohydrate (X_C, % dw)	microalgae lipid (X_L, % dw)	Microalgae ash (X_A, % dw)	*Chlorella*, *Scenedesmus*, *Chlorogloeopsis*, *Spirulina*, and defatted biomass; 300 °C, 30 min
	Biocrude yield (% dw) = $0.45*X_P + 0.22*X_C + 0.85*X_L$			R^2=0.985	
	SR yield (% dw) = $0.41*X_C + 0.18*X_A$			R^2=0.879	

Literature	Raw materials					Reaction conditions
Sheng et al. (2018)	Soya protein (X_P, wt.%)		Glucose (X_C, wt.%)		Castor oil (X_L, wt.%)	Model compounds + *Nanochloropsis*; 280 °C, 60 min
	Biocrude yield (wt.%) = $0.385*X_P + 0.025*X_C + 0.9*X_L + 0.052* X_LX_P/lX_L-X_Pl + 0.093* X_LX_C/lX_L-X_Cl + 0.003* X_PX_C/lX_P-X_Cl$					
Hietala et al. (2016)	Protein (X_{Pro}, wt.%)	Carbohydrate (X_{Cab}, wt.%)	Saturated lipid (X_{Sat}, wt.%)	Mono-saturated lipid (X_{Mon}, wt.%)	Poly-saturated lipid (X_{Pol}, wt.%)	multiple algae species (co-cultivated); 350 °C, 20 min
	Biocrude yield (wt.%) = $10.7 + 575*X_{Sat} - 4130*X^2_{Mon} + 65*X^2_{Pro} + 51.2*X^2_{Car} + 223*X_{Sat}X_{Mon} - 928*X_{Sat}X_{Car} + 316*X_{Mon}X_{Car} -514*X_{Pol}X_{Pro} + 547*X_{Pol}X_{Cab}$				R^2=0.97	
Déniel et al. (2017b)	Cellulose+hemicellulose + sugar (X_1, wt.% daf)		Protein (X_2, wt.% daf)	Lignin (X_3, wt.% daf)	Lipid (X_4, wt.% daf)	model compounds; 300 °C, 60 min
	Biocrude yield (wt.% daf) = $0.05*X_1 + 0.95*X_4 + 0.18*X_1X_2 + 0.79*X_1X_3 + 0.45*X_1X_4 + 0.23*X_2X_3 + 0.44*X_2X_4 – 0.3*X_3X_4$				R^2 =0.998	
	SR yield (wt.% daf) = $0.64*X_3$				R^2=0.86	

2.4 HTL of biomass model compounds

Biomass is generally composed of protein, lipid and carbohydrates (including hemicellulose, cellulose and lignin). It is well-known that HTL of biomass is a complex process, which involves many chemical interactions among these individual components. Therefore, using the biomass model compounds instead of actual biomass is helpful to better understand the underlying mechanisms of HTL reaction pathways.

HTL can easily break protein peptide bonds and subsequently generate amino acids. The produced amino acids are highly possible to be further degraded in hot compressed water *via* decarboxylation and deamination, which contributes to the carbon dioxide and ammonia production respectively. Meanwhile, amino acids can go through cyclization and other rearrangement processes in hydrothermal media, resulting in water-insoluble biocrude. The formation of diketopiperazine (DKP) from HTL of protein was reported in Madsen et al. (2017b), Meetani et al. (2010) and Torri et al. (2012a). Madsen et al. (2017b) also stated that amino acids might be dimerized to form DKP prior to deamination or decarboxylation.

Lipid is chemically defined as triglyceride, which can be hydrolyzed into fatty acids, diglycerides, monoglycerides and esters at subcritical water media. The product distribution from HTL of lipid highly depended on the HTL reaction conditions (such as temperature and residence time) (Alenezi et al., 2009; Shin et al., 2012). Alenezi et al. (2009a) studied the hydrolysis kinetics of sunflower oil under subcritical water conditions, and reported that hydrolysis reaction of sunflower oil required higher energy to start converting triglycerides into diglycerides as compared to the subsequent steps. The produced fatty acids could act as acid catalysts for the hydrolysis reaction, which positively contributed to a high fatty acid yield. The thermal stability of fatty acids under subcritical water conditions was investigated by Shin et al. (2012), and they suggested that fatty acids remained stable at 300 °C or below.

Cellulose is a polysaccharide molecule that consists of hundreds to thousands glucose monomers. These glucose monomers are linked by β-1,4-glycosidic bond, which results in highly crystallized structure, strong inter- and intramolecular hydrogen bonds within cellulose, and strong resistance to swelling in water (Peterson et al., 2008). Hydrothermal decomposition of cellulose has been well studied, and more information can be found in Cantero et al. (2013), Deguchi et al. (2006), Mok et al. (1992), Sasaki et al. (2000) and Yin and Tan, (2012). Above 250 °C, cellulose

can be rapidly hydrolyzed into oligomers and glucose monomers. The generated glucose monomers can be further fragmented into erythrose, glycoaldehyde, glyceraldehyde, pyruvaldehyde and dihydroxyacetone etc, and isomerized into fructose *via* well-known Lobry le Bruny-Alberda Van Ekenstein transformation (LBET) (Cantero et al., 2013). Dehydration of fructose can further produce 5-hydroxymethyl-furfural (5-HMF) (Lü and Saka, 2012; Putten et al., 2013). The retro-aldol condensation can be involved as well to produce furfural from fructose (Aida et al., 2007; Lü and Saka, 2012).

In comparison with cellulose, limited literature on HTL of hemicellulose has been reported. Hemicellulose is typically considered as a heteropolymer, which comprises hundreds of xylose, mannose, glucose and other sugar monomers. It can be hydrolyzed relatively easily as compared to cellulose due to the different bonding (α-1,4-glycosidic bond) between hemicellulose sugar monomers. Hemicellulose hydrolysis can be initialized at 180 °C, and a considerable amount of monomeric sugars can be obtained within a couple of minutes (Bobleter, 1994; Mok and Antal Jr, 1992). Although relatively less severe HTL conditions are required to degrade hemicellulose, comparable chemical compositions of xylan and cellulose biocrude have been reported in Gao et al. (2011) and Li et al. (2016). Similar reaction networks were proposed for hydrothermal decomposition of d-xylose (Aida et al., 2010) and cellulose (Cantero et al., 2013) as well.

Lignin is a complex high molecular weight compound that prevalently comprises methoxy phenolics. A complete hydrothermal decomposition of lignin requires severe conditions to obtain valuable chemicals and oil production (Kang et al., 2013). Using subcritical water (around 300 °C) for lignin decomposition mainly generates water-soluble phenolic compounds and insoluble solid residue along with limited amount of non-polar biocrude. The density of hydrothermal media has been reported to be a critical factor for lignin hydrolysis. Higher density of reaction media seems to improve lignin hydrolysis efficiency (Barbier et al., 2012; Wahyudiono et al., 2008). The HTL biocrude obtained from lignin was reported to be mainly composed of phenolic compounds (guaiacol and creosol), as well as some lignin monomers (such as vanillin, apocynin and 4-hydroxy-3-methoxy-benzenepropanol). Barbier et al. (2012) used the lignin monomers to explore the lignin decomposition pathways, and suggested that hydrolysis of ether bonds (C-O) and alkylation of aromatics rings were critical steps for lignin degradation. The hydrolytic cleavage of C-O linkages in lignin model compounds with the assistance of water-tolerant Lewis acids was

investigated as well (Yang et al., 2014), unfortunately, no corresponding reaction pathways were proposed.

2.5 Hydrothermal co-liquefaction of different biomass

In addition to the above-mentioned efforts, hydrothermal co-liquefaction of different biomass has recently attracted many research interests. Biomass is usually bulky and has low energy density and inconsistent properties/compositions over seasons. It is difficult to collect sufficient quantity of one type biomass in a region to make the overall production economically viable (Li et al., 2016). Thus, co-liquefaction can significantly reduce the logistics costs associated with collection and transportation of biomass. Another benefit of co-liquefaction is the improved processability of slurry feedstock for continuous processes (Sintamarean et al., 2017). More importantly, co-liquefaction has the potential to increase the yield and modify the physicochemical properties of obtained biocrude *via* altering the biochemical composition of the feedstock mixture (Yang et al., 2017). The yield/properties of HTL biocrude is highly associated with the chemical composition of the subject feedstock. Biomass feedstock typically consists of protein, lipid and carbohydrates. Co-liquefying feedstocks with different biochemical compositions might enhance biocrude yield/quality *via* chemical reactions between biochemical components at hydrothermal media. For instance, Maillard reactions between protein and carbohydrates (Peterson et al., 2010), and amide formation from protein and lipid were observed previously (Chiaberge et al., 2013).

The co-liquefaction effect (CE) is defined as synergistic effect (SE), antagonistic effect (AE) or additive effect. A certain combination of two or more biomass may enhance biocrude yield, termed as SE that essentially is a comparison between actual yield of mixed feedstock and the calculated mass-averaged yield. It is generally believed that the SE on biocrude yield originates from the positive interaction among breakdown products and intermediates from co-processed biomass. Many types of biomass have been hydrothermally co-liquefied for biocrude production, including microalgae, macroalgae, rice husk/straw, aspen/pine wood sawdust, plastics, spent coffee grounds, spent mushroom compost, sewage and pulp/paper sludge, animal manure and crude glycerol etc. Chen et al. (2014a) conducted a study on co-liquefaction of microalgae (MA) and swine manure (SM) at 300 °C for 60 min. As the proportion of SM increased from 0 to 50%, the biocrude yield remained constant at ~23 dwt.%, whereas biocrude yield increased to the highest point of 35.7 dwt.% when further increasing the SM mass ratio to 75%. Unfortunately, the CE on

biocrude yield was not discussed in their work. Therefore, the biocrude yield at different SM/MA mass ratios in Chen et al. (2014a) were adapted, and the CE on biocrude yield were then quantitatively evaluated as shown in Table 2.3. It can be observed from Table 2.3 that co-liquefaction of 75:25 SM/MA exhibited a weak SE of 2.2 dwt.% on biocrude yield.

A representative agriculture waste, rice husk (RH) was used to co-liquefy with microalgae (MA) by Gai et al. (2015a) at 300 °C for 60 min. When increasing the proportion of MA from 0 to 100%, the biocrude yield showed a steady increase from 13.9 wt.% to 43.6 wt.%. Similar to the study conducted by Chen et al. (2014a), although the general trend of biocrude yield was reported for co-liquefaction of MA/RH at varying mass ratios, the CE on biocrude yield was not explicitly discussed in Gai et al. (2015a). Thus, the effort on adapting the data from Gai et al. (2015a) was made to quantitatively assess the CE as well. It can be noted from Table 2.3 that co-liquefaction of MA/RH resulted in SE on biocrude yield at all studied MA/RH mass ratios, with the highest SE (8.7 wt.%) at MA/RH ratio of 50:50. Lignocellulosic biomass are abundantly available, such as pine wood, aspen wood and willow wood etc., and they have been used to co-liquefy with other types of biomass. Saba et al. (2018) carried out the co-liquefaction of loblolly pine (LP) wood with digested sewage sludge in 300 °C subcritical water for 30 min. Different with the SE on biocrude yield as reported by aforementioned co-liquefaction studies, a 1.9 dwt.% AE on acetone-recovered biocrude yield was observed for co-liquefaction of 50:50 LP/sludge.

Although many attempts have been made to hydrothermally co-liquefy various feedstocks for biocrude production, most of them simply compare the experimental biocrude yield of mixed feedstock with the calculated mass-averaged value of individual feedstock, to determine whether co-liquefaction generated positive or negative effect on biocrude yield. Many of the reported SE or AE on biocrude yield were less than 5 wt.% (Chen et al., 2014a; Pedersen et al., 2015; Saba et al., 2018). In a typical liquefaction operation at a lab scale, the experimental error on biocrude yield is usually in the range of 2 wt.% to 5 wt.%. Therefore, the claimed SE or AE lower than 5 wt.% is subject to a critical examination for its significance and reliability.

Table 2.3 Hydrothermal co-liquefaction effect (CE) on biocrude yield from the mixtures of biomass.

MA	SM	75:25 MA/SM			50:50 MA/SM			25:75 MA/SM			Ref.
		Expt	Calc	CE	Expt	Calc	CE	Expt	Calc	CE	
26	36	25.8	28.5	-2.7	22	21	1	35.7	33.5	2.2	Chen et al. (2014a)[a]

CG	SM	75:25 CG/SM			50:50 CG/SM			25:75 CG/SM			Ref.
		Expt	Calc	CE	Expt	Calc	CE	Expt	Calc	CE	
27	24	68	26.3	41.8	35	25.5	9.5	25	24.8	0.3	Xiu et al. (2011b)[b]

NG	AW	75:25 NG/AW			50:50 NG/AW			25:75 NG/AW			Ref.
		Expt	Calc	CE	Expt	Calc	CE	Expt	Calc	CE	
17.7	42.3	21.0	23.9	-2.9	32.5	30	2.5	44	36.2	7.8	Pedersen et al. (2015)[c]

SMC	SD	67:33 SMC/SD			50:50 SMC/SD			33:67 SMC/SD			25:75 SMC/SD			Ref.
		Expt	Calc	CE	Expt	Calc	CE	Expt	Calc	CE	Expt	Calc	CE	
47.9	20.7	23	38.8	-15.8	21.2	34.3	-13.1	17.9	29.8	-11.9	15.5	27.5	-12.0	Jasiūnas et al. (2017)[d]

SL	M	S	W	PF	33:67 SL/M			33:67 SL/S			33:67 SL/W			33:67 SL/PF			Ref.
					Expt	Calc	CE	Expt	Calc	CE	Expt	Calc	CE	Expt	Calc	CE	
42.6	22.8	29.1	25.9	31.1	47.1	36.0	11.0	41.0	38.1	2.9	41.0	37.0	4.0	45	38.8	6.2	Biller et al. (2018)[e]

ALP=AM	AS	CLP	CM	CS	50:50 ALP/AM			50:50 ALP/AS			50:50 CLP/CM			50:50 CLP/CS			Ref.
					Expt	Calc	CE	Expt	Calc	CE	Expt	Calc	CE	Expt	Calc	CE	
11.8	9	1	3	22	14.6	11.8	2.8	8.5	10.4	-1.9	3.3	2	1.3	8.5	11.5	-3.0	Saba et al. (2018)[f]

CG	EP	86:14 CG/EP			83:17 CG/EP			80:20 CG/EP			75:25 CG/EP			67:33 CG/EP			Ref.
		Expt	Calc	CE	Expt	Calc	CE	Expt	Calc	CE	Expt	Calc	CE	Expt	Calc	CE	
32.5	13.4	38	29.3	8.7	43.2	29.3	13.9	41	28.7	12.3	17	27.7	-10.7	18	26.1	-8.1	Lu et al. (2017)[g]

CP	RH	80:20 CP/RH			60:40 CP/RH			50:50 CP/RH			40:60 CP/RH			20:80 CP/RH			Gai et al. (2015a)[h]
		Expt	Calc	CE	Expt	Calc	CE	Expt	Calc	CE	Expt	Calc	CE	Expt	Calc	CE	
43.6	13.9	38.5	37.7	0.8	38	31.7	6.3	37.5	28.8	8.7	30	25.8	4.2	28	19.8	8.2	

a: MA = mixed-culture algae; SM = swine manure. Biocrude recovery solvent = toluene; Yield = dwt.% (dry basis)
b: CG = crude glycerol; SM = swine manure. Biocrude recovery solvent = acetone; Yield = dwt.% (dry basis)
c: NG = neat glycerol; AW = aspen wood. Biocrude recovery solvent = diethyl ether; Yield = wt.% (daf)
d: SMC = spent mushroom compost; SD = sawdust. Biocrude recovery solvent = acetone; Yield = wt.% (daf)
e: SL = sludge; M = Miscanthus; S = Switchgrass; W = willow; PF = Pine Flakes. Biocrude recovery solvent = dichloromethane; Yield unit = wt.% (daf)
f: ALP = Loblolly Pine (acetone); AM = Manure (acetone); AS = Sludge (acetone); CLP = Loblolly Pine (cyclohexane); CM = Manure (cyclohexane); CS = Sludge (cyclohexane). Yield unit = dwt.% (dry basis)
g: CG= crude glycerol; EP = *Enteromorpha prolifera.* Biocrude recovery solvent = acetone; Yield unit = dwt.% (dry basis)
h: CP = *Chlorella pyrenoidosa*; RH = rice husk. Biocrude recovery solvent = toluene; Yield unit = wt.%

2.6 Microwave-assisted biomass processing

2.6.1 Fundamentals of microwave (MW) heating

Microwaves are electromagnetic waves with frequencies ranging from 0.3 to 300 GHz, corresponding to wavelengths varying from 1 m to 0.001 m. The standard operating frequency of microwave-assisted synthesis reactor is 2.45 GHz, which means that the direction of the electromagnetic filed changes 2.45 billion times per second. When microwaves are transmitted, the constantly fluctuating electromagnetic field direction results in continuous alignment and realignment of dipoles in polar liquids. These alignment and realignment of dipoles, together with the migration of ions if exist any (as a result of the electromagnetic field), lead to the enormous friction and subsequent internal energy inside the material. The accumulated internal energy is further dispersed as heat, and the materials can be consequently heated up (Aguilar-Reynosa et al., 2017).

The microwave dielectric heating depends on both the polarizability of molecules (known as dielectric constant) and the material's inherent dissipation of electromagnetic energy (known as dielectric loss). The ratio of dielectric loss to dielectric constant is termed as loss tangent (tan δ), which evaluates the ability of a specific solvent/material to convert microwave energy into heat at a given frequency and temperature. The loss tangent of different solvents at 2.45 GHz and 20 °C is presented in Table 2.4. In general, solvents used for MW-assisted synthesis can be classified by their loss tangent as high (tan >0.5), medium (0.1 < tan <0.5) and low (tan <0.1). Water can be considered only a medium microwave absorbing solvent with a loss tan of 0.123.

Table 2.4 The loss tangent (tan $\boldsymbol{\delta}$) of different solvents at 2.45 GHz and 20 °C.

Solvent	tan δ	Solvent	tan δ
Ethylene glycol	1.350	Acetonitrile	0.062
Ethanol	0.941	Acetone	0.054
Methanol	0.659	Tetrahydrofuran	0.047
Acetic acid	0.174	Dichloromethane	0.042
Water	0.123	Toluene	0.040
Chloroform	0.091	Hexane	0.020

Microwave thermal effects are usually referred to its efficient heating manner due to the selective absorption of microwave energy by polar substances. The existence of non-thermal (athermal) effect of microwave irradiation is still a controversial topic, even though a few studies

have hypothesized that MW athermal effects might be attributed to the disruption of hydrogen bonds during MW heating (Eskicioglu et al., 2007b; Hong et al., 2004; Hoz et al., 2005).

2.6.2 Comparison of MW heating and conventional heating

As mentioned previously, microwave irradiation takes advantage of 'microwave dielectric heating' phenomena that involves dipolar polarization and ionic conduction mechanisms. It is characterized with non-contact, volumetric and faster heating, as opposed to the conventional heating that materials within reactors are heated through slow conduction and convection processes. The detailed comparison of MW heating and conventional heating is presented in Table 2.5.

Moreover, green chemistry is heavily promoted recent years, and 'safer solvent', 'design for energy efficiency' and 'use of renewable feedstocks' are three key principles among the 12 principles of green chemistry (Anastas and Warner, 2000). Microwave-assisted hydrothermal liquefaction of biomass, that uses water as reaction medium, microwave irradiation as heating method and renewable biomass as feedstocks, exhibits the promising potential for biofuel production in a green and sustainable manner.

Table 2.5 Comparison of microwave heating and conventional heating adapted from Bundhoo, (2018).

Microwave heating	Conventional heating	Remarks
Non-contact heating	Contact heating	With non-contact heating, the subject material is heated directly as opposed to conventional heating where the contained wall is heated more severely.
Lower energy consumption	Higher energy consumption	Although MW irradiation is not 100% energy efficient (energy loss during conversion of electrical energy into microwaves), it is however less energy-consuming than conventional heating. This is due to considerable energy that is required for heating the container wall prior to heat the subject materials under conventional heating.
Rapid heating	Slow heating	Microwave energy is directly absorbed by subject material and transferred as heat, resulting in rapid heating. The subject material is heated by convective heat transfer from reactor wall to subject material, and by conduction from the material surface to the material core.
Shorter reaction time requirement	Longer reaction time requirement	MW irradiation yield similar or higher quality products in shorter reaction times as opposed to conventional heating.
Volumetric heating	Superficial heating	Volumetric heating ensures uniform heat distribution in the material unlike superficial heating which occurs at the surface
Higher level of control	Lower level of control	MW heating can be immediately switched on and off, and the energy applied to the material can be more precisely pre-determined based on per unit weight or volume basis.
Improved product yields	Lower product yields	Owing to the mechanism of MW heating, better product yields have been obtained as opposed to conventional heating.

2.6.3 MW-assisted conversion for biofuels production

MW-assisted pretreatment of lignocellulosic biomass has been extensively studied to improve bio-ethanol production from fermentable sugars. MW irradiation has been reported to assist the breakdown of lignocellulosic biomass in which cellulose is typically protected inside the lignin wall and complex hemicellulose chains. This pretreatment process improves the accessibility of cellulose molecules for the subsequent cellulose hydrolysis into simple sugar, resulting in sufficient bio-ethanol production from lignocellulosic biomass (Aguilar-Reynosa et al., 2017). MW-assisted pretreatment of sludge that is the mostly studied feedstock for bio-methane production has been widely investigated as well. The increased bio-methane production from anaerobic digestion of MW-irradiated substrates was observed due to enhanced solubilization of organics in liquid phase for microbial bacteria. Pino-Jelcic et al. (2006) reported a 16.4% increase in bio-methane production from MW pre-treated sludge as compared to that of untreated sludge. A similar observation was reported by Eskicioglu et al. (2007a), that a 17% increase in biogas was obtained from anaerobic digestion of MW-irradiated sludge than its control run.

The thermochemical techniques typically used to convert biomass and waste materials into value-added products can be generally referred to torrefaction for biochar production, fast pyrolysis or HTL for bio-oil production and gasification for syngas production. In terms of torrefaction, it can be further classified into dry torrefaction and wet torrefaction (or hydrothermal carbonization). Gronnow et al. (2012) compared MW-assisted dry torrefaction with conventional heating, and observed a higher HHV for MW-torrefied biochar than that of biochar obtained through conventional heating at the same process temperature. Tumuluru et al. (2012) reported that comparable HHV values were obtained for MW-torrefied and conventionally torrefied corn stover biochar, but less process time was required for MW-assisted one. MW irradiation has been applied to assist hydrothermal carbonization as well (Elaigwu and Greenway, 2016a, 2016b). They reported that higher hydrochar HHV and shorter process time were obtained by using MW irradiation as opposed to conventional heating, while the hydrochar from two heating methods had comparable SEM, FTIR, BET surface area, TGA and NMR results.

Many attempts have been made to study the MW-assisted gasification of biomass for syngas (a gas mixture of CO and H_2) production. For instance, (Xiao et al., 2015) reported that a higher conversion efficiency (46%) was observed for MW-assisted gasification of rice straw biochar,

while only 9.5% for conventional gasification. Lahijani et al. (2014) carried out the MW-assisted gasification of oil palm shell in the presence of CO_2, and compared MW-assisted and conventional gasification as well. They stated that a higher conversion rate and more CO_2 to CO were obtained under MW irradiation than under convectional heating.

Bio-oil production *via* fast pyrolysis usually requires low moisture content feedstocks. Although dried feedstocks have poor MW absorption ability, MW-assisted pyrolysis for bio-oil production has been widely investigated. The addition of MW absorbers such as carbon materials, metal oxides and hydroxides into pyrolysis feedstocks was commonly conducted to increase reaction temperature and enhance pyrolytic process (Yin, 2012; Bundhoo, 2018). Various feedstocks have been tested in MW-assisted pyrolysis for biocrude production, such as corn stover (Ren et al., 2014), bamboo (Dong and Xiong, 2014), rice straw (Huang et al., 2013) and switchgrass (Mohamed et al., 2016). Upon comparison of MW-assisted and conventional pyrolysis, MW-assisted pyrolysis required less processing time than conventional pyrolysis (Domínguez et al., 2005; Huang et al., 2016). Robinson et al. (2015) reported that biocrude with better quality was obtained from MW-assisted pyrolysis of larch woodchips. Similar to pyrolysis, biocrude is the target product for HTL of biomass and waste materials. Unfortunately, MW-assisted HTL (MW-HTL) of biomass for biocrude production has been limitedly investigated (Remón et al., 2019; Lorente et al., 2019). Therefore, it is highly necessary to evaluate the feasibility of MW-HTL, and compare the quality of MW-HTL products with that of products obtained from conventional HTL.

Chapter 3: The Impact of Downstream Processing Methods on Yield and Physicochemical Properties of Hydrothermal Liquefaction Bio-oil

Contribution statement:

I was responsible for raw materials collection, experiment design and conduction, data analysis and manuscript preparation.

3.1 Abstract

Hydrothermal liquefaction (HTL) is considered as a promising thermochemical conversion technology for crude bio-oil (biocrude) production from biomass. However, the influence of downstream processing methods (such as biocrude recovery methods and solvents used) were rarely investigated. We examined the effect of solvents and extraction methods on the yield and physicochemical properties of biocrude from *Chlorella sp.* (*C. sp.*), spent coffee grounds (SCG), and a mixture of the two. It was found that the extraction method had no effect on the yield and physicochemical properties of biocrude from either *C. sp.,* SCG or a mixture of the two. However, the solvent used for biocrude recovery had crucial effects. Dichloromethane (DCM) was determined to be a favorable one from biocrude yield and chemical yield perspective. It was also noticed that the synergetic effects claimed in co-liquefaction of *C. sp.* and SCG were highly dependent on the solvent used as well. This study calls attention to the impact of various recovery procedures on the yield/physicochemical properties of HTL bio-oil.

3.2 Introduction

In the study of hydrothermal liquefaction of biomass, different downstream processing procedures have been used to recovery biocrude, which can cause significant variations on the yield and physicochemical properties of the resulting biocrude. This makes the literature results less comparable even for the same feedstock and under similar liquefaction conditions, and thus hinder facilitating process optimization and better understanding of reaction mechanisms under

HTL conditions. The more detailed information of inconsistent downstream processing procedures has been reviewed in section 2.2.

There is also an increasing research interest in blending various feedstock for co-liquefaction such as paper-mill sludge with waste newspaper (Zhang et al., 2011) and sewage sludge with teacake (Zhai et al., 2015). One motivation is to explore potential positive co-liquefaction effect that is usually referred as synergistic effect (SE), in which the actual yield of a mixture is higher than the mass-averaged yield. SE was observed in some of these studies even though the underlying SE from blending these biomass were not well understood (Xiu et al., 2011a; Jin et al., 2013). For instance, Jin et al. (2013) carried out co-liquefaction of microalgae (*Spirulina platensis*) and macroalgae (*Entermorpha prolifera*) and used dichloromethane to recover biocrude; a SE of 3.2 wt.% on biocrude yield was observed. However, each co-liquefaction study used different biocrude recovery solvents. If the yield of biocrude is strongly affected by the solvent used, the SE results in the literature might be biased due to extraction solvents used, and thus make it difficult to truly reflect SE that takes place in the process of co-liquefaction. Some mixed feedstock that did not show SE using certain solvents, might exhibit significant SE using other extraction solvents. There are currently no appropriate ways to address this fundamental research limitation with HTL as researchers can only rely on the extracted bio-oil to evaluate the performance of liquefaction. However, it is essential to examine the influence of extraction solvents on the research outcomes of SE in co-liquefaction, which could provide more information, and potential discovery of some hidden SE and prevent underestimation of the advantages of certain feedstock combinations.

This chapter examined three commonly used extraction methods, namely filtration (solvent dissolving at room temperature), Soxhlet extraction and microwave-assisted extraction. Hexane, acetone, dichloromethane (DCM), and tetrahydrofuran (THF) were selected as extraction solvents, representing varied degrees of polarity. *Chlorella sp*. microalgae (*C. sp.*), spent coffee grounds (SCG) and *C. sp.*/SCG (50/50 by mass) were liquefied under identical reaction conditions, to assess whether co-liquefaction (*C. sp.*/SCG) can produce more desirable biocrude or not as compared to that of individual *C. sp.* and SCG. Biocrude yield, chemical yields and dynamic viscosity were used to evaluate the influence of extraction procedures and feedstock used. The impact of extraction solvents on the co-liquefaction effect was investigated as well.

3.3 Materials and methods

3.3.1 Materials

Wet spent coffee grounds were collected from Tim Hortons, Truro, Canada, and oven dried at 105 °C for 24 hours. Dried microalgae (*Chlorella. sp.*) was purchased from Buy Algae, Meridian, American. ACS reagent grade hexane and acetone were purchased from Fisher Scientific Ltd. Dichloromethane (ACS reagent grade), inhibitor-free tetrahydrofuran (>99.9%) and naphthalene D8 standard were purchased from Sigma Aldrich Ltd. All chemicals were used as received.

3.3.2 Biomass feedstock characterization

The proximate analysis and feedstock chemical composition analysis of *C. sp.* and SCG were conducted by SGS lab (Guelph) at Ontario, Canada. The moisture, ash, lipid, protein, lignin, acid detergent fiber (ADF) and neutral detergent fiber (NDF) content were measured by following methods, AOAC 930.15, AOAC 942.05, AOAC 945.16, AOAC 990.03, AOAC 973.18, NFTA 4.1 and NFTA 5.1 respectively. The cellulose and hemicellulose content were calculated based on the ADF and NDF percentage. The lignin, cellulose and hemicellulose for SCG was 24.0%, 26.8% and 22.5% respectively. Unfortunately, the lignin, ADF and NDF percentage for *C. sp.* (very fine powder) were not obtained due to the crucible clogging problems during testing. The element analysis of *C. sp.* and SCG was conducted in a Perkin Elmer 2400 CHNS elemental analyzer on Agricultural Campus, Dalhousie University. The obtained results from feedstock characterization are presented in Table 3.1.

Table 3.1 Characterization of biomass feedstock, *Chlorella sp*. microalgae (*C. sp.*), spent coffee grounds (SCG), and 50/50 *C. sp.*/SCG by mass.

	C. sp.	SCG	*C. sp.*/SCG[a]
Moisture content (%)	6.53	4.58	5.56
Ash (%)	5.59	1.30	3.45
Lipid (%)	0.90	9.51	5.21
Protein (N × 6.25) (%)	63.23	14.22	38.73
Carbohydrate[b] (%)	23.75	70.39	47.07
C	49.53	51.77	50.65
H	6.97	7.31	7.14
O	31.44	37.49	34.47
N	10.42	2.29	6.36
S	1.64	1.14	1.39

Notes: a, the biochemical composition of *C. sp.*/SCG was calculated by 50% *C. sp.* + 50% SCG.
b, hydrocarbon content was calculated by 100 % - the sum of moisture, lipid, protein and ash content.

3.3.3 Hydrothermal liquefaction processes

Hydrothermal liquefaction experiments were carried out in a 100 mL stainless-steel autoclave (Parr Instrument, 4590 micro-reactor) equipped with an A2140HC magnetic stirrer and a 4848 reactor controller. In a typical conversion process, five grams of dried feedstock were weighed and loaded into the reaction vessel, followed by the addition of 40 grams distilled water, giving a water/feedstock mass ratio of 9:1. The reaction vessel was then sealed and transferred to the autoclave support stand, and the magnetic stirrer was started. The reaction vessel was then pressurized with high purity nitrogen at 5 MPa for 3 mins to detect the potential leaking. If no leaking was detected, the reaction vessel was subsequently purged with nitrogen to remove originally existing air, and then re-pressurized to 1 MPa. About 35-38 mins were required to heat the reactor up to 290 °C, and the reaction was held at 290 °C for 10 mins.

Once the reaction was completed, the reactor was cooled down to 25 °C by quenching with a cold-water bath for 5 mins. The magnetic stirrer was then stopped, and the gaseous phase was vented into a fume hood. The reactor was then opened. The aqueous phase containing certain amounts of solids was transferred into a centrifuge tube, which was centrifuged at 3200 rpm for 10 mins to separate aqueous phase and solids. The aqueous phase within the centrifuge tube was then discharged, and remaining solids were collected into a prepared beaker for downstream extraction processes to obtain crude bio-oil.

3.3.4 Downstream extraction processes

3.3.4.1 Solvent filtration

The solids remaining in the reaction vessel were carefully scooped into the beaker containing solids from the centrifuge step. About 50 mL organic solvent was used to rinse centrifuge tube, reactor and stirrer, and poured in the previously used beaker. Eventually, a solvent-solid mixture was formed in the beaker. Vacuum filtration with Buchner funnel and Whatman No. 5 filter paper was applied to separate the solvent-solid mixture. The solids remaining on the filter paper were washed with an extra 50 mL of solvent to recover the remaining oil content, resulting in about 100 mL solvent-biocrude mixture in total.

3.3.4.2 Soxhlet extraction

Similar to the solvent filtration procedure, the solids within the reactor were first collected. The reactor, stirrer and centrifuge tube were rinsed with 50 mL solvent and stored in a beaker. The solvent-solid mixture was then carefully transferred into a soxhlet extraction vessel (50 mL capacity) with a pre-weighed cellulose thimble inside. An additional 50 mL of solvent was added into the Soxhlet extraction vessel. The Soxhlet extraction was held for four hours. Once the Soxhlet extraction was completed, the organic solvent dissolving 'bio-oil' was vacuum filtered through a Buchner funnel with Whatman No. 5 filter paper to remove any solid particles. Another 10 mL solvent was used to rinse the filter paper. Finally, approximately 110 mL solvent-biocrude mixture was obtained from Soxhlet extraction process.

3.3.4.3 Microwave-assisted extraction

This process is different from the solvent filtration and Soxhlet extraction, in that the solids remaining in centrifuge tube were directly transferred into a 100 mL microwave extraction vessel, along with 50 mL solvent-solid mixture, obtained by rinsing the reactor, stirrer and centrifuge tube. The microwave-assisted extraction was carried out in a laboratory microwave reactor (Anton Paar-Multiwave Pro) by using the following power programing: reaching 250 Watts microwave power within 2 mins; holding microwave power at 250 Watts for 15 mins; and cooling down to 45 °C. A low agitation speed was used during extraction. Once the microwave-assisted extraction was completed, the solvent-solid mixture was vacuum filtered through a Buchner funnel with Whatman No. 5 filter paper, and extra 50 mL solvent was used to recover the remaining oil on the solids and filter paper, giving about 100 mL solvent-biocrude mixture in total.

3.3.4.4 Solvent Removal

For each extraction method, the resulting solvent-biocrude mixture was transferred to a pre-weighed Erlenmeyer flask to remove the organic solvent by rotary vacuum evaporation. The vacuum (-0.7 bar) and evaporation temperature (70 °C) was applied for hexane, THF and acetone extracted samples, and the same vacuum pressure but different evaporation temperature (45 °C) was applied for removing DCM due to its much lower boiling point. Finally, the crude bio-oil product was obtained and weighed. Crude bio-oil from each experimental run was stored in a 4 mL amber glass vial, followed by nitrogen gas purge to blow out the remaining air in the headspace

of the vial. All obtained crude bio-oil samples were stored at 4 °C fridge. The yield of crude bio-oil was calculated as a mass percentage and defined as follows:

$$Y_{oil}\,(\text{wt. \%}) = \frac{\text{Mass of biocrude}}{\text{Mass of feedstock}} \times 100\% \quad (3.1)$$

3.3.5 Synergistic effect (SE) calculation

The synergistic effect (SE) from co-liquefaction of *C. sp.* and SCG is evaluated as follows:

$$\text{SE}\,(\%) = \frac{Y_{MA/SCG} - Y_{theo}}{Y_{theo}} \times 100$$

$$= \frac{Y_{MA/SCG} - (X_{SCG} \times Y_{SCG} + X_{MA} \times Y_{MA})}{Y_{theo}} \times 100 \quad (3.2)$$

where $Y_{C.\,sp./SCG}$ denotes the actual yield from co-liquefaction of *C. sp.* and SCG, and Y_{theo} indicates the theoretical mass-averaged yield of each feedstock. X_{SCG} and $X_{C.\,sp.}$ are the mass fraction in mixed feedstock which were 0.5. Y_{SCG} and $Y_{C.\,sp.}$ represent the yield obtained from liquefaction of individual SCG and *C. sp.* respectively.

3.3.5 Biocrude oil characterization

The GC-MS detectable chemical compounds of crude bio-oils were identified and further quantified by using naphthalene D8 as an internal standard. About 3 mg crude bio-oil sample was loaded into a 5 mL volumetric flask, followed by the addition of 50 uL internal standard solution (1000 ug/mL naphthalene D8). The same type of organic solvent used for crude bio-oil extraction was added into the 5 mL volumetric flask, resulting in a sample solution containing approximately 600 ug/mL biocrude and 10 ug/mL internal standard. Such prepared sample solution was filtered through a 0.2 um syringe filter before being injected into GC-MS system.

GC-MS analysis was performed using a Perkin Elmer Clarus 680 GC coupled with a Clarus SQ8 MS. The GC injection port was operated at 280 °C in a splitless mode, and 1 mL/min helium was used as the carrier gas. The injection volume was 1 uL. A Rxi-5ms column (30 m × 0.25 mm × 0.25 um) with a low-polarity phase was used. An initial oven temperature was set at 50 °C and held for 2 mins, then increased to 280 °C at a heating rate of 15 °C/min and held for 12 mins, giving a total run time of 30 mins. In terms of MS settings, an electron impact (EI) source with electron energy of 70 eV was used. The source and transfer line temperature was 150 °C and 200 °C respectively. Data was acquired in 45-400 m/z scan mode, and a solvent delay of five mins

was applied to protect the MS. Fifty peaks based on the integrated peak areas in total ion chromatogram (TIC) were identified by using the NIST library, and they were further quantified by using the internal standard. These fifty chemical compounds were then categorized into eight groups: hydrocarbons, esters, amides, amines, ketones, phenols, acids and others.

The viscosity of crude bio-oil was measured using a Brookfield CAP 2000+ (low torque) viscometer at 60 °C. Cone 01, 05 and 09 (viscosity testing spindles) were used to test biocrude viscosity after calibrating with standard fluids. The spindle speed was 100 rpm in all measurements.

3.3.6 Experimental design and data analysis

A full factorial design (3×4×3) was used in this study, involving three factors, namely extraction methods (filtration, Soxhlet and microwave-assisted), solvents (hexane, acetone, DCM and THF) and feedstocks (*C. sp.*, SCG and 50/50 *C. sp.*/SCG). The yield of crude bio-oil, biocrude chemical yields and dynamic viscosity were selected as the response. Duplication of each combination was applied, giving 72 experimental runs in total. The data were analyzed in Minitab 17 by using Analysis of Variance (ANOVA).

3.4 Results and discussion

3.4.1 Crude bio-oil yield (wt.% of biomass mass)

3.4.1.1 Effects of downstream extraction methods and solvents

Biocrude yield (wt.%) is a commonly used parameter that assesses the performance of hydrothermal liquefaction as a bio-oil fraction is the primary target product. Fig. 3.1a shows the yield of *C. sp.* biocrude recovered using different downstream extraction methods and solvents. It was found that the yields of biocrude derived from *C. sp.* were not significantly influenced by the extraction methods used, but were however impacted by the extraction solvent remarkably. The yield of biocrude extracted by DCM and THF were both much higher than those obtained by acetone and hexane, by an order of DCM (30.95 wt.%) ≈ THF (30.04 wt.%) > acetone (23.19 wt.%) > hexane (9.44 wt.%). This was mainly attributed to their different solvent dielectric constants as shown in Table 3.2. Hexane has a low dielectric constant of 1.89 and acetone has a high one of 21.0 while both DCM and THF have moderate dielectric constants, 9.08 and 7.52 respectively (Vogel et al., 1996). The organic solvents with moderate dielectric constants are generally capable of dissolving both polar and non-polar chemical compounds (Smallwood, 2012).

Therefore, using DCM and THF resulted in relatively high biocrude yields; hexane gave the lowest biocrude yield. Valdez et al. (2011) investigated the impact of solvent on biocrude yield using hexane and DCM with low to moderate dielectric constants in the HTL of microalgae *Nannochloropsis sp*. They reported a yield of DCM-extracted biocrude of 30 wt.% comparable to 30.95 wt.% obtained in our study. However, there was a fairly large variation on hexane-extracted biocrude yield between this reported study (Valdez et al., 2011) and our study (32 wt.% vs 9.44 wt.%). The reason behind this variation is not clear, it might be caused by using different microalgae strains, reaction systems and HTL conditions.

For feedstock SCG, different extraction methods did not significantly change the biocrude yield when using solvents such as acetone, DCM and THF as shown in Fig. 3.1b. This observation suggested that acetone (32.94 wt.%), DCM (34.37 wt.%) and THF (38.29 wt.%) were effective solvents for biocrude recovery, and the extraction methods used made insignificant difference. However, when hexane was used, Soxhlet extraction (23.02 wt.%) was able to collect more biocrude than filtration (15.20 wt.%). This might be due to the formation of co-solvent (hexane-water) in the process of Soxhlet extraction. It was noticed in our experiments that the wet solid residues obtained after liquefaction of SCG, contained a certain amount of water, and the water was then introduced into Soxhlet extraction system along with the solid residues. Co-existence of hexane and water led to a positive co-solvent (hexane-water) effect in the process of biocrude recovery. This positive co-solvent effects between non-polar and polar solvents have been well documented in the field of bio-compounds extraction (Azwanida, 2015).

In terms of *C. sp.* and SCG mixture, the effects of extraction methods and solvents on the biocrude yield are illustrated in Fig. 3.1c. There was no significant variation on the yield of biocrude recovered by three extraction methods when using acetone, DCM and THF. Acetone, DCM and THF demonstrated strong biocrude recovery ability, as evidenced by the yields of 29.33 wt.%, 35.46 wt.% and 37.58 wt.% respectively. Due to the existence of a small amount of water, Soxhlet extraction exhibited better performance than filtration when hexane was used as an extraction solvent, similar to the observation in the HTL of SCG.

In general, the effect of downstream extraction methods on biocrude yield is insignificant. Taking the operation costs into consideration, filtration is recommended for the recovery of biocrude oil from the HTL product mixture. The effectiveness of extraction solvents is in the

following order: DCM ≈ THF > acetone > hexane. If biocrude yield is a primary optimization parameter, solvents with moderate dielectric constant are favorable, for example DCM and THF.

Table 3.2 Properties of extraction solvents used in this study (Vogel et al., 1996).

	Hexane	Acetone	DCM	THF
Formula	C_6H_{14}	C_3H_6O	CH_2Cl_2	C_4H_8O
Boiling point (°C)	69.00	56.05	39.80	65.00
Density (g/mL)	0.66	0.78	1.33	0.88
Solubility in water (g/100g)	0.01	Miscible	1.32	30.00
Dielectric constant at 20 °C	1.89	21.01	9.08	7.52
General descriptions	non-polar, low dielectric constant	polar, high dielectric constant	low polarity, moderate dielectric constant	moderate polarity, moderate dielectric constant

Note: DCM = dichloromethane; THF = tetrahydrofuran.

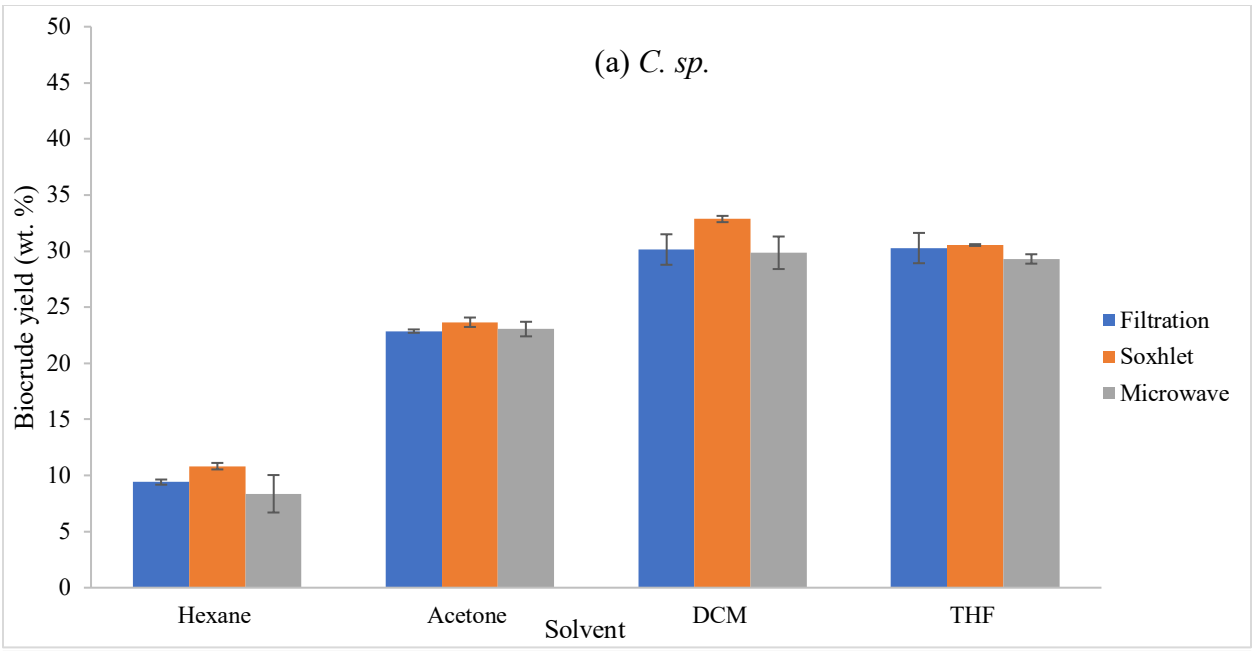
(a) C. sp.
Biocrude yield (wt. %)
50
45
40
35
30
25
20
15
10
5
0
Hexane
Acetone
DCM
THF
Solvent
Filtration
Soxhlet
Microwave

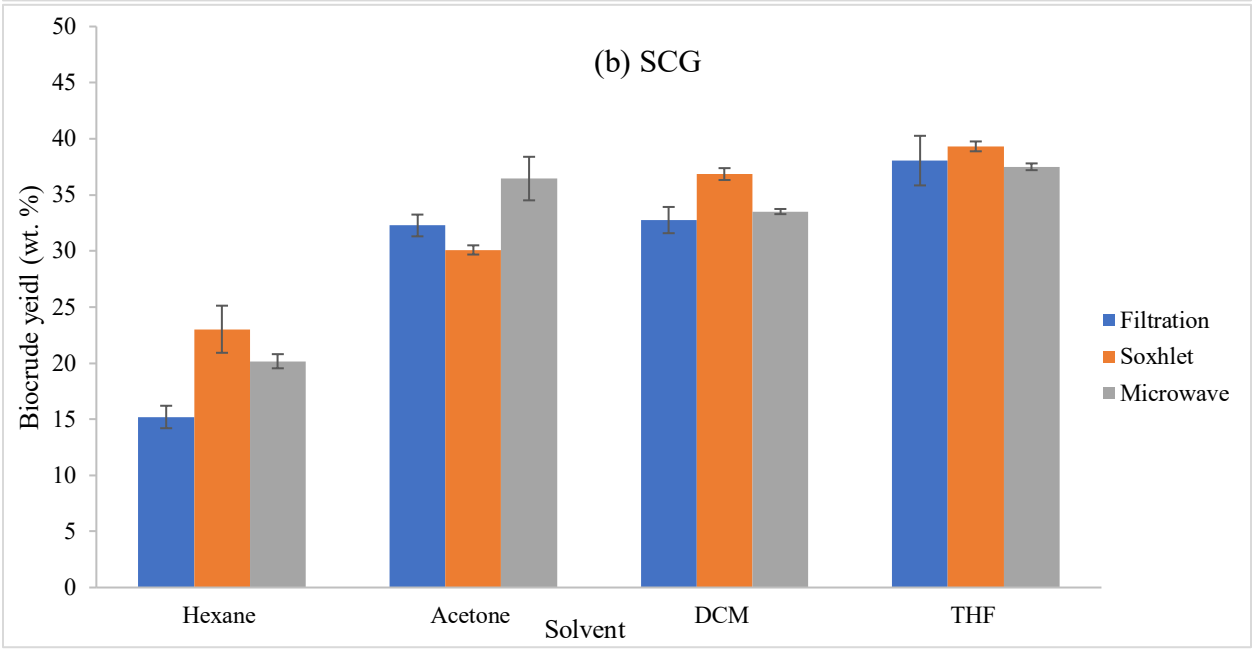
(b) SCG
Biocrude yeidl (wt. %)
50
45
40
35
30
25
20
15
10
5
0
Hexane
Acetone
DCM
THF
Solvent
Filtration
Soxhlet
Microwave

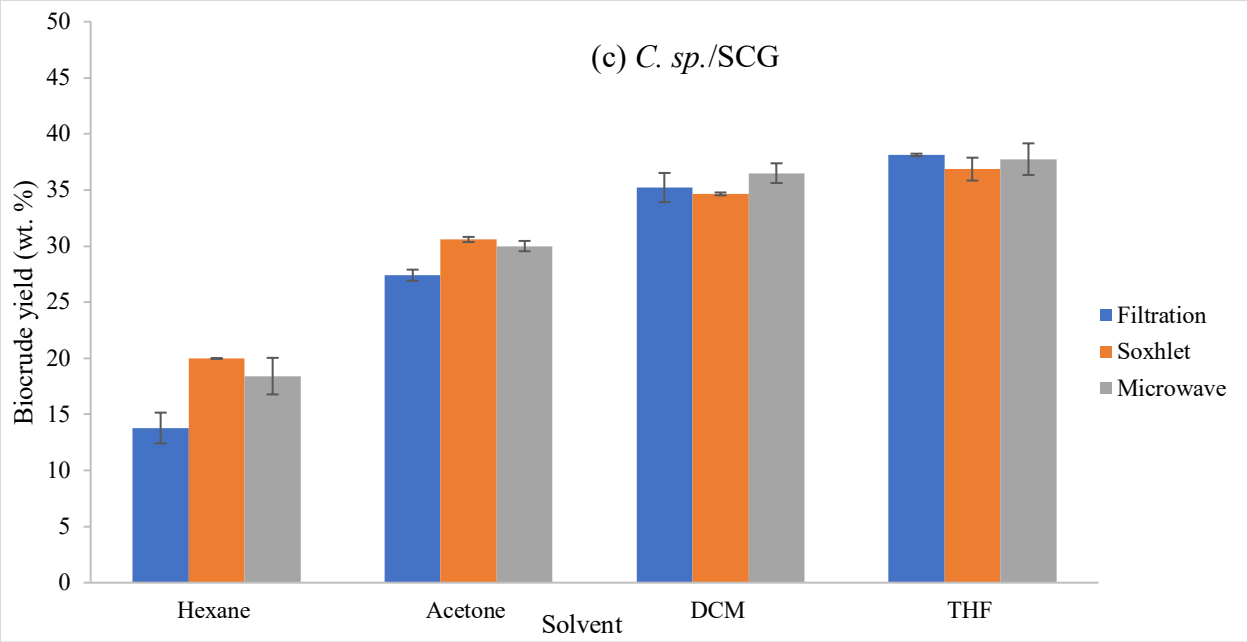

Fig. 3.1 The yield of crude bio-oil derived from (a) *Chlorella sp*. microalgae (*C. sp.*), (b) spent coffee grounds (SCG) and (c) 50/50 *C. sp.*/SCG using different extraction methods (filtration, Soxhlet and microwave) and solvents (hexane, acetone, dichloromethane (DCM) and tetrahydrofuran (THF)).

3.4.1.2 Effects of feedstock

The impact of feedstock (*C. sp.*, SCG and *C. sp.*/SCG) on the biocrude yield was analyzed and presented in Table 3.3. It was clearly observed that SCG and *C. sp.*/SCG had comparable biocrude yields, and they were higher than that of *C. sp.* regardless of extraction methods and solvents used. This is due to the fact that SCG and *C. sp.*/SCG had higher lipid content than *C. sp.* (here a microalgae specie with low lipid content), in which a high lipid content has been proved to be remarkably beneficial for biocrude formation (Biller and Ross, 2011; Teri et al., 2014). Combining the results presented in section 3.4.1.1, we can conclude that the extraction solvent and feedstock were the crucial factors for biocrude yield rather than the extraction method. This was further supported by the Analysis of Variance (ANOVA) as presented in Supplemental materials Table S3.1. The Fisher F-test value, a statistical indicator for the degree of contribution from the experimental factor, was 733.66, 215.64 and 12.87 respectively for solvent, feedstock and extraction method, demonstrating that the extraction method was a much less influential factor for biocrude yield compared to the extraction solvent and feedstock.

Table 3.3 The yield of crude bio-oil (wt.%) derived from *Chlorella sp*. microalgae (*C. sp.*), spent coffee grounds (SCG) and *C. sp.*/SCG.

	Filtration			Soxhlet			Microwave		
	C. sp.	SCG	*C. sp.*/SCG	*C. sp.*	SCG	*C. sp.*/SCG	*C. sp.*	SCG	*C. sp.*/SCG
Hexane	9.4±0.2	15.2±1.0	13.8±1.4	10.8±0.3	23.0±2.1	20.0±0.0	8.4±1.7	20.2±0.6	18.4±1.6
Acetone	22.9±0.2	32.3±1.0	27.4±0.5	23.7±0.4	30.8±0.1	30.6±0.2	23.1±0.7	36.5±1.4	30.0±0.5
DCM	30.1±1.4	32.8±1.2	35.2±1.3	32.9±0.3	36.9±0.5	34.7±0.1	29.9±1.5	33.5±0.1	36.5±0.9
THF	30.3±1.4	38.1±2.2	38.1±0.1	30.5±0.1	39.3±0.4	36.9±1.0	29.3±0.4	37.5±0.3	37.8±1.4

Notes: DCM = dichloromethane; THF = tetrahydrofuran

3.4.1.3 Synergetic effect on biocrude yield in co-liquefaction

Feedstock optimization (co-liquefaction of various feedstock) aims to increase oil yield, control the composition/properties of bio-crude oil and make full use of all kinds of available biowastes. Hereby, *C. sp.* and SCG were chosen as a representative feedstock combination and co-liquefied under an identical reaction condition. The SE on biocrude yield for different extraction solvents were presented in Table 3.4. Varied SE on biocrude yield were resulted, 19.95% for using hexane, 10.00% for THF, 7.54% for DCM and 2.82% for acetone.

SE on biocrude yield originate from the reaction process of HTL. The enhancement on biocrude yield (SE) if existing, should come from the interactions among different components in the feedstock mixture and would depend on the reaction parameters such as temperature, pressure, mass ration of feedstock and reaction medium and catalyst (Gai et al., 2015a; Wu et al., 2017). However, each study used different solvents to collect biocrude which might have resulted in inconsistent SE even for the same feedstock mixture under the same liquefaction conditions. For example, in our previous study on co-liquefaction of SCG with several lignocellulosic feedstock, acetone was used to recover biocrude. It was found that SCG with corn stalk was the best combination with a SE of 20% on biocrude yield, while there was a negative SE for feedstock combination of SCG with white pine bark. This conclusion was valid only when acetone was used for the post-reaction collection of biocrude oil. If another solvent was used, the outcomes might be different. This also holds true for other relevant studies that investigated the synergy in co-liquefaction of different feedstock (Jin et al., 2013; Xiu et al., 2011b). Therefore, future works on the co-liquefaction SE need to be aware of the solvents' influence as illustrated in this study.

Table 3.4 The co-liquefaction synergy effect (SE, %) on biocrude yield.

Solvent	Yield of *C. sp.* (wt.%)	Yield of SCG (wt.%)	Yield of *C. sp.*/SCG (wt.%)	SE (%)
Hexane	9.54	19.46	17.39	19.95
THF	30.04	38.29	37.58	10.00
DCM	30.95	34.99	35.46	7.54
Acetone	23.19	33.86	29.33	2.82

Notes: DCM = dichloromethane; THF = tetrahydrofuran; *C. sp.* = *Chlorella sp*. microalgae; SCG = spent coffee grounds.

3.4.2 Biocrude chemical yields (wt.% of feedstock mass)

In addition to the biocrude yield, it is necessary to investigate the impact of extraction methods, solvents and feedstock on the chemical composition of biocrude. GC-MS analysis was carried out to serve this purpose. Peaks in Total Ion Chromatogram (TIC) were identified and further classified into eight distinct chemical groups, including hydrocarbons, esters, amides, amines, ketones, phenols, acids and others. These eight chemical groups were quantified based on the feedstock mass, being referred as the biocrude chemical yields (wt.% of feedstock mass), illustrating in the following equation:

$$\text{Chemical yield} = \frac{\text{feedstock mass} \times \text{biocrude yield} \times \text{biocrude chemical compositions}}{\text{feedstock mass}} \times 100$$

The ANOVA analysis was conducted to evaluate the significance of studied variables on the chemical yields as presented in supplemental materials Table S3.2. The extraction method was found to be an insignificant factor for chemical yields, but solvents and feedstock exhibited considerable influence on the chemical yields. Table 3.5 shows the impact of solvents and feedstocks on chemical yields (wt.% of feedstock mass) after excluding extraction method effect.

From Table 3.5, DCM extracted biocrude had a higher hydrocarbon yield (1.05-1.42 wt.%) than the other three solvents (0.14-0.69 wt.%) for all three feedstocks. Hexane and THF had comparable hydrocarbon yields, and they were greater than that of acetone. Acetone is much more polar than other solvents and therefore was less effective for dissolving non-polar hydrocarbons. Microalgae were liquefied in a reported research (Valdez et al., 2011), and about 1.12 wt.% and 0.99 wt.% of hydrocarbons were extracted by DCM and hexane respectively. These were in agreement with our results that hydrocarbon yield of DCM- *C. sp.* and hexane- *C. sp.* was 1.42 wt.% and 0.52 wt.% respectively. Yu et al. (2017) used carbohydrate-rich aspen wood as a HTL feedstock and

DCM as biocrude recovery solvent, and reported a hydrocarbon yield of 3.35 wt.%, which was much higher than that of SCG (1.05 wt.%) recovered by DCM in our study.

For ester yield, DCM was able to extract more esters than other solvents (hexane, acetone and THF) from *C. sp.* and *C. sp.*/SCG. However, when SCG was used as feedstock, DCM only had a comparable ester yield (0.50 wt.%) to acetone (0.58 wt.%). This was mainly because acetone was as effective as DCM in recovering biocrude from carbohydrate-rich SCG, but acetone exhibited weaker extraction ability for *C. sp.* and *C. sp.*/SCG as compared to DCM.

In terms of amide yield, DCM was also superior to the other three solvents, and a general order can be concluded as DCM > acetone > THF ≈ hexane for all three feedstock. *C. sp.*/SCG had higher amide yields of 0.8-2.47 wt.% than *C. sp.* (0.33-1.64 wt.%) and SCG (0.09-0.31 wt.%) for all four solvents. This was attributed to the chemical reaction between *C. sp.* and SCG during co-liquefaction process. Microalgae contained an extremely low amount of lipids (0.90 wt.%) and a high amount of proteins (63.23 wt.%), while SCG comprised 9.51 wt.% lipids and 14.22 wt.% proteins. Therefore, co-liquefaction of *C. sp.* and SCG allowed the protein in *C. sp.* to react with lipid in SCG, which then generated high amide yield. Chiaberge et al. (2013) has reported that amide yields were highly dependent on the coexistence of proteins and lipids. Under hydrothermal conditions, the proteins can be rapidly hydrolyzed into amino acids and subsequently degraded into various intermediates such as ammonia and amine (Sato et al., 2004). The generated intermediates from protein hydrolysis then reacted with fatty acids from lipid hydrolysis to form amides eventually (Simoneit et al., 2003). The high amide yield from HTL of *C. sp.*/SCG was further proved by its low yield of amine and acid, which were consumed during amide formation.

Ketones and phenols have been widely identified in biocrudes from various biomass feedstock, and they are believed to originate from the carbohydrate decomposition in HTL processes (Biller et al., 2016; Lee et al., 2016; Yu et al., 2017). The solvent influence on ketone yields were observed as DCM ≈ acetone > THF ≈ hexane for SCG and *C. sp.*/SCG. However, when *C. sp.* was used as feedstock, DCM (0.9 wt.%) had higher ketone yield than acetone (0.58 wt.%). This is because DCM- *C. sp.* (30 wt.%) had higher biocrude yield that acetone- *C. sp.* (23 wt.%). The solvent impact on phenol yields can be ranked in the order of DCM > acetone > THF ≈ hexane, while feedstock did not exhibit significant influence on phenol yields. Phenols are typically obtained from lignin decomposition, which required severe hydrothermal conditions

(temperature greater than 350 °C). The HTL temperature used in this study was only 290 °C, which was not able to sufficiently decompose lignin in the subject feedstock. Therefore, *C. sp.*, SCG and *C. sp.*/SCG had similar phenol yields, although SCG and *C. sp.*/SCG had higher lignin contents than *C. sp.*. The comparison in the effects of solvent and feedstock on each chemical yield is presented in Table 3.6.

Table 3.5 Impact of downstream extraction solvents and feedstock on biocrude chemical yields (wt.% of feedstock mass) after excluding extraction method effect.

	C. sp.				SCG				*C. sp.*/SCG			
	Hexane	Acetone	DCM	THF	Hexane	Acetone	DCM	THF	Hexane	Acetone	DCM	THF
Hydrocarbons	0.52±0.05	0.33±0.03	1.42±0.09	0.54±0.03	0.69±0.13	0.14±0.02	1.05±0.08	0.58±0.06	0.62±0.05	0.21±0.03	1.09±0.09	0.52±0.06
Esters	0.25±0.01	0.87±0.05	1.60±0.11	0.45±0.02	0.22±0.03	0.58±0.05	0.50±0.07	0.25±0.03	0.49±0.02	0.96±0.07	1.49±0.07	0.51±0.05
Amides	0.33±0.03	0.97±0.08	1.64±0.07	0.54±0.04	0.09±0.01	0.21±0.02	0.31±0.05	0.11±0.02	0.83±0.03	1.35±0.09	2.47±0.15	0.8±0.08
Ketones	0.02±0.01	0.58±0.06	0.90±0.05	0.23±0.02	0.05±0.01	0.18±0.02	0.17±0.02	0.07±0.01	0.03±0.01	0.42±0.06	0.40±0.06	0.07±0.00
Phenols	0.32±0.04	0.37±0.01	0.55±0.03	0.23±0.02	0.14±0.05	0.30±0.04	0.41±0.03	0.22±0.02	0.20±0.02	0.22±0.01	0.37±0.03	0.14±0.02
Amines	0.08±0.01	0.23±0.03	0.34±0.02	0.12±0.01	0.02±0.00	0.11±0.03	0.27±0.02	0.10±0.00	0.05±0.13	0.13±0.02	0.25±0.03	0.11±0.01
Acids	0.01±0.01	0.08±0.03	0.01±0.01	0.03±0.02	0.03±0.01	0.15±0.03	0.44±0.11	0.05±0.01	0.04±0.02	0.05±0.02	0.04±0.02	0.04±0.02
Others	0.02±0.00	0.08±0.03	0.11±0.03	0.03±0.01	0.02±0.01	0.07±0.01	0.08±0.01	0.05±0.01	0.07±0.02	0.05±0.01	0.10±0.02	0.05±0.01
Total	1.54±0.10	3.51±0.18	6.57±0.17	2.17±0.05	1.25±0.17	1.73±0.10	3.22±0.15	1.43±0.10	2.34±0.10	3.38±0.16	6.20±0.31	2.25±0.10

Notes: DCM = dichloromethane; THF = tetrahydrofuran; *C. sp.* = *Chlorella sp*. microalgae; SCG = spent coffee grounds.

Table 3.6 The general orders for the solvent and feedstock effects based on chemical yields (wt.%).

Chemicals Yield	Solvents	Feedstock
Hydrocarbons	DCM > hexane ≈ THF > acetone	*C. sp.* ≈ SCG ≈*C. sp.*/SCG
Esters	DCM > acetone > THF ≈ hexane	*C. sp.*/SCG ≈*C. sp.* > SCG
Amides	DCM > acetone > THF ≈ hexane	*C. sp.*/SCG > *C. sp.* > SCG
Ketones	DCM > acetone > THF ≈ hexane	*C. sp.* > *C. sp.*/SCG > SCG
Phenols	DCM > acetone > THF ≈ hexane	*C. sp.*> SCG ≈*C. sp.*/SCG
Amines	DCM > acetone > THF > hexane	*C. sp.* > *C. sp.*/SCG ≈ SCG
Acids	DCM = acetone > THF ≈ hexane	SCG > *C. sp.*/SCG ≈*C. sp.*
Others	DCM = acetone > THF ≈ hexane	SCG ≈*C. sp.*/SCG ≈*C. sp.*
Total	DCM > acetone > THF ≈ hexane	*C. sp.*/SCG = *C. sp.* > SCG

Notes: DCM = dichloromethane; THF = tetrahydrofuran; *C. sp.* = *Chlorella sp*. microalgae; SCG = spent coffee grounds.

3.4.3 Bio-oil dynamic viscosity

Crude bio-oils are known to be highly viscous, which can cause problems for pipeline transportation and downstream treatments in refinery plants. There is no standard testing method for biocrude viscosity yet, and the biocrude viscosity can vary significantly under different testing conditions. In this section, the influence of extraction methods, solvents and feedstock on the dynamic viscosity of crude bio-oils were investigated as presented in Table 3.7. Using different extraction methods for biocrude recovery did not cause much variation on the viscosity of biocrude. For instance, the viscosity of SCG bio-oils recovered by hexane were comparable (around 12 cP) using three extraction methods. However, solvents and feedstock did influence the viscosity.

Biocrudes recovered by hexane had much lower viscosity (10-40 cP) than using acetone, DCM and THF for all three feedstock. It was likely due to that hexane-recovered biocrude contained mainly non-polar low molecular weight compounds, which therefore exhibited relatively low viscosity. In terms of the other three solvents, it was observed that *C. sp.* biocrude recovered by DCM had the highest viscosity (1265-1375 cP) compared to those of acetone (749-918 cP) and THF (841-889 cP). However, feedstock SCG showed a different trend, in which DCM extracted biocrude had lower viscosity than acetone and THF. In terms of *C. sp.*/SCG, comparable viscosities (around 500 cP) were observed for DCM, acetone and THF. In terms of the other three solvents influence, it was observed that *C. sp.* biocrude recovered by DCM had the highest viscosity (1265-1375 cP) compared to those of acetone (749-918 cP) and THF (841-889 cP). However, feedstock SCG showed a different trend, in which DCM extracted biocrude had lower viscosity than acetone and THF. For *C. sp.*/SCG, comparable viscosities (around 500 cP) were observed for DCM, acetone and THF.

As for the effects from feedstock, biocrudes from *C. sp.* had the highest viscosity among three feedstock used, and these *C. sp.* bio-oils were non-flowable at room temperature (poor flowability) with an exception of hexane extracted crude oil (good flowability). Jarvis et al. (2017) reported that the viscosity of HTL biocrude generated from *Chlorella* was 295 cSt (about 325 cP) at 40 °C, which was much lower than 749-1375 cP (60 °C) obtained from the present work. Although SCG bio-oils exhibited the lowest viscosity among three feedstock, they were all non-flowable at room temperature (including hexane extracted bio-oil). The reason for such poor flowability escaped our understanding. *C. sp.*/SCG bio-oil had a moderate viscosity, which was between *C. sp.* and SCG

for all solvents used. *C. sp.*/SCG biocrudes from all four solvents exhibited fairly good flowability at room temperature, and this made the co-liquefaction biocrudes more desirable than those from *C. sp.* or SCG. Xiu et al. (2010) reported that the viscosity (25.4 cP) of biocrude derived from co-liquefaction of manure and free fatty acids was tremendously lower than that of individual manure (843 cP). Similar improvement on biocrude viscosity was also observed in our previous study as well (Yang et al., 2017). Therefore, co-liquefaction of *C. sp.* and SCG was preferred based on the biocrude viscosity and flowability. Overall, hexane and *C. sp.*/SCG was the most desirable extraction solvent and feedstock if consider solely from viscosity/flowability perspective.

Table 3.7 The dynamic viscosity of crude bio-oils derived from *Chlorella sp*. microalgae (*C. sp.*), spent coffee grounds (SCG) and *C. sp.*/SCG by using different downstream processing methods and solvents.

	C. sp.			SCG			*C. sp.*/SCG		
	Filtration	Soxhlet	Microwave	Filtration	Soxhlet	Microwave	Filtration	Soxhlet	Microwave
Hexane	36±4	24±2	40±10	10±0.6	12±0.8	14±0.2	23±0.7	20±2	19±3
Acetone	749±118	918±58	876±304	100±10	120±10	NA	450±156	441±9	530±106
DCM	1375±NA	1328±264	1265±64	44±2	60±7	39±10	341±128	516±7	478±109
THF	889±128	841±62	858±105	NA	681±126	400±100	549±93	505±59	464±198

Notes: 1, DCM = dichloromethane; THF = tetrahydrofuran.
2, The dynamic viscosity of biocrude were tested at 100 rpm and 60 °C

A summary table was generated to illustrate the effects of extraction methods, solvents, feedstock on the biocrude yield, chemical yields and dynamic viscosity in Table 3.8. The downstream extraction method was not a critical factor for biocrude yield and physicochemical properties, and filtration was thus considered as the most desirable extraction method due to its ease of operation and low costs. DCM was proved to be an effective solvent mainly due to its strong extraction ability of bio-oil chemicals. Co-liquefaction of *C. sp.* and SCG was advantageous over HTL of individual *C. sp.* and SCG considering the increased yields and favorable properties.

Table 3.8 Summary of the effects of extraction methods, solvents and feedstock on biocrude yield and physicochemical properties.

Biocrude physicochemical properties	Downstream extraction methods	Downstream extraction solvents	Feedstock
Biocrude yield (wt.% of feedstock mass)	filtration ≈ Soxhlet ≈microwave-assisted	DCM≈THF > acetone > hexane	*C. sp.*/SCG ≈ SCG > *C. sp.*
Biocrude chemical yield (wt.% of feedstock mass)	filtration ≈ Soxhlet ≈ microwave-assisted	DCM > acetone > THF≈ hexane	*C. sp.*/SCG ≈*C. sp.* > SCG
Dynamic viscosity (cP)	filtration ≈ Soxhlet ≈ microwave-assisted	Biocrudes recovered by hexane had lowest dynamic viscosity	*C. sp.* > *C. sp.*/SCG > SCG

Notes: DCM = dichloromethane; THF = tetrahydrofuran; *C. sp.* = *Chlorella sp*. microalgae; SCG = spent coffee grounds; *C. sp.* /SCG = 50/50 *C. sp.* /SCG by mass.

3.5 Conclusions

This study investigated the influence of recovery methods (filtration, Soxhlet and microwave-assisted) and solvents (hexane, acetone, DCM and THF) on the yield and physicochemical properties of biocrude from *Chlorella sp.* (*C. sp.*), spent coffee grounds (SCG), and a mixture of the two. It was found that using different downstream extraction methods did not significantly affect the yield and physicochemical properties of biocrude from either *C. sp.,* SCG or a mixture of the two. Filtration was therefore recommended as a suitable extraction method due to its ease of operation and low costs. The recovery solvent was proven to strongly impact the yield/physicochemical properties of biocrude. DCM was a favorable biocrude recovery solvent from both biocrude yield and chemical yields perspective. It was also noticed that the synergy claims for co-liquefaction of *C. sp.* and SCG were highly dependent on the solvent used as well. It is therefore essential to take the influence of recovery solvent into consideration when claiming co-liquefaction effect on biocrude yield. In general, inconsistent recovery procedures did lead to varied biocrude yield and physicochemical properties. Awareness of such influence particular from solvents needs to be embedded when comparing research results in literature, optimizing process parameters, studying synergistic effect in co-liquefaction and exploring HTL reaction mechanisms.

3.6 Supplementary materials

Table S3.1 The Analysis of Variance (ANOVA) table for biocrude yield (wt.%).

Source	DF	Adj MS	F-value
Solvent	3	1451.05	733.66
Extraction method (EM)	2	25.45	12.87
Feedstock	2	426.49	215.64
Solvent*EM	6	10.18	5.15
Solvent*Feedstock	6	16.24	8.21
Feedstock*EM	4	5.54	2.80
Solvent*EM*Feedstock	12	5.27	2.66
Error	36	1.98	
Total	71		

Notes: DF= degree of freedom; Adj MS= adjusted mean squares.

Table S3.2 The p-values for Analysis of Variance (ANOVA) of the chemical yields.

Chemicals	Solvent	Extraction method	Feedstock
Hydrocarbon	0.000	0.137	0.030
Ester	0.000	0.057	0.000

Chemicals	Solvent	Extraction method	Feedstock
Amide	0.000	0.181	0.000
Amine	0.000	0.544	0.000
Ketone	0.000	0.058	0.000
Phenol	0.000	0.525	0.000
Acid	0.003	0.969	0.000

Note: P-value < 0.05 indicates significant difference between two mean values at the 5% level of significance.

3.7 Transition section

Chapter 3 assessed the influence of HTL downstream processing methods on the yield and physicochemical properties of biocrude. Filtration with dichloromethane was suggested to be favourable for downstream biocrude recovery, which was then consistently applied into other HTL experiments in this project. Since there is a lack of prediction models for the yield of HTL products, as well as the limited understanding on the product formation pathways, it is therefore necessary to use biomass model components coupled with statistical design to develop HTL product yield prediction models, and also to gain more insights of reaction pathways during HTL of biomass. The detailed experimental design, prediction model development and reaction pathways exploration were presented in Chapter 4.

Chapter 4: Hydrothermal Liquefaction of Biomass Model Components for Product Yield Prediction and Reaction Pathways Exploration

Contribution statement:

I was responsible for raw materials collection, experiment design and conduction, part of data analysis and manuscript preparation.

4.1 Abstract

Prediction models for biocrude yield and solid residue (SR) yield were developed by using a mixture design of five model components, including xylan (hemicellulose), crystalline cellulose, alkaline lignin, soya protein and soybean oil in this study. The model predictability was verified by using actual feedstock as well as a mixture of model components based on feedstock biochemical composition. The biocrude yield, SR yield and quantitative chemical yields obtained from bio-oil characterization were used to explore the possible reaction pathways as well as synergistic and/or antagonistic interactions between two studied model components. It was found that both hemicellulos and lipid (H*Lip) and cellulose and lipid (C*Lip) interactions had synergistic effect on the biocrude yield, while SR yield was antagonistically decreased by the cellulose and lignin (C*Lig) interaction. Maillard reactions between protein and carbohydrates and amide formation from protein and lipid were observed. The carbohydrates and lipid interactions had a variety of effects on the acid yield, hydrocarbon yield and ketone yield, but lignin and lipid behaved independently in the HTL processes.

4.2 Introduction

A number of attempts have also been made to predict HTL biocrude yield by kinetic modelling, and/or the biomass model compounds modelling (on the basis of biomass chemical compositions) (Biller and Ross, 2011; Teri et al., 2014; Leow et al., 2015; Sheng et al., 2018; Hietala et al., 2017; Déniel et al., 2017b; Sheehan and Savage, 2017; Hietala et al., 2016). For instance, Biller and Ross, (2011) first used model compounds (protein, lipid and carbohydrates) to

develop a linear prediction model for biocrude yield by using "compounds additive" approach. Sheng et al. (2018b) used castor oil, soya protein and glucose as model compounds and a non-linear regression modelling as a statistical tool and developed a prediction model for HTL biocrude yield that involved cross-interactions between model components; this newly developed model was proven to provide more accurate prediction than the previous models. More detailed information of HTL product yield modeling was provided in section 2.3. The currently available models either had unsatisfactory representativeness (monomers as model components), or only focused on lipid, protein and carbohydrate with limited consideration on the difference between cellulose, hemicellulose, and lignin, or provided only linear additive models assuming each component behaved independently under HTL conditions. Therefore, it is necessary to develop prediction models which use five representative model components and consider interaction effects between five components. Such models can more accurately predict product yields, and be used to assess the potential of various biomass feedstocks as well as their co-liquefaction feasibility to achieve the optimal use of all kinds of biomass resources for energy production.

In addition to model bio-oil yield and the contribution from each individual component in biomass to the product distribution, it is essential to explore the potential chemical reactions between these components. This will provide fundamental knowledge for tailoring the HTL product distribution, and better understanding of the synergistic effects, if they exist, when mixed feedstock (co-liquefaction) is applied. It is generally agreed that hydrothermal decomposition of biomass is a complicated process involving many kinds of chemical reactions. Therefore, biomass model compounds instead of actual biomass have been used to elucidate the biomass decomposition mechanisms under HTL conditions. Hydrolysis is typically considered as the first degradation step in a HTL process, resulting in oligomers and monomers intermediates (Déniel et al., 2016; Peterson et al., 2008). Monosaccharides can be obtained from hemicellulose/cellulose hydrolysis (Sasaki et al., 2000; Mok and Antal Jr, 1992), methoxyphenol derivatives from lignin (Garrote et al., 1999), amino acids from protein (Déniel et al., 2017a), and fatty acids and monoglycerides from lipid (Gao et al., 2011). These generated intermediates are not stable under hydrothermal conditions, and are highly susceptible to dehydration, decarboxylation, isomerization, retro-aldol reaction, aldol condensation, and other inter- and intra-molecular reactions. Unfortunately, the reactions between two or more model compounds at subcritical water medium are rarely investigated, though Maillard reaction between protein and carbohydrates

(Yang et al., 2015a; Zhang et al., 2016), and amide formation between protein and lipid (Madsen et al., 2017b) were reported in a few studies that used microalgae as feedstocks. The potentially existing interactions between hemicellulose, cellulose and lignin, as well as between carbohydrates and lipid were still unclear. Déniel et al. (2017a) attempted the hydrothermal conversion of mixtures of model monomers (such as glucose-glutamic acid and guaiacol-linoleic acid), and provided valuable information on the interactive effects. They suggested that using model biopolymers instead of monomers would provide a better representation of actual biomass. Pedersen and Rosendahl, (2015) also recommended that more work needed to be conducted for understanding the unsatisfactory predictability between model compounds and actual biomass.

This chapter aims to develop prediction models for HTL products by using biopolymers instead of monomers and response surface methodology of a mixture design as the statistical method. Protein, hemicellulose, cellulose, lignin and lipid were used for the first time as five representative biomass model components to develop the predication models, which allow a quick estimation of HTL product yield based on the biochemical composition of feedstock. The pathways of reactions between two model components at subcritical water conditions were investigated as well, which would contribute to the advancement and fundamental knowledge on reaction mechanism of biomass under liquefaction conditions.

4.3 Materials and methods

4.3.1 Materials

ACS reagent grade dichloromethane (DCM), DCM (MS grade) and naphthalene D8 standard were purchased from Sigma Aldrich Ltd. Soybean oil and microcrystalline cellulose were supplied by Alfa Aesar. Xylan from corn core and alkaline lignin were purchased from TCI America. Unflavored soy protein isolate was purchased from Myprotein Canada. Soybean oil, microcrystalline cellulose, xylan, alkaline lignin, and soy protein isolate was used to represent biomass lipid, cellulose, hemicellulose, lignin, protein respectively. All these chemicals were used as received.

4.3.2 Experiment operation procedures

4.3.2.1 Hydrothermal liquefaction processes

Please refer to the section 3.3.3.

4.3.2.2 Downstream biocrude recovery processes

Please refer to section 3.3.4.1 and 3.3.4.4 for solvent (dichloromethane) filtration washing and evaporation respectively.

4.3.3 Biocrude characterization

Please refer to section 3.3.6.

4.3.4 Experiment design and data analysis

A Simplex-Centroid mixture design that has 36 formulations of five components (protein, hemicellulose, cellulose, lignin, and lipid) was analyzed using Minitab Version 18 software. The biocrude yield, SR yield and GC-MS detected chemical groups were selected as the response variables. Complete analyses of these response variables were conducted using the methods described in Montgomery (Montgomery, 2017). The analyses included verifying the validity of normal distribution and constant variance assumptions on the error terms. Independence assumption was valid due to the random run orders. This was followed by testing the significance of each model term, constructing contour plots, and performing response optimization to identify the optimum proportions that jointly maximize or minimize the desired response variables. Principle component analysis (PCA) was also conducted to investigate correlations between feedstock chemical compositions, HTL product yields and biocrude chemical groups.

4.4 Results and discussion

4.4.1 Development and application of prediction models

4.4.1.1 HTL products yield of individual model component

Biomass feedstock mainly consists of protein, lipid and carbohydrates, in which carbohydrates are typically referred to hemicellulose, cellulose and lignin. It is necessary to investigate their individual contributions to HTL product yield before studying their mixtures. The HTL products yields of individual model component are presented in Table 4.1.

The biocrude yield from HTL of lipid was extremely high (95.86 wt.%) along with low yields of SR, aqueous phase (AqP) and gaseous phase products, which were in agreement with other relevant studies (Biller and Ross, 2011; Déniel et al., 2017b; Teri et al., 2014). HTL of individual protein had a biocrude yield of 19.91 wt.%, SR yield of 6.6 wt.% and a relatively high AqP+gas yield (73.49 wt.%). This was mainly because protein could be easily hydrolyzed into water-soluble amino acids under HTL reaction condition, and amino acids were further degraded into gaseous

products (such as carbon dioxide and ammonia *via* decarboxylation and deamination respectively) (Peterson et al., 2008). Hemicellulose (xylan) had a SR yield of 20.98 wt.%, and this was contributed to either incomplete decomposition of xylan or intensive repolymerization of xylan hydrolysis intermediates. A low biocrude yield (5.27 wt.%) and high AqP+gas yield (73.75 wt.%) from HTL of xylan evidenced that enormous amounts of xylan decomposition products were water-soluble and highly susceptible to gas formation. Mok and Antal Jr, (1992) also reported that hot compressed water was able to solubilize hemicellulose efficiently within 10-15 mins. The biocrude yield and SR yield from HTL of cellulose was 14.23 wt.% and 32.43 wt.% respectively, along with a moderate AqP+gas yield (53.34 wt.%). In comparison with hemicellulose, cellulose had a higher SR yield as expected, because more severe hydrothermal conditions were typically required to achieve sufficient cellulose decomposition. HTL of cellulose had a higher biocrude yield and a lower AqP+gas yield than hemicellulose. These observations can be explained from two aspects, i) due to a relatively incomplete hydrolysis of cellulose, some short-chain oligomers were recovered by DCM and simply resulted in the high biocrude yield for cellulose; ii) the decomposition intermediates from cellulose tended to interact or/and rearrange to form biocrude *via* aldol condensation. Lignin had the lowest biocrude yield (3.93 wt.%) and highest solid residue yield (40.58 wt.%), which illustrated the difficulty of obtaining sufficient lignin decomposition under subcritical water condition (Toor et al., 2011).

In general, HTL of carbohydrates (hemicellulose, cellulose and lignin) tended to generate less bio-oil and more solid residue as compared to that of lipid and protein. In terms of the biocrude yield, it was ranked in the following order of lipid >> protein > cellulose > hemicellulose ⩾ lignin, while the order of lignin > cellulose > hemicellulose > protein > lipid was proposed for SR yield. These results were consistent with many reported studies (Biller and Ross, 2011; Déniel et al., 2017b; Li et al., 2017; Teri et al., 2014).

Table 4.1 Hydrothermal liquefaction (HTL) products yield from individual model component.

	Protein	Hemicellulose	Cellulose	Lignin	Lipid
Biocrude yield (wt.%)	19.91±0.24	5.27±0.61	14.23±0.16	3.93±0.52	95.86±0.94
Solid residue (wt.%)	6.60±0.74	20.98±5.52	32.43±3.10	40.58±2.01	1.34±0.23
AqP+gas (wt.%)	73.49±0.49	73.75±4.91	53.34±3.25	55.49±1.48	2.81±0.71

Notes: AqP = aqueous phase; AqP + gas = 100% - (biocrude yield + solid residue)

4.4.1.2 Prediction model for biocrude yield and solid residue (SR) yield

HTL of binary, ternary, quaternary and quinary mixtures of model components was conducted to develop prediction models for biocrude yield and SR yield. The mathematical models that only include significant terms were provided in Table 4.2. The R^2 (*adj*) for biocrude yield and SR yield was 95.62% and 86.16% respectively, which demonstrated very high strength of the model in describing the experimental data. The p-values of the test that indicate the significance of the model terms were included in supplemental materials Table S4.1. The biocrude and SR yield prediction model containing all model terms are provided in Table S4.2, along with respective 96.35% and 85.66% of R^2 (*adj*). It is necessary to mention that excluding the insignificant terms from prediction model does not cause much difference on the value of R^2 (*adj*).

The predictability of the developed models in Table 4.2 (only including significant terms) was assessed by using model feedstocks, which were prepared by mixing five representative components (hemicellulos, cellulose, lignin, lipid and protein) according to the biochemical compositions of actual feedstocks, spent coffee grounds (SCG) and microalgae (MA). The predicted biocrude yield and SR yield, as well as the corresponding experimental results of model and actual feedstocks were presented in Table 4.3.

The experimental biocrude yields from model feedstocks were reasonably close to the predicted biocrude yields and within the confidence interval, which validated the predictability of the biocrude yield model. In terms of SR yield, its prediction model exhibited less accuracy as compared to biocrude yield model. Model feedstock MA had a comparable experimental SR yield with the predicted value (8.54 wt.% vs 11.09 wt.%). This weak predictability can be seen that the R^2_{adj} for SR yield model was much lower than that of biocrude (86.16% vs 95.62%) as shown in supplemental materials Table S4.2.

HTL of actual feedstocks (SCG and MA) were carried out to further evaluate the predictability of developed models. SCG had comparable biocrude yields of predicted and experimental values (22.62 wt.% vs 24.74 wt.%). A similar variation between predicted and experimental biocrude yield (ranging from -0.9 to 4.8 wt.%) was reported by Déniel et al. (2017b), in which blackcurrant pomace, raspberry achenes, brewer's spent grain and grape marc were used as actual feedstocks. However, MA had a lower predicted biocrude yield (21.03 wt.%) than the experimental biocrude yield (28.14 wt.%) in this study. Déniel et al. (2017b) also found that the

predicted biocrude yield for high-protein and low-lipid feedstocks were generally lower than the actual yield when adapting available data in the literature to test the predictability of biocrude yield model that they developed. They inferred that the use of a model monomer (glutamic acid) to represent protein instead of a model polymer has caused the underestimated biocrude yield. However, Deniel's assumption cannot explain our results from MA (high-protein and low-lipid feedstock), as in our study model polymer (soya protein) not monomer was used to represent protein. An alternative explanation for the underestimated biocrude yield could be a remarkable contribution of lipid to the predicted biocrude yield. A slight decrease in lipid percentage would significantly decrease the predicted biocrude yield, but slightly less lipid content in actual feedstock does not necessarily decrease the experimental biocrude yield that much. Therefore, predicted biocrude yield from high protein and low-lipid feedstocks were lower than the experimental yield.

In terms of SR yield from actual feedstocks, MA had a slightly higher predicted yield (11.09 wt.%) than the experimental yield (7.26 wt.%). The experimental SR yield was about 8 wt.% higher than the predicted SR yield observed for SCG. This is more likely to be the case in which for carbohydrate-rich raw feedstocks as fibers are not linked to each other in model mixture, contrarily to real biomass (Déniel et al., 2017b). It is also worth pointing out that the biomass characterization methods, ash content, experimental operation procedures and even the organic solvents used in downstream product recovery might be influential factors for the model development and related predication capability (Li et al., 2017).

Table 4.2 The prediction models (only including significant terms) for biocrude yield and solid residue (SR) yield from hydrothermal liquefaction of model components.

Model components	Soya protein (X_1, wt.%)	Xylan (X_2, wt.%)	Microcrystalline cellulose (X_3, wt.%)	Alkaline lignin (X_4, wt.%)	Soybean oil (X_5, wt.%)
Biocrude yield (wt.%) = $19.88*X_1 + 4.29*X_2 + 12.00*X_3 + 2.13*X_4 + 95.18*X_5 + 59.04*X_2X_5 + 37.94*X_3X_5$					R^2 (*adj*) = 95.62%
SR yield (wt.%) = $5.88*X_1 + 21.04*X_2 + 31.65*X_3 + 39.29*X_4 + 0.57*X_5 - 86.33*X_3X_4$					R^2 (*adj*) = 86.16%

Table 4.3 Predicted and experimental yields of biocrude and solid residue (SR) from hydrothermal liquefaction of model and actual feedstocks.

	Pred biocrude (wt.%)	95% CI for biocrude	Expt biocrude (wt.%)	Pred SR (wt.%)	95% CI for SR	Expt SR (wt.%)
Model SCG	22.62	20.8-24.44	22.24	18.32	16.85-19.80	24.17
Actual SCG			24.74			26.76
Model MA	21.03	17.09-24.97	23.38	11.09	8.33-13.85	8.54
Actual MA			28.14			7.26

Notes: SCG=spent coffee grounds; MA=microalgae; CI=confidence interval
SCG composition: protein=0.15, hemicellulose=0.23, cellulose=0.27, lignin=0.25, lipid=0.10
MA composition: protein=0.72, hemicellulose=0.07, cellulose=0.13, lignin=0.07, lipid=0.01

4.4.2 Optimization of biochemical compositions

Although many attempts have been made to optimize HTL process conditions via experimental design (such as RSM and ANOVA) (Hardi et al., 2017; Song et al., 2017), limited efforts have been contributed to optimize the feedstock biochemical compositions for obtaining high biocrude yield and low SR yield. These developed prediction models in Table 4.2 were further used to generate contour plots, which were utilized to obtain the optimal setting of biochemical compositions that jointly maximize biocrude yield and minimize SR yield. There are two commonly used HTL feedstocks, lignocellulosic and algal biomass. Lignocellulosic biomass is typically rich in carbohydrates with low lipid content and almost no protein. Algal biomass generally contains a high protein content, moderate amount of lipid, and small amount of carbohydrates (especially low in lignin content) (Jones and Mayfield, 2012). The contour plots for biocrude yield and SR yield were therefore generated based on the biochemical compositions of lignocellulosic and algal feedstocks as shown in Fig. 4.1.

From Fig. 4.1a and 4.1b, a maximum of 26 wt.% of biocrude yield and a minimum of 15 wt.% of SR yield can be achieved from the HTL of lignocellulosic feedstocks assuming the feedstock contains 10% lipid and 0% protein. The optimal setting for carbohydrates that provides maximum biocrude yield and minimum SR yield are determined to be 20% hemicellulose, 50% cellulose and 20% lignin. As for HTL of algal biomass, protein content was set at 50% and the absence of lignin was assumed. It can be clearly observed that lipid is a crucial factor for both biocrude yield and SR yield from Fig. 4.1c and 4.1d. A high amount of lipid in algal biomass can remarkably benefit biocrude formation. A biocrude yield of 60 wt.% and SR yield of 2.5 wt.% can be produced from algal biomass that contains 50% protein and 45%-50% lipid. These obtained optimal settings could

be the valuable references for co-liquefaction applications that mix feedstocks with various biochemical compositions.

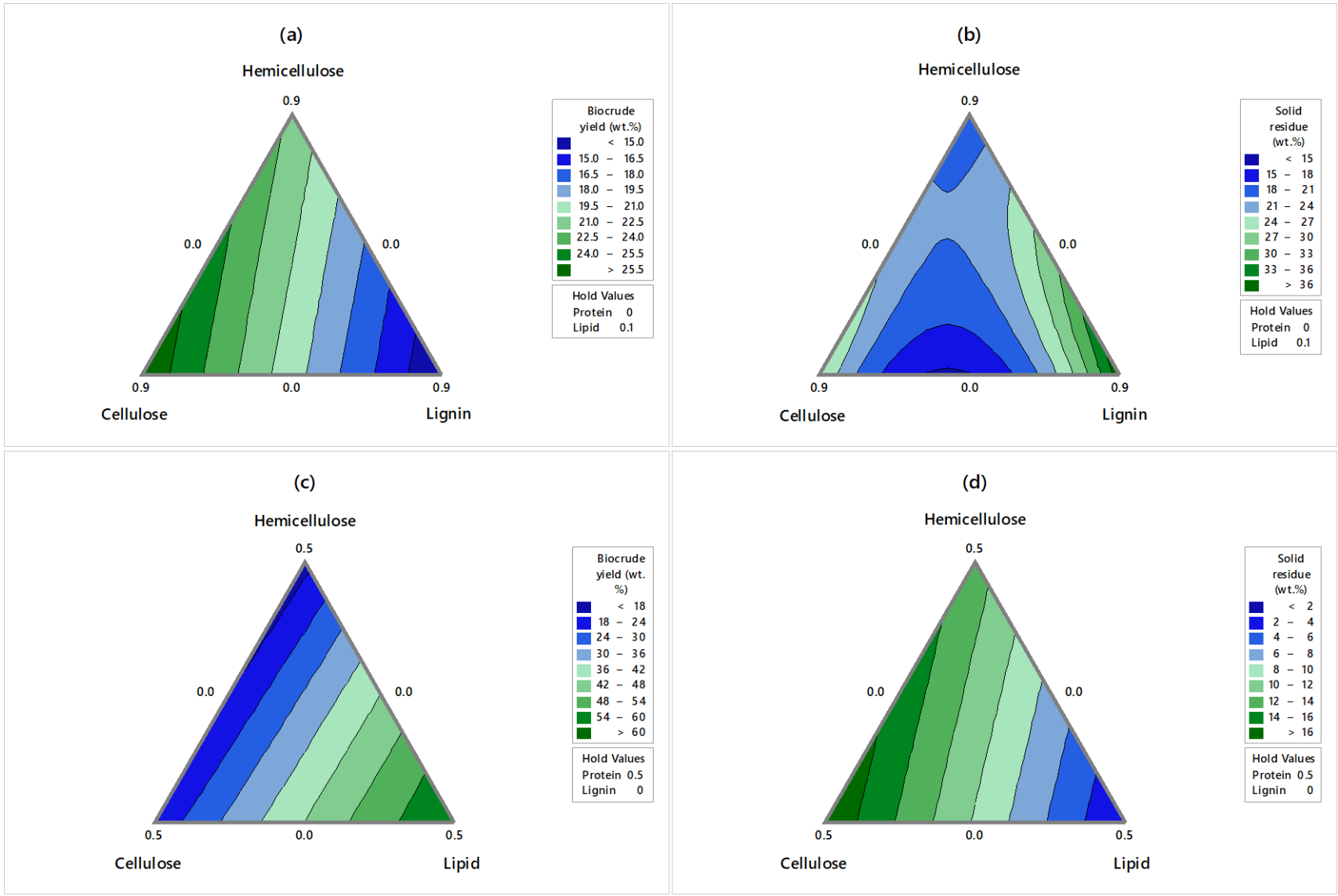

Fig. 4.1 The contour plot for biocrude yield (a) and (c), and solid residue (b) and (d) from hydrothermal liquefaction of lignocellulosic and algal biomass respectively.

4.4.3 Reaction pathways exploration

4.4.3.1 General correlations between studied variables

In addition to the model development and optimization of biochemical composition of feedstock, the chemical compounds of crude bio-oils derived from model component mixtures were quantitatively identified *via* GC-MS and then classified into 11 chemical groups, including acid, ester, amide, amine, diketopiperazine (DKP), aldehyde, ketone, phenol, furan, hydrocarbon, and others. It is notable that only GC-MS detectable chemicals in bio-oil were reported in this study.

The results of these representative chemical groups can be coupled with feedstock biochemical compositions and HTL product yield to investigate the correlations between them. The principle component analysis (PCA) that has been previously implemented in the relevant studies (Madsen et al., 2017a; Pedersen and Rosendahl, 2015) was adapted to gain overview information on the correlations between feedstock chemical compositions, HTL product yields and biocrude chemical groups. The loading plot of PCA was used to explore the above-mentioned correlations as shown in Fig. 4.2.

From Fig. 4.2, it can be observed that cellulose, hemicellulose and lignin was in close relation to the SR yield, suggesting that these three components tended to form solid residue during the HTL process. The presence of lipid favored the biocrude yield, and protein did not exhibit clearly defined correlation with HTL product yield. However, protein was strongly correlated with the formation of amine and DKP that are nitrogen-containing chemical groups. Lipid was featured with fatty acid and ester formation, which were most likely produced by lipid hydrolysis at subcritical water medium. Interestingly, amide was located between lipid and protein in the loading plot of PCA, which suggested the possible chemical reaction to form amide through interaction between fatty acid from lipid and nitrogen-containing compounds from protein. Aldehyde had a moderate correlation with carbohydrates, and the rest of chemical groups seemed not to have well-defined correlation with biochemical compositions. The detailed identification of biocrude chemical compounds were provided in the subsequent sections.

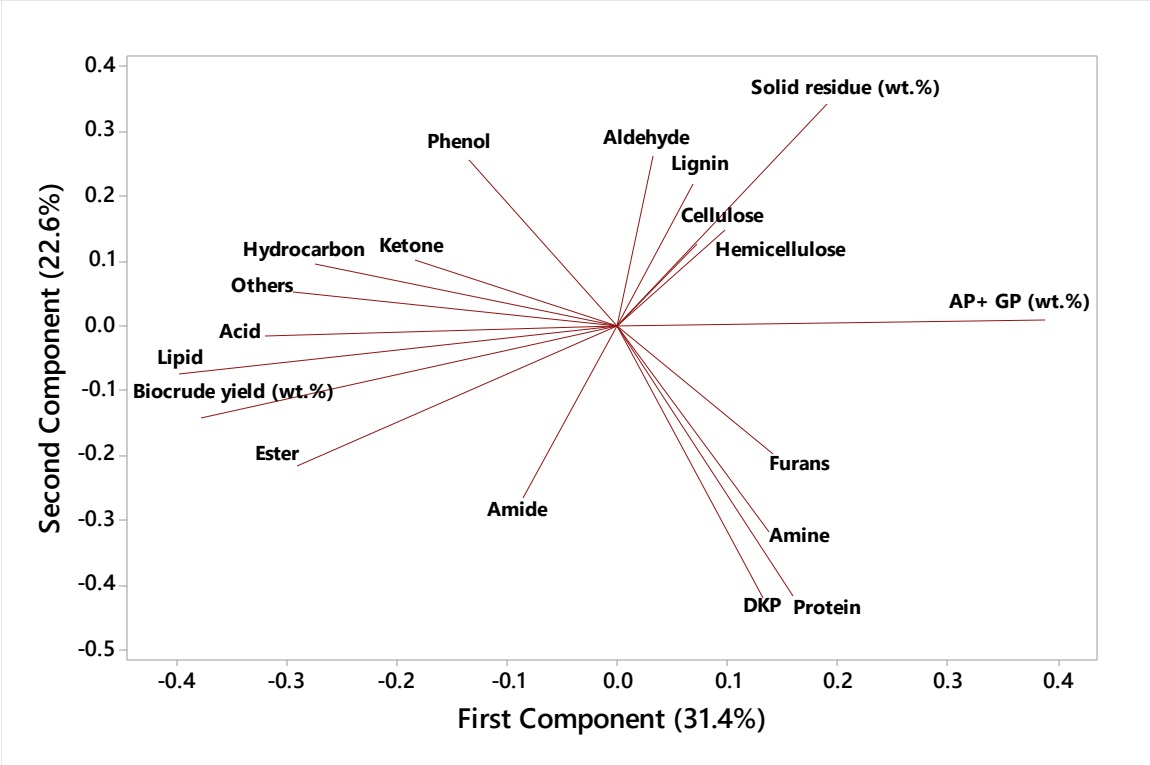

Fig. 4.2 The loading plot from principle component analysis (PCA) for investigating the correlations among feedstock biochemical compositions, product yields and biocrude chemical groups.

4.4.3.2 GC-MS results for HTL of individual model component

The featured chemical compounds in the biocrudes derived from individual model components were first investigated and presented in Table 4.4. These results agree well with a number of studies that have explored and summarized the HTL of individual model components and related mechanisms (Alenezi et al., 2009; Croce et al., 2017; Déniel et al., 2016; Q. Li et al., 2016; Pedersen and Rosendahl, 2015; Peterson et al., 2008; Teri et al., 2014).

Table 4.4 The chemical composition of biocrudes (mg/g of feedstock mass) from hydrothermal liquefaction of individual model components.

	Protein	Lipid	Cellulose	Hemicellulose	Lignin
Acid	-	124.7	0.1	-	-
Aldehyde	-	-	4.6	6.5	1.8
Amide	28	5.5	-	-	0.5
Amine	6.7	0.8	0.2	-	0.6
DKP	30.9	-	-	-	-
Furan	2.5	-	1.4	0.4	-

	Protein	Lipid	Cellulose	Hemicellulose	Lignin
Ester	1.7	151.2	1.3	0.1	1.2
Hydrocarbon	-	6.6	0.7	0.2	-
Ketone	1.6	1.1	3.9	1.3	2.6
Phenol	0.4	7.5	1.8	0.9	16.2
Others	-	2.7	0.4	0.1	0.8

Note: DKP = diketopiperazine

HTL biocrude derived from individual protein was featured with the presence of nitrogen-containing chemicals, such as DKP (30.9 mg/g), amide (28.0 mg/g) and amine (6.7 mg/g). DKP was the most abundant chemical in the protein biocrude, including 3,6-diisopropylpiperazine-2,5-dione, 3,6-bis(2-methylpropyl)-2,5-piperazinedione and pyrrolo-pyrazine-1,4-dione. Amide and amine were represented by methyldodecanamide and pyrrolidine respectively. The formation of DKP from HTL of protein has been reported in Madsen et al. (2017b), Meetani et al. (2010) and Torri et al. (2012a) as well. In particular, Madsen et al. (2017b) suggested that amino acids might be dimerized to form DKP prior to deamination or decarboxylation. They also stated that competition of different reactions could affect the formation or/and degradation of DKP during HTL process, as observed that high-protein feedstock of *C. vulgaris* did not produce DKP, but high-protein feedstock of *N. gaditana* and low-protein feedstock of *L. hyperborean* did.

There were two main chemical groups within lipid biocrude, fatty acid (124.7 mg/g) and ester (151.2 mg/g). It is worthwhile mentioning that monoglycerides were observed in GC-MS chromatogram, and they were classified into the chemical group of ester due to the presence of ester functional group. The representative chemical compounds for lipid biocrude were 9,12-octadecadienoic acid, butyl 9,12-octadecadienoate and 2,3-dihydroxypropyl-9,12-octadecadienoic ester. The product distribution from HTL of lipid highly depended on the HTL reaction conditions (such as temperature and residence time) (Alenezi et al., 2009; Shin et al., 2012). Alenezi et al. (2009a) studied the hydrolysis kinetic of sunflower oil under subcritical water conditions, and reported that hydrolysis reaction of sunflower oil required higher energy to start converting triglycerides into diglycerides as compared to the subsequent steps. The produced fatty acids acted as acid catalysts for the hydrolysis reaction, which positively contributed to the high fatty acid yield. The thermal stability of fatty acids under subcritical water conditions was investigated by Shin et al. (2012), and they found that fatty acids remained stable at 300 °C or below. This was in agreement with our observations. In our study, soybean oil (triglyceride) contained a large

proportion of C18:2 carbon chains, and HTL of soybean oil resulted in fatty acids and esters containing identical C18:2 carbon chains.

Biocrude from HTL of cellulose mainly consisted of aldehyde (4.6 mg/g) and ketone (3.9 mg/g). Furfural was the major compound in aldehyde chemical group, and the presence of 5-hydroxymethyl-furfural (5-HMF) was observed as well. Ketone group was featured by 1-(2-furanyl)-ethanone, 3-methyl-1,2-cyclopentanedione and 2,5-hexanedione. Some benzofurans (such as 7-methyl-benzofuran) were observed as well. Hydrothermal decomposition of cellulose has been well studied, and relevant information can be found in Cantero et al. (2013), Deguchi et al. (2006), Mok et al. (1992) Sasaki et al. (2000) and Yin and Tan, (2012). Similar to cellulose, the HTL biocrude from hemicellulose mainly comprised aldehyde (6.5 mg/g) and ketone (1.3 mg/g). Comparable chemical compositions of xylan and cellulose biocrude have been reported in Gao et al. (2011) and Li et al. (2016). A similar reaction network has been proposed for hydrothermal decomposition of d-xylose (Aida et al., 2010) and cellulose (Cantero et al., 2013). The HTL biocrude from lignin were featured by phenolic compounds (such as guaiacol and creosol), as well as some lignin monomers (such as vanillin, apocynin and 4-hydroxy-3-methoxy-benzenepropanol). These were consistent with other related studies (Wahyudiono et al., 2008; Yong and Matsumura, 2013).

4.4.3.3 Synergistic and antagonistic effects

Synergistic effect (SE) is considered to originate from the positive interaction among breakdown products and intermediates from mixed model components. Antagonistic effect (AE) is an opposite to SE. The SE and AE between model components were investigated to better understand the HTL product distributions and reaction pathways. Analysis of Variance (ANOVA) from mixture design was carried out to evaluate the significance of potentially existing SE and AE on biocrude yield, SR yield and chemical yields. Due to the constraints of statistical model used for mixture design analysis, only the effects from either two components interaction were presented as shown in Table S4.1 (biocrude and SR yield) and Table 4.5 (chemical yields).

The SE of H*Lip and C*Lip on the biocrude yield were observed. Since HTL of lipid was able to generate extremely high biocrude yield, these observed SE benefitted the biocrude production from hemicellulose and cellulose. It was therefore assumed that the degradation intermediates from HTL of lipid (such as free fatty acids) simultaneously interacted with the

degradation intermediates from hemicellulose and cellulose (such as furfural and glyceraldehyde) at subcritical water condition, which eventually positively contributed to the overall biocrude yield. Déniel et al. (2017a) observed the SE on biocrude yield from glucose-linoleic acid mixture as well. A marginally significant SE of C*Lig was observed for biocrude yield, along with an AE on SR yield as illustrated in supplementary materials Table S4.1. Alkaline lignin was used in this study, and C*Lig interaction might drive retro-aldol reactions that are more likely to occur in alkaline media, resulting in a higher biocrude yield and lower SR yield. A similar observation has been reported in Déniel et al. (2017b) that HTL of cellulose with alkaline lignin favored the biocrude yield at the expense of char formation due to the basic environment created by the alkalinity of lignin.

The chemical yields were used to investigate the SE and AE as well. The influence of Maillard reactions between carbohydrates (hemicellulose, cellulose and lignin) and protein on the chemical yields were explored at first. It can be seen from Table 4.5, there were AE of P*H and P*C on the aldehyde and furan yield. As previously mentioned, furfural was the major compound within aldehyde group in the biocrude derived from individual hemicellulose and cellulose. Alkylated benzofurans have been observed for hemicellulose and cellulose biocrude as well. Both furfural and benzofurans were highly reactive at hydrothermal condition, which can simultaneously react with degradation intermediates from protein, giving the AE of P*H and P*C on aldehyde and furan yield. This can be supported by the absence of both furfural and benzofurans in the biocrude derived from the P*H and P*C mixture. Peterson et al. (2010) have provided the kinetic evidence for the existing Maillard reaction between glucose and glycine. Although it is widely accepted that hydrothermal decomposition of lignin favored the phenolic compounds generation instead of aldehyde, the interaction between model protein and lignin has not been previously reported. In this study, the AE of P*Lig was observed for the phenolic compounds and DKP, revealing that the Maillard reaction between protein and lignin occurred through phenolics and DKP interaction.

Apart from Maillard reaction, amide formation from the interaction between protein and lipid has been reported in some studies (Chiaberge et al., 2013; Madsen et al., 2017b). There was also a SE of P*Lip on the amide yield observed in this study. Interestingly, a SE of P*Lip was observed for ester yield as well. This might be attributed to the consumption of free fatty acids during amide formation that drove the lipid hydrolysis toward the direction of free fatty acid and monoglyceride

formation, which positively contributed to the ester yield. The interactions between lipid and carbohydrates in HTL process were rarely studied, however, a SE of H*Lip on the acid yield was observed in this study. It is assumed that the abundantly available degradation intermediates (such as short chain carboxylic acids) from hemicellulose hydrolysis were beneficial for more complete lipid hydrolysis. Specifically, the existing mono-, di-, and tri-glycerides were hydrolyzed more completely into free fatty acids under acidic hydrothermal environment created by the decomposition of hemicellulose.

In terms of C*Lip, there was a synergistic effect on the hydrocarbon yield. Similar observation has been reported in (Déniel et al., 2017a) where the successive reduction of octanoic acid into octane was observed. Ketone yield was also synergistically increased when cellulose and lipid were both present. This was reflected by the formation of a fairly large amount of dihydro-5-tetradecyl-furanone ($C_{18}H_{34}O_2$) and tetrahydro-6-tridecyl-pyran-2-one ($C_{18}H_{34}O_2$) in the biocrude derived from C*Lip mixture. These two compounds were isomers and classified into the ketone group in our study. When cellulose and lipid were both present, these two ketone compounds might be formed through the fragmentation and hydrogenation of fatty acid chains from lipid hydrolysis, followed by the alkylation of hydrocarbon chain on the hydrogenated furfural and furans that originated from cellulose hydrolysis. This assumption can be supported by the AE of C*Lip on the furfural and furan yield. It should be mentioned that the effect of H*Lip and C*Lip on chemical yields were not identical even though hemicellulose and cellulose exhibited comparable biocrude compositions as determined in section 4.4.3.2. No significant Lig*Lip interactive effect on chemical yields was detected, indicating their independent behaviours in the HTL processes.

As for the effects of interactions among carbohydrates (H*C, H*Lig and C*Lig) on chemical yields, AE on aldehyde yield were observed for all of them. When cellulose coexisted with lignin, an AE of C*Lig was observed for phenol yield. It was due to that aldehyde and phenol reacted with each other under hydrothermal condition and resulted in the lower aldehyde and phenol yields but a synergistic increase in the biocrude yield as mentioned previously. The general decomposition pathways of five studied model components, as well as some observed SE and AE were summarized in Fig. 4.3.

Table 4.5 Analysis of variance (ANOVA) p-values and adjusted R^2 for chemical group yields. Significant effects, and whether these effects are synergistic or antagonistic are shown in bold.

Source	Acid	Aldehyde	Furan	Ester	Hydrocarbon	Ketone	Phenol	Amide	Amine	DKP
P*H	0.927	**0.00 (-)**	**0.001(-)**	0.820	0.950	0.908	0.248	0.428	0.109	0.224
P*C	0.543	**0.001(-)**	**0.001(-)**	0.569	0.784	0.289	0.570	**0.015(-)**	0.119	**0.001(-)**
P*Lig	0.304	0.107	**0.001(-)**	0.504	0.462	0.566	**0.030(-)**	0.331	0.764	**0.001(-)**
P*Lip	0.656	0.815	**0.001(-)**	**0.001(+)**	**0.001(-)**	0.939	**0.038(-)**	**0.001(+)**	0.120	0.574
H*Lip	**0.018(+)**	0.336	0.474	0.131	0.620	0.180	0.947	0.921	0.372	0.274
C*Lip	0.087	**0.001(-)**	**0.001(-)**	0.064	**0.009(+)**	**0.003(+)**	0.354	0.223	0.687	0.457
Lig*Lip	0.066	0.772	0.520	0.257	0.075	0.827	0.088	0.542	0.332	0.512
H*C	0.691	**0.001(-)**	**0.001(-)**	0.840	0.533	0.979	0.210	0.959	0.872	0.834
H*Lig	0.527	**0.001(-)**	0.719	0.893	0.715	0.871	0.082	0.845	0.858	0.484
C*Lig	0.871	**0.001(-)**	**0.003(-)**	0.423	0.467	0.327	**0.004(-)**	0.843	0.534	0.779
R^2_{adj}	90.4%	90.3%	92.2%	79.5%	68.7%	27.2%	81.1%	59.1%	50.2%	95.5%

P = Protein, H = Hemicellulose, C = Cellulose, Lig = Lignin, and Lip = Lipid, DKP = diketopiperazine
(+) = synergistic effect; (-) = antagonistic effect

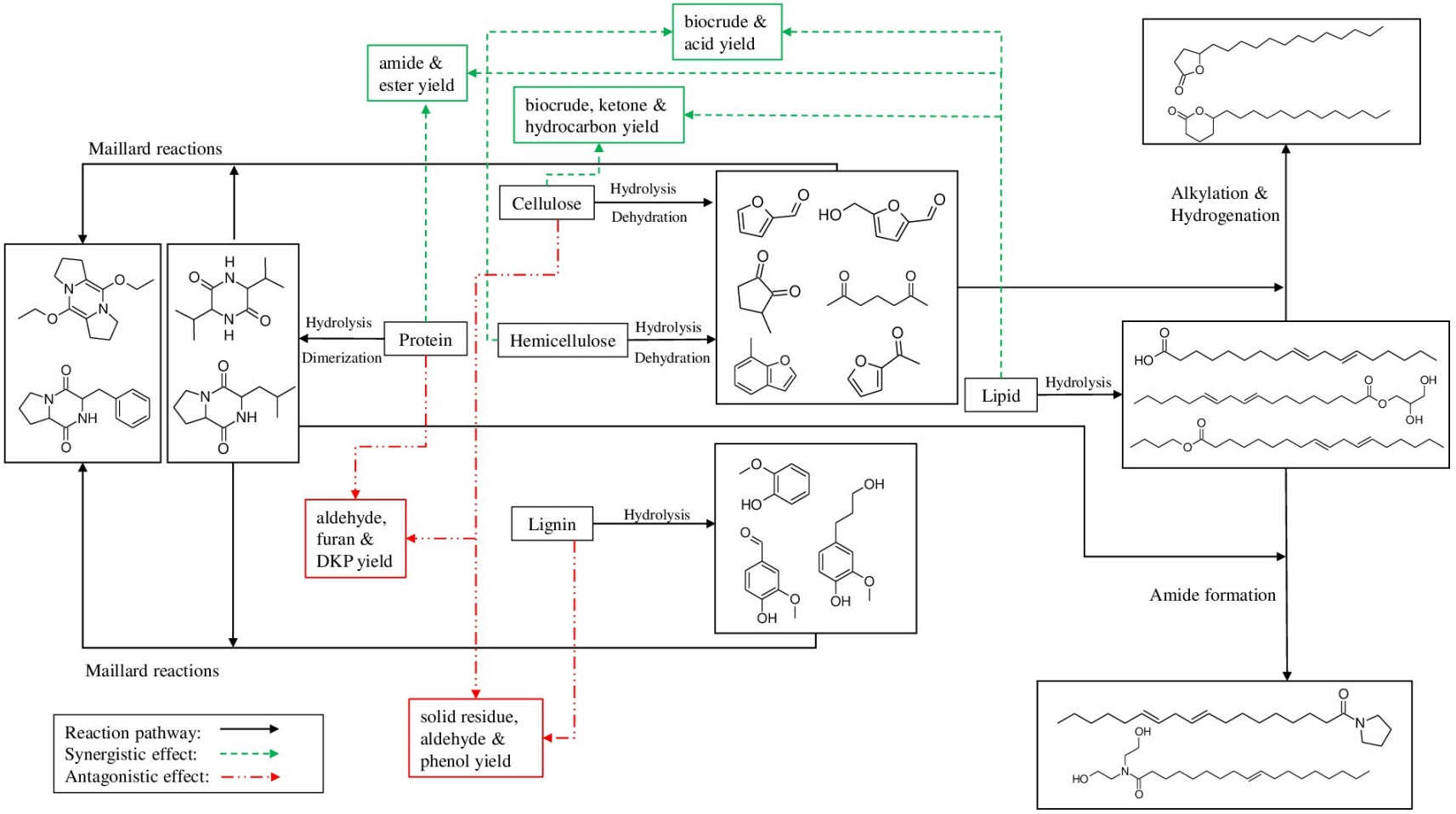

Fig. 4.3 Decomposition pathways of individual model components and related interactions.

4.5 Conclusions

The contribution of individual model components to HTL biocrude and solid residue formation was in the order of: lipid >> protein > cellulose > hemicellulose ≥ lignin, and lignin > cellulose > hemicellulose > protein > lipid respectively. Combining all studied mixtures (individual, binary, ternary, quaternary and quinary), prediction models including interactive terms were developed, for the biocrude yield and SR yield. The model predictability was verified by using the model and actual feedstocks (spent coffee grounds and microalgae). These models were further used to generate the contour plots, in which the optimal biochemical composition settings for jointly maximizing biocrude yield and minimizing SR yield were determined.

The featured chemical groups were identified for biocurdes derived from HTL of individual model components. Aldehyde was the most abundant chemical for both hemicellulose and cellulose biocrude. Lignin biocrude was featured by phenolic derivatives. Protein biocrude mainly consisted of nitrogenous compounds, such as diketopiperazine. Lipid biocrude had high content of fatty acid and ester. The synergistic and antagonistic interactions between pairs of model components on biocrude, SR and chemical yields were explored as well. Both H*Lip and C*Lip exhibited SE on biocrude yield. The interaction between cellulose and lignin (C*Lig) had AE on SR yield. As for the interactive effects on chemical yields, Maillard reactions between protein and carbohydrates, as well as amide formation from protein and lipid interaction were observed. The carbohydrates and lipid interactions had a variety of effects on the acid yield (by H*Lip), hydrocarbon yield and ketone yield (by C*Lip). No significant Lig*Lip interactive effect on chemical yields was observed, indicating their independent behaviours in HTL processes. These results shed light on the interaction between decomposition intermediates in HTL conversion of biomass components.

4.6 Supplemental materials

Table S4.1 The regression coefficients and corresponding p-values for biocrude yield and solid residue (SR) yield prediction model. Significant model terms are shown in bold.

		Biocrude yield (wt.%)		Solid residue yield (wt.%)	
		Coefficient	p-value	Coefficient	p-value
Regression			0.000		0.000
Linear					
	P	19.88	-	5.88	-
	H	4.29	-	21.04	-
	C	12.00	-	31.65	-

		Biocrude yield (wt.%)		Solid residue yield (wt.%)	
		Coefficient	p-value	Coefficient	p-value
	Lig	2.13	-	39.29	-
	Lip	95.18	-	0.57	-
Quadratic					
	P*H	33.20	0.060	1.07	0.935
	P*C	14.95	0.380	-21.34	0.118
	P*Lig	-18.69	0.275	17.48	0.196
	P*Lip	24.35	0.159	-8.36	0.530
	H*C	-1.41	0.933	12.41	0.354
	H*Lig	20.42	0.234	0.22	0.987
	H*Lip	59.04	**0.002**	-13.85	0.302
	C*Lig	32.86	0.062	-86.33	**0.000**
	C*Lip	37.94	**0.034**	-4.74	0.721
	Lig*Lip	1.94	0.908	8.09	0.543
R^2		97.81%		91.39%	
R^2 (*adj*)		96.35%		85.66%	

Notes: P = Protein, H = Hemicellulose, C = Cellulose, Lig = Lignin, and Lip = Lipid

Table S4.2 The prediction models (including all model terms) for biocrude yield and solid residue (SR) yield from hydrothermal liquefaction of model components.

Model components	Soya protein (X_1, wt.%)	Xylan (X_2, wt.%)	Microcrystalline cellulose (X_3, wt.%)	Alkaline lignin (X_4, wt.%)	Soybean oil (X_5, wt.%)	
Biocrude yield (wt.%) = $19.88*X_1 + 4.29*X_2 + 12.00*X_3 + 2.13*X_4 + 95.18*X_5 + 33.20*X_1X_2 + 14.95*X_1X_3 - 18.69*X_1X_4 + 24.35*X_1X_5 - 1.41*X_2X_3 + 20.42*X_2X_4 + 59.04*X_2X_5 + 32.86*X_3X_4 + 37.94*X_3X_5 + 1.94*X_4X_5$						R^2 (*adj*) = 96.35%
SR yield (wt.%) = $5.88*X_1 + 21.04*X_2 + 31.65*X_3 + 39.29*X_4 + 0.57*X_5 + 1.07*X_1X_2 - 21.34*X_1X_3 + 17.48*X_1X_4 - 8.36*X_1X_5 + 12.41*X_2X_3 + 0.22*X_2X_4 - 13.85*X_2X_5 - 86.33*X_3X_4 - 4.74*X_3X_5 + 8.09*X_4X_5$						R^2 (*adj*) = 85.66%

4.7 Transition section

Chapter 4 used five representative biomass model components along with statistical mixture design to develop the prediction model for HTL product yield. Meanwhile, the chemical interactions between biomass model components were assessed to better understand the reaction pathways during HTL of biomass. However, the prediction model development and reaction pathways exploration in Chapter 4 were conducted under a constant HTL processing condition. If a variety of HTL process variables were incorporated into the prediction model, this would allow broader applications of prediction models. Moreover, how the chemical interactions between

biomass model components are influenced by changing HTL process variable has been rarely investigated. Therefore, Chapter 5 aims to develop more advanced prediction models for the prediction of HTL product yield *via* a mixture design of biomass model components coupled with process variables, as well as to evaluate the impact of process variables on the chemical interactions between biomass model components.

Chapter 5: Advanced Models for the Prediction of Product Yield in Hydrothermal Liquefaction *via* a Mixture Design of Biomass Model Components Coupled with Process Variables

Contribution statement:

I was responsible for raw materials collection, experiment design and conduction, part of data analysis and manuscript preparation.

5.1 Abstract

This chapter developed advanced models for the prediction of hydrothermal liquefaction (HTL) products yield *via* a mixture design of biomass model components coupled with process variables. The model components used were soya protein, a mixture of cellulose and xylan, alkaline lignin and soybean oil for a representative of protein, saccharide, lignin and lipid respectively. Reaction temperature (270-320 °C), time (5-20 min) and mass ratio of water/feedstocks (6:1-12:1) were chosen as the process variables of interest. The developed predictive models for biocrude yield and solid residue (SR) yield showed high accuracy (R^2_{adj} of 94.6% and 93.2%, respectively), and were further validated using modelled feedstock and actual feedstock. These models can be used either to optimize HTL conditions when feedstock is known, or to optimize the composition of feedstock when reaction conditions are given. It was also observed that within the experimental design range, relatively mild HTL conditions eliminated alkaline lignin-lipid interaction and protein-lipid interaction, and thus enhanced biocrude formation; while more severe HTL conditions were preferred to reduce solid residue formation through promoting protein-saccharide interaction and saccharide-alkaline lignin interaction.

5.2 Introduction

Recently, the development of quantitative models for the prediction of HTL product yield is gaining interest. As the product yield in a HTL process is greatly influenced by process variables such as reaction temperature, time, mass ratio of water to feedstock (Akhtar and Amin, 2011), a

statistical tool (central composite design, CCD) has been widely used to predict product distributions and to obtain optimal reaction settings (Gan and Yuan, 2013; Zhu et al., 2018; Hardi et al., 2017). For instance, Hardi et al. (2017) recently applied a face centered central composite design of HTL temperature, time and feedstock concentration to predict the yield of HTL products from sawdust and their properties as well. However, these kind of prediction models consist of only model terms for process variables, and they only work well for the specific feedstock used in the corresponding studies.

The HTL product yield is also highly associated with the nature of the feedstock used in the HTL process. Several attempts, therefore, have been made to develop predictive models based on the biomass composition, which allows the estimation of HTL product yield for various types of feedstock (Yang et al., 2018b; Lu et al., 2018). Although some progress was made in modelling HTL product yield based on the biomass composition, these prediction models did not take the process variables as model input. These models are only able to predict HTL products' yield for feedstocks under a specific set of reaction conditions. Kinetics-based modelling of HTL reaction networks advanced this research (Sheehan and Savage, 2017; Valdez et al., 2014). Because kinetics-based models can predict HTL product yields at different reaction temperature/time based on feedstock composition, and such models have good prediction accuracy and are also more useful (Valdez et al., 2014; Vo et al., 2016). However, the process variables incorporated into kinetics-based models were limited to reaction temperature and time, excluding the mass ratio of water to feedstock, which was also a critically influential variable in an HTL process. Thus, it is necessary to develop models that incorporate not only the biochemical composition of feedstock but also the most important process variables. Mixture design of using biomass model components along with various process variables holds promise for broadly useful prediction of HTL product yield. A comparison of different modelling approaches is presented in Table 5.1.

Table 5.1 A comparison of different prediction models for HTL product yield.

Types of prediction models	Considering composition of feedstock	Incorporating process variables?	References
CCD for process variables	No, only works for a specific feedstock	Yes, a variety of process variables	Hardi et al. (2017)
Model compounds	Yes, works for a variety of feedstock	No, at a specific HTL condition	Lu et al. (2018)
Kinetic model	Yes, works for a variety of feedstocks	Yes, but only limited to reaction temperature and time	Valdez et al. (2014)

Types of prediction models	Considering composition of feedstock	Incorporating process variables?	References
Mixture design + process variables	Yes, works for a variety of feedstocks	Yes, a variety of process variables	current study

Note: CCD = central composite design

In addition to the development of advanced prediction models for HTL product yield, it is essential to better understand the HTL product formation pathways under different reaction conditions. HTL of biomass is a complicated process involving many kinds of chemical interactions between feedstock's biochemical components, such as Maillard reaction between carbohydrates and protein and amide formation between lipid and protein (Gai et al., 2015b). These interactions were also influenced by varying process variables. Although this is an interesting and fundamental subject, it was rarely investigated.

The objective of this chapter is to develop advanced prediction models for HTL product yield by using a mixture design of both process variables and feedstock composition. Soya protein, a mixture of cellulose and xylan, alkaline lignin and soybean oil were chosen as representative model components for protein, saccharide, lignin and lipid respectively. The process variables studied included reaction temperature (270-320 °C), time (5-20 min) and mass ratio of water/feedstocks (6:1-12:1). The developed prediction models will be useful to evaluate the potential of various biomass feedstock and their mixtures under different HTL conditions, opening the way to co-process all available bio-resources. In addition, the impact of process variables on HTL of individual model components as well as how the interactions between model components were affected by changing process variables were investigated. These results will be valuable for exploring the reaction pathways of product formation under different liquefaction conditions.

5.3 Materials and methods

5.3.1 Materials

Please refer to section 4.3.1, and saccharide was obtained by evenly mixing (50/50 by mass) microcrystalline cellulose with hemicellulose (corn core xylan supplied by TCI America).

5.3.2 Experiment operation procedures

5.3.2.1 Hydrothermal liquefaction process

Please refer to section 4.3.2.1, and the studied variables with coded levels were presented in Table 5.2. The representative heating profile was provided in supplemental file (Fig. S5.1).

Table 5.2 Hydrothermal liquefaction (HTL) process variables and coded levels.

Process variables	Levels		
	-1	0	+1
Temperature (°C)	270	295	320
Time (min)	5	12.5	20
Mass ratio of water to feedstock	6:1	9:1	12:1

5.3.2.2 Biocrude recovery process

Please refer to section 4.3.2.2.

5.3.2.3 Biocrude characterization

Please refer to section 4.3.2.3.

5.3.3 Experiment design and data analysis

A Simplex-Centroid mixture design of four model components (protein, saccharide, lignin and lipid), coupled with three process variables (reaction temperature, time and mass ratio), was created and analyzed using Minitab Version 18.1 software (Minitab Inc., State College, PA, USA). Half fractional design for three process variables led to a total of 4 combinations. For each combination of the process variables, the Simplex-Centroid mixture design has 20 runs, resulting in 80 runs (4×20) in total. This design is a special class of response surface experiments that uses different proportions of the ingredients or components to develop mathematical models, following by the optimization of studied subjects; and is commonly used in many industrial product design and development activities. The biocrude yield and SR yield were selected as the response variables. Complete analyses of these response variables were conducted using the methods described in Section 11.6 of Montgomery, (2017).

The analyses included verifying the validity of normal distribution and constant variance assumptions on the error terms. Independence assumption was met due to the randomization of the run orders. This was followed by testing the significance of each model term shown in Table S5.1, constructing contour plots, and performing response optimization to identify the optimum proportions that jointly maximize biocrude yield and minimize SR yield.

5.4 Results and discussion

5.4.1 Model development and optimization

5.4.1.1 Prediction model for biocrude yield and solid residue yield

It has been widely reported that HTL of carbohydrate (including saccharide and lignin) tended to generate less bio-oil and more solid residue as compared to that of protein and lipid (Biller and Ross, 2011; Peterson et al., 2008; Teri et al., 2014). Our experimental results complimented these previous studies. As observed, the biocrude yield (wt.%) from HTL of pure model components was in the following order, lipid (97.8 ± 1.6) >> protein (18.4 ± 3.0) > saccharide (9.9 ± 0.7) > lignin (2.5 ± 0.7); while for solid residue yield, the order was lipid (0.7 ± 0.2) < protein (4.7 ± 0.4) << saccharide (30.9 ± 4.1) ≈ lignin (30.5 ± 4.1).

HTL of individual, binary, ternary and quaternary mixtures of model components at different reaction conditions (270 ^{o}C vs. 320 ^{o}C, 5 min vs. 20 min and 6:1 vs. 12:1) were carried out to develop prediction models for biocrude yield and SR yield. The Analysis of Variance (ANOVA) for biocrude yield and SR yield are presented in supplementary materials Table S5.1. The yield prediction models that include only significant model terms are provided in Table 5.3. In Supplementary materials Table S5.2, the models including all model terms are also presented. The R^2 (*adj*) for biocrude yield and SR yield was 94.6% and 93.2% respectively as shown in Table 5.3, which indicated very high strength of the model in describing the relationship. It is worthwhile to mention that excluding the insignificant terms in prediction model does not cause much difference in the value of R^2 (*adj*), as can be seen when comparing the R^2 (*adj*) in Table 5.3 and Table S5.2.

Model validation was performed using model feedstock and actual feedstock. The model feedstock was prepared by mixing four model components according to the biochemical composition of the actual feedstock, spent coffee grounds (SCG). SCG has been identified as a desirable HTL feedstock in our previous study (Yang et al., 2016b), and the composition of SCG used was 15% of protein, 50% of saccharide, 25% of lignin and 10% of lipid. Three HTL conditions were included to liquefy SCG in hot compressed water such as 270 °C, 5 min, 6:1; 295 °C, 12.5 min, 9:1; and 320 °C, 20 min and 12:1. The predicted and experimental yields for HTL of model and actual feedstock under different HTL conditions are presented in Table 5.4. Comparing the experimental yield to the predicted value in the HTL of model SCG, the difference in yields was in a range of 2-6 wt.%, indicating a moderate to good prediction performance under

various reaction conditions. HTL of actual SCG were carried out to further assess the predictability of the developed models. It was observed that although HTL of actual SCG had a higher biocrude yield than that of model SCG and predicted values, they were within the prediction interval. HTL of actual SCG gave a higher SR yield than the predicted value of model SCG. This is most likely because the actual SCG contained 75% of cross-linked carbohydrates (hemicellulose, cellulose and lignin), but they were not inherently linked to each other in the model SCG (simply a mixture of hemicellulose, cellulose and lignin), resulting in less solid residue formation from HTL of model SCG. Such observation, namely lower SR yields from model feedstocks were reported by Déniel et al. (2017b) as well, in which HTL of food processing residues were conducted at 300 °C, 60 min and 15 wt.% of feedstock loading.

Overall, within the experimental range in this study, the models developed had a high R^2 (*adj*) and they are adequate for the prediction of biocrude yield and SR yield from HTL of SCG under different reaction conditions. Future efforts are needed to further verify the applicability of the models using a broad spectrum of feedstock and HTL conditions.

Table 5.3 The prediction models (only including significant model terms) for biocrude yield and solid residue (SR) yield from hydrothermal liquefaction of model components. *Coefficients are calculated for coded process variables.*

	Biomass model components				Process variables			
	Soya protein (X_1, wt.%)	Saccharide (X_2, wt.%)	Alkaline lignin (X_3, wt.%)	Soybean oil (X_4, wt.%)	Temperature (X_5, °C)	Time (X_6, min)	Mass ratio of Water/feedstock (X_7)	
Biocrude yield (wt.%) = $19.99*X_1 + 9.75*X_2 + 1.75*X_3 + 97.37*X_4 - 33.1*X_1X_4 + 26.4*X_2X_3 + 59.8*X_2X_4 - 65.6*X_3X_4 - 25.46*X_3X_4X_5 - 18.93*X_1X_4X_6 - 38.63*X_1X_4X_7$								R^2 (*adj*) = 94.6%
SR yield^0.5 (wt.%) = $2.184*X_1 + 5.396*X_2 + 5.514*X_3 + 0.870*X_4 + 6.025*X_1X_3 - 2.051*X_2X_3 + 4.349*X_3X_4 + 0.455*X_3X_5 - 2.957*X_1X_2X_5 - 3.396*X_2X_3X_5 - 1.838*X_1X_2X_6 - 0.339*X_2X_7 - 0.359*X_3X_7$								R^2 (*adj*) = 93.2%

Note: solid residue yield (wt.%) was statistically transformed by square root to achieve satisfactory normality and constant variance.

Table 5.4 The predicted and experimental yields from model feedstock and actual feedstock at three different hydrothermal liquefaction conditions.

		270 °C, 5 min, 6:1	295 °C, 12.5 min, 9:1	320 °C, 20 min, 12:1
Biocrude (wt.%)	Predicted value	23.7	22.2	20.7
	Prediction interval	12.4 – 35.1	10.9 – 33.6	9.4 – 32.1
	HTL of model SCG	20.1 ± 0.5	24.6 ± 1.4	24.3 ± 1.2
	HTL of actual SCG	23.3 ± 3.0	28.1 ± 1.0	26.3 ± 0.7
SR (wt.%)	Predicted value	30.2	20.9	13.2
	Prediction interval	22.4 – 39.2	14.4 – 27.4	8.3 – 19.4
	HTL of model SCG	32.9 ± 2.9	23.1 ± 0.9	17.9 ± 0.5
	HTL of actual SCG	36.2 ± 2.2	25.0 ± 0.2	21.1 ± 0.4

Note: SR = solid residue; HTL = hydrothermal liquefaction; SCG = spent coffee grounds

5.4.1.2 Optimization of process variables

The developed prediction models shown in Table 5.3 were further used to generate contour plots to obtain the optimal setting of process variables that jointly maximize biocrude yield and minimize SR yield. The biochemical composition of SCG (15% of protein, 50% of saccharide, 25% of lignin and 10% of lipid) was used in this case study. The biocrude and SR yield contour plots including process variables are shown in Fig. 5.1a-f, in which Fig. 5.1a-1b, 5.1c-1d and 5.1e-1f present the contour plot of temperature *vs* time, temperature *vs* mass ratio, and time *vs* mass ratio respectively.

It was observed from Fig. 5.1a-1b that when the mass ratio of water/feedstock was set at the center value of 9:1, a maximum biocrude yield of 22.8 wt.% was obtained in HTL of SCG at a temperature of 270-280 °C and a reaction time between 5 -11 min; however, under such a HTL condition, a high solid residue (about 25.0 wt.%) was generated. To obtain less SR formation, a more severe HTL condition is required, such as a higher reaction temperature of 310-320 °C and longer reaction time of 12-20 min. Similar patterns were observed from the contour plot of temperature *vs* mass ratio (Fig. 5.1c-1d) and time *vs* mass ratio (Fig. 5.1e-1f), where biocrude formation in HTL of SCG was favored at milder conditions, and more severe HTL conditions were required to attain a relatively low SR yield. Therefore, the optimal reaction setting for satisfactory

biocrude yield and SR yield from HTL of SCG was determined to be temperature of 290-300 °C, time of 10-15 min and mass ratio (water/feedstock) of 8:1-10:1. This was supported by the HTL of actual SCG as presented in Table 5.4, in which a HTL condition of 295 °C, 12.5 min and 9:1 resulted in high biocrude yield (28.1 wt.%) with a relative low solid residue formation (25.0 wt.%). It is also worthwhile to mention that the optimization of process variables for HTL of other feedstocks (other than SCG used in this study) can be performed using the developed prediction models, as long as the biochemical composition of the feedstock is known.

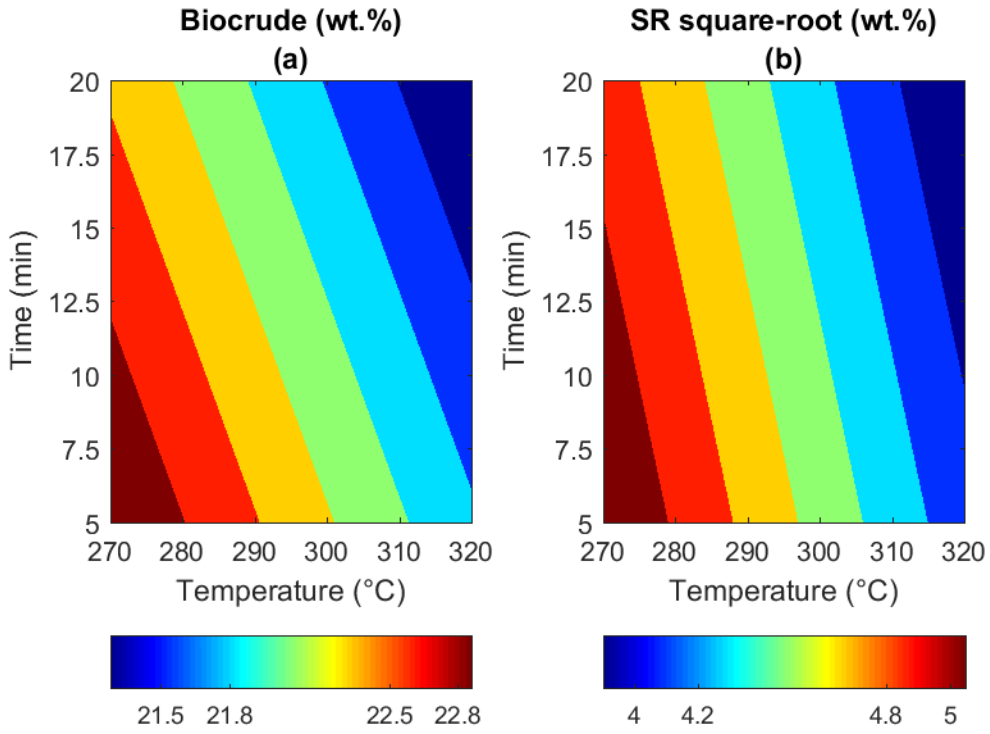

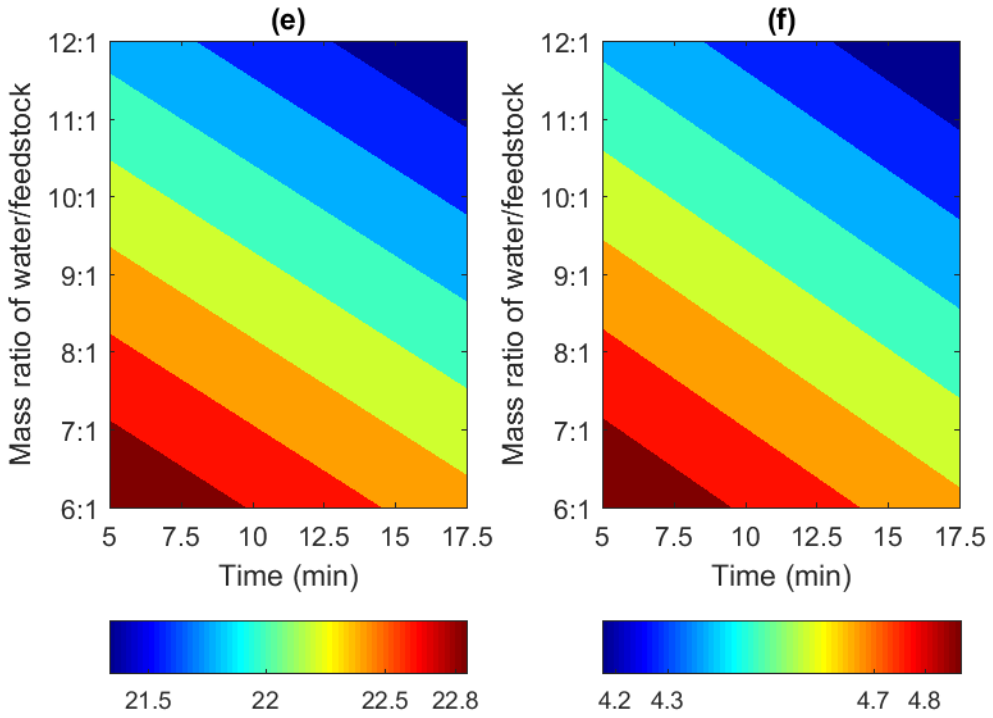

Fig. 5.1 Contour plots for biocrude yield (a), (c) and (e), and solid residue (SR) (b), (d) and (f) from hydrothermal liquefaction of spent coffee grounds. Square root values of SR yiled are shown in the plots.

5.4.1.3 Optimization on biochemical composition of feedstock

In addition to the optimization of process variables *via* the developed prediction models present in Table 5.3, the models can also be used to optimize feedstock's biochemical composition at a given HTL condition. The response optimizer in Minitab 18.1 software and the partial model in Table 5.3 was utilized to obtain the optimum feedstock composition. The studied HTL conditions were 1) 270 °C, 5 min and 6:1, and 2) 320 °C, 20 min and 12:1. The respective optimization on feedstock's biochemical composition are shown in supplementary material Fig. S5.2 and Fig. S5.3.

From Fig. S5.2, when the biocrude yield was targeted at 40 wt.% with a minimum amount of SR formation, an optimal biochemical composition of 70.5% protein, 8.1% saccharide, 0% lignin and 21.4% of lipid was suggested under HTL condition of 270 °C, 5 min and 6:1. It is notable that this suggested optimum feedstock composition was reasonably identical to most of

microalgae feedstocks, which have been widely reported to contain high protein content, moderate amount of lipid and a small amount of carbohydrate (Chen et al., 2013; Jones and Mayfield, 2012; Pragya et al., 2013). Thus, microalgae feedstocks would be sufficiently decomposed at HTL condition of 270 °C temperature, 5 min reaction time and 6:1 mass ratio of water/feedstock, to obtain 40.5 wt.% of biocrude yield and only 6.1 wt.% of SR yield as estimated by the models. These results were in good agreement with those reported in other relevant studies (Koley et al., 2018; López Barreiro et al., 2013). From Fig. S5.3, an optimal biomass composition of 12.0% of protein, 30.3% of saccharide, 22.0% of lignin and 37.7% of lipid was recommended to obtain 39.8 wt.% of biocrude yield and 10.3 wt.% of SR yield at HTL condition of 320 °C temperature, 20 min reaction time and 12:1 mass ratio of water/feedstock. This indicated that more severe HTL conditions were required to decompose carbohydrate-rich feedstocks to obtain high biocrude yield and minimize solid residue formation.

In general, the developed prediction models performed well on the optimization of HTL process variables when the biochemical composition of feedstock is given, and/or the optimization of biochemical compositions at a given HTL condition. Therefore, the comprehensive and advanced models incorporating both feedstock and operation terms will be a useful tool to predict the yield of solid residue and biocrude derived from various feedstocks under different HTL reaction conditions.

5.4.2 Effects of process variables on individual model component

In order to better understand biomass decomposition pathways at varied HTL conditions, it is necessary to examine the effect of process variables on HTL of individual model components, including protein, saccharide, alkaline lignin and lipid. The biocrude and SR yield from HTL of individual model components at varied conditions are presented in Fig. S5.4 in supplementary material file. It can be clearly observed from Fig. S5.4a that HTL of pure lipid generated an extremely high biocrude yield (>95.8 wt.%) along with a negligible amount of SR, and this is in agreement with other reported studies (Déniel et al., 2017b; Teri et al., 2014). Within the experimental design range, changing reaction temperature, time and mass ratio of water/feedstock did not lead to large difference in yields.

HTL of pure protein had the second highest biocrude yield (14.4-22.3 wt.%) among the four studied model components, along with the low and consistent SR yield (about 5 wt.%) under varied HTL conditions as shown in Fig. S5.4b. Elevating the HTL temperature from 270 °C to

320 °C increased the biocrude yield from 14.4 wt.% to 22.3 wt.%, implying that a higher temperature might enhance the recombination of protein degradation intermediates in hot compressed water to form biocrude. Yang et al. (2015a) also reported a slight increment in biocrude yield from the HTL of pure protein when increasing temperature from 260 °C to 300 °C. About 10 wt.% of biocrude yield was obtained from the HTL of pure saccharide (Fig. S5.4c), but the corresponding SR yield (about 30 wt.%) was much higher than that of pure lipid and protein. A decline in SR yield from 37.2 wt.% to 24.6 wt.% was observed for the HTL of pure saccharide when increasing mass ratio of water/feedstock from 6:1 to 12:1. This is due to the fact that the presence of a large amount of water promoted saccharide hydrolysis into water-soluble chemicals and therefore eliminated solid residue formation (Yin et al., 2010). As for the HTL of alkaline lignin, a very low biocrude yield (<5 wt.%) but a high SR yield were observed under different HTL conditions as shown in Fig. S5.4d. HTL of alkaline lignin at 320 °C resulted in a higher SR yield (36 wt.%) than that of at 270 °C (24.9 wt.%) A similar observation was reported by Yuan et al. (2010), and they stated that a higher reaction temperature favored the phenolic compounds combination and increased solid residue formation *via* the condensation reaction of the degradation intermediates.

5.4.3 Effects of process variables on the interactions between model components

For the biocrude formation, three significant interaction effects (lignin*lipid*temperature, protein*lipid*time and protein*lipid*mass ratio) were identified by ANOVA as shown in Table S5.1. As for the solid residue formation, the effects of protein*saccharide*temperature, saccharide*lignin*temperature and protein*saccharide*time interaction were determined to be significant.

5.4.3.1 Alkaline lignin-lipid interaction on biocrude

Fig. 5.2 shows the influence of HTL temperature on the interaction between alkaline lignin and lipid during biocrude formation. A general trend that can be clearly observed, that is, increasing feedstock's alkaline lignin content decreased the biocrude yields when holding the lipid content at a constant level (either 12.5%, 33.3% or 50%). When a feedstock contains 50% of lipid, increasing alkaline lignin content at 270 ºC led to a decrease in biocrude yield from 52.5 wt.% to 35.5 wt.%; however, a much larger decrease in biocrude yield (from 55.9 wt.% to 17.2 wt.%) was observed at temperature of 320 ºC. A greater decrement in biocrude yield was observed for 320 ºC (vs. 270 ºC) when the feedstock lipid content was 33.3% and 12.5% as well. We hypothesized that

a higher reaction temperature (320 ºC) could hydrolyze lipid more readily and generate a large amount of free fatty acids, which reacted with alkaline cations (such as K^+ from alkaline lignin) to form more soap, resulting in a much lower biocrude yield at 320 ºC (17.2 wt.%). Holliday et al. (1997) used subcritical water to hydrolyze soybean, linseed and coconut oil, and reported that greater than 97% conversion (to free fatty acids) were obtained at temperature of 260-280 °C and reaction time of 15-20 min. Alenezi et al. (2009) provided kinetics evidence on sunflower oil hydrolysis under subcritical conditions, and stated that increasing temperature promoted the hydrolysis rate of sunflower oil. Such produced free fatty acids are known to form undesirable saponified products in the presence of alkali cations, as widely reported in oleochemical industry and biodiesel production field (King et al., 1999;Yang et al., 2016b).

The above-mentioned observations should raise the awareness of using basic or/and alkaline catalysts (such as KOH, NaOH and K_2CO_3) in hydrothermal conversion of lipid-rich biomass at high temperature (> 300 ºC). This was in agreement with Xu et al. (2014). They investigated the biocrude production from planktonic algae biomass by catalytic HTL with NaOH as a catalyst, and reported that with an increase in reaction temperature, the liquefaction yield increased first and then started decreasing when temperature was above 300 ºC. Zhu et al. (2015) carried out the HTL of barley straw with alkali catalyst (K_2CO_3) at different temperature (280-400 ºC), and stated that low temperature favored the formation of biocrude, with a maximum yield of 34.9 wt.% at 300 ºC. Ross et al. (2010) studied the influence of various alkali (KOH and $NaCO_3$) and organic acids (acetic acid and formic acid) on the yield of biocrude from microalgae at the reaction temperature ≥ 300 ºC, and they reported that the biocrude yield was higher when using an organic acid catalyst than alkali catalyst.

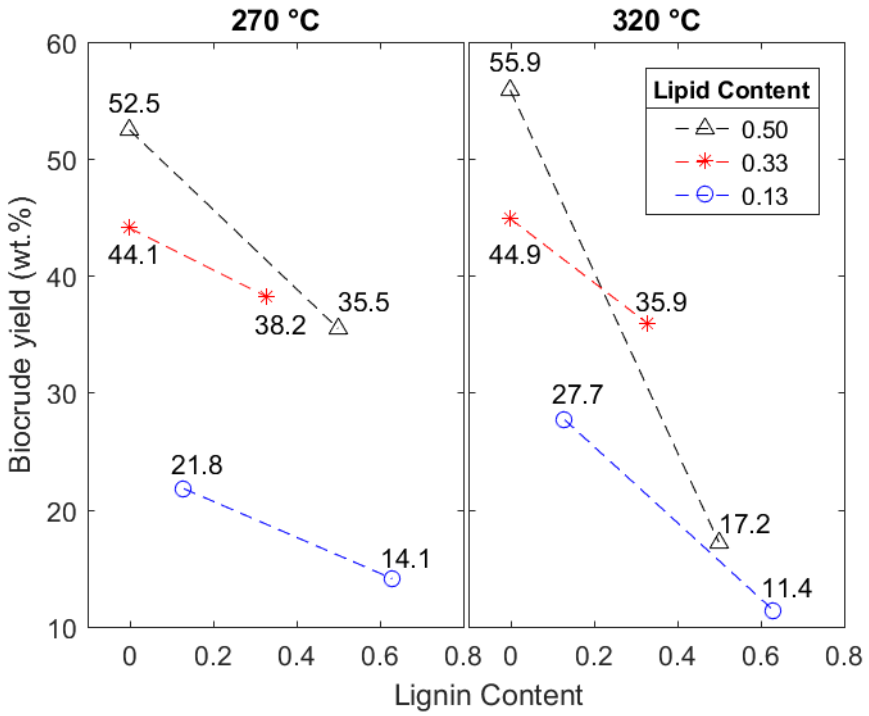

Fig. 5.2 Influence of temperature (270 ºC vs. 320 ºC) on alkaline lignin and lipid interaction during biocrude formation.

5.4.3.2 Protein-lipid interaction on biocrude

The impact of reaction time (5 min vs. 20 min) on the interaction between protein and lipid are presented in Fig. 5.3. As for the feedstock containing 50% of lipid, increasing protein content bumped up the biocrude yield (from 43.5 wt.% to 51.1 wt.%) at a reaction time of 5 min; a long reaction time (20 min) led to an opposite trend of the biocrude yield, decreasing from 46.0 wt.% to 39.4 wt.% when increasing feedstock protein content. This suggests that reaction time had a critical influence on biocrude formation involving protein and lipid interaction, and a shorter reaction time (5 min) was preferred to obtain relatively high biocrude yields. When the lipid content of feedstock was lower than 50 wt.%, the influence of reaction time was negligible.

The lipid and protein interaction in a hydrothermal medium has been previously reported to produce fatty amides that are highly soluble in aqueous phase (Chiaberge et al., 2013; Madsen et al., 2017b). Specifically, fatty amides can be formed through the chemical reactions between lipid hydrolysis products (fatty acids) and protein decarboxylation products (ammonia and amine) under hydrothermal conditions. It is well known that hot compressed water can easily break protein peptide bonds to generate amino acids, which subsequently degrade through decarboxylation and deamination processes (Peterson et al., 2008). Klingler et al. (2007) conducted the kinetic study of

amino acid decomposition, and reported that about 50% of starting amino acids (glycine and alanine in this case) degraded in 5-15 seconds at 350 °C and 34 MPa. Sato et al. (2004) also illustrated that hot compressed water can rapidly decompose amino acids (within 2-3 min) into ammonia, amines and various organic acids. The HTL reaction time applied in this study was 5 min and 20 min, in which should be long enough to readily decompose protein. However, a reaction time of 5 min was not capable of hydrolyzing vegetable oil into fatty acids readily as reported by Alenezi et al. (2009). At 300 °C, only about 10 mol.% of fatty acids were obtained after 5 min, but more than 80 mol.% of fatty acids were generated after 20 min (Alenezi et al., 2009). Combining these reported studies and our experimental data, we concluded that a shorter reaction time (5 min) was desirable to gain more biocrude from model protein-lipid mixture; this is likely that a shorter reaction time led to incomplete lipid hydrolysis and therefore less rapid formation of water-soluble fatty amides, ultimately resulting in higher biocrude yield.

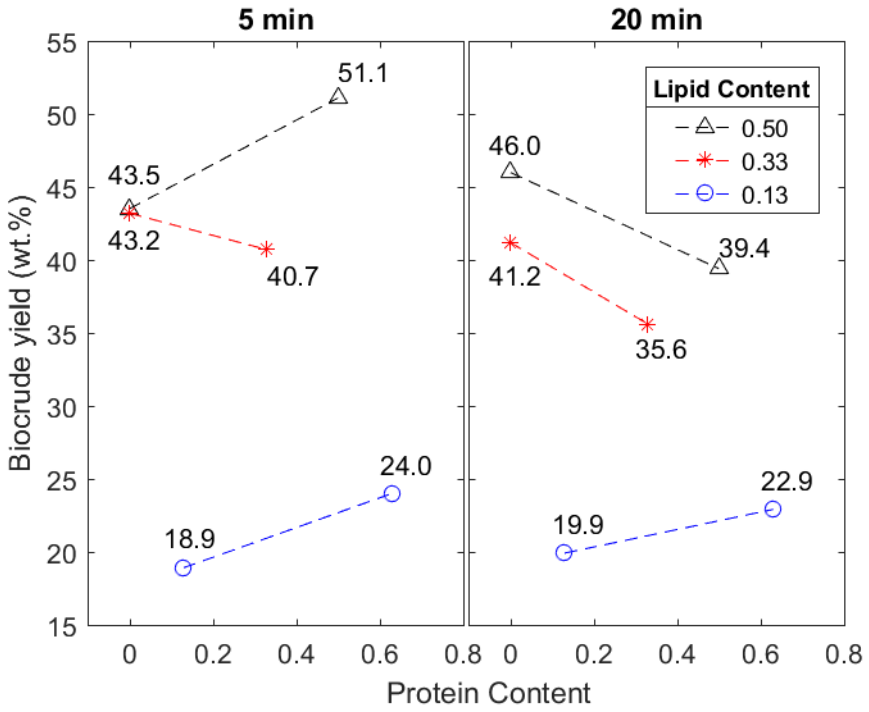

Fig. 5.3 Influence of reaction time (5 min vs. 20 min) on protein and lipid interaction during biocrude formation.

Fig. 5.4 illustrates the influence of mass ratio of water/feedstock on the interaction between protein and lipid during biocrude formation. When the lipid content of feedstock was relatively high (33.3% and 50%), increasing feedstock protein content generated more biocrude at

a mass ratio of 6:1; however, using a higher mass ratio of water/feedstock (12:1) produced less biocrude. This indicates that a high mass ratio of water/feedstock did not favor biocrude formation from protein-lipid mixture. Similar to the influence of reaction time on protein-lipid interaction as mentioned previously, this relatively low biocrude yield at 12:1 water/feedstock mass ratio (vs. 6:1) might be due to the extensive formation of water-soluble fatty amides. King et al. (1999) carried out soybean oil hydrolysis under hydrothermal conditions, and reported that higher water/feedstock ratio led to more complete hydrolysis and therefore larger amounts of fatty acids. Unfortunately, no available literature has reported the influence of mass ratio of water/feedstock on protein degradation products yet. Therefore, more research efforts are desired to investigate the mass ratio influence on HTL of protein, which will be helpful to better understand the interaction between protein and lipid under varied hydrothermal conditions.

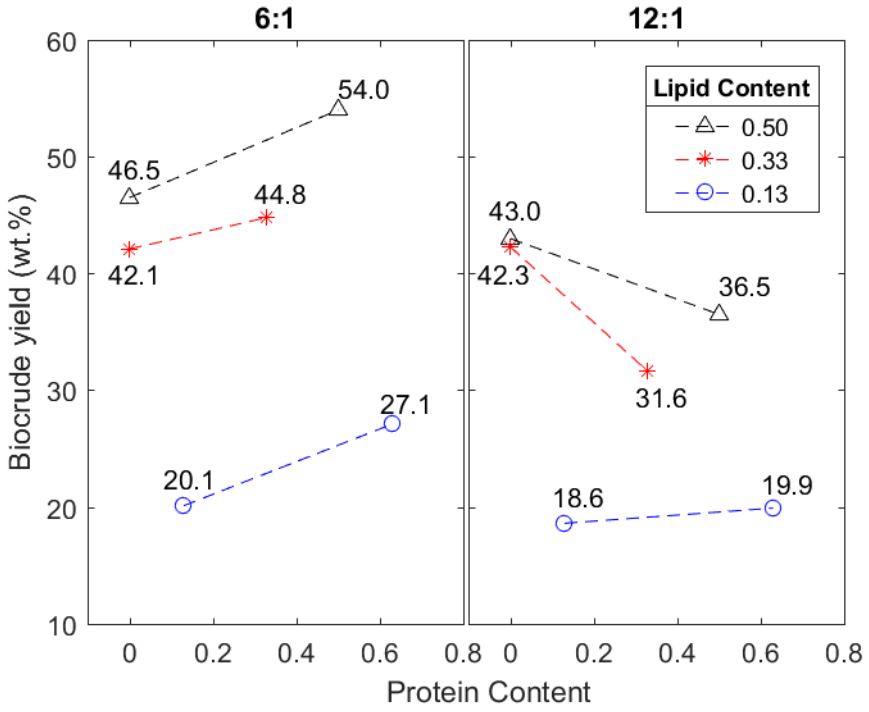

Fig. 5.4 Influence of mass ratio of water/feedstock (6:1 vs. 12:1) on protein and lipid interaction during biocrude formation.

To summarize section 5.4.3.1 and 5.4.3.2, in order to obtain a higher biocrude yield, a low HTL temperature was favorable to eliminate soap formation from alkaline lignin and lipid interaction; shortening reaction time and lowering mass ratio of water/feedstock were desirable to reduce fatty amides formation from protein and lipid interaction.

5.4.3.3 Saccharide-protein interaction on solid residue

Reaction temperature and reaction time exhibited comparable influence on protein and saccharide interaction during solid residue formation as shown in Fig. 5.5 and Fig. 5.6 respectively. At a saccharide content of 33.3%, increasing feedstock protein content led to more SR formation at 270 °C and 5 min, however, a decrement in SR yield was observed at 320 °C and 20 min. In terms of saccharide content at the levels of 12.5% and 50%, larger decrements in SR yield were observed at conditions of 320 °C and 20 min than those of 270 °C and 5 min, when the protein content of feedstock was increased. Thus, using different HTL temperature and reaction time did lead to varied SR formation involving protein and saccharide interaction. The interaction between saccharides and protein in subcritical water has been widely reported (Teri et al., 2014; Yang et al., 2015a; Zhang et al., 2016), which is known as Maillard reaction. Peterson et al. (2010) has provided kinetics evidence for the existing Maillard reaction as well. Maillard reaction typically undergoes the formation of Schiff base and Amadori adducts, dehydration and fragmentation, and aldol condensation to eventually form brown color melanoidins. Both Teri et al. (2014b) and Yang et al. (2015a) stated that more severe HTL conditions were required to produce more biocrude yield through Maillard reaction occurred between protein and saccharide. Yang et al. (2015a) also demonstrated that more severe HTL conditions could decrease the solid residue formation from the mixture of protein and saccharide. These reported observations echoed our findings that 320 °C and 20 min were preferred to generate less solid residue when protein and saccharide were involved in the liquefaction process.

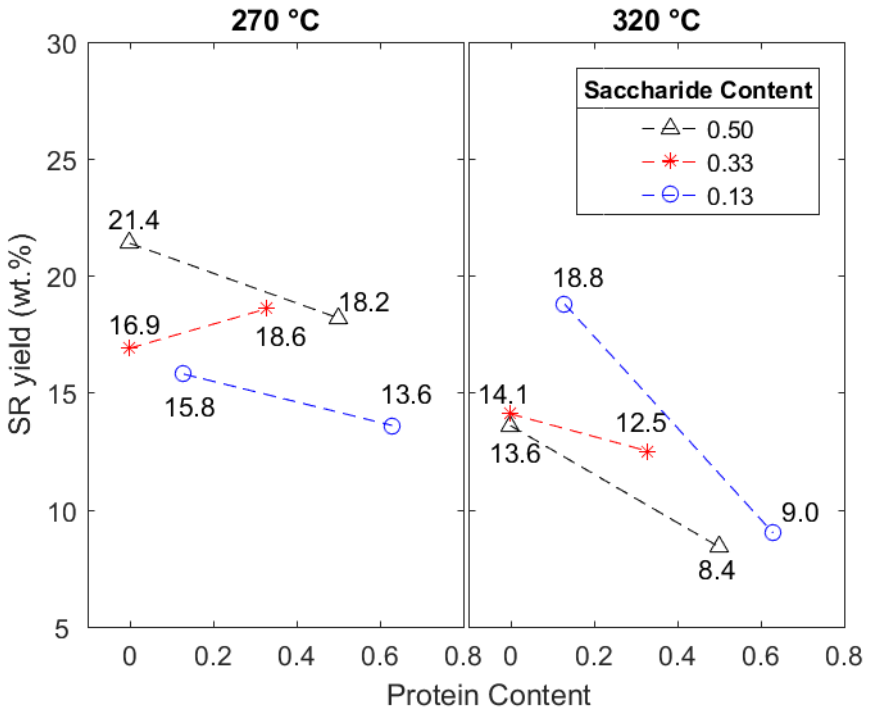

Fig. 5.5 Influence of reaction temperature (270 ºC vs. 320 ºC) on protein and saccharide interaction during solid residue (SR) formation.

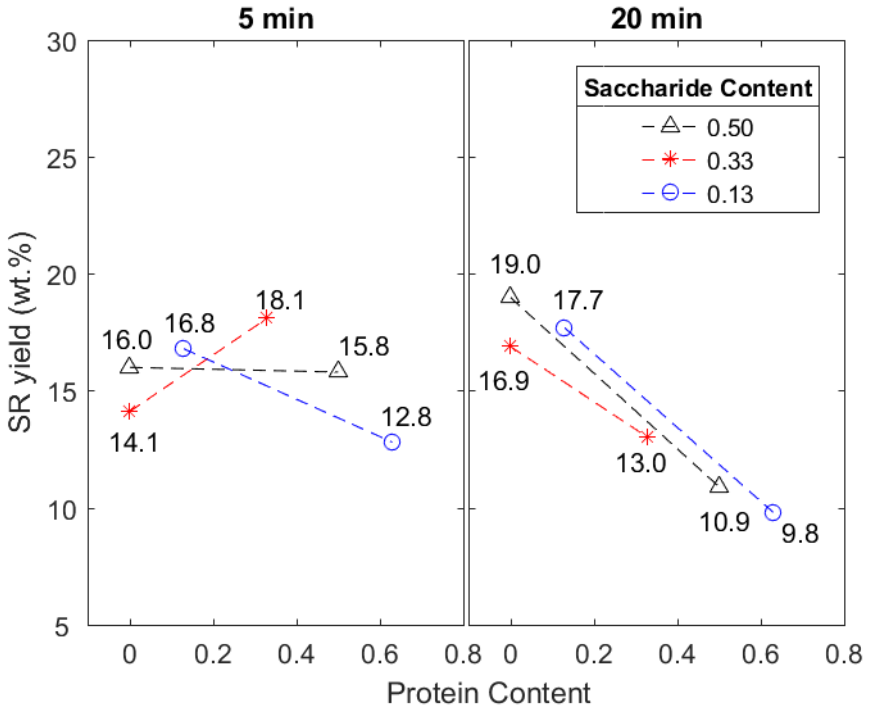

Fig.5.6 Influence of reaction time (5 min vs. 20 min) on protein and saccharide interaction during solid residue (SR) formation.

5.4.3.4 Saccharide-lignin interaction on solid residue

Fig. 5.7 shows that when the feedstock contained 50% of alkaline lignin, increasing saccharide content at 270 °C raised the SR yield from 24.0 wt.% to 33.5 wt.%; however, the SR yield decreased at 320 °C from 24.4 wt.% to 17.1 wt.% when increasing the saccharide content. When the lignin content of feedstock was lower than 50 wt.%, the above-mentioned influence of temperature was negligible. This might be attributed to that a high HTL temperature promoted the retro-aldol reactions that usually happened during carbohydrate decomposition and were more likely to occur in alkaline media, resulting in less SR formation at 320 °C (Kang et al., 2013). Déniel et al. (2017b) studied the interaction between cellulose (one of saccharides) and alkaline lignin at HTL condition of 300 °C and 60 min, and reported that HTL of cellulose with alkaline lignin favored the biocrude formation at an expense of char formation due to the basic environment created by the alkalinity of lignin. Therefore, high HTL temperature was desirable for reducing SR formation *via* saccharide and alkaline lignin interaction.

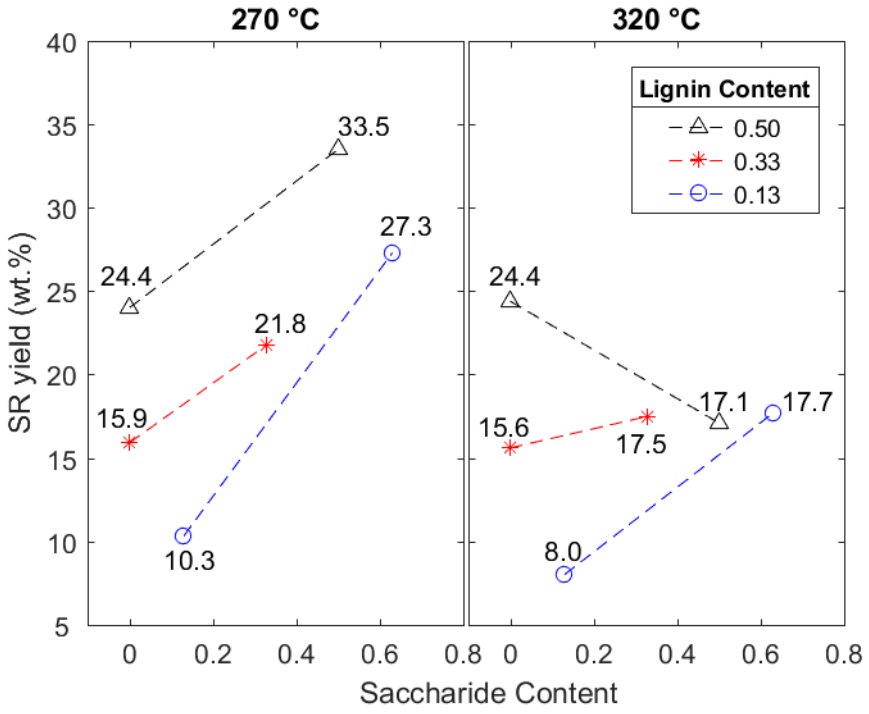

Fig. 5.7 Influence of reaction temperature (270 ºC vs. 320 ºC) on saccharide and lignin interaction during solid residue (SR) formation.

Overall, to minimize SR formation, more severe HTL conditions (320 ºC and 20 min) were required to promote Maillard reaction from interaction between protein and saccharide; high temperature was also preferred to accelerate the retro-aldol reaction between saccharide and alkaline lignin.

5.4.4 GC-MS analysis of biocrude

The biocrudes produced from individual model component and their binary mixtures were analyzed *via* GC-MS. For the biocrudes derived from individual model component, they are featured by certain characteristic chemical compounds. For instance, protein-based biocrude was featured with the nitrogen-containing compounds, such as 3,6-bis(2-methylpropyl)-2,5-piperazinedione and 3,6-diisopropylpiperazin-2,5-dione. The presence of these nitrogen-containing diketopiperazines (DKP) in biocrude have been previously reported (Torri et al., 2012; J. Yang et al., 2018b). The biocrude derived from individual saccharide was rich in furfural and 5-hydroxymethyl-furfural (5-HMF). The mechanisms of furfural and 5-HMF generation from saccharide decomposition under hydrothermal conditions have been well studied, and relevant information can be found in literature (Deguchi et al., 2006; Li et al., 2016; Sasaki et al., 2000). Alkaline lignin-based biocrude mainly consisted of phenolic compounds in this study. The representative compounds in lignin biocrude were guaiacol, vanillin, apocynin and 4-hydroxy-3-methoxy-benzenepropanol. These were consistent with prior works (Wahyudiono et al., 2008). The biocrude derived from lipid was featured by fatty acids and esters (including monoglycerides), such as hexadecanoic acid, 9,12-octadecadinenoic acid and glyceryl 2-octadecadienote. Various fatty acids were also identified in the biocrude from HTL of sunflower oil as recently reported by Gollakota and Savage, (2018).

As for the biocrude from HTL of protein-saccharide mixture, its total ion chromatogram (TIC) was comparable with that of protein biocrude rather than saccharide biocrude. It is necessary to mention that although furfural was the main component in saccharide biocrude, only a trace amount of furfural was identified in the biocrude derived from protein-saccharide mixture. This indicated that certain chemical interactions between protein and saccharide under hydrothermal conditions occurred, and most likely to be the Maillard reaction as previously reported (Teri et al., 2014; Yang et al., 2015b). The biocrude derived from protein-alkaline lignin mixture was comprised of featured compounds from HTL of individual model component, such as DKP from protein and guaiacol from lignin. The presence of phenylmethyl-pyrazine-1,4-dione (a chemical

compound of DKP coupled with benzene ring) was also observed in the biocrude derived from protein-alkaline lignin mixture, presumably due to the chemical interaction between protein and lignin.

In terms of the biocrude from HTL of protein-lipid mixture, its TIC was different with that of individual protein and lipid. There were much less 3,6-bis(2-methylpropyl)-2,5-piperazinedione and 9,12-octadecadinenoic in the biocrude derived from protein-lipid mixture as compared to that of individual protein and lipid respectively. Trace fatty amides were recognized in protein-lipid biocrude. These were in consistent with previous studies (Chiaberge et al., 2013; Déniel et al., 2017a). Déniel et al. (2017a) used glutamic acid and linoleic acid as a representative of protein and lipid respectively, and stated that the difference in the chemical composition of glutamic acid-linoleic acid biocrude evidenced the chemical interactions between glutamic acid and linoleic acid under hydrothermal conditions. Chiaberge et al. (2013b) carried out a mass spectrometric study on the HTL products from a mixture of amino acid and fatty acid, and recognized the fatty amide formation through condensation reaction between fatty acids and the decarboxylation products of amino acids.

The biocrude derived from saccharide-alkaline lignin mixture was rich in guaiacol but lack of furfural. This is consistent with the observation reported by Déniel et al. (2017a), that guaiacol remained as the main component in biocrude derived from glucose-guaiacol mixture. Some alkylation products of guaiacol were identified in saccharide-alkaline lignin biocrude such as 4-hydroxy-3-methoxyphenyl-propanone, due to the presence of furfural decomposition intermediates. It is interesting to note that the biocrude from HTL of saccharide-lipid mixture contained a certain amount of furfural, which was not observed in the biocrude derived from saccharide-protein mixture and saccharide-lignin mixture. This might be that the generation of fatty acids from lipid hydrolysis inhibited the furfural degradation that is known to produce various organic acids; however, the readily happened Maillard reaction between furfural and protein degradation intermediates led to the absence of furfural in the biocrude derived from saccharide-protein mixture. Moreover, the alkalinity of the alkaline lignin also accelerated the furfural degradation, and therefore no furfural was found in the biocrude derived from saccharide-alkaline lignin mixture.

Plenty of monoglycerides (such as glyceryl 2-octadecadienote) were observed in lipid biocrude as mentioned previously, however, much less monoglycerides but abundant

octadecadienoic acid methyl esters were recognized in the biocrude derived from HTL of alkaline lignin-lipid mixture. This indicates that transesterification might occur to convert monoglycerides into fatty acid methyl esters during hydrothermal processing of alkaline lignin-lipid mixture. Since the transesterification is well known to be accelerated under alkaline environment (Yang et al., 2016b, 2016a), it is therefore concluded that the alkalinity played an important role in the formation of octadecadienoic acid methyl ester as observed in this study.

5.5 Conclusions

This is the first study that offers advanced models for predicting product yields as functions of feedstock composition (protein, saccharide, lignin and lipid) and process variables (temperature, time and mass ratio of water/feedstock). The developed models had R^2 (*adj*), 94.6% and 93.2% for biocrude yield and SR yield respectively, indicating a high accuracy of the models. The model predictability was further validated by using modeled feedstock and actual feedstock (spent coffee grounds, SCG) under different HTL conditions. The developed prediction models performed well on either the optimization of HTL process variables when the biochemical composition of feedstock is given, or the optimization of biochemical composition at a given HTL condition.

In addition to the model development and optimization, it was also found that within the experimental design range, the interaction between biomass model components were affected by process variables. To obtain a high biocrude yield, low HTL temperatures were preferred to eliminate soap formation resulting from alkaline lignin and lipid interaction; short reaction time and low mass ratio of water/feedstock were desirable to reduce fatty amides formation from protein and lipid interaction. In order to reduce solid residue formation, severe HTL conditions (320 ºC and 20 min) were required to promote Maillard reaction between protein and saccharide; and high temperatures was beneficial to accelerate the retro-aldol reaction between saccharide and alkaline lignin.

5.6 Supplemental materials

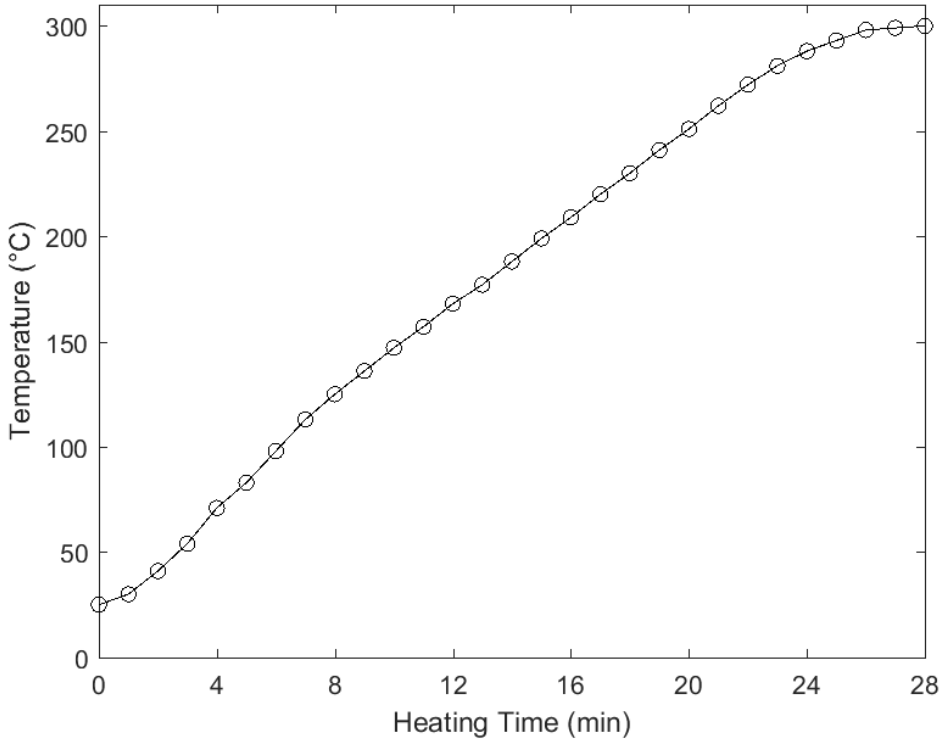

Fig. S5.1 The representative heating profile for 100 mL stainless-steel autoclave (Parr Instrument, 4590 micro-reactor).

Table S5.1 The Analysis of Variance (ANOVA) table for biocrude yield (wt.%) and solid residue yield (wt.%) along with the regression coefficients. Significant model terms are shown in bold.

	Biocrude yield (wt.%)		Solid residue yield[a] (wt.%)	
	Coefficient	P-Value	Coefficient	P-Value
Regression		0.000		0.000
Component Only				
Linear		0.000		0.000
Protein	17.16	-	2.16	-
Saccharide	8.57	-	5.59	-
Lignin	0.40	-	5.51	-
Lipid	97.66	-	0.82	-
Quadratic		0.000		0.000
Protein*Saccharide	14.20	0.212	-1.02	0.154
Protein*Lignin	15.90	0.163	6.05	**0.000**
Protein*Lipid	-32.10	**0.007**	1.13	0.113
Saccharide*Lignin	27.40	**0.019**	-2.15	**0.004**
Saccharide*Lipid	59.80	**0.000**	-0.82	0.250

Lignin*Lipid	-65.60	**0.000**	4.41	**0.000**
*Component * Temperature*				
Linear		0.437		0.025
Protein*Temperature	4.70	0.075	-0.10	0.547
Saccharide*Temperature	-0.92	0.722	0.18	0.270
Lignin*Temperature	0.71	0.783	0.53	**0.002**
Lipid*Temperature	-1.46	0.573	0.05	0.751
Quadratic		0.039		0.000
Protein*Saccharide*Temperature	6.30	0.575	-2.69	**0.000**
Protein*Lignin*Temperature	8.50	0.455	-1.34	0.062
Protein*Lipid*Temperature	-2.80	0.806	-0.33	0.635
Saccharide*Lignin*Temperature	18.80	0.103	-3.82	**0.000**
Saccharide*Lipid*Temperature	7.60	0.501	-0.58	0.412
Lignin*Lipid*Temperature	-36.20	**0.003**	0.96	0.178
*Component * Time*				
Linear		0.955		0.590
Protein*Time	0.12	0.963	-0.06	0.692
Saccharide*Time	0.48	0.854	0.20	0.227
Lignin*Time	-1.42	0.584	-0.14	0.376
Lipid*Time	-1.45	0.577	-0.10	0.540
Quadratic		0.288		0.040
Protein*Saccharide*Time	5.80	0.607	-2.42	**0.001**
Protein*Lignin*Time	14.70	0.198	0.05	0.941
Protein*Lipid*Time	-23.20	**0.046**	0.83	0.243
Saccharide*Lignin*Time	2.80	0.804	0.50	0.478
Saccharide*Lipid*Time	-1.20	0.913	0.06	0.932
Lignin*Lipid*Time	12.00	0.293	0.54	0.446
*Component * Mass ratio*				
Linear		0.758		0.004
Protein*Mass ratio	-3.36	0.199	-0.08	0.633
Saccharide*Mass ratio	-0.07	0.979	-0.55	**0.001**
Lignin*Mass ratio	-0.70	0.786	-0.33	**0.046**
Lipid*Mass ratio	-0.77	0.767	-0.21	0.198
Quadratic		0.314		0.126
Protein*Saccharide*Mass ratio	2.40	0.832	1.28	0.074
Protein*Lignin*Mass ratio	5.50	0.628	-0.31	0.663
Protein*Lipid*Mass ratio	-28.30	**0.016**	0.98	0.169
Saccharide*Lignin*Mass ratio	5.60	0.622	1.38	0.055
Saccharide*Lipid*Mass ratio	-7.20	0.522	-0.03	0.965
Lignin*Lipid*Mass ratio	3.00	0.793	-0.77	0.279
Lack-of-Fit	0.052		0.315	
R^2_{adj}	95.03%		94.27%	

Table S5.2 The prediction model (including all model terms) for biocrude yield and solid residue (SR) yield from hydrothermal liquefaction of model components. Coefficients are calculated for coded variables and significant terms are shown in bold.

	Biomass model components				Process variables			
	Soya protein (X_1, wt.%)	Saccharide (X_2, wt.%)	Alkaline lignin (X_3, wt.%)	Soybean oil (X_4, wt.%)	Temperature (X_5, °C)	Time (X_6, min)	Mass ratio of Water/feedstock (X_7)	
Biocrude yield (wt.%) = **$17.16*X_1 + 8.57*X_2 + 0.4*X_3 + 97.66*X_4$** + $14.2*X_1X_2 + 15.9*X_1X_3$ **$– 32.1*X_1X_4 + 27.4*X_2X_3 + 59.8*X_2X_4$** $– 65.6*X_3X_4 + 4.7*X_1X_5 – 0.92*X_2X_5 + 0.71*X_3X_5 – 1.46*X_4X_5 + 6.3*X_1X_2X_5 + 8.5*X_1X_3X_5 – 2.8*X_1X_4X_5 + 18.8*X_2X_3X_5 + 7.6*X_2X_4X_5$ **$– 36.2*X_3X_4X_5$** $+ 0.12*X_1X_6 + 0.48*X_2X_6 – 1.42*X_3X_6 – 1.45*X_4X_6 + 5.8*X_1X_2X_6 + 14.7*X_1X_3X_6$ **$– 23.2*X_1X_4X_6$** $+ 2.8*X_2X_3X_6 – 1.2*X_2X_4X_6 + 12*X_3X_4X_6 – 3.36*X_1X_7 – 0.07*X_2X_7 – 0.7*X_3X_7 – 0.77*X_4X_7 + 2.4*X_1X_2X_7 + 5.5*X_1X_3X_7$ **$– 28.3*X_1X_4X_7$** $+ 5.6*X_2X_3X_7 – 7.2*X_2X_4X_7 + 3*X_3X_4X_7$							R^2 (*adj*) = 95%
SR yield^0.5 (wt.%) = **$2.16*X_1 + 5.59*X_2 + 5.51*X_3 + 0.82*X_4$** $– 1.02*X_1X_2$ **$+ 6.05*X_1X_3$** $+ 1.13*X_1X_4$ **$– 2.15*X_2X_3$** $– 0.82*X_2X_4$ **$+ 4.41*X_3X_4$** $– 0.1*X_1X_5 + 0.18*X_2X_5$ **$+ 0.53*X_3X_5$** $+ 0.05*X_4X_5$ **$– 2.69*X_1X_2X_5$** $– 1.34*X_1X_3X_5 – 0.33*X_1X_4X_5$ **$– 3.82*X_2X_3X_5$** $– 0.58*X_2X_4X_5 + 0.96*X_3X_4X_5 – 0.06*X_1X_6 + 0.2*X_2X_6 – 0.14*X_3X_6 – 0.1*X_4X_6$ **$– 2.42*X_1X_2X_6$** $+ 0.05*X_1X_3X_6 + 0.83*X_1X_4X_6 + 0.5*X_2X_3X_6 + 0.06*X_2X_4X_6 + 0.54*X_3X_4X_6 – 0.08*X_1X_7$ **$– 0.55*X_2X_7$ $– 0.33*X_3X_7$** $– 0.21*X_4X_7 + 1.28*X_1X_2X_7 – 0.31*X_1X_3X_7 + 0.98*X_1X_4X_7 + 1.38*X_2X_3X_7 – 0.03*X_2X_4X_7 – 0.77*X_3X_4X_7$							R^2 (*adj*) = 94%

Note: A square root transformation was applied on solid residue yield (wt.%) to meet normal distribution and constant variance of the error terms assumptions.

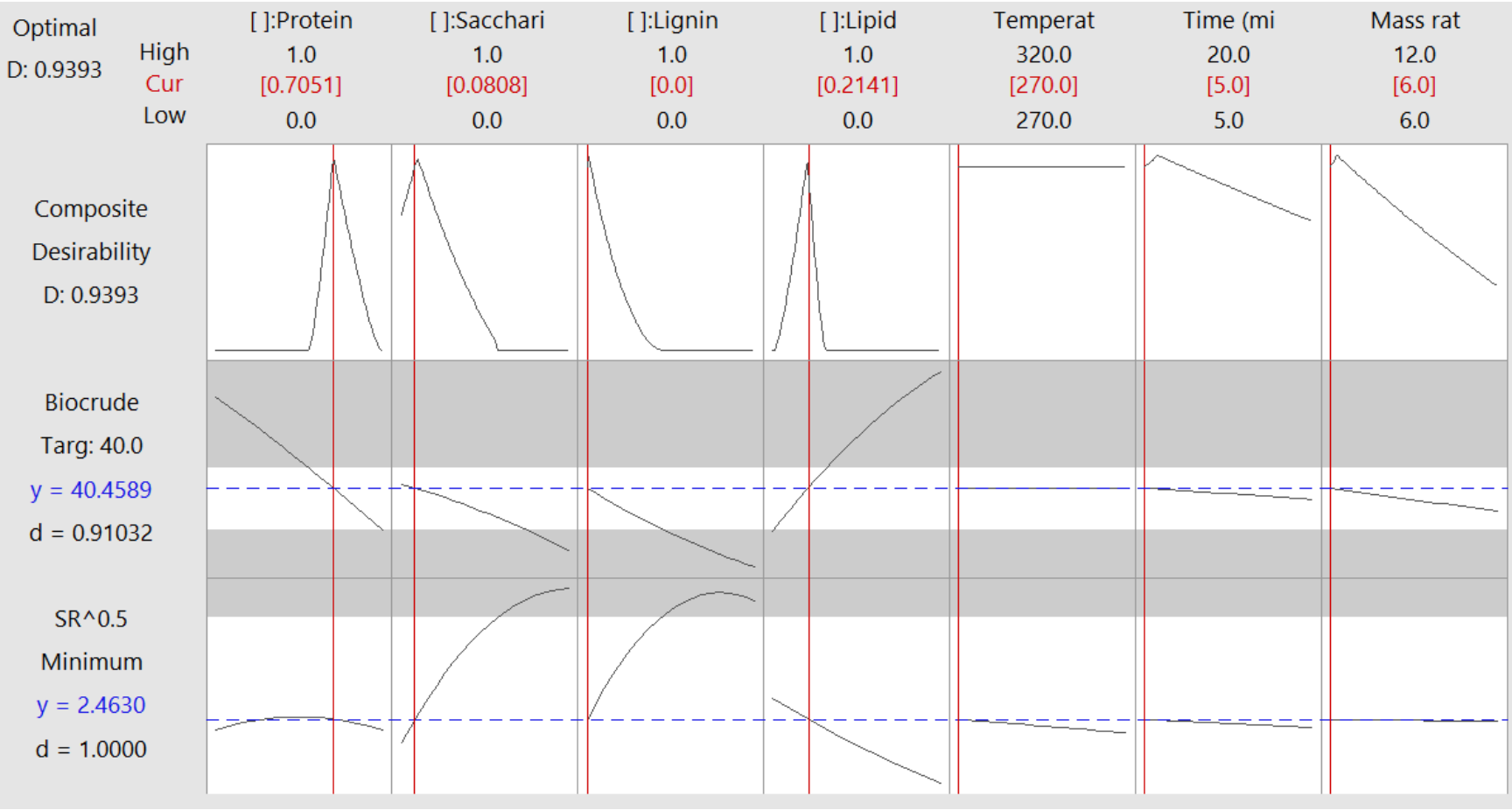

Fig. S5.2 The optimum of feedstock biochemical compositions at hydrothermal liquefaction condition of 270 °C reaction temperature, 5 min time and 6:1 mass ratio of water/feedstock.

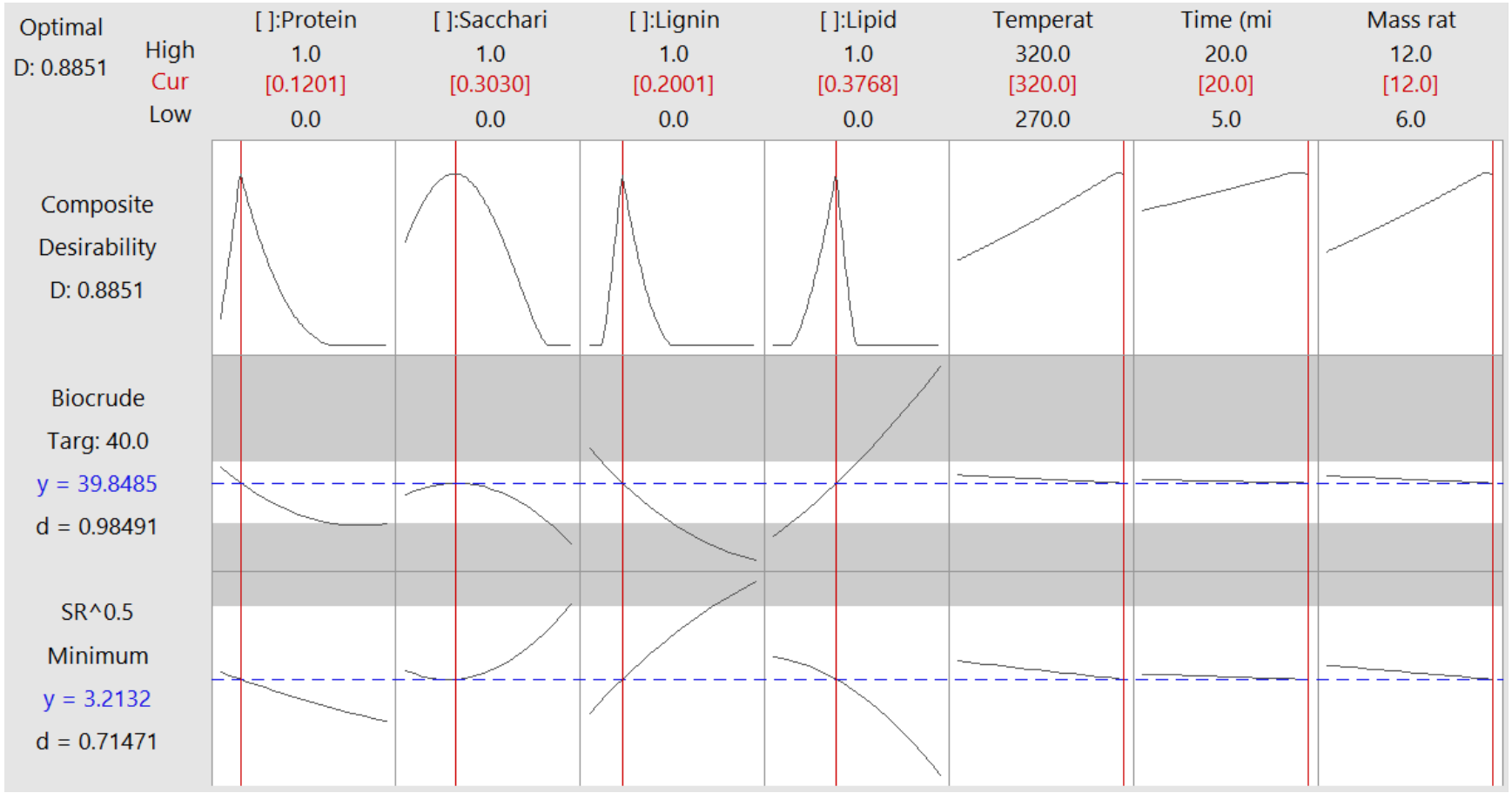

Fig. S5.3 The optimum of feedstock biochemical compositions at hydrothermal liquefaction condition of 320 ºC reaction temperature, 20 min time and 12:1 mass ratio of water/feedstock.

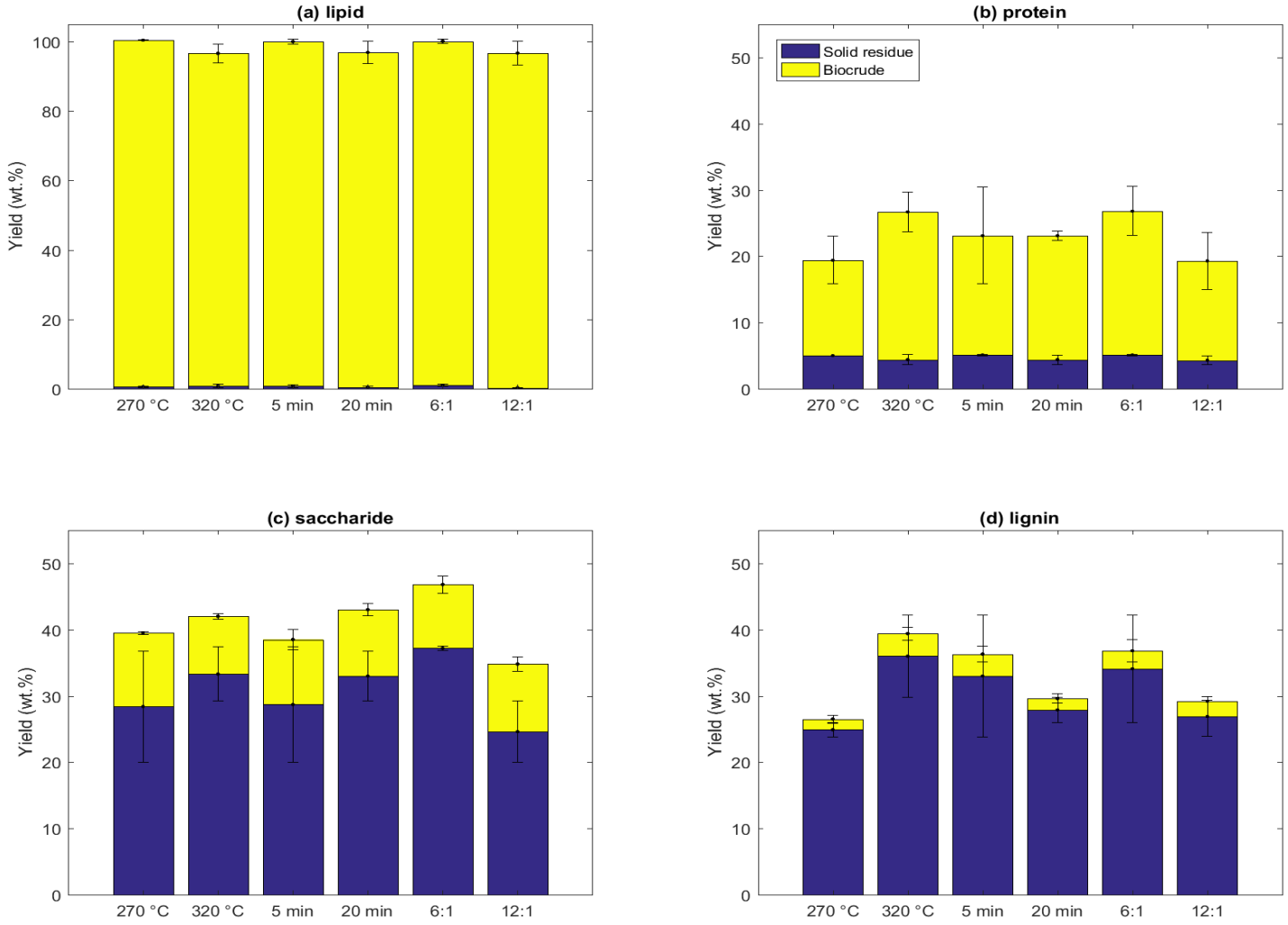

Fig. S5.4 The yield of biocrude and solid residue for hydrothermal liquefaction of individual model components at varied conditions.

5.7 Transition section

Chapter 5 developed broadly applicable models for the prediction of HTL product yield *via* a mixture design of biomass model components coupled with process variables. How the chemical interactions between biomass model components are influenced by changing process variables were investigated as well. Besides the co-liquefaction of biomass model components, hydrothermal co-liquefaction of different types of actual biomass has recently attracted much research interest as it might lead to desirable co-liquefaction effect (CE) on biocrude yield/quality. Although some attempts have been made to study the CE, how significant the observed CE is when taking experimental error into consideration has not been investigated yet. Therefore, Chapter 6 aims to statistically determine the significance of observed CE, and to explore how the CE is influenced by changing mixing ratios.

Chapter 6: Co-liquefaction Effect on Product Yield: Statistical Determination and Mixing Ratio's Influence

Current state:

A version of this chapter is under preparation for a submission to Energy Conversion and Management.

Contribution statement:

I was responsible for raw materials collection, part of experiment design, conduction and data analysis, and manuscript preparation.

6.1 Abstract

To assess the co-liquefaction effect (CE) on product yield, binary mixtures (50:50 by mass) of food waste (spent coffee grounds), microalgae (*Chlorella. sp.*), marine macroalgae (red seaweed) and lignocellulosic biomass (sawdust) were hydrothermally liquefied under identical conditions. A synergistic effect on biocrude yield was observed in the co-liquefaction of spent coffee grounds and *Chlorella. sp.* (6.3 wt.% or 23.0%), as well as spent coffee grounds and sawdust (3.1 wt.% or 13.8%). Co-liquefying spent coffee grounds/red seaweed, *Chlorella. sp.*/red seaweed and *Chlorella. sp.*/sawdust showed positive values of CE on biocrude yield, but these numbers were not statistically significant when considering the experimental error, and thus there was no synergetic effect in the three feedstock combinations. The effect of mixing ratio on CE was also explored in this chapter. Co-liquefaction of spent coffee grounds and *Chlorella. sp.* at a mixing ratio of 50:50 led to more desirable CE on biocrude yield than that of 25:75 and 75:25. Co-liquefaction of spent coffee grounds and sawdust at a mixing ratio of 25:75 or 50:50 was favored over 75:25 in terms of CE on biocrude yield. Although the CE on biocrude yield was not remarkably influenced by the mixing ratio for *Chlorella. sp.*/sawdust, increasing the proportion of protein-rich *Chlorella. sp.* resulted in much less solid residue yield. Changing mixing ratios exhibited negligible impact on CE when red seaweed was co-liquefied with other feedstocks. It is also worthwhile to mention that using the absolute CE or relative CE as the response might lead to different conclusions when studying the influence of mixing ratio on the CE.

6.2 Introduction

Hydrothermal co-liquefaction of various feedstock is believed to be advantageous over hydrothermal liquefaction (HTL) of individual feedstock due to its potential synergistic effect on yield/quality of biocrude, and low logistics costs for feedstock collection and transportation. Several feedstocks have been evaluated for co-liquefaction, such as microalgae, lignocellulosic biomass, municipal sludge, food processing waste, marine species, crude glycerol and even plastics waste etc.

Co-liquefaction effects on biocrude yield were indeed observed in previous co-liquefaction studies, as defined simple additive effect, synergistic effect (SE, in the range of 2.2 wt.% to 45.1 wt.%), or antagonistic effect (AE, in the range of 1 wt.% to 15.8 wt.%). Gai et al. (2015a) co-liquefied microalgae (*Chlorella pyrenoidosa*) and rice husk in hot compressed water at 300 °C for 60 min, and a highest SE (8.7 wt.%) on toluene-recovered biocrude yield was observed for 50:50 microalgae/rick husk. Co-liquefaction of spent coffee grounds and corn stalk was reported to have a 5.4 wt.% SE on acetone-recovered biocrude yield (Yang et al., 2017). AE on biocrude yield were also reported (Brilman et al., 2017; Lu et al., 2017), for instance, a 1.9 dwt.% AE on acetone-recovered biocrude yield was observed for the co-liquefaction of 50% loblolly pine wood and 50% digested sewage sludge (Saba et al., 2018). The detailed summary of the CE reported in the previous co-liquefaction studies was provided in section 2.5. unfortunately, the significance of the claimed SE or AE was not statistically determined when accounting for the experimental error.

Although many attempts have been made to study hydrothermal co-liquefaction of biomass, each study had its specific focus on the type of mixed biomass feedstock. For instance, Xiu and coworkers (Xiu et al., 2010; Ye et al., 2012) focused on the co-liquefaction of swine manure and glycerol, and Wu and coworkers (Wu et al., 2017) emphasized on the co-liquefaction of plastics and microalgae. However, the applied co-liquefaction conditions were usually different between research groups, making the reported results less comparable. Another challenge is the inconsistency of downstream processing procedures used by research groups, which might result in misleading conclusions when comparing the co-liquefaction effect. For example, the type of organic solvent used to recover biocrude was influential to the claimed SE on biocrude yield (Yang et al., 2018a; Saba et al., 2018), even though identical feedstock and experimental operations were applied. This was mainly due to that the yield of bio-crude is highly associated with the

physicochemical properties of organic solvents used. Therefore, it is necessary to conduct a thorough co-liquefaction study that include a variety of biomass mixtures, and such a study should be carried out with identical condition and downstream processing procedures to ensure proper data comparability.

This study aims to statistically and thoroughly determine the hydrothermal co-liquefaction effect on product yield. Binary mixtures of four representative biomass, food waste (spent coffee grounds, A), microalgae (*Chlorella. sp.*, B), marine species (red seaweed, C) and lignocellulosic biomass (sawdust, D), gave six combinations in total (AB, AC, AD, BC, BC and CD). The identical reaction conditions and downstream processing procedures were applied to ensure the data comparability. A statistical method, one-sample t-test was used to evaluate if the SE or AE on product yield is significantly greater than zero or less than zero respectively. This chapter also investigated whether the SE or AE was favored at certain biomass mixing ratios for each studied combination, and the optimal mixing ratio for each combination was then suggested.

6.3 Materials and methods

6.3.1 Materials

Spent coffee grounds was collected from Tim Hortons at Truro, Canada, maple sawdust was provided by the wood shop on Dalhousie Agricultural Campus, and red seaweed was purchased from Stirling's Farm Market, Truro. All of them were oven dried at 105 °C for 24 h before being used in the experiments. Dried microalgae (*Chlorella. sp.*) was purchased from Buy Algae, Meridian, American, and was used as received. Dichloromethane (ACS reagent grade) was supplied by EMD Millipore Cooperation and used as received.

6.3.2 Biomass feedstock characterization

The biochemical composition of red seaweed and sawdust were characterized by the methods that have been used for spent coffee grounds and *Chlorella. sp.* as described in section 3.3.2.

6.3.3 Hydrothermal co-liquefaction processes

The hydrothermal co-liquefaction temperature, time and feedstock concentration used in this study was 320 °C, 10 min and 10 wt.% respectively. Liquefaction processes were identical to that of section 3.3.3, and solvent extraction method (dichloromethane) was used to recover biocrude.

The gas yield was calculated using ideal gas law as shown in equation (6.1)

$$\text{Gas yield (wt. \%)} = \frac{\text{Mass of gas}}{\text{Mass of feedstock}} \times 100\% \quad (6.1)$$

$$= \frac{\Delta n \times M}{Mass\ of\ feedstock} \times 100\% = \frac{\left(\frac{\Delta P \times V}{RT}\right) \times M}{Mass\ of\ feedstock} \times 100\%$$

where V = 0.06 L, R = 0.08314 (L·bar)/(mol·K), T = 298 K, since the majority of HTL gas is carbon dioxide, then the molecular weight (M) of gas is assumed to be 44 g/mol (Brown et al., 2010; Wang et al., 2013).

The aqueous phase yield was calculated using equation (6.2),

$$\text{Aqueous phase yield} = 100\% - \text{biocrude yield} - \text{solid residue yield} - \text{gas yield} \quad (6.2)$$

6.3.4 Co-liquefaction effect evaluation

Hydrothermal co-liquefaction effect on product yield is commonly referred to the incremental difference between experimental yield and calculated mass-averaged yield, namely the absolute co-liquefaction effect on product yield as shown in equation (6.3):

$$\text{Absolute co-liquefaction effect (wt.\%)} = Y_{A/B} - Y_{\text{mass-averaged}} \quad (6.3)$$

$$= Y_{A/B} - (X_A \times Y_A + X_B \times Y_B)$$

where $Y_{A/B}$ denotes the actual yield from co-liquefaction of A and B, and $Y_{\text{mass-averaged}}$ indicates the calculated mass-averaged yield. X_A and X_B are the mass fraction in the mixed feedstock. Y_A and Y_B represent the yield obtained from liquefaction of individual A and B respectively.

Relative co-liquefaction effect on product yield was also used by some studies for better data comparability as shown in equation (6.4) (Yang et al., 2018a; Yang et al., 2017a; Brilman et al., 2017a). Using relative co-liquefaction effect (%) can prevent the inconsistency of the basis that is used to define yield, such as weight basis (wt.%), dry weight basis (dwt.%), and dry ash free basis (wt.%, daf). Researchers must be aware of the difference between absolute value and relative value when comparing the co-liquefaction effect.

$$\text{Relative co-liquefaction effect (\%)} = \left(\frac{\text{absolute co-liquefaction effect}}{\text{mass-averaged yield}}\right) \times 100\% \quad (6.4)$$

6.3.5 Data analysis

For each of the six combinations, one-sample t-test (Montgomery, 2017) was conducted to test whether the SE or AE is significantly greater than zero or less than zero respectively. To do

this, the null hypothesis was H_0: SE or AE = 0, which represents no significant SE or AE exists. An alternative hypothesis was H_a: SE > 0 or AE < 0, which represents there is significant SE or AE. A confidence level of 95% was used for the test, and if p-value < 0.05, then rejects H_0 and accepts H_a, indicating there is significant SE or AE. If p-value > 0.05, then accepts H_0 and rejects H_a, indicating no significant SE or AE.

For each of the six combinations, the influence of feedstock mixing ratio (three levels: 50:50, 75:25, and 25:75) on CE was studied using an one-way analysis of variance method. Fisher's least significant difference (LSD) method was then applied to generate the letter grouping. Letter grouping that does not share the same letter indicates significant difference between two mean values. In contrast, letter grouping that shares the same letter indicates non-significant difference.

6.4 Results and discussion

6.4.1 Biochemical composition of studied feedstock

The product yield from HTL of biomass is highly dependent on the proportion of chemical constituents in feedstock. Four representative biomass feedstocks chosen to study CE are food waste (spent coffee grounds), microalgae (*Chlorella sp.*), marine macroalgae (red seaweed) and lignocellulosic biomass (sawdust). The feedstocks' biochemical composition are presented in Table 6.1, and they vary from each other. The largely different biochemical composition of studied feedstocks allows us to thoroughly assess the CE when co-processing either two of them.

Chlorella sp. microalgae used had a high protein content (63.2%), which is common for a microalgae feedstock. There is only 0.9% lipid in the used *Chlorella sp*. microalgae. The biochemical composition of sawdust was characterized by its high carbohydrate content, including 46.2% cellulose, 23.2% lignin and 19.8% hemicellulose. These data were comparable to the composition of sawdust used in other liquefaction studies (Jensen et al., 2017). Spent coffee grounds exhibited a relatively balanced biochemical composition, containing 9.5% lipid and 14.2% protein. It is notable that much lower ash content was observed for spent coffee grounds, *Chlorella sp*. and sawdust, however, red seaweed that is a marine macroalgae specie had high ash content (29.4%). A high content of ash and/or minerals in marine macroalgae was reported by Jin et al. (2013) and Barreiro et al. (2015) as well.

Table 6.1 Biochemical composition of spent coffee grounds, Chlorella sp. microalgae, red seaweed and sawdust.

	Spent coffee grounds	*Chlorella sp*. microalgae	Red seaweed	Sawdust
Moisture content (%)	4.6	6.5	1.0	2.1
Ash (%)	1.3	5.6	29.4	0.1
Lipid (%)	9.5	0.9	0.5	0.2
Protein (N × 6.25) (%)	14.2	63.2	24.5	1.9
Hemicellulose	22.5	5.9[c]	16.5	19.8
Cellulose	26.8	11.8[c]	4.1	46.2
Lignin	24.0	5.9[c]	1.8	23.2

Note: the carbohydrate composition of microalgae (very fine powder) were not able to be obtained due to the crucible clogging problems during testing. Therefore, lignin, hemicellulose and cellulose composition for microalgae was assumed to be 1/4 of carbohydrate, 1/4 of carbohydrate and 1/2 of carbohydrate respectively base on testing experience and literatures.

6.4.2 Hydrothermal liquefaction of single feedstock

HTL of individual biomass was conducted to investigate their product distributions prior to co-process either two of them. All experiment runs were carried out at 320 °C for 10 min with a 10 wt.% feedstock concentration, and dichloromethane was used to recovery biocrude. The product yields from HTL of single feedstock were presented in Table 6.2.

HTL of *Chlorella sp*. at 320 °C for 10 min led to the highest biocrude yield (30.7 wt.%) and the lowest solid residue (SR) yield (4.1 wt.%) among four feedstocks studied. A relatively high aqueous phase (AqP) yield (47.5 wt.%) and a gas yield (17.8 wt.%) were obtained for HTL of *Chlorella sp*. as well. This is mainly because of a high protein content in *Chlorella sp*., which could be easily hydrolyzed into water-soluble amino acids under HTL reaction condition, and amino acids were further degraded into gaseous products (such as carbon dioxide and ammonia *via* decarboxylation and deamination respectively) (Peterson et al., 2008). HTL of sawdust generated a 20.6 wt.% biocrude yield and the highest SR yield (30.6 wt.%) along with 35.4 wt.% AqP yield and 13.3 wt.% gas yield. The high SR yield can be attributed to a high content of cellulose and lignin in sawdust, making it hard to be decomposed under the applied processing conditions (Toor et al., 2011).

Marine macroalgae (red seaweed) is a rarely studied feedstock in HTL field, and HTL of it gave only 15.0 wt.% biocrude yield along with 12.6 wt.% SR yield. The majority of red seaweed was turned into AqP (58.2 wt.%), presumably due to its high content of minerals that could be

readily dissolved in water. A high solubility of minerals in subcritical water was also observed by Barreiro et al, in which HTL of marine macroalgae was carried out (Barreiro et al., 2015). In comparison with other three feedstocks, HTL of spent coffee grounds resulted in a relatively even product distribution, including 24.5 wt.% biocrude yield, 23.5 wt.% SR yield, 37.0 wt.% AqP yield and 15.1 wt.% gas yield. This is likely due to a balanced proportion of lipid, protein, cellulose, hemicellulose and lignin in spent coffee grounds as shown in Table 6.1.

In general, the product distributions from HTL of individual feedstocks were highly associated with their biochemical compositions, and these obtained results will be helpful to better understand the co-liquefaction's product formation.

Table 6.2 The product yield (wt.%) from hydrothermal liquefaction of individual biomass.

Product yield (wt.%)	Food waste	Microalgae	Marine macroalgae	Lignocellulosic biomass
	spent coffee grounds	*Chlorella sp*.	red seaweed	sawdust
Biocrude	24.5	30.7	15.0	20.6
Solid residue	23.5	4.1	12.6	30.6
Aqueous phase	37.0	47.5	58.2	35.4
Gas	15.1	17.8	14.2	13.3

Note: 1, AqP denotes to aqueous phase. Aqueous phase yield = 100 – Biocrude yield – Solid residue yield – Gas yield
2, processing conditions: 320 °C, 10 min, 10 wt.% feedstock concentration, dichloromethane as the biocrude recovery solvent.

6.4.3 Significance of co-liquefaction effect

Binary mixtures of four representative feedstocks were hydrothermally co-liquefied at a fixed mixing ratio of 50:50, giving six combinations in total (AB, AC, AD, BC, BD and CD). The identical reaction conditions and downstream processing procedures were applied to ensure the data comparability. One-sample t-test was used to determine the significance of the observed co-liquefaction effect (CE) on biocrude yield, SR yield, AqP yield and gas yield, and the results were presented in Table 6.3. Both absolute CE (wt.%) and relative CE (%) were used the response in this chapter.

Hydrothermally co-liquefying spent coffee grounds with microalgae (AB) at a 50:50 mixing ratio resulted in a highly significant SE on biocrude yield, either expressed in an absolute value of 6.3 wt.% or a relative value of 23.0% as shown in Table 6.3; meanwhile, a highly significant AE

on SR yield was observed, indicating that biomass was more readily converted into biocrude during co-liquefaction. An insignificant CE on gas yield and a significant AE on AqP yield suggested that the biocrude formation from water-soluble intermediates/chemicals was favored by co-liquefaction as compared to HTL of individual A and B. Yang et al. (2018a) reported a 7.5% relative SE on biocrude yield from co-liquefaction of spent coffee grounds with microalgae at 290 °C, which was lower than 23.0% in this study. This difference in relative SE was likely due to the different processing temperatures (290 °C vs. 320 °C), indicating that temperature could substantially influence CE and deserves more attention in the future study on co-liquefaction.

As for the co-liquefaction of spent coffee grounds with red seaweed (AC), the CE on biocrude yield was not significant even though the positive value of absolute CE (0.8 wt.%) and relative CE (3.9%) were obtained. A highly significant SE on SR yield were observed along with a significant AE on AqP and gas yield. There are three potential explanations for the observations: 1) co-liquefaction of A and C inhibited the decomposition of biomass mixture into water-soluble products and subsequently suppressed the formation of gases from water-soluble chemicals (e.g., light weight acids). 2) solid spent coffee grounds was readily converted into water-soluble products, then the repolymerization of these water-soluble chemicals were favored to form SR due to the presence of minerals in red seaweed. 3) previous two speculations that involve certain degree of chemical interactions between co-liquefied feedstocks, the observed SE on SR yield might be simply caused by the physical deposit of red seaweed minerals on the SR that is more readily available during co-liquefaction than HTL of individual red seaweed.

The absolute and relative SE values of 3.1 wt.% and 13.8% respectively were observed for co-liquefaction of spent coffee grounds and sawdust (AD). However, there was no significant CE on SR yield as shown in Table 6.3. It is plausible that co-liquefaction of A and D did not enhance the conversion of biomass into biocrude but favored the biocrude formation from originally water-soluble intermediates. This assumption is confirmed by a marginally significant AE on AqP yield along with insignificant CE on gas yield. The enhanced biocrude yield and suppressed AqP yield from co-liquefaction of AD can be rationally explained from feedstock biochemical composition perspective. Specifically, spent coffee grounds had a relatively high lipid content (9.5%) and sawdust was featured with 19.8% hemicellulose and 46.2% cellulose as shown in Table 6.1, in which the chemical interaction of lipid-hemicellulose and lipid-cellulose promoted the biocrude

formation as proven in our previous study (Yang et al., 2018b). The degradation intermediates from HTL of lipid (such as fatty acids) simultaneously interacted with the degradation intermediates from hemicellulose and cellulose (such as water-soluble furfural and glyceraldehyde etc.) at subcritical condition, which contributed to the biocrude formation while reduced AqP yield.

Similar to co-liquefaction of A and C, co-liquefaction of microalgae and red seaweed (BC) led to an insignificant CE on biocrude yield as shown in Table 6.3. A marginally significant SE (absolute value 2.6 wt.% or relative value 4.8%) on AqP yield was observed, while with a significant AE on SR yield and gas yield. Hence, it is reasonable to believe that co-liquefaction of B and C favored the formation of AqP products at the expense of char and gas formation. These observations might be highly associated with the presence of abundant minerals in red seaweed and protein in *Chlorella sp*. microalgae. Minerals assisted the decomposition of protein into water-soluble compounds and inhibited the gases formation from intermediates in aqueous phase, or alternatively, the protein degradation intermediates promoted the red seaweed decomposition into water-soluble products and diminished the gas formation as well.

Hydrothermal co-liquefaction of *Chlorella sp*. microalgae and sawdust (BD) did not show any significant CE on biocrude yield in this study, even though Gai et al. (Gai et al., 2015a) stated that co-liquefying microalgae (*Chlorella pyrenoidosa*) with lignocellulosic biomass (rice husk) led to a SE on biocrude yield. Brilman et al. (2017) reported an opposite result that co-liquefying microalgae with pine wood exhibited a AE on biocrude yield. Unfortunately, the significance of these previously reported CE was not statistically evaluated. These conflicting results might also be caused by inconsistent processing conditions and biocrude recovery method used in these studies. As seen from Table 6.3, co-liquefaction of B and D led to a significant AE on SR yield. This is likely due to that the nitrogen-containing intermediates from protein degradation assisted the decomposition of carbohydrate in sawdust into water-soluble products, resulting in the AE on SR yield. A positive CE on AqP yield (1.2 wt.% or 2.9%) was observed even though it was not significant.

In terms of co-liquefaction of red seaweed and sawdust (CD), there was a marginally significant AE (absolute value of -2.4 wt.% or relative value of -13.3%) on biocrude yield and a highly significant SE (absolute value of 2.2 wt.% or relative value of 10.3%) on SR yield. This might be caused by the presence of minerals in red seaweed, which inhibited/terminated the

biocrude formation from carbohydrates intermediates and instead favored the repolymerization to form more SR. Jasiūnas et al. (2017) also reported a AE on biocrude yield from co-liquefaction of aspen wood sawdust and spent mushroom compost that contained a fairly large amount of minerals. The reported AE on biocrude yield was attributed to more gases being generated during co-liquefaction, in which minerals in spent mushroom compost were believed to assist gas formation from hemicellulose-rich aspen wood sawdust (Jasiūnas et al., 2017). Different from above-mentioned AE on biocrude yield, Saba et al. (2018) observed a SE on biocrude yield from co-liquefaction of loblolly pine wood and cow manure that had a high content of minerals as well; they stated that the organic acids produced from loblolly pine wood promoted the biocrude formation during co-liquefaction.

In summary, both co-liquefaction of AB and AD had significant SE on biocrude yield along with AE on AqP yield. Although co-liquefaction of AC, BC and BD all had positive CE on biocrude yield, but they were not statistically significant when taking the experimental error into consideration. Co-liquefaction of CD led to a significant AE (-2.4 wt.% or -13.3%) on biocrude yield and a SE (2.2 wt.% or 10.3%) on SR yield; this might be caused by the presence of minerals in red seaweed, which inhibited/terminated the biocrude formation from the decomposition intermediates from carbohydrate-rich sawdust. Overall, it is highly necessary to determine the significance of CE on product yield, this is mainly due to the follow three aspects: 1) if every co-liquefaction study uses one-sample t-test (taking experimental errors into consideration) or other proper statistical methods to assess the significance of observed CE, then the reliability of reported CE and data comparability between studies would be improved. 2) with knowing the significance of observed CE on each product stream, researchers would have stronger confidence on the speculation of product formation pathways during co-liquefaction. 3) with the better understanding on the product formation pathways during co-liquefaction, we can incorporate the biochemical composition of individual biomass to elucidate the potential reasons for the observed CE on product yield during co-liquefaction.

Table 6.3 The statistical significance level of hydrothermal co-liquefaction effect for six studied biomass combinations.

	Biocrude		Solid residue		Aqueous phase		Gas	
	Absolute CE (wt.%)	Relative CE (%)	Absolute CE (wt.%)	Relative CE (%)	Absolute CE (wt.%)	Relative CE (%)	Absolute CE (wt.%)	Relative CE (%)
AB	6.3***	23.0***	-1.2***	-8.5***	-4.7**	-11.2**	-0.4	-2.7
AC	0.8	3.9	0.7***	3.7***	-1.0*	-2.1*	-0.4**[a]	-3.0**[a]
AD	3.1***	13.8***	0.1	0.4	-3.0*	-8.2*	0.9	6.3
BC	0.1	0.4	-0.9**	-10.2**	2.6*	4.8*	-1.8**[a]	-11.1**[a]
BD	0.3	1.3	-2.9***	-16.5***	1.2	2.9	1.8[b]	8.6[b]
CD	-2.4*	-13.3*	2.2***	10.3***	-1.2	-2.5	1.3[b]	9.7[b]

Notes: *** denotes highly significant level; ** denotes significant level; * denotes marginally significant level; no * denotes that the value is not significantly different from zero; A = spent coffee grounds; B = microalgae (*Chlorella. sp.*); C = red seaweed; D = sawdust.

a: the normality test cannot be carried out as four replicated runs gave the identical yields, and the value is considered to be significant.

b: the normality test was not satisfactory even though the data transformation has been attempted, and therefore the significance of the value might be biased.

6.4.4 Influence of mixing ratio of feedstock on co-liquefaction effect

The mixing ratio of biomass feedstocks is an important variable for hydrothermal co-liquefaction studies, and the influence of mixing ratio on CE was explored for each of six feedstock combinations. A statistical method, one-way analysis of variance coupled with Fisher's least significant difference (LSD), was applied to test whether different mixing ratios led to significantly different CE.

For a mixture of spent coffee grounds (A) and *Chlorella. sp.* microalgae (B) as shown in Fig. 6.1, a mixing ratio of 50:50 favoured the positive CE (6.3 wt.% or 23.0%) on biocrude yield as compared to that of 25:75 (1.3 wt.% or 4.5%) and 75:25 (2.1 wt.% or 8.2%). No significantly different CE was observed for the gas yield when changing the mixing ratio. As for the mixing ratio of 25:75 AB, its CE on SR yield was comparable with that of 50:50, however, it had a 1.3 wt.% or 3% of CE on AqP yield as compared to that of -4.7 wt.% or -11.2% for 50:50. This indicates that a high proportion of microalgae in the co-liquefied mixture favoured the AqP yield rather than biocrude yield, which is mainly because microalgae contained a high content of protein that can be readily degraded into water-soluble products. In terms of the mixing ratio of 75:25 AB, its CE on AqP yield was similar to that of 50:50, but it exhibited less desirable CE on SR yield. This suggests that a high percent of spent coffee grounds in the AB mixture inhibited the conversion pathway (from solid biomass to biocrude), resulting in a relatively low biocrude yield. Therefore, co-liquefaction of AB at a mixing ratio of 50:50 was the most desirable as it promoted the biocrude formation from biomass mixture and reduced SR and AqP yield as well.

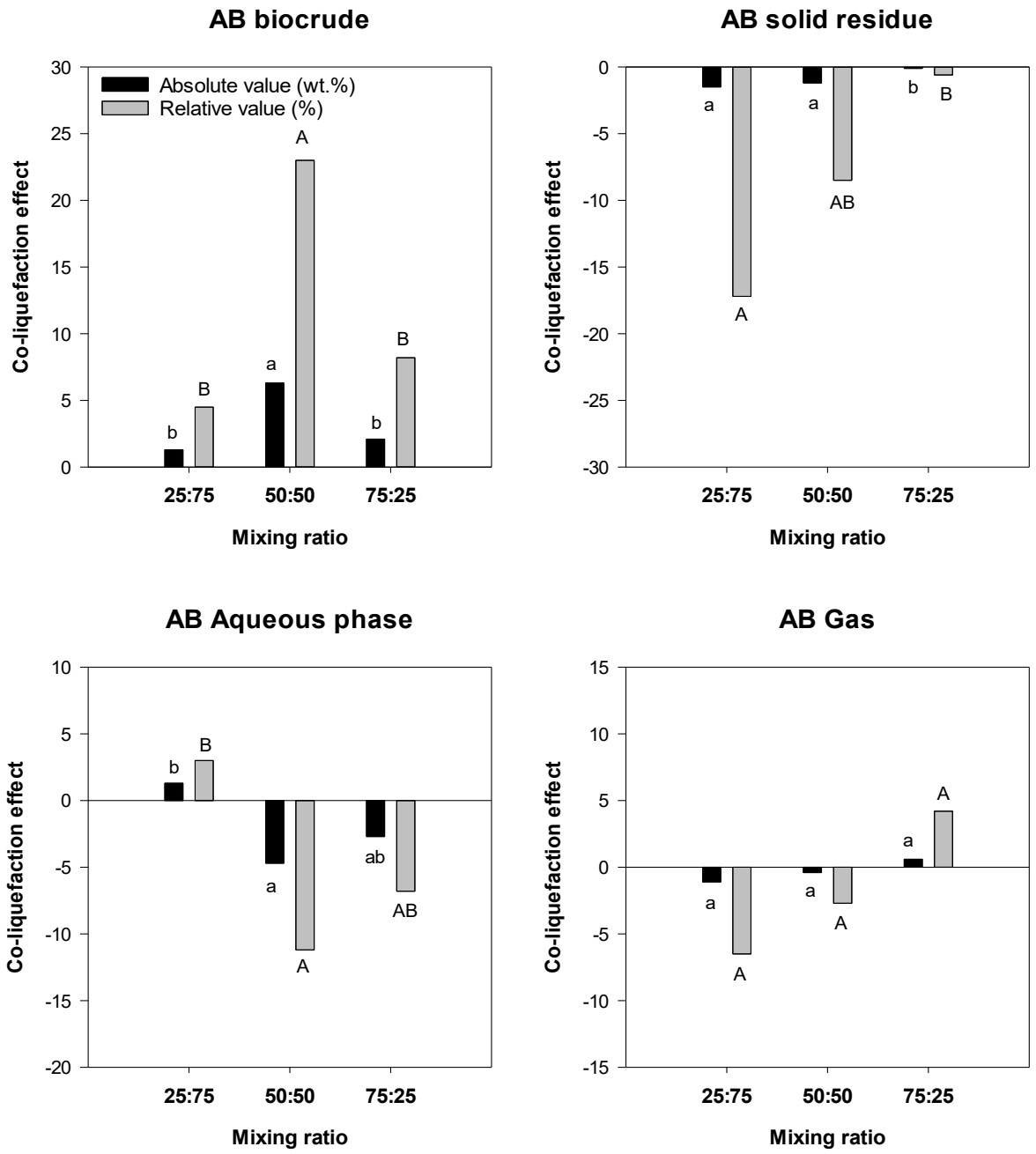

Fig. 6.1 The influence of mixing ratio on the co-liquefaction effect for spent coffee grounds (A) and *Chlorella sp.* microalgae (B). 95% confidence level was applied. Letter grouping that does not share the same letter indicates significant difference between two mean values.

In terms of the CE in the co-liquefaction of A (spent coffee grounds) and D (sawdust) as shown in Fig. 6.2, changing mixing ratios did not remarkably influence the CE on SR yield and gas yield. However, increasing the proportion of spent coffee grounds (reducing sawdust content) led to a gradual decline of positive CE (from 21.5% to 4.2%) on biocrude yield. This was evidenced by the weaker negative CE (from -13.2% to 0.7%) on AqP yield. These indicate that co-

liquefaction of AD favoured the biocrude formation from AqP products, and the extent of this favourability steadily became weaker when reducing sawdust content in the co-liquefied mixture. As mentioned in section 6.4.3, the underlying mechanism for the positive CE on biocrude yield from co-liquefaction of AD might be due to the lipid-hemicellulose and lipid-cellulose interactions, in which the fatty acids from spent coffee grounds lipid and water-soluble furfurals from sawdust hemicellulose/cellulose interacted with each other and ultimately promoted the biocrude yield. The lipid in spent coffee grounds can be easily hydrolysed into fatty acids in subcritical water, but the decomposition of hemicellulose especially cellulose in sawdust into furfurals was much harder. When only a small amount of sawdust existed in the co-liquefied mixture, the availability of furfurals was very limited, resulting in weak chemical interactions. Therefore, the biocrude formation from AqP products was suppressed when reducing the sawdust content in the co-liquefied mixture.

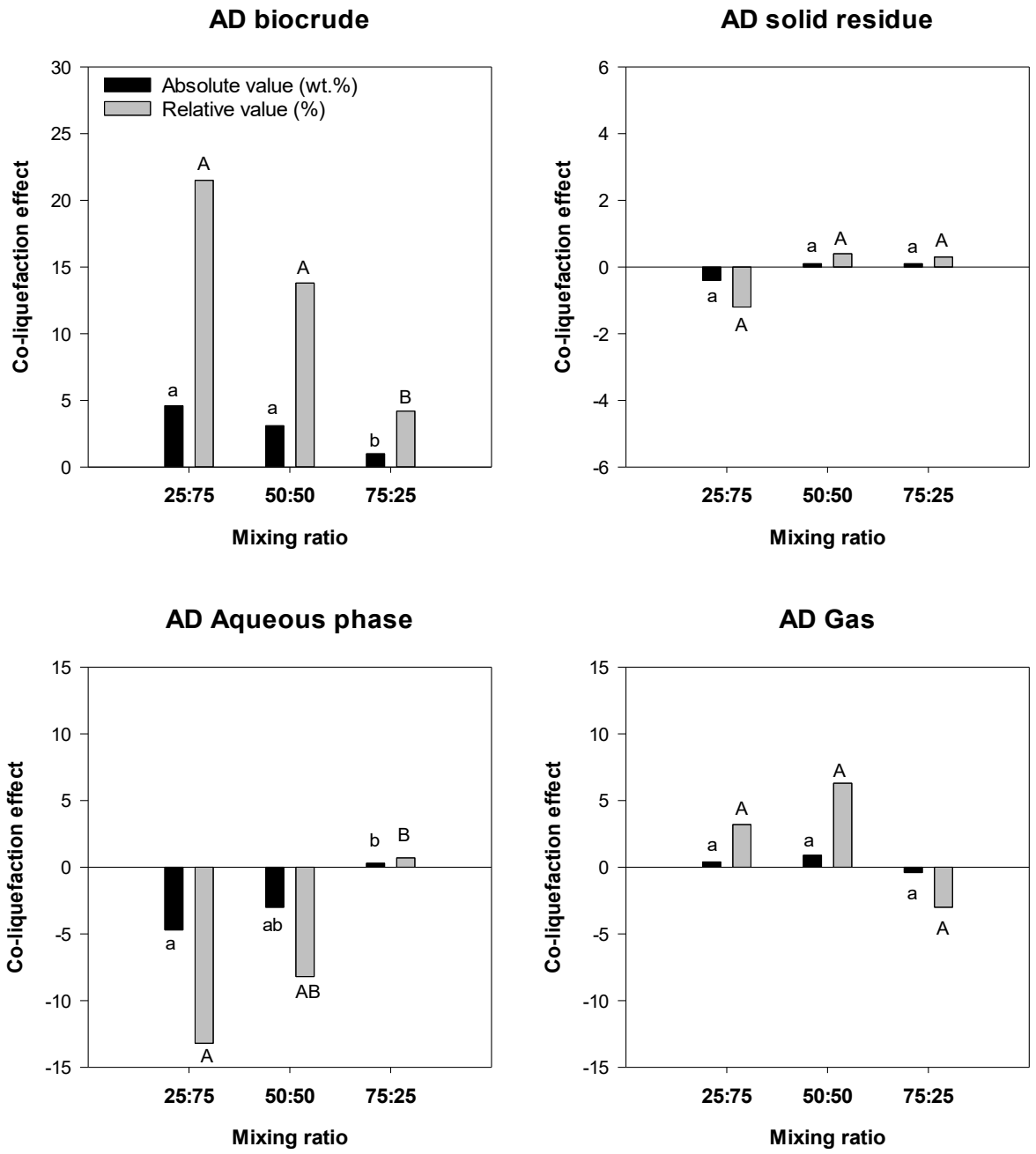

Fig. 6.2 The influence of mixing ratio on the co-liquefaction effect for spent coffee grounds (A) and sawdust (D). 95% confidence level was applied. Letter grouping that does not share the same letter indicates significant difference between two mean values.

As for the effect of mixing ratio on the CE in co-liquefaction of *Chlorella sp.* microalgae and sawdust (BD), it can be observed from Fig. 6.3 that applying different mixing ratios did not significantly impact the CE on biocrude yield and AqP yield. A different observation was reported by Feng et al. (Feng et al., 2018) that the strongest CE (2.3 wt.%) on biocrude yield was achieved at a mixing ratio of 50:50 microalgae (*Spirulina*) and a lignocellulosic plant (*Spartina alterniflora*)

at 340 °C for 30 min in water-ethanol medium. Gai et al. (2015a) co-liquefied the microalgae (*Chlorella pyrenoidosa*) with rice husk at 300 °C for 60 min in subcritical water, and found that the mixing ratio was influential for the biocrude yield, unfortunately, the co-liquefaction effects were not quantified. Although co-liquefaction of BD at different mixing ratios led to comparable CEs on biocrude yield, changing mixing ratio exhibited significant influence on the SR yield and gas yield as shown in Fig. 6.3. Increasing the proportion of protein-rich microalgae in the mixture resulted in more desirable CE on SR yield, and this was likely due to the nitrogen-containing intermediates from protein degradation enhanced the decomposition of carbohydrate-rich sawdust. As for the CE on gas yield, increasing the percent of microalgae from 25% to 75% altered the positive CE into negative CE, and unfortunately the exact reason remains unclear.

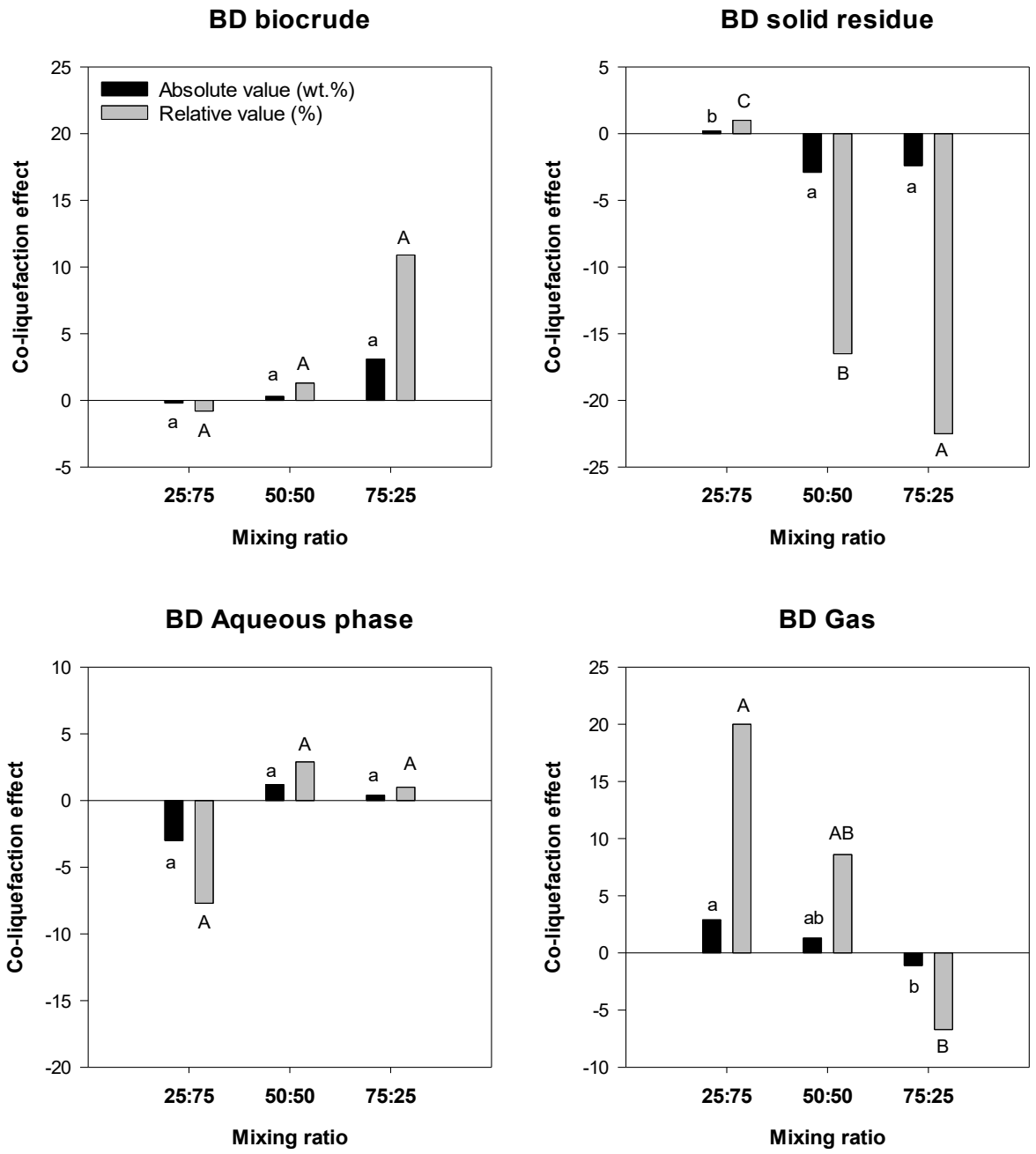

Fig. 6.3 The influence of mixing ratio on the co-liquefaction effect for *Chlorella sp.* microalgae (B) and sawdust (D). 95% confidence level was applied. Letter grouping that does not share the same letter indicates significant difference between two mean values.

The impact of mixing ratio on CE in the co-liquefaction of A (spent coffee grounds) and C (red seaweed) was presented in Fig. 6.4. It can be noticed that both the absolute and relative CE on product yield were quite low (around ±1 wt.% and ±5% respectively), and the CE on the biocrude, SR, AqP and gas yield were all not significantly affected by changing mixing ratios. Insignificant CE on biocrude yield was observed in section 6.4.3 that a mixing ratio of 50:50 was

applied, and altering the mixing ratio into 25:75 or 75:25 did not promote the CE on biocrude yield. Although co-liquefaction of AC at a mixing ratio of 50:50 led to a SE on SR yield and AE on AqP, changing mixing ratios once again exhibited limited influence on the CE for SR and AqP yield.

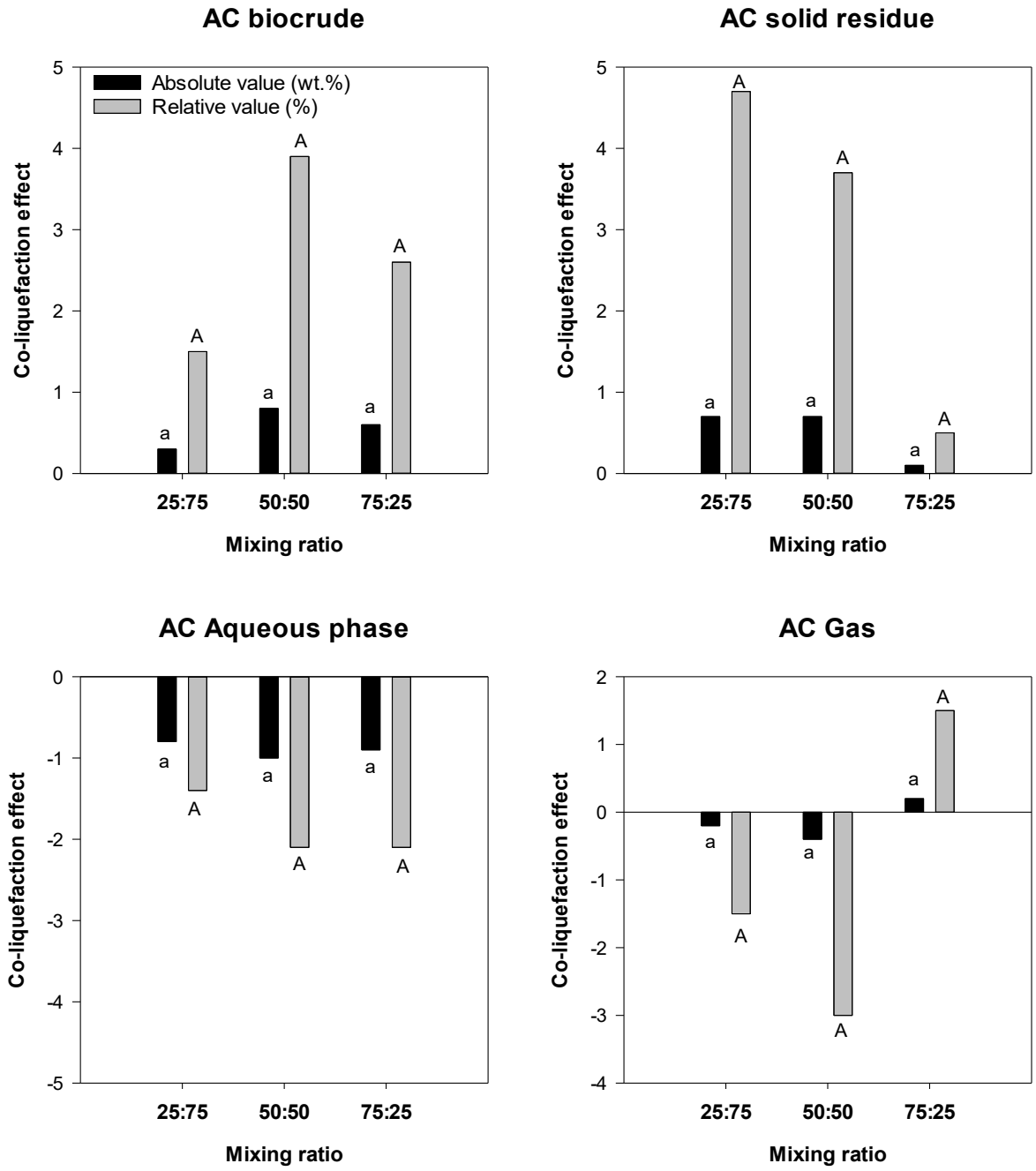

Fig. 6.4 The influence of mixing ratio on the co-liquefaction effect for spent coffee grounds (A) and red seaweed (C). 95% confidence level was applied. Letter grouping that does not share the same letter indicates significant difference between two mean values.

The influence of mixing ratio on the CE from co-processing B (*Chlorella sp.*) and C (red seaweed) was negligible for all product streams as shown in Fig. 6.5, meanwhile, co-liquefaction of BC favored the formation of AqP products at the expense of char and gas formation. Jin et al. (Jin et al., 2013) hydrothermally co-liquefied microalgae (*Spirulina platensis*) with macroalgae (*Entermorpha prolifera*) with different mixing ratios at 340 °C for 40 min, and reported that all the CE on biocrude yield were positive and a highest CE (3.2 dwt.%) was obtained at the mixing ratio of 50:50. Although the mixing ratio was considered to be influential for the CE in Jin et al. (2013), the significance of observed difference was not statistically assessed.

Referencing the insignificant impact of mixing ratio for co-liquefaction of AC (spent coffee grounds/red seaweed) as shown in Fig. 6.4, when red seaweed was used as one of co-liquefied biomass, the influence of mixing ratio on the CE is likely to be insignificant. This was confirmed by co-liquefaction of red seaweed with sawdust (CD) as shown in Fig. 6.6, in which altering mixing ratio did not significantly influence the CE on biocrude yield, AqP yield, gas yield and SR yield (except absolute CE). These observations suggested that when red seaweed was co-liquefied with other feedstocks, it behaved quite consistently regardless of varying mixing ratios. Jasiūnas et al. (2017) used high-mineral content spent mushroom compost to co-liquefied with aspen wood sawdust at different mixing ratios, and a constant CE (around -10 wt.%, daf) on biocrude yield were observed as well. This previously reported result was in agreement with co-liquefaction of CD in our study that about -2 wt.% CE on biocrude yield was observed for all three mixing ratios.

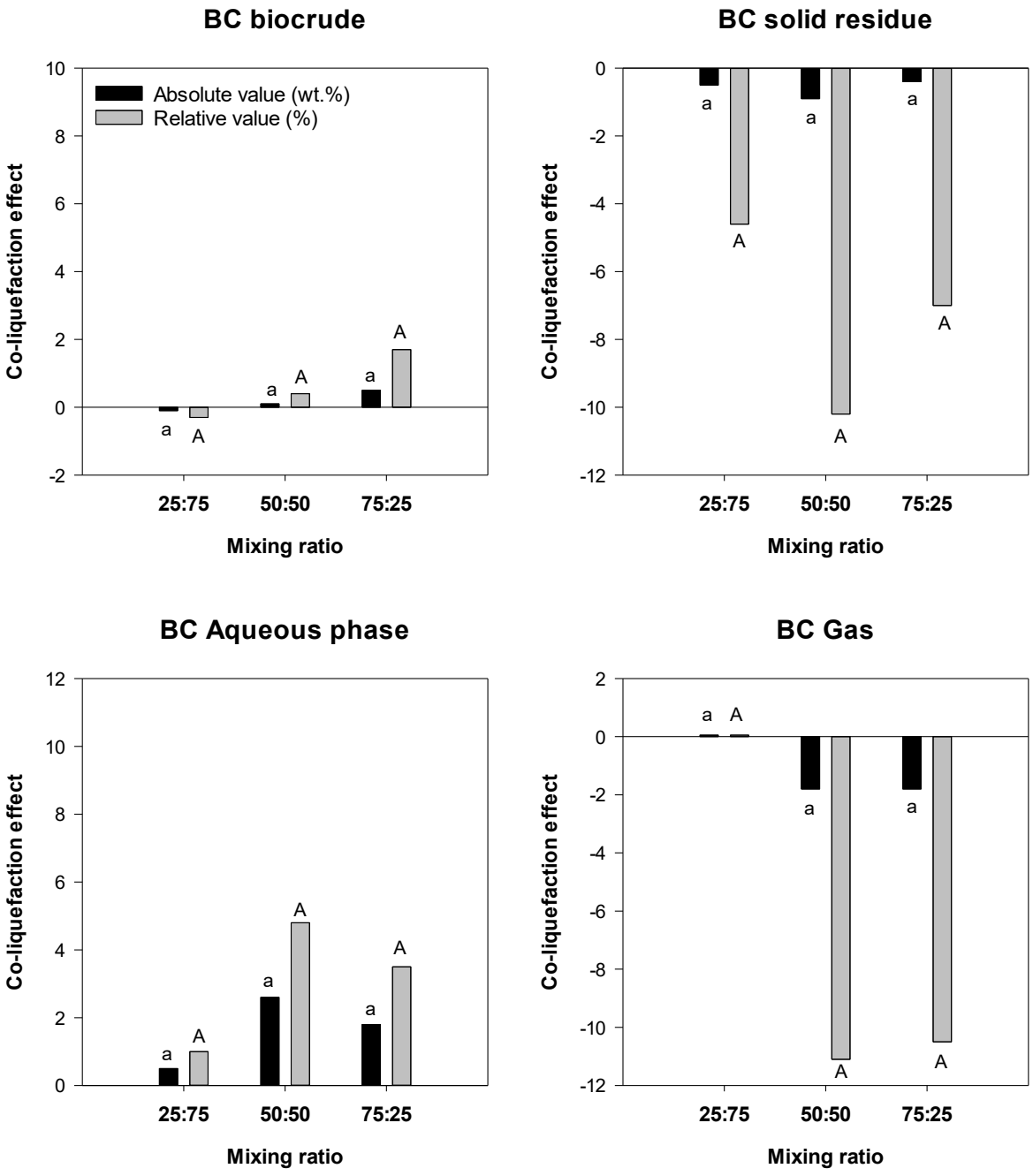

Fig. 6.5 The influence of mixing ratio on the co-liquefaction effect for *Chlorella sp.* microalgae (B) and red seaweed (C). 95% confidence level was applied. Letter grouping that does not share the same letter indicates significant difference between two mean values.

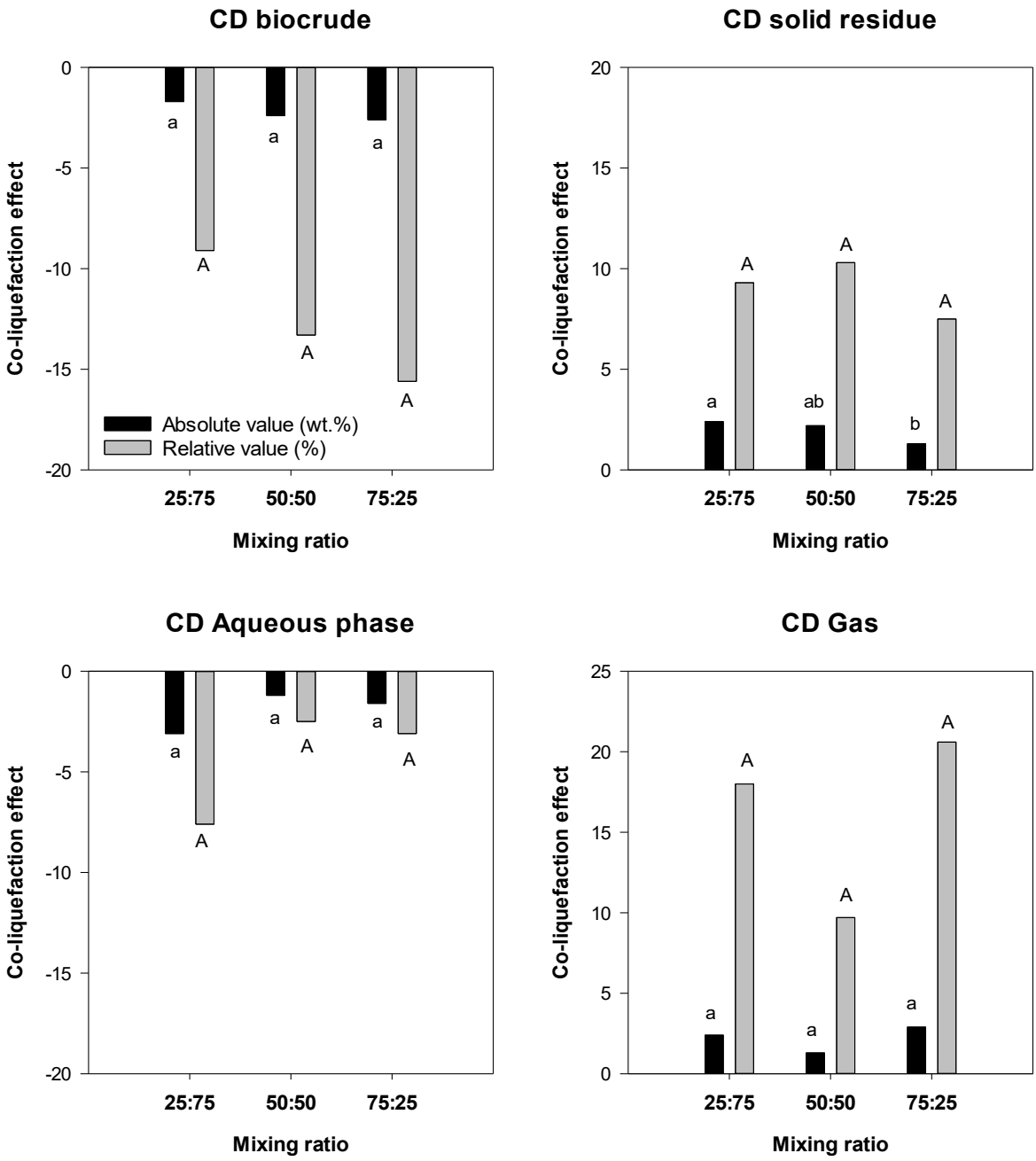

Fig. 6.6 The influence of mixing ratio on the co-liquefaction effect for red seaweed (C) and sawdust (D). 95% confidence level was applied. Letter grouping that does not share the same letter indicates significant difference between two mean values.

When an absolute CE was used as a response in co-liquefaction of CD, a mixing ratio of 50:50 and 75:25 had comparable CE (-2.9 wt.% and -2.4 wt.% respectively) on SR yield, and both of them were significantly stronger that that of 25:75 (0.2 wt.%). Interestingly, when a relative CE was employed as the response, a different result was observed, in which a mixing ratio of 50:50 and 75:25 no longer had comparable CE on SR yield instead 75:25 had significantly stronger CE

than 50:50 (-22.5% vs. -16.5% respectively). These observations indicate that using absolute CE or relative CE as response might lead to different conclusions for investigating the influence of mixing ratio on CE, as illustrated in Table 6.4.

The relative CE was calculated/standardized based on the mass-fraction-averaged value as shown in equation (6.4), and the mass-averaged value varied with the mixing ratios. For instance, the mass-averaged value of SR yield for a mixing ratio of 25:75, 50:50 and 75:25 CD was 17.1 wt.%, 21.6 wt.% and 26.1 wt.% respectively as presented in Table 6.4. Within each mixing ratio, the experimental error/variance of absolute CE was proportionally transformed by a specific mass-averaged value into relative CE, as evidenced by the identical coefficient of variation within each mixing ratio. For instance, a mixing ratio of 50:50 had a coefficient of variation of 37.07 for both absolute CE and relative CE.

With the aim to study the influence of mixing ratios by considering all three mixing ratios' data as an overall dataset, different coefficients of variations were obtained for overall absolute CE and overall relative CE (30.30 vs. 36.35 respectively). This is because the experimental error/variance of overall absolute CE was not proportionally transformed into overall relative CE by a specific mass-averaged value. Therefore, when inputting all three mixing ratios' data into statistical analysis to test whether changing mixing ratios altered the CE, using the absolute CE or relative CE as the response might lead to different conclusions. Researchers need to be aware of "trick" when studying the influence of mixing ratios on the CE.

Table 6.4 The absolute and relative co-liquefaction effect (CE) on solid residue yield from hydrothermal co-liquefaction of red seaweed and sawdust.

	Absolute CE (wt.%)	Mass-fraction-averaged value (wt.%)	Relative CE (%)
25:75	1.804	17.129	10.533
25:75	1.538	17.129	8.976
25:75	0.771	17.129	4.500
25:75	1.038	17.129	6.057
Coefficient of variation	36.38		36.40
50:50	3.033	21.633	14.022
50:50	2.833	21.633	13.097
50:50	1.433	21.633	6.626
50:50	1.600	21.633	7.396
Coefficient of variation	37.07		37.07
75:25	2.463	26.138	9.421

	Absolute CE (wt.%)	Mass-fraction-averaged value (wt.%)	Relative CE (%)
75:25	2.463	26.138	9.421
75:25	2.263	26.138	8.656
75:25	2.529	26.138	9.676
Coefficient of variation	4.74		4.75
Overall coefficient of variance	36.35		30.30

Notes:

1, equation (6.4): relative co-liquefaction effect (%) = $\left(\frac{\text{absolute co-liquefaction effect}}{\text{mass-fraction-averaged value}}\right) \times 100\%$

2, four replicates on each mixing ratio were carried out in this study.
3, three decimal place was used to ensure better data comparability

6.5 Conclusions

Binary mixtures (50:50 by mass) of four biomass feedstocks, food waste (spent coffee grounds, A), microalgae (*Chlorella. sp.*, B), marine macroalgae (red seaweed, C) and lignocellulosic biomass (sawdust, D), were hydrothermally liquefied under identical conditions. A statistical method, one-sample t-test, was used for the first time to determine the significance of the observed CE on biocrude yield, SR yield, AqP yield and gas yield. A synergistic effect on biocrude yield was observed for both co-liquefaction of AB (6.3 wt.% or 23.0%) and AD (3.1 wt.% or 13.8%), coupling with an antagonistic effect on AqP yield. Though co-liquefaction of AC, BC and BD had positive CE on biocrude yield, but they were not statistically significant when taking the experimental error into consideration. Co-liquefaction of red seaweed and sawdust (CD) led to an antagonistic effect (-2.4 wt.% or -13.3%) on biocrude yield along with a synergistic effect (2.2 wt.% or 10.3%) on SR yield, indicating that the interaction between mineral-rich red seaweed and carbohydrate-rich sawdust diminished the biocrude formation. In general, it is highly necessary to determine the significance of CE on product yield to gain confidence on the observed CE and better understand the product formation pathways during co-liquefaction.

The effect of mixing ratio on CE was also investigated in this chapter. Co-liquefaction of AB at a mixing ratio of 50:50 presented a favorable CE on biocrude yield as compared to that of 25:75 and 75:25. Co-liquefaction of AD at a mixing ratios of 25:75 or 50:50 was more desirable than 75:25 in terms of CE on biocrude yield. As for the co-liquefaction of BD, the CE on biocrude yield was not remarkably influenced by changing mixing ratios, but increasing the proportion of protein-

rich microalgae resulted in much less solid residue. It was observed that changing mixing ratios did not significantly influence the CE on product yield when red seaweed was co-liquefied with others feedstock, as demonstrated in combinations of AC, BC and CD. Coincidently, red seaweed was the only mineral-rich feedstock (29.4 wt.%) compared to other three counterparts (in the range of 0.1 -5.6 wt.%), however, the explicit role of minerals played during co-liquefaction remains unclear. It is also notable that using absolute CE or relative CE as the response in statistical analysis might lead to different conclusions when studying the mixing ratio effect on the CE, and researchers need to be aware of such a twist.

6.7 Transition section

Chapter 6 statistically evaluated the significance of co-liquefaction effect from hydrothermal co-liquefaction of a variety of biomass. The influence of mixing ratio on the CE was also investigated. Process temperature has been proved to be one of most critical variables for HTL of single feedstock, which would certainly impact co-liquefaction effect. Thus, chapter 7 aims to study the effect of temperature on co-liquefaction effect, and to explore whether the temperature effect depends on the level of mixing ratio.

Chapter 7: Co-liquefaction Effect on Product Yield: Influence of Temperature and Its Interaction with Other Variables

Current state:

A manuscript based on this chapter is under preparation.

Contribution statement:

I was responsible for raw materials collection, part of experiment design, conduction and data analysis, and manuscript preparation.

7.1 Abstract

The influence of temperature (320 °C vs. 270 °C) and whether temperature interacts with mixing ratio to affect co-liquefaction effect (CE) were explored in this chapter. A higher co-processing temperature (320 °C) led to more favourable CE on biocrude yield for spent coffee grounds/*Chlorella. sp.* and red seaweed/sawdust, regardless of mixing ratios. However, the temperature effect was dependent on the level of mixing ratio for co-liquefaction of spent coffee grounds/sawdust and *Chlorella. sp.*/sawdust. A low temperature of 270 °C was preferred to obtain more desirable CE on biocrude yield for spent coffee grounds/red seaweed at all mixing ratios of interest in this study. The CE on biocrude yield from co-liquefaction of *Chlorella. sp.*/red seaweed was not affected by either temperature or mixing ratio. When the feedstock combination was also considered as an influential factor, it exhibited much more impact on the CE as compared to that of temperature and mixing ratio. Spent coffee grounds/*Chlorella. sp.* was a favourable combination, and co-liquefying them at 320 °C with a mixing ratio of 50:50 (by mass) led to the most desirable CE (net increment of 6.3 wt.%) on biocrude yield. The loading plot from principle component analysis suggested that if there was a co-liquefaction synergism on biocrude yield, then an antagonism was likely to be observed for solid residue yield, and *vice versa*.

7.2 Introduction

Many studies on co-liquefaction have attempted to identify the co-liquefaction effect (CE, either synergistic, antagonistic or additive) on product yield. The processing temperature has been proved to be one of most critical factors for biocrude production from HTL of biomass. Nazari et al. (2017) carried out the HTL of sawdust and sludge mixture and observed the profound

temperature influence on the product yield. Likewise, Hardi et al. (2017) and Yang et al. (2016a) used response surface methodology to optimize the HTL condition for sawdust and K-cup respectively, and a significant temperature influence on the product yield was reported. These evidences encouraged us to ask: to what extend the processing temperature would affect the CE on product yield? Unfortunately, this has not been assessed in research field of hydrothermal co-liquefaction.

In terms of the statistical analysis method in co-liquefaction studies, the most commonly used one is one-factor-at-a-time method with standard deviation/error (Gai et al., 2015a; Leng et al., 2018; Zhang et al., 2011). It evaluates the effect of the studied factors separately (one-factor-at-a-time), and the observed factors' influence are called main effects. However, only evaluating the main effect could be misleading when two or more factors are involved. This is because the effect of one factor might depend on the level of another factor, termed as interaction effect or 'it depends' effect. For instance, if temperature and mixing ratio are the studied factor in a co-liquefaction study, the effect of temperature might depend on the level of mixing ratio. However, the effect of temperature and mixing ratio interaction (if exist any) on CE has not been explored yet, and using the traditional one-factor-at-a-time method limits the investigation on the "it depends" effect.

This chapter assessed the temperature influence on CE and explored whether its effect on CE depends on the mixing ratio. The binary mixtures used in this chapter were identical to those in c hapter 6. For each binary mixture, the main and interaction effects of temperature (270 °C, 320 °C) and mixing ratio (25:75, 50:50, 75:25) were determined using a 2 × 3 factorial design analysis with four replications.

7.3 Materials and methods

7.3.1 Materials

Please refer to Section 6.3.1

7.3.2 Feedstock characterization

Please refer to Section 6.3.2

7.3.3 Hydrothermal co-liquefaction processes

The applied temperature was 270 °C, and the rest was identical to that described in section 6.3.3.

7.3.4 Co-liquefaction effect calculation

Please refer to section 6.3.4

7.3.5 Data analysis

The factorial design analysis was applied to evaluate the influence of studied factors on the co-liquefaction effect. The validity of normal distribution and constant variance assumptions on the error terms was verified by examining the residuals as described in Montgomery, (2017). Once the significant effects were determined, multiple means comparison was carried out to obtain the letter grouping at 95% confidence level. Letter grouping that does not share the same letter indicates a significant difference between two mean values. In contrast, letter grouping that shares the same letter indicates non-significant difference.

7.4 Results and discussion

7.4.1 Temperature influence on HTL of individual feedstock

The biochemical compositions of four studied feedstocks (spent coffee grounds, *Chlorella sp*. microalgae, red seaweed and sawdust) were presented and detailly discussed in section 6.4.1. The temperature influence on the product yield from HTL of individual feedstock is presented in Table 7.1. It is worthwhile to mention that the product yields at 320 °C were adapted from section 6.4.2 to compare with those at 270 °C herein.

For HTL of individual spent coffee grounds, increasing temperature from 270 °C to 320 °C did not significantly influence the biocrude yield, however, much less solid residue along with higher AqP yield was observed as shown in Table 7.1. This indicates that raising temperature promoted the formation of water-soluble products from spent coffee grounds during liquefaction processes.

A significantly higher biocrude yield was obtained for the HTL of *Chlorella sp*. at 320 °C (30.7 wt.%) than that at 270 °C (21.2 wt.%), and this was further verified by a much lower SR and AqP yield at 320 °C. Brown et al. (Brown et al., 2010) also reported that increasing the processing temperature favoured the biocrude formation from HTL of *Nannochloropsis sp.,* in which 43 wt.% biocrude yield was obtained at 350 °C compared to that of 38 wt.% at 250 °C.

HTL of mineral-rich red seaweed resulted in the lowest biocrude yield among the four feedstocks studied, and increasing temperature from 270 °C to 320 °C significantly improved the biocrude yield from 8.9 wt.% to 15.0 wt.%. The promoted biocrude formation at 320 °C was

coupled with much lower SR and AqP yield. These data were comparable with that in the study conducted by Zhou et al. (2010), in which a marine macroalgae (*Enteromorpha prolifera*) was hydrothermally liquefied at varied temperature (220 °C to 320 °C) for 10 min.

In terms of the temperature influence on HTL of sawdust, changing temperature seems to have negligible influence on the SR and AqP yield as shown in Table 7.1, but a lower biocrude yield was observed at 320 °C (20.6 wt.%) as compared to that at 270 °C (24.7 wt.%). This is likely due to that there was a temperature threshold during HTL of sawdust, after which the biocrude yield began to decrease. This was in agreement with other related studies (Zhu et al., 2015; Xu and Lad, 2008).

Table 7.1 Temperature influence (270 °C vs. 320°C) on the product yield (wt.%) from hydrothermal liquefaction of individual biomass. Significant difference was shown in bold.

Product yield (wt.%)	Spent coffee grounds		*Chlorella sp.*		Red seaweed		Sawdust	
	270 °C	320 °C	270 °C	320 °C	270 °C	320 °C	270 °C	320 °C
Biocrude	21.9	24.5	**21.2**	**30.7**	**8.9**	**15.0**	**24.7**	**20.6**
Solid residue	**32.7**	**23.5**	**9.5**	**4.1**	**16.7**	**12.6**	29.1	30.6
Aqueous phase[a]	**30.4**	**37.0**	**53.4**	**47.5**	**63.8**	**58.2**	35.1	35.4
Gas[b]	15.1	15.1	16.0	17.8	10.7	14.2	11.1	13.3

Note: a, Aqueous phase yield = 100 – Biocrude yield – Solid residue yield – Gas yield

b, the normality test was not satisfactory even though the data transformation has been attempted, and therefore the significance of the value might be biased.

7.4.2 Temperature influence on co-liquefaction effect

7.4.2.1 Analysis of Variance (ANOVA)

The influence of temperature on the co-liquefaction effect (CE) were further explored, as well as how interaction between temperature and mixing ratio influences the CE. For the six combinations (AB, AC, AD, BC, BD and CD), the results were statistically analyzed as shown in Table 7.2.

It can be seen from Table 7.2 that co-liquefaction of spent coffee grounds and microalgae (AB) was not as sensitive to temperature as to mixing ratio, because only relative CE on SR yield and absolute CE on gas yield were significantly influenced by temperature. The temperature was observed to interact with the mixing ratio at a marginally significant level for absolute CE on biocrude yield and relative CE on SR yield. The more detailed discussions were provided in section

7.4.2.2. Different from co-liquefaction of AB, only the main effects were observed for co-liquefaction of AC, and co-liquefaction of AD was not sensitive to mixing ratio at all. Co-liquefaction of BC had comparable responses to the temperature and mixing ratio compared to that of HTL of CD, in which the CE on SR yield were significantly influenced by temperature, mixing ratio and their interaction. Co-liquefaction of BD was also highly dependent on the applied processing conditions. With knowing the significance of temperature, mixing ratio and their interaction influence on the CE, more detailed result interpretation and discussion were provided in the following section.

Table 7.2 ANOVA p-values for the temperature and mixing ratio influence on co-liquefaction effect (CE).

		CE on biocrude yield		CE on SR yield		CE on AqP yield		CE on gas yield	
	Source of variation	Abs (wt.%)	Rel (%)	Abs (wt.%)	Rel (%)	Abs (wt.%)	Rel (%)	Abs (wt.%)	Rel (%)
AB	Temp	0.635	0.700	0.203	**0.010**	0.131	0.130	**0.025**	0.20
	Ratio	**0.014**	**0.024**	**0.007**	**0.001**	**0.030**	**0.038**	**0.05**	**0.049**
	Temp*ratio	**0.098**	0.15	0.605	**0.073**	0.102	0.125	0.549	0.421
AC	Temp	0.148	**0.061**	**0.000**	**0.000**	0.190	0.229	**0.015**	**0.009**
	Ratio	0.513	0.749	**0.001**	**0.006**	0.687	0.844	0.176	0.124
	Temp*ratio	0.686	0.797	0.103	0.326	0.647	0.759	0.692	0.571
AD	Temp	**0.006**	**0.005**	**0.000**	**0.000**	0.244	0.316	0.304	0.310
	Ratio	0.180	0.137	0.351	0.372	0.123	0.150	0.573	0.609
	Temp*ratio	**0.025**	**0.019**	0.790	0.803	0.192	0.216	0.925	0.929
BC	Temp	0.367	0.348	**0.000**	**0.000**	0.547	0.453	0.999	0.829
	Ratio	0.828	0.830	**0.012**	**0.034**	0.442	0.431	**0.025**	**0.036**
	Temp*ratio	0.977	0.956	**0.015**	**0.009**	0.862	0.835	0.862	0.768
BD	Temp	**0.000**	**0.000**	**0.000**	**0.000**	**0.000**	**0.000**	0.632	0.356
	Ratio	**0.000**	**0.000**	**0.000**	**0.000**	**0.009**	**0.002**	**0.001**	**0.000**
	Temp*ratio	**0.045**	**0.02**	**0.000**	**0.094**	0.569	0.562	0.290	0.384
CD	Temp	**0.079**	**0.038**	**0.000**	**0.000**	0.666	0.742	0.585	0.850
	Ratio	0.792	0.337	**0.000**	**0.000**	0.733	0.506	**0.085**	**0.051**
	Temp*ratio	0.680	0.953	**0.003**	**0.014**	0.535	0.511	0.135	**0.071**

Note: A = spent coffee grounds, B = microalgae, C = red seaweed, D = sawdust, SR = solid residue, AqP = aqueous phase, abs = absolute, rel = relative, temp = temperature, ratio = mixing ratio.

7.4.2.2 Influence on relative co-liquefaction effect (CE)

Since using the relative CE (%) can prevent the inconsistency of the basis that is used to define yield, it was utilized as the response in this section. The influence of process variables on the CE for co-liquefaction of spent coffee grounds and microalgae (AB) was presented in Table 7.3. The CE on biocrude yield, AqP yield and gas yield was not significantly influenced by varying

temperature for the co-liquefaction of AB. Therefore, the mixture of AB behaved consistently under different processing temperatures. Although the CE on biocrude yield was sensitive to mixing ratio, the effect of temperature did not depend on the applied mixing ratio (p-value = 0.15 > 0.05, insignificant interaction of temperature and mixing ratio). As for the CE on SR yield, a much stronger CE was observed for 320 °C (-17.2%) than 270 °C (-5.0%) at a mixing ratio of 25:75, however, a comparable CE was observed for 320°C and 270 °C at other mixing ratios (50:50 and 75:25). In other words, the influence of temperature depended on the level of mixing ratio for the CE on SR yield. Therefore, for co-liquefaction of AB, the most favourable CE on SR yield can be obtained at 320 °C and 25:75 (-17.2%).

Table 7.3 The temperature and mixing ratio influence on co-liquefaction effect (CE) from spent coffee grounds and *Chlorella sp*. microalgae mixture.

		25:75	50:50	75:25
Biocrude	270 °C 320 °C	10.1 b	20.0 a	7.6 b
SR	270 °C	-5.0 ab	-4.6 ab	0.0 a
	320 °C	-17.2 c	-8.5 b	-0.6 a
AqP	270 °C 320 °C	1.4 a	-6.7 b	-4.0 ab
Gas	270 °C 320 °C	-13.8 a	-7.1 ab	-1.5 b

Notes: SR = solid residue; AqP = aqueous phase; Letter grouping that does not share the same letter indicates significant difference between two mean values.

As for co-liquefaction of spent coffee grounds and red seaweed (AC), no significant interaction between temperature and mixing ratio was observed as shown in Table 7.4. The CE on biocrude yield was affected by temperature at a marginally significant level (p-value = 0.061), in which a lower temperature (270 °C) favoured the CE (8.6%) on biocrude yield. This was confirmed by a stronger CE (negative) on SR yield at 270 °C compared to that at 320 °C. The enhanced biocrude formation along with the inhibited solid residue from co-liquefaction of AC at 270 °C might be caused by a high content of minerals in red seaweed. It is plausible that the soap formation between minerals (e.g., K^+) and lipid in spent coffee grounds was diminished at lower temperature, and therefore led to a favourable CE on biocrude yield at 270 °C. The inhibition on soap formation at lower temperature has been observed previously (Yang et al., 2019a). The CE on gas yield at 270 °C (16.7%) was much higher than that at 320 °C (1.3%), however, the CE on AqP yield was not affected by changing temperature even though the gases are usually considered to originate

from aqueous phase containing the volatile and water-soluble chemicals. Therefore, the reason for the stronger CE on gas yield at 270 °C remains unclear.

Table 7.4 The temperature and mixing ratio influence on co-liquefaction effect (CE) from spent coffee grounds and red seaweed mixture.

		25:75	50:50	75:25
Biocrude	270 °C	8.6 a		
	320 °C	2.7 b		
SR	270 °C	-4.2 b		
	320 °C	2.9 a		
	270 °C 320 °C	0.3 a	1.3 a	-3.6 b
AqP	270 °C 320 °C	-3.34		
Gas	270 °C	16.7 a		
	320 °C	1.3 b		

Notes: SR = solid residue; AqP = aqueous phase; Letter grouping that does not share the same letter indicates significant difference between two mean values.

In terms of co-liquefaction of spent coffee grounds and sawdust (AD), temperature and mixing ratio interactively influenced the CE on biocrude yield as presented in Table 7.5. At the mixing ratio of 25:75, a strong CE (21.5%) on biocrude yield was observed for 320 °C, but a -2.9% CE was observed for 270 °C; insignificant difference was observed between 270 °C and 320 °C at other mixing ratios. This means that the effect of temperature on the CE was dependent on the level of mixing ratio. A highest CE (21.5%) on biocrude yield can be obtained at 320 °C with a mixing ratio of 25:75 for co-liquefaction of AD. It can also be noticed that the formation of solid residue at 320 °C was less intensive than that at 270 °C. These observations were likely due to that a higher temperature promoted the decomposition of carbohydrate-rich sawdust, in which the generated intermediates interacted with the lipid in spent coffee grounds, ultimately led to a high CE (positive) on biocrude formation. The hemicellulose-lipid and cellulose-lipid interaction in subcritical water have been proved to positively contribute to the biocrude formation (Yang et al., 2018b). Both temperature and mixing ratio did not influence the CE on AqP yield and gas yield for the co-liquefaction of AD in this study.

Table 7.5 The temperature and mixing ratio influence on co-liquefaction effect (CE) from spent coffee grounds and sawdust mixture.

		25:75	50:50	75:25
Biocrude	270 °C	-2.9 b	0.5 b	1.16 b
	320 °C	21.5 a	8.8 b	0.4 b

		25:75	50:50	75:25
SR	270 °C	6.8 a		
	320 °C	-0.2 b		
AqP	270 °C	-5.3		
	320 °C			
Gas	270 °C	-1.9		
	320 °C			

Notes: SR = solid residue; AqP = aqueous phase; Letter grouping that does not share the same letter indicates significant difference between two mean values.

Opposite to co-liquefaction of AD, neither temperature nor mixing ratio was influential for the CE on biocrude yield for co-liquefaction of BC as illustrated in Table 7.6. However, the CE on SR yield were very sensitive to the temperature and mixing ratio for co-liquefaction of BC. The influence of temperature on the biocrude yield from co-liquefaction of microalgae (*Spirulina platensis*) and macroalgae (*Entermorpha prolifera*) was also reported to be much less profound than on SR yield (Jin et al., 2013). Negative CE on SR yield was observed when co-processing BC at 320 °C regardless of mixing ratios; but if 270 °C was applied to co-process BC, a 17.3% CE on SR yield was observed at a mixing ratio of 75:25 BC. This indicates that at a high temperature with a high proportion of microalgae in BC mixture, the repolymerisation of break-down intermediates was favoured to form more solid residues.

Table 7.6 The temperature and mixing ratio influence on co-liquefaction effect (CE) from *Chlorella sp*. microalgae and red seaweed mixture.

		25:75	50:50	75:25
Biocrude	270 °C	-1.8		
	320 °C			
SR	270 °C	-2.7 bc	6.3 b	17.3 a
	320 °C	-4.6 c	-10.2 c	-7.0 c
AqP	270 °C	2.4		
	320 °C			
Gas	270 °C	1.9 a	-12.2 b	-12.8 b
	320 °C			

Notes: SR = solid residue; AqP = aqueous phase; Letter grouping that does not share the same letter indicates significant difference between two mean values.

Microalgae and lignocellulosic biomass are the two mostly studied feedstock for biocrude production from HTL of biomass, mainly due to the fast-growing rate of microalgae and the large availability of lignocellulosic biomass (e.g., forest/agriculture wastes). Therefore, more studies on co-liquefaction of microalgae and lignocellulosic biomass were carried out than co-liquefaction of other feedstocks (Gai et al., 2015a; Feng et al., 2018; Hu et al., 2018). Although the influence of

temperature and mixing ratio was investigated in the previous studies, no attempt has been made to explore whether the effect of temperature depended on the level of mixing ratio. Our experimental results showed that the temperature and mixing ratio did interactively affect the CE on biocrude yield in the co-liquefaction of *Chlorella sp*. microalgae and sawdust (BD) as shown in Table 7.7.

At a mixing ratio of 75:25, there was a comparable CE on biocrude yield for 270 °C and 320 °C; however, at a mixing ratio of 25:75 or 50:50, a more desirable CE was observed at 320 °C compared to that at 270 °C. This was in agreement with the results from Feng et al, (2018) that CE on biocrude yield was favoured at higher temperature when co-liquefying microalgae (*Spirulina*) and macroalgae (*Spatina alterniflora*) at a mixing ratio of 50:50. As for the CE on SR yield in this study, only a marginally significant interaction of temperature and mixing ratio was observed (p-value = 0.098 in Table 7.2), and a -22.5% CE can be obtained at 320 °C and 75:25 BD.

According to the results above, it can be concluded that 320 °C with a mixing ratio of 75:25 appeared to be the best processing condition for co-liquefaction of BD (a 10.9% CE on biocrude yield and -22.5% CE on SR yield). This might be caused by a basic environment created by protein decomposition, which promoted the biocrude formation *via* retro-aldol condensation of intermediates from carbohydrate-rich sawdust decomposition. The retro-aldol condensation has been proved to likely occurs at the basic condition (Yang et al., 2018b; Déniel et al., 2017b).

Table 7.7 The temperature and mixing ratio influence on co-liquefaction effect (CE) from *Chlorella sp*. microalgae and sawdust mixture.

		25:75	50:50	75:25
Biocrude	270 °C	-24.8 d	-12.2 c	8.2 ab
	320 °C	-0.8 b	1.3 ab	10.9 a
SR	270 °C	48.5 a	37.9 b	26.1 c
	320 °C	1.0 d	-16.5 e	-22.5 e
AqP	270 °C	-12.8 b		
	320 °C	-1.3 a		
	270 °C 320 °C	-13.0 b	-4.4 a	-3.7 a
Gas	270 °C 320 °C	15.9 a	6.7 b	-5.2 c

Notes: SR = solid residue; AqP = aqueous phase; Letter grouping that does not share the same letter indicates significant difference between two mean values.

As seen from Table 7.8, co-liquefaction of red seaweed with sawdust resulted in a -20.9% and -12.7% CE on biocrude yield for 270 °C and 320 °C respectively. This can be confirmed by the higher positive CEs on SR yield at 270 °C than that at 320 °C. These observations were opposite to co-liquefaction of AC that red seaweed was also involved, in which a low temperature favoured the biocrude formation and inhibited SR yield. These suggested that the difference between spent coffee grounds and sawdust played certain roles during co-liquefaction processes. When co-processing spent coffee grounds and red seaweed, a low temperature can diminish the soap formation from lipid in spent coffee grounds and minerals in red seaweed, which therefore contributed a high biocrude yield. However, higher temperature was preferred for co-liquefaction of red seaweed and sawdust to readily decompose carbohydrate-rich sawdust. Sintamarean et al. (2017) attempted to co-liquefy the willow with red, green and brown seaweed, but the influence of temperature and mixing ratio on the CE was not studied. Instead, they aimed to improve the pumpability of willow slurries in continuous HTL processes by co-liquefying willow with macroalgae.

Table 7.8 The temperature and mixing ratio influence on co-liquefaction effect (CE) from red seaweed and sawdust mixture.

		25:75	50:50	75:25
Biocrude	270 °C	-20.9 b		
	320 °C	-12.7 a		
SR	270 °C	21.9 a	24.6 a	14.1 b
	320 °C	9.3 c	10.3 c	7.5 c
AqP	270 °C	-4.8		
	320 °C			
Gas	270 °C	1.0 c	18.4 abc	32.0 a
	320 °C	18.0 abc	9.7 bc	20.6 ab

Notes: SR = solid residue; AqP = aqueous phase; Letter grouping that does not share the same letter indicates significant difference between two mean values.

Overall, the relative CE was used as the response in this section, and a processing temperature of 320 °C and a mixing ratio of 25:75 or 50:50 were desirable for co-liquefaction of AB. Mixing ratio was not influential for co-liquefaction of AC and the low temperature (270 °C) favoured the CE on biocrude and SR yield. Differently, a high temperature was preferred for co-liquefaction of CD even though the undesirable CE on biocrude and SR yield were observed. As for the temperature influence on co-liquefaction of AD and BD, its effect on the CE (biocrude yield) depended on the level of mixing ratio. A high CE of 21.5% on biocrude yield can be obtained at

320 °C with a mixing ratio of 25:75 for co-liquefaction of AD, and this was slightly different from co-liquefaction of BD that 320 °C with a mixing ratio of 75:25 appeared to be the best processing condition. Interestingly, the CE on biocrude yield from co-liquefaction of BC was affected neither by temperature nor by mixing ratio in this study. It is challenging to conclude a generally favorable co-processing condition for six feedstock combinations, nor to suggest a combination that had the best co-liquefaction performance, mainly due to their largely different biochemical compositions.

7.4.3 Three-way interaction

The influence of temperature and how it interacts with mixing ratio to affect the CE in HTLs of AB, AC, AD, BC, BD and CD were investigated individually in Section 7.4.2. However, if the type of mixed feedstock is coupled in as a studied factor, then questions arise: does the type of mixed feedstock play a more important role than temperature and mixing ratio regarding the CE? and does the type of mixed feedstock significantly interact with temperature and mixing ratio to influence the CE? To answer the questions, a 2 × 3 × 6 factorial design analysis was performed, and the p-values from ANOVA were presented in Table 7.9.

From Table 7.9, it can be seen that CE was more sensitive to the type of mixed feedstock than temperature and mixing ratio as its p-values were all lower than 0.05. Although the temperature and mixing ratio interaction was determined to be significant for relative CE on biocrude yield in HTL of AD and BD in Section 7.4.2, their interaction was no longer significant when the type of mixed feedstock was taken into consideration as shown in Table 7.9. Instead, the temperature×type and ratio×type interaction became significant, and these further confirmed that the type of mixed feedstock had the strongest influence on the CE. As for the three-way interaction (temperature×ratio×type), the absolute CE on biocrude yield, the absolute CE on SR yield and relative CE on SR yield were significantly influenced by the three-way interaction. Since the biocrude is the primary product from HTL of biomass, how the absolute CE on biocrude yield was influenced by the three-way interaction was plotted in Fig. 7.1 and discussed as follows. It was observed from Fig. 7.1 that co-liquefaction of AC, BC and CD were less sensitive to the alteration of temperature and mixing ratio than the rest three combinations (AB, AD and BD). At a mixing ratio of 25:75, co-liquefaction of AD (4.6 wt.% CE on biocrude yield) was more favorable than other feedstock combinations regardless of temperature. Co-liquefaction of spent coffee grounds

and microalgae (AB) at a mixing ratio of 50:50 and 320 °C had the strongest CE (6.3 wt.%) on biocrude yield in this study, and no feedstock combination stood out at a mixing ratio of 75:25.

Table 7.9 ANOVA p-values that show the significance of the main and interaction effects on co-liquefaction effect (CE). Significant effects are shown in bold.

	CE on biocrude yield		CE on SR yield		CE on AqP yield		CE on gas yield	
Source of variation	Abs (wt.%)	Rel (%)	Abs (wt.%)	Rel (%)	Abs (wt.%)	Rel (%)	Abs (wt.%)	Rel (%)
Temp	**0.001**	**0.001**	**0.001**	**0.001**	**0.058**	0.103	0.261	0.594
Ratio	0.113	0.563	**0.001**	**0.088**	0.116	0.057	0.128	0.225
Type	**0.001**	**0.001**	**0.001**	**0.001**	**0.001**	**0.001**	**0.001**	**0.001**
Temp*Ratio	**0.058**	0.136	**0.001**	0.207	0.874	0.828	0.442	0.939
Temp*Type	**0.001**	**0.002**	**0.001**	**0.001**	**0.001**	**0.001**	**0.011**	**0.004**
Ratio*Type	**0.001**	**0.001**	**0.001**	**0.001**	**0.047**	**0.013**	**0.002**	**0.002**
Temp*Ratio*Type	**0.051**	0.157	**0.001**	**0.001**	0.315	0.243	0.908	0.480

Notes: SR = solid residue; AqP = aqueous phase; abs = absolute; rel = relative; temp = temperature; ratio = mixing ratio; Type = the type of mixed feedstock

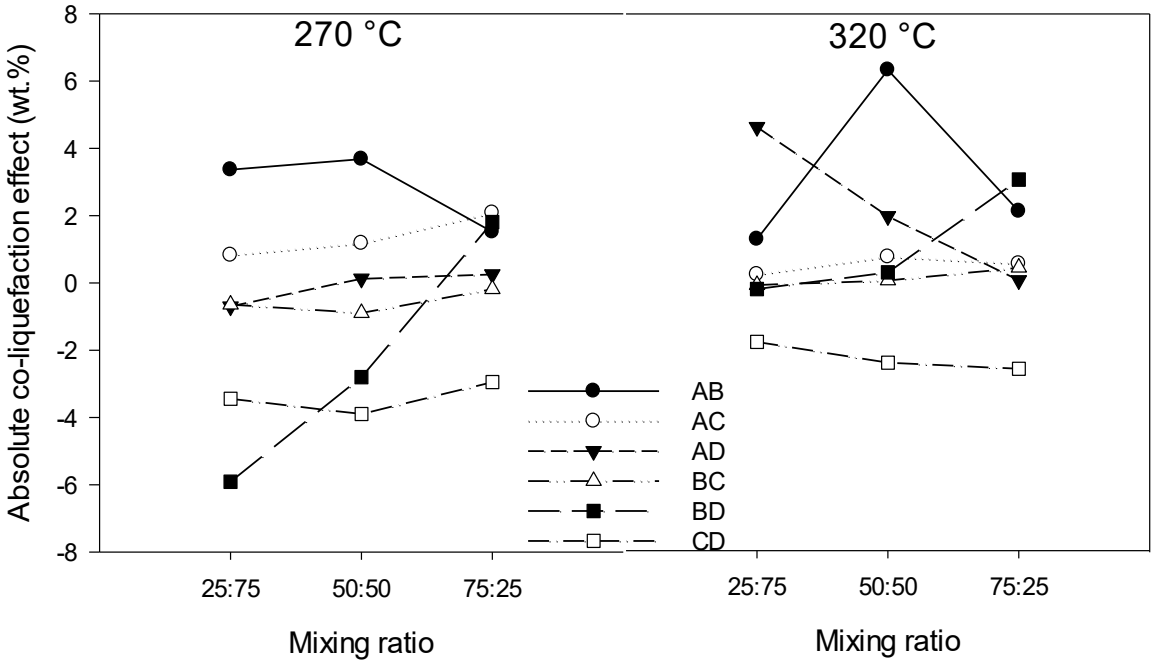

Fig. 7.1 The three-way interaction for the absolute co-liquefaction effect on biocrude yield.

7.4.4 Principle component analysis on co-liquefaction effect

Since a large set of data was involved in this study, principle component analysis (PCA) was applied to gain an overview on the influence of the type of mixed feedstock (combination), mixing ratio and temperature on the CE. Fig. 7.2 showed that AB and CD can be readily separated based on the first component, indicating that co-liquefaction of AB and CD were largely different with each other in terms of CE. This further verified the obtained results in Section 7.4.2 and 7.4.3. The CE from other studied combinations were considered to be comparable as they were clustered together in Fig. 7.2. Similarly, the mixing ratios (25:75, 50:50, 75:25), as well as temperatures (250 °C and 270 °C) were clustered together as shown in Fig. 7.3a and Fig. 7.3b respectively. These PCA results echoed the statement in Section 7.4.3. that the type of mixed feedstock had a stronger impact on the CE than mixing ratio and temperature.

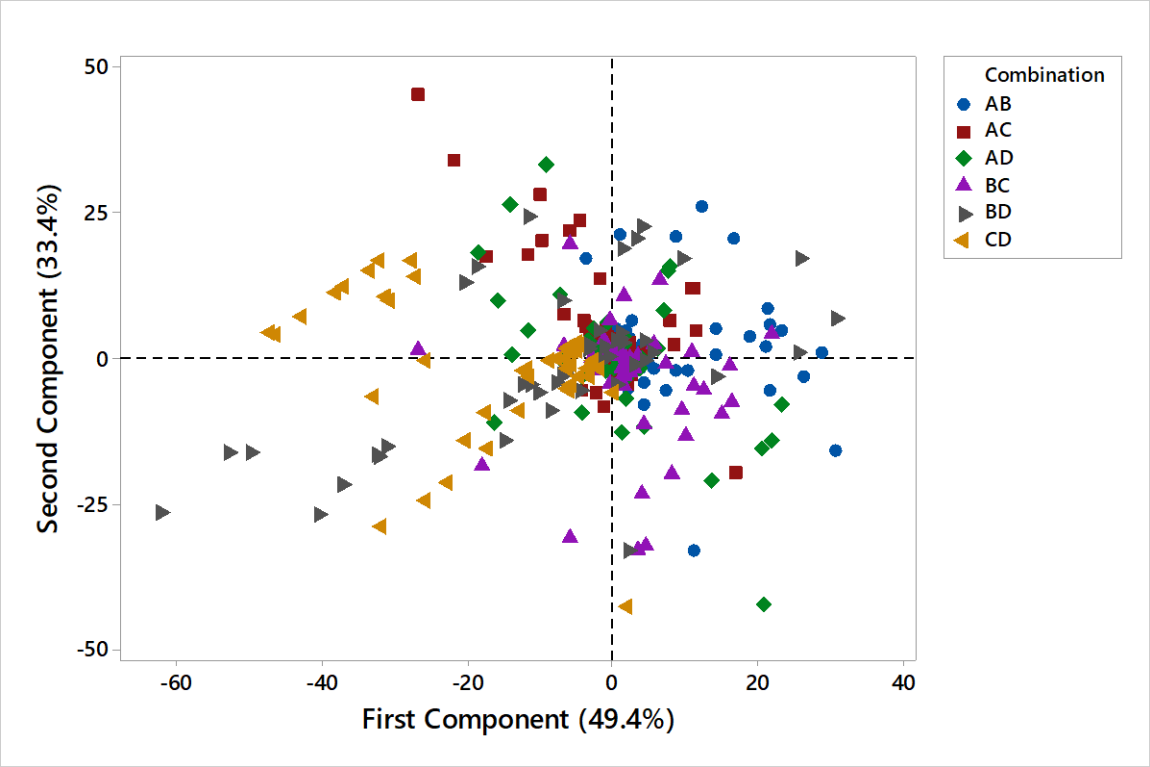

Fig. 7.2 The score plot from principle component analysis (PCA) for investigating the influence of feedstock combinations on co-liquefaction effect. A, B, C and D denotes spent coffee grounds, *Chlorella sp*. microalgae, red seaweed and sawdust respectively.

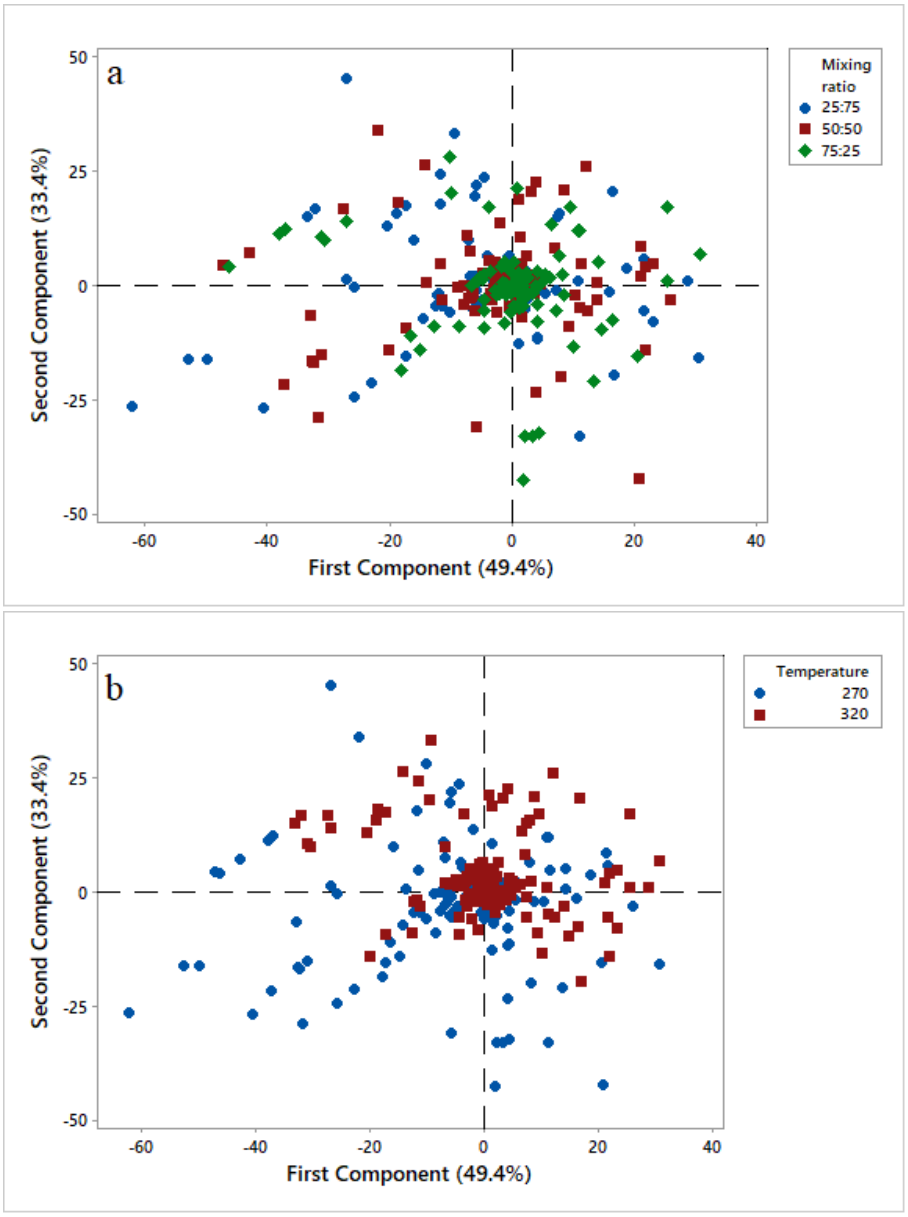

Fig. 7.3 The score plot from principle component analysis (PCA) for investigating the influence of mixing ratio (a) and temperature (b) on co-liquefaction effect.

Loading plot from PCA was also generated to study the correlation among studied variables, CE on biocrude, SR, AqP and gas yield as shown in Fig. 7.4. It can be seen that biocrude and SR were negatively correlated as they were positioned on the opposite sides. This indicates that if a positive CE exists for biocrude yield, a negative CE is likely to be observed for SR yield, and vice versa. A similar pattern was observed for AqP and gas yield.

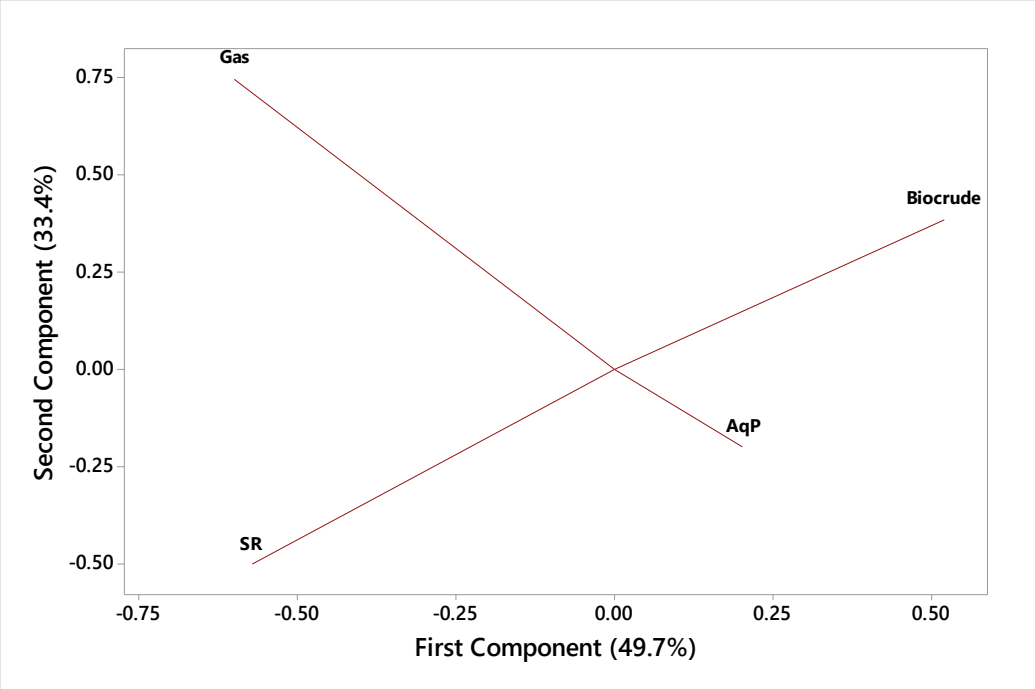

Fig. 7.4 The loading plot from principle component analysis (PCA) for investigating the correlation between co-liquefaction effect on biocrude yield, solid residue (SR) yield, aqueous phase (AqP) yield and gas yield.

7.5 Conclusions

This chapter explored the temperature influence and how it interacts with mixing ratio to affect co-liquefaction effect (CE). Prior to studying the temperature influence on CE, its influence on HTL of single feedstock was assessed. It was found that increasing temperature from 270 °C to 320 °C significantly improved the biocrude yield for HTL of *Chlorella. sp.* and red seaweed, but the biocrude yield from spent coffee grounds remained constant and a significant decline in the biocrude yield was observed for sawdust.

In term of the CE on biocrude yield, a relatively high co-processing temperature (320 °C vs. 270 °C) was favourable for spent coffee grounds/*Chlorella. sp.* and red seaweed/sawdust, regardless of mixing ratios; however, the temperature effect was dependent on the level of mixing ratio for co-liquefaction of spent coffee grounds/sawdust and *Chlorella. sp.*/sawdust, suggesting the existence of interaction between temperature and mixing ratio. As for the co-liquefaction of spent coffee grounds/red seaweed, a lower temperature (270 °C) led to more desirable CE on biocrude yield, and no interaction between temperature and mixing ratio was observed. The CE on

biocrude yield from co-liquefaction of *Chlorella. sp.*/red seaweed was not affected by either temperature or mixing ratio.

When the feedstock combination was also considered as a factor, and a factorial design analysis revealed that feedstock combination was much more influential than temperature and mixing ratio in terms of CE on product yield. This was further confirmed by the principle component analysis (PCA) that spent coffee grounds/*Chlorella. sp*. and red seaweed/sawdust can be readily separated by the first principle component. Spent coffee grounds/Chlorella. sp. was a favourable combination, and co-liquefying them at 320 °C with a mixing ratio of 50:50 (by mass) led to the most desirable CE (net increment of 6.3 wt.%) on biocrude yield. Moreover, the loading plot from PCA suggested that if there was a positive CE on biocrude yield, then a negative CE was likely to be observed for solid residue yield, and *vice versa*. A similar pattern was observed for the aqueous phase yield and gas yield as well.

7.7 Transition section

Chapter 7 studied the influence of temperature and its interaction with other factors (mixing ratio and even feedstock combination) on the co-liquefaction effect. In addition to co-liquefaction of different types of biomass to improve biocrude yield, process intensification techniques (e.g., microwave irradiation) might also enhance biocrude formation. Unfortunately, microwave-assisted HTL (MW-HTL) of biomass has been rarely investigated. Therefore, Chapter 8 focuses on evaluating the technical feasibility of MW-HTL of spent coffee grounds that has been proven to be a desirable feedstock for biocrude production through HTL.

Chapter 8: Microwave-assisted Hydrothermal Liquefaction of Spent Coffee Grounds

Current state:

A manuscript based on this chapter is under preparation.

Contribution statement:

I was responsible for raw materials collection, part of experiment design, conduction and data analysis, and manuscript preparation.

8.1 Abstract

Microwave-assisted hydrothermal liquefaction (MW-HTL) of biomass has not been investigated very much, and this chapter evaluated the influence of heating rate (4.5-13.5 °C/min), temperature (250-270 °C), feedstock concentration (8.3-14.3 wt.%) and reaction time (0-30 min) on the product yield/quality from MW-HTL of spent coffee grounds (SCG). It was observed that heating rate was not influential for biocrude yield, but a high heating rate substantially reduced the solid residue (SR) formation. The biocrude yield was significantly affected by temperature, in which increasing temperature from 250 °C to 270 °C promoted biocrude yield (19.6 wt.% vs. 24.8 wt.% respectively). A lower feedstock concentration led to a more favourable product distribution (e.g., a higher biocrude yield and lower SR). The optimal processing condition for MW-HTL of SCG was a heating rate of 13.5 °C/min, temperature of 270 °C, feedstock concentration of 8.3 wt.% and reaction time of 20 min. Under such conditions, a biocrude yield of 30.1 wt.% and SR yield of 28.6 wt.% were obtained. It was also found that the product yield/quality from HTL of SCG were comparable between two different heating methods (MW irradiation vs. conventional heating).

8.2 Introduction

Different from conventional heating that the subject material is heated by convective heat transfer from reactor wall and by the heat conduction from the material surface to the material core, microwave heating is featured with non-contact, uniform heat distribution, faster heating and lower energy consumption. Microwave irradiation/heating has been proven to be more favorable than conventional heating in the biofuels production, such as bio-ethanol (Chen et al., 2018), bio-methane (Pino-Jelcic et al., 2006) and syngas (Xiao et al., 2015). Crude bio-oil production from fast pyrolysis of biomass under microwave irradiation has been investigated as well. Various

feedstocks have been examined in MW-assisted pyrolysis for biocrude production, such as corn stover (Ren et al., 2014), bamboo (Dong and Xiong, 2014), rice straw (Huang et al., 2013) and switchgrass (Mohamed et al., 2016). Upon comparison of MW-assisted and conventional pyrolysis, a shorter process time was required for MW-assisted pyrolysis than conventional pyrolysis (Domínguez et al., 2005; Huang et al., 2016). Robinson et al. (2015) reported that biocrude with better quality was obtained from MW-assisted pyrolysis of larch woodchips as compared to that of conventional pyrolysis.

Similar to fast pyrolysis, biocrude is the target product for HTL of biomass. Unfortunately, MW-HTL of biomass for biocrude production has been rarely investigated (Remón et al., 2019; Lorente et al., 2019). Only recently Clark and his coworkers carried out the microwave-assisted and catalytic HTL of a mixture of pine and spruce (Remón et al., 2019), as well as the brewers' spent grain (Lorente et al., 2019). These two studies examined the effect of temperature, pressure, time and catalyst loading on the products' yield and physicochemical properties, and thus contributed valuable knowledge to MW-HTL of biomass. However, the influence of heating rate on the MW-HTL biocrude yield/quality was not investigated by Clark and coworkers, and this limits the understanding on biomass decomposition behavior during a MW heating process. Also, stainless batch reactors with conventional heating were widely used in HTL studies, which however did not allow a fast heating (usually only around 10 °C/min) and had relatively poor heating rate controllability as compared to that of microwave reactor. Therefore, using microwave reactor is ideal for studying the heating rate's influence on HTL of biomass.

This chapter assessed the technical feasibility of MW-HTL of spent coffee grounds (SCG) that has been determined to be a suitable HTL feedstock in our previous studies (L. Yang et al., 2016b). The influence of heating rate, temperature, feedstock concentration and time on the product yield was investigated. This chapter also compared the product yield/quality from MW-HTL and conventional HTL to deepen the understanding of microwave effect, which has not been explored in the research field of HTL.

8.3 Materials and methods

8.3.1 Materials

Please refer to section 3.3.1.

8.3.2 Microwave-assisted hydrothermal liquefaction processes

Hydrothermal liquefaction experiments were carried out in a Multi-wave PRO microwave from Anton Parr GmbH (Graz, Austria), and two 80 mL quartz vessels (NXQ80, up to 300 °C and 80 bar) were used as the reactor. In a typical run, 3 g feedstock were weighed and loaded into each quartz vessel along with the magnetic stirrer, followed by the addition of pre-calculated amount of distilled water based on the feedstock concentrations. The reaction vessels were then purged by nitrogen gas to remove existing air and quickly capped by a self-sealing lip-type seal (PTFE-TFM). The sample-containing vessels plus seal were weighed before locating them in the position 1 and 5 of the 8-position-rotor (Antor Parr, S8). The vessel in position 1 was equipped with a temperature sensor (T-probe S) to simultaneously record the reaction temperature. The vessel in position 5 was considered as a replicate. Another two vessels that did not contain samples but comparable amounts of low-polarity solvent (octane) were located in position 3 and 7 for rotor symmetry reasons.

A ramp time was set based on the heating rates of interest, and the reaction was stopped once the pre-set reaction time was reached. The magnetic stirrer (low mode, around 200 rpm) was stopped after reaction, and the reaction vessels were cooled down to 70 °C by a built-in fan in the microwave cavity. The gas in reaction vessels was then vented into fume hood *via* the gas releasing system in the seal. After gas releasing, the reaction vessel plus seal was weighed again to obtain the gas yield based on the gravimetric difference. The seal was finally removed from the reaction vessel, and the following product recovery procedures can be referred to Section 3.3.4.1.

The experimental process of conventional HTL were identical to that of in Section 3.3.3.

8.3.3 Product characterization

Please refer to Section 3.3.5.

8.3.4 Experimental design and data analysis

A 2^k factorial design of heating rate (4.5 °C/min vs. 13.5 °C/min), temperature (250 °C vs. 270 °C) and feedstock concentration (8.3 wt.% vs. 14.3 wt.%) was applied to assess their influence on product yield/quality. The validity of normal distribution and constant variance assumptions on the error terms was verified by examining the residuals as described in Montgomery, (2017).

8.4 Results and discussion

8.4.1 Influence of process variables on product yield

8.4.1.1 Analysis of variance (ANOVA)

The effect of heating rate, temperature and feedstock concentration on the product yield from MW-HTL of SCG were evaluated by ANOVA, and the obtained p-values were presented in Table 8.1. It can be clearly observed that the interaction effects (either two-way or three-way) were not significantly important for the product yield. Heating rate was not influential for biocrude yield, but the SR yield was significantly affected by varying heating rates. The process temperature was crucial for biocrude, SR and gas yield, but not for AqP yield. This was in agreement with the study of Lorente et al. (2019), in which temperature was not significantly important for the AqP yield from microwave-assisted and catalytic HTL of brewers' spent grain. The feedstock concentration exhibited a profound influence on the biocrude, SR and AqP yield, and only a marginally significant influence was observed for gas yield ($0.05 < \text{p-value} = 0.094 < 0.1$). These effects were interpreted and discussed in detail in the following section.

Table 8.1 ANOVA p-values that show the significance of the main and interaction effects on product yield (wt.%) from microwave-assisted hydrothermal liquefaction of spent coffee grounds. Significant effects are shown in bold.

	Biocrude yield	SR yield	AqP yield	Gas yield
Liner				
Heating rate	0.966	**0.033**	0.792	0.426
Temperature	**0.001**	**0.000**	0.449	**0.004**
Concentration	**0.049**	**0.000**	**0.007**	0.094
Two-way interaction				
Heating rate*Temperature	0.331	0.313	0.349	0.467
Heating rate*Concentration	0.812	0.898	0.750	0.276
Temperature*Concentration	0.648	0.108	0.223	0.702
Three-way interaction				
Heating rate*Temperature*Concentration	0.250	0.506	0.167	0.249

Note: SR = solid residue; AqP = aqueous phase

8.4.1.2 Heating rate influence

The influence of heating rate (4.5 °C/min vs. 13.5 °C/min) on the product distribution from MW-HTL of SCG was illustrated in Fig. 8.1. Using different heating rates led to almost identical biocrude, AqP and gas yield. However, a relatively large variation on SR yield was found, in which increasing heating rate significantly ($\text{p-value} = 0.033 < 0.05$) reduced the SR yield from 39.7 wt.%

to 38.5 wt.%. This was in agreement with the reported results, that a high heating rate eliminated the SR formation from HTL of corn stover and pretreated aspen wood chips (Zhang et al., 2008) and native grassland perennial (Zhang et al., 2009). Unfortunately, the heating rate influence on the biocrude yield and AqP yield were not accessible in their studies as they were considered as a whole and defined as the liquid yield (acetone soluble oil + aqueous phase products).

Different from Zhang and his coworkers' studies that HTL was carried out at a specified temperature, Brand et al. (2014) explored the influence of heating rate (2 °C/min vs. 20 °C/min) on HTL of pine sawdust at varied HTL temperatures ranging from 250-350 °C. At the temperature of 250 °C and 280 °C, heating rate was observed to be an insignificant factor for biocrude yield. However, a significant impact of heating rate was reported at the temperature of 315 °C and 350 °C. These observations suggested that the influence of heating rate on the biocrude yield depended on the level of applied temperature (heating rate and temperature interaction), in which heating rate only exhibited a significant impact on biocrude yield at the reaction temperature ≥ 315 °C. According to the reported results from Brand et al. (2014), the insignificant interaction between heating rate and temperature observed in our study (as shown in Table 8.1) was likely due to the relatively low temperature range (250-270 °C). Kamio et al. (2008) also investigated the heating rate effect on HTL of cellulose at the reaction temperature ranging from 170-280 °C, and reported that increasing the heating rate did not promote the cellulose decomposition, which is opposite to the above-mentioned results.

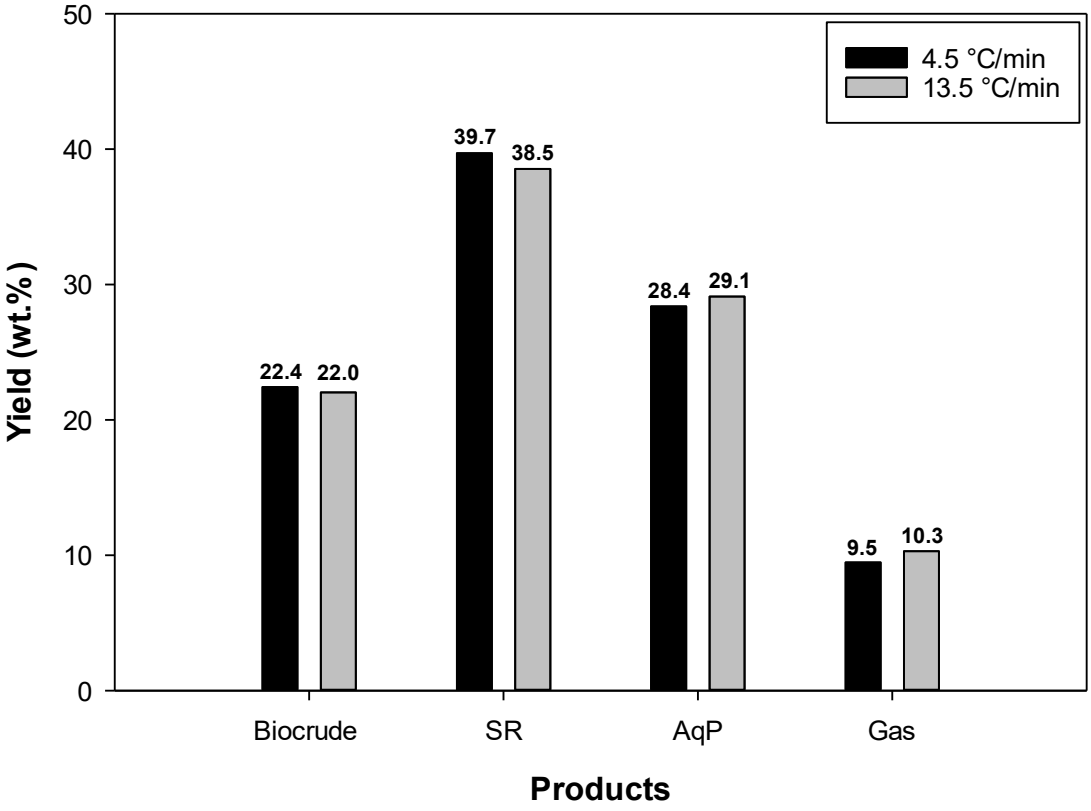

Fig. 8.1 The influence of heating rate on the yield of products from microwave-assisted hydrothermal liquefaction of spent coffee grounds. SR and AqP denotes solid residue and aqueous phase respectively.

8.4.1.3 Reaction temperature influence

As for the temperature influence on the product yield, increasing temperature from 250 °C to 270 °C resulted in significant improvement on biocrude yield from 19.6 wt.% to 24.8 wt.%. This can be verified by the much lower SR yield at 270 °C, indicating that SCG biomass was more readily converted into biocrude at 270 °C than that of 250 °C. Remón et al. (2019) carried out a MW-HTL of a mixture of pine and spruce at 50 bar for 0 min and in the absence of catalyst, and also reported that a higher temperature (250 °C vs. 150 °C) favoured the biocrude formation and eliminated SR. In comparison with our study and the study of Remón et al. (2019), slightly different results were reported in Lorente et al. (2019) that MW-HTL of brewers' spent grain was investigated. Increasing temperature from 180-220 °C was found to promote the biocrude yield at the expense of SR formation under MW irradiation, but further increasing temperature to 250 °C led to a decline in biocrude yield and a higher SR yield. It was attributed to two aspects by the

authors: 1) HTL of biomass is usually endothermic at low temperature and exothermic at high temperature. Although the biocrude yield can be raised with an increase in temperature, it could reach a point after which an increase in temperature suppresses liquefaction. 2) the decreased biocrude yield might be due to the increased gas formation *via* cracking and/or pyrolysis at the higher temperature.

Temperature was not influential for the AqP yield from MW-HTL of SCG in this study, unfortunately, the temperature influence on the AqP yield was inaccessible in Remón et al. (2019) as the AqP yield was not treated as a response. Lorente et al. (2019) reported a higher AqP yield (30.2 wt.%) at 250 °C than that of 9.3 wt.% at 180 °C, and this observation was different from ours. It is likely due to a relatively high temperature range used in our study (250-270 °C) compared to that of 180-250 °C in Lorente et al. (2019), in which 250 °C was sufficient enough to decompose SCG into water-soluble products under MW irradiation. In terms of the temperature effect on the gas yield from MW-HTL of SCG, increasing temperature from 250 °C to 270 °C promoted the gas yield from 8.3 wt.% to 11.6 wt.% as shown in Fig. 8.2. This was in agreement with both Remón et al. (2019) and Lorente et al. (2019), and the observed increase of gas yield was attributed to the more extensive biocrude cracking and/or low-molecular acids/phenols evaporation from aqueous phase at a high temperature.

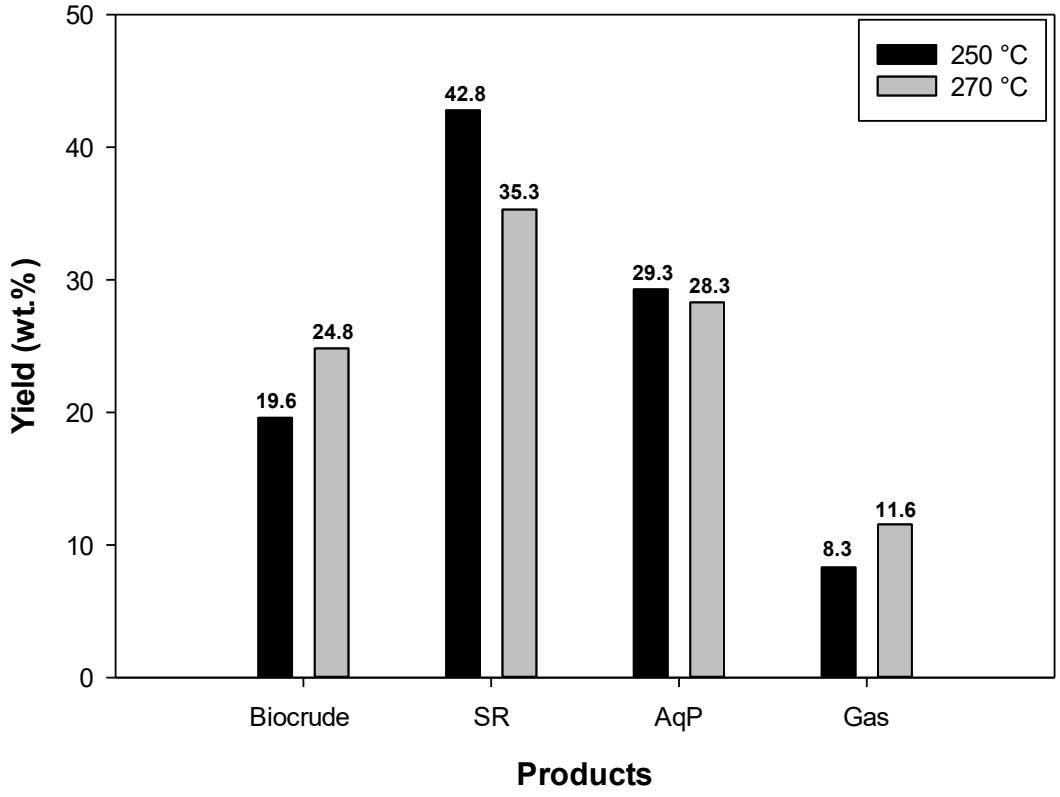

Fig. 8.2 The influence of temperature on the product yield from microwave-assisted hydrothermal liquefaction of spent coffee grounds. SR and AqP denotes solid residue and aqueous phase respectively.

8.4.1.4 Feedstock concentration influence

The effect of feedstock concentration on the product distribution from MW-HTL of SCG was presented in Fig. 8.3. A higher feedstock concentration (14.3 wt.% vs. 8.3 wt.%) inhibited the biocrude and AqP formation from SCG biomass, as evidenced by a much higher SR yield (36.5 wt.% vs. 41.6 wt.%). The gas yield was influenced by feedstock concentration at a marginally significant level (p-value = 0.094 as shown in Table 8.1). Remón et al. (2019) and Lorente et al. (2019) are the only currently available literature on MW-HTL of biomass, unfortunately, the effect of feedstock concentration was not investigated in these two studies.

A few attempts have been made to use ethylene glycol rather than hot-compressed water as the processing medium to carry out the MW-assisted liquefaction of biomass (Liu et al., 2013), while using organic solvent could lead to different product distribution as compared to using hot-compressed water. Liu et al. (2013) utilized ethylene glycol to conduct the MW-assisted

liquefaction of *Ulva prolifera* at 170 °C and the presence of 0.64 wt.% of sulfuric acid as a catalyst, and reported a comparable observation with ours that increasing feedstock concentration resulted in higher SR yield. The same research group then carried out a similar MW-assisted liquefaction of a brown seaweed feedstock (*Sargassum polycystu)* (Guo et al., 2012), and they observed that at a temperature of ~180 °C with 8 wt.% sulfuric acid as a catalyst, increasing feedstock concentration initially decreased but then increased the SR yield. Unfortunately, a proper explanation for these observations was not available in Guo et al. (2012). The effect of feedstock concentration was investigated in our previous HTL of SCG study (Yang et al., 2016b) that conventional heating was applied. It was found that increasing feedstock concentration gradually reduced the biocrude yield along with improved SR yield, and this was in a good agreement with our current study that microwave irradiation was used as a heating method. It therefore seems that microwave heating did not alter the feedstock concentration influence on product distribution as compared to conventional heating.

Combining the influence of heating rate, temperature and feedstock concentration, it can be concluded that a heating rate of 13.5 °C/min, reaction temperature of 270 °C and feedstock concentration of 8.3 wt.% was the favourable reaction setting for MW-HTL of SCG to obtain the highest biocrude yield and the lowest SR yield within the scope of this study.

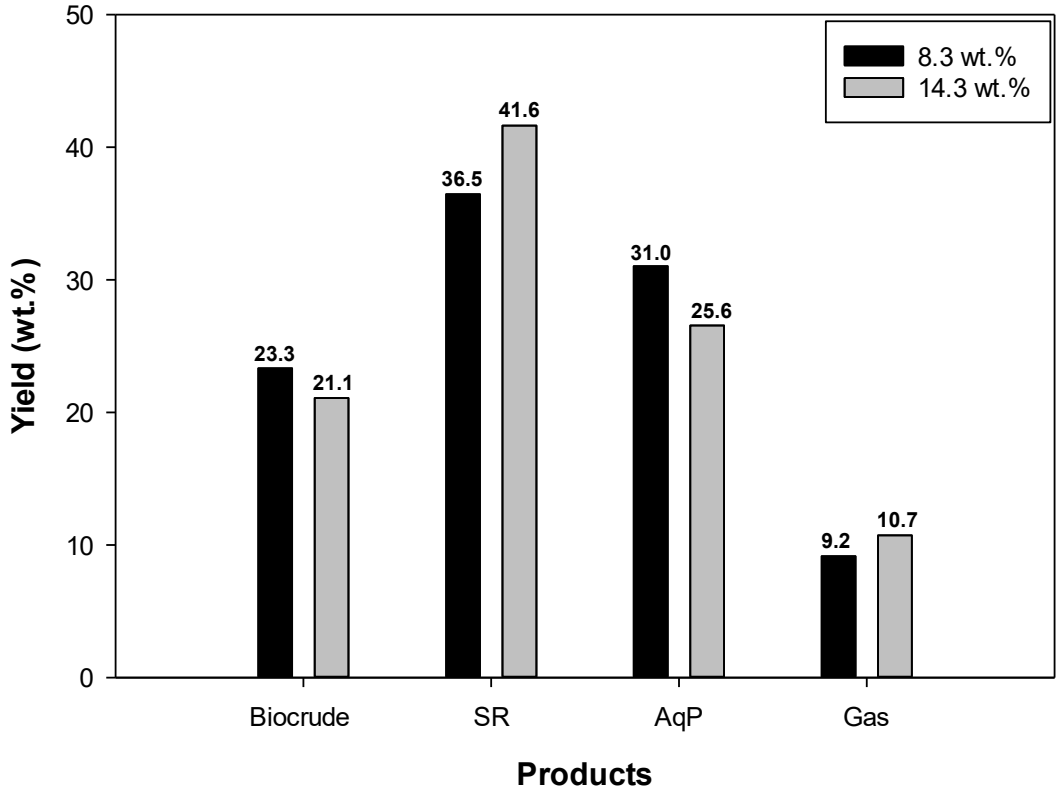

Fig. 8.3 The influence of feedstock concentration on the product yield from microwave-assisted hydrothermal liquefaction of spent coffee grounds. SR and AqP denotes solid residue and aqueous phase respectively.

8.4.1.5 Reaction time influence

The influence of reaction time was evaluated based on the optimal heating rate (13.5 °C/min), temperature (270 °C) and feedstock concentration (8.3 wt.%) as concluded in last section. As shown in Fig. 8.4, when a reaction time of 0 min was applied for MW-HTL of SCG, a fairly high biocrude yield (20.9 wt.%) was obtained. This suggested that SCG was partially decomposed into biocrude during the heating time. Increasing the reaction time from 0 min to 20 min gradually improved the biocrude yield (from 20.9 wt.% to 30.1 wt.%) and gas yield as well at the expense of SR and AqP yield. However, a further increase in reaction time to 30 min led to a slight decline in biocrude yield (by 1.8 wt.%). Thus, a reaction time of 20 min was considered to be the optimal reaction time for MW-HTL of SCG in this study. This result was different from both Remón et al. (2019) and Lorente et al. (2019) in which the favourable reaction time was 1.9 h and 2 h respectively. The observed difference might be from a variety of contributors such as the relatively

low temperature applied in Remón et al. (2019) and Lorente et al. (2019), and/or different downstream processing methods and biocrude recovery solvents used.

In summary, although heating rate was not influential for biocrude yield, the SR yield was significantly decreased by increasing heating rate. Temperature was the most impactful factor for biocrude yield in MW-HTL of SCG, and a higher temperature (270 °C vs. 250 °C) resulted in more biocrude formation (19.6 wt.% vs. 24.8 wt.% respectively). A low feedstock concentration (8.3 wt.%) favoured the biocrude and AqP formation. The optimal conditions for MW-HTL of SCG was a heating rate of 13.5 °C/min, reaction temperature of 270 °C, feedstock concentration of 8.3 wt.% and reaction time of 20 min, under which a biocrude yield of 30.1 wt.%, SR yield of 28.6 wt.%, AqP yield of 28.0 wt.%, and gas yield of 13.3 wt.% can be obtained.

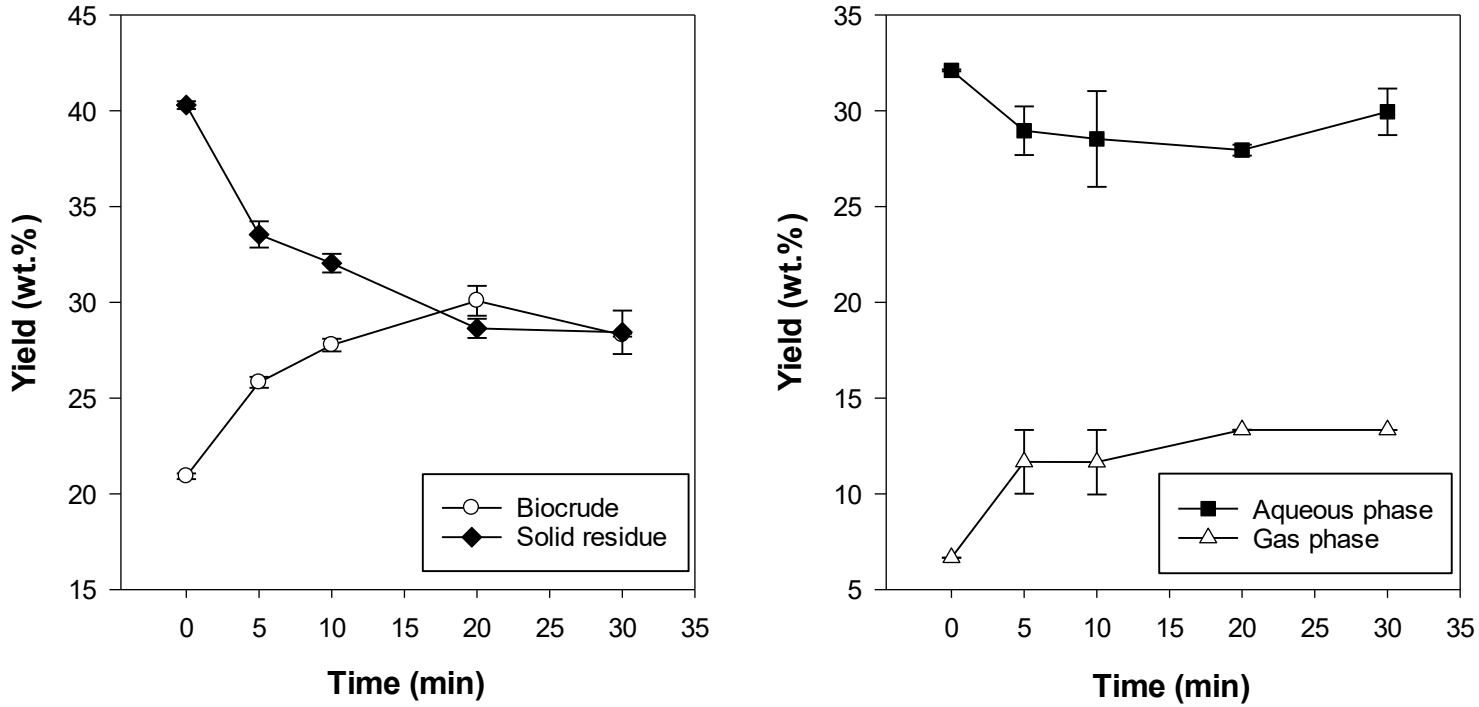

Fig. 8.4 The influence of reaction time on the product yield from microwave-assisted hydrothermal liquefaction of spent coffee grounds at the condition of 270 °C, 8.3 wt.% and 13.5 °C/min.

8.4.2 Comparison of product yield/quality from microwave and conventional heating

8.4.2.1 Product distribution

The optimal processing conditions for MW-HTL of SCG were obtained in section 8.4.1, however, the question on what the product yield/quality would be if conventional heating is applied remains unclear. To answer this question, the conventional HTL of SCG was carried out by using a 100 mL Parr stainless-steel batch reactor, and was referred as stream 2 in Table 8.2. The Parr reactor had a heating rate of 10 °C/min, but the optimal heating rate for MW-HTL of SCG was 13.5 °C/min. In order to ensure data comparability, MW-HTL of SCG with 10 °C/min was then conducted and referred as stream 1. The optimal conditions for MW-HTL of SCG was denoted as stream 3. Moreover, our previous study suggested that a reaction temperature of 295 °C, feedstock concentration of 10.0 wt.% and reaction time of 12.5 min (stream 4) was the optimal processing conditions for conventional HTL of SCG. The detailed comparison and discussion on stream 1-4 were provided as follow.

Table 8.2 The product distribution from hydrothermal liquefaction of spent coffee grounds for four studied streams.

	Stream 1	Stream 2	Stream 3	Stream 4
	Microwave 270 °C 10 °C/min 8.3 wt.% 20 min	Conventional 270 °C 10.0 °C/min 8.3 wt.% 20 min	Microwave 270 °C 13.5 °C/min 8.3 wt.%, 20 min	Conventional 295 °C 10.0 °C/min 10 wt.%, 12.5 min
Biocrude	27.8 ab	25.7 b	30.1 a	28.1 ab
SR	28.5 a	27.1 ab	28.6 a	25.0 b
AqP	33.7 b	33.9 b	28.0 c	38.0 a
Gas	10.0 b	13.3 a	13.3 a	8.9 b

Note: Letter grouping that does not share the same letter indicates significant difference between two mean values.

As shown in Table 8.2, the biocrude yield from stream 1 was not significantly higher than stream 2 (27.8 wt.% vs. 25.7 wt.% respectively), indicating that microwave irradiation had comparable performance with conventional heating during SCG biocrude formation. This was evidenced by the analogous SR and AqP yield between stream 1 and 2, even though stream 2 had slightly higher gas yield than stream 1. Stream 3 (30.1 wt.%) had significantly higher biocrude yield than stream 2 (25.7 wt.%), however, it is not adequate to compare stream 2 with stream 3

(due to their different heating rates), with the aim to study the influence of heating methods on biocrude yield. In terms of the product distribution under optimal conditions, stream 3 and 4 was observed to have similar biocrude yield (30.1 wt.% vs. 28.1 wt.% respectively), which further demonstrated the comparable performance of microwave heating and conventional heating. Stream 4 had a much higher AqP yield than stream 3, and this was likely caused by the relative high temperature in stream 4 that promoted the conversion of SR into AqP products and somehow inhibited the gas formation from AqP. Overall, no significant enhancement on biocrude yield was observed for MW-HTL of SCG when comparing with conventional HTL of SCG. More research efforts are needed to further evaluate the influence of microwave irradiation on the product yield by using a broader spectrum of biomass feedstock, and even the biomass model components and their mixtures.

8.4.2.2 Biocrude quality

The chemical composition of obtained biocrudes were presented in Table 8.3. Ester accounted for the largest proportion based the relative peak area, followed by amine and phenol. Biocrude from stream 1 and 2 had similar chemical composition, and this suggested that using different heating methods did not alter the biocrude chemical composition. As for the biocrude obtained under two different optimal conditions, their chemical composition was not identical. Stream 4 had significantly less ester, amine but more amide as compared to stream 3, presumably due to that the amide formation from ester and amine reaction was favoured at a relatively high temperature (295 °C) in stream 4. Similar with biocrude chemical composition, the higher heating value (HHV) for stream 1 and stream 2 was comparable (around 32 MJ/kg), even though stream 4 exhibited greater HHV than stream 3.

Table 8.3 The chemical composition (peak area %) and higher heating value (HHV, MJ/kg) of biocrudes from hydrothermal liquefaction of spent coffee ground.

	Stream 1	Stream 2	Stream 3	Stream 4
	Microwave 270 °C 10 °C/min 8.3 wt.% 20 min	Conventional 270 °C 10.0 °C/min 8.3 wt.% 20 min	Microwave 270 °C 13.5 °C/min 8.3 wt.%, 20 min	Conventional 295 °C 10.0 °C/min 10 wt.%, 12.5 min
Acid	3.6 a	3.1 a	4.0 a	6.1 a
Alcohol	2.8 b	2.1 b	2.1 b	11.1 a

	Stream 1	Stream 2	Stream 3	Stream 4
	Microwave 270 °C 10 °C/min 8.3 wt.% 20 min	Conventional 270 °C 10.0 °C/min 8.3 wt.% 20 min	Microwave 270 °C 13.5 °C/min 8.3 wt.%, 20 min	Conventional 295 °C 10.0 °C/min 10 wt.%, 12.5 min
Amide	0.9 b	1.1 b	1.0 b	4.0 a
Amine	11.7 b	11.7 b	14.8 a	12.1 b
DKP	6.0 a	5.1 a	5.6 a	3.6 a
Ester	56.4 a	58.2 a	54.7 a	35.4 b
Furan	-	1.7	-	-
Hydrocarbon	4.1 b	4.2 b	4.5 ab	8.7 a
Ketone	5.9 a	1.9 a	6.6 a	6.0 a
Phenol	7.9 a	11.3 a	8.4 a	13.0 a
HHV	32.0 b	31.7 b	31.3 b	33.5 a

8.5 Conclusions

Microwave-assisted hydrothermal liquefaction of spent coffee grounds (MW-HTL of SCG) was proved to be technically feasible in this chapter. Within the experimental design range, it was found that temperature was the most influential factor for biocrude yield, and a high temperature favoured the biocrude formation. Changing heating rate exhibited negligible effect on biocrude yield, however, increasing heating rate from 4.5 °C/min to 13.5 °C/min significantly reduced the SR formation. Using a lower feedstock concentration (8.3 wt.%) led to more biocrude formation than that of 14.3 wt.% feedstock concentration. A biocrude yield of 30.1 wt.%, SR yield of 28.6 wt.%, AqP yield of 28.0 wt.% and gas yield of 13.3 wt.% were obtained under an optimal reaction temperature of 270 °C, heating rate of 13.5 °C/min, feedstock concentration of 8.3 wt.% and reaction time of 20 min.

It was also observed that MW irradiation showed a negligible enhancement (by ~2.0 wt.%) on biocrude yield in the HTL of SCG, and the chemical compositions of biocrudes obtained from MW irradiation and conventional heating were comparable.

8.7 Transition section

Chapter 8 demonstrated that it was technically feasible to hydrothermally liquefy spent coffee grounds under microwave irradiation, and comparable biocrude yields were observed for microwave-assisted HTL and conventional HTL. However, the influence of heating methods (microwave irradiation vs. conventional heating) on HTL of biomass model components and their mixtures remains unclear. Chapter 9 therefore carried out a thorough comparison in product yield/quality between microwave-assisted and conventional HTL by using both model components and actual feedstocks.

Chapter 9: Influence of Heating Method on Hydrothermal Liquefaction of Biomass Model Components

Current state:

A manuscript based on this chapter is under preparation.

Contribution statement:

I was responsible for raw materials collection, part of experiment design, conduction and data analysis, and manuscript preparation.

9.1 Abstract

A few attempts have been recently made to study the microwave-assisted hydrothermal liquefaction (MW-HTL) of biomass, but a thorough comparison of microwave irradiation and conventional heating on liquefaction of biomass is still missing. HTL of biomass model components and their mixtures were carried out under both MW irradiation and convention heating in this chapter. In comparison with conventional heating, MW irradiation led to a lower biocrude yield from saccharide, comparable biocrude yield from protein or lignin, and higher biocrude yield from lipid. HTL of saccharide-containing binary mixtures (saccharide-protein, saccharide-lignin, saccharide-lipid) under MW irradiation generated less biocrude but more solid residue (SR) than conventional heating. MW-HTL of protein-lipid and lignin-lipid resulted in higher biocrude yield but lower SR yield. The mixture design analysis revealed that heating methods did not substantially alter the model components' interaction under HTL conditions. As for biocrude chemical composition, heating method exhibited slight and/or negligible influence on the biocrudes obtained from HTL of model components and their mixtures.

9.2 Introduction

Microwave-assisted heating has been widely used for biofuels production, such as crude bio-oil production from pyrolysis (Mohamed et al., 2016), biomass pre-treatment for the production of bio-ethanol (Chen et al., 2018), bio-methane (Pino-Jelcic et al., 2006) and syngas (Xiao et al., 2015). A few attempts on microwave-assisted hydrothermal liquefaction (MW-HTL) of biomass have also been conducted, and MW-HTL was suggested to be an efficient route for biocrude production (Lorente et al., 2019; Remón et al., 2019). Unfortunately, a comparison in product

yield/quality between MW-HTL and conventional HTL is still not available in the literature, and such an attempt was only made in this thesis (Chapter 8).

Biomass is mainly composed of four components, protein, lipid, saccharide and lignin, and different types of biomass usually have largely different biochemical composition. The degradation profile of each component differs from one another, and the interactions among these components during HTL process could occur (Yang et al., 2018b; Lu et al., 2018; Yang et al., 2019). The influence of heating methods (MW irradiation vs. conventional heating) on the yield/quality of product obtained from individual biomass components and their mixtures remains unclear, which prevents from gaining insights into the influence of heating method.

This study therefore aims to investigate the influence of heating methods on the product yield/quality from HTL of biomass model components and their mixtures. Soya protein, a mixture of cellulose and xylan (50/50 by mass), alkaline lignin and soybean oil were used as the representative model component for protein, saccharide, lignin and lipid respectively. HTL of individual, binary, ternary and quaternary model component mixtures were conducted under MW irradiation and conventional heating to assess the heating method's influence. MW-HTL and conventional HTL of actual biomass were also carried out to verify the heating method's influence on product yield/quality.

9.3 Materials and methods

9.3.1 Materials

Please refer to section 5.3.1.

9.3.2 Hydrothermal liquefaction processes

For the MW-HTL processes, please refer to section 8.3.2. For the conventional HTL processes, please refer to section 4.3.2.1. The processing conditions were 270 °C, 20 min, 10 °C/min heating rate and 8.3 wt.% feedstock concentration for both MW-HTL and conventional HTL.

9.3.3 Product characterization

Please refer to the section 3.3.5.

9.3.4 Experimental design and analysis

A Simplex-Centroid mixture design (without augment points) of four components (protein, saccharide, lignin and lipid) was applied, resulting in four individual components, six binary mixtures, four ternary mixtures and one quaternary mixture. Complete analyses of the response variables were conducted using the methods described in Montgomery, (2017) and Minitab Version 18 software. The analyses included verifying the validity of normal distribution and constant variance assumptions on the error terms. Independence assumption was valid due to the random run orders.

9.4 Results and discussion

9.4.1 Influence of heating method on individual components

Biomass feedstock mainly consists of protein, saccharide, lignin and lipid, and it is necessary to explore the heating method effect on HTL of individual model component before studying their mixtures. The product yields from MW-HTL and conventional HTL of protein, saccharide, lignin and lipid were presented in Fig. 9.1.

Regarding protein, MW-HTL had comparable biocrude yield, relatively low SR yield and much higher AqP yield compared to conventional HTL. This suggested that MW irradiation promoted protein decomposition into aqueous phase products. It is worthwhile to mention that a relatively large experimental error (3-5 wt.%) was involved in obtaining gas yield in this study, as the gas yield from MW-HTL and conventional HTL was determined by two different methods. The gas yield from MW-HTL was obtained from the gravimetrical weight difference before and after reaction, but the gas yield from conventional HTL was calculated by using ideal gas law with the assumption that only carbon dioxide exists in the gas. As for the chemical composition of protein-based biocrude shown in Table 9.1, MW-HTL and conventional HTL had a comparable chemical composition, in which diketopiperazine (DKP) accounted for the largest proportion (~63%). The formation of DKP during HTL of protein has been reported in Madsen et al. (2017b) and Yang et al. (2018b).

MW-HTL of saccharide led to a lower biocrude yield (10.2 wt.%) along with a higher SR yield (35.0 wt.%) than conventional HTL (biocrude yield of 15.6 wt.% and SR yield of 30.6 wt.%). This was likely that MW irradiation enhanced the repolymerization of saccharide decomposition intermediates to form more solid residue rather than biocrude. The chemical composition of

saccharide-based biocrudes were slightly different between MW-HTL and conventional HTL, even though they were both featured with aldehyde (e.g., furfural). MW-HTL led to a relatively low percent of aldehyde (49.3%) than conventional HTL (67.3%), presumably due to MW irradiation promoted the interaction of highly reactive furfural with other intermediates.

Comparable product yields from HTL of alkaline lignin were obtained for two different heating methods. Extremely low biocrude yields (2.7-3.4 wt.%) were observed for HTL of alkaline lignin, suggesting very limited conversion of alkaline lignin into biocrude under either MW irradiation or conventional heating. Conventional HTL of alkaline lignin at 350 °C was studied by Lu et al. (2018), and a very low biocrude yield (1.4 wt.%) was reported as well. The lignin-based biocrudes mainly consisted of phenolic compounds, such as guaiacol, creosol, vanillin and apocynin etc. A smaller proportion of phenol along with a greater percent of hydrocarbon were observed for MW-HTL compared to conventional HTL, suggesting the existence of interconversion between phenolics and hydrocarbon under microwave irradiation.

HTL of lipid resulted in a remarkably high biocrude yield, a negligible amount of SR and gas yield of ~5 wt.% along with negative AqP yield. These suggested that HTL of lipid consumed a small amount of hot-compressed water to hydrolyse lipid into intermediates (e.g., short-chain fatty acids and glycerol), which were then partially decomposed into gaseous products. In particular, HTL of lipid under MW irradiation resulted in >100 wt.% of biocrude yield (103.9 wt.%) that was higher than that of 97.9 wt.% for conventional heating, and the exact reason for the observed difference remains unclear. In terms of biocrude chemical composition, MW-HTL and conventional HTL had comparable performance, in which fatty acid esters accounted for ~85%. It is notable that a variety of fatty acid monoglycerides were detected, and they were grouped as ester in this study due to the presence of ester functional group in monoglyceride. The low proportion of fatty acid but abundantly available monoglycerides in lipid-based biocrudes seemingly due to the relatively low HTL temperature used (270 °C), which was not capable of hydrolysing monoglycerides into fatty acids readily. This assumption could be supported by a few previous works on HTL of lipid at a relatively high temperature, for instance, Lu et al. (2018) conducted HTL of soybean oil at 350 °C and observed a vast number of fatty acids in the obtained biocrude. Yang et al. (2018b) reported an almost equivalent amount of fatty acid and ester in the biocrude obtained from HTL of soybean oil at 290 °C.

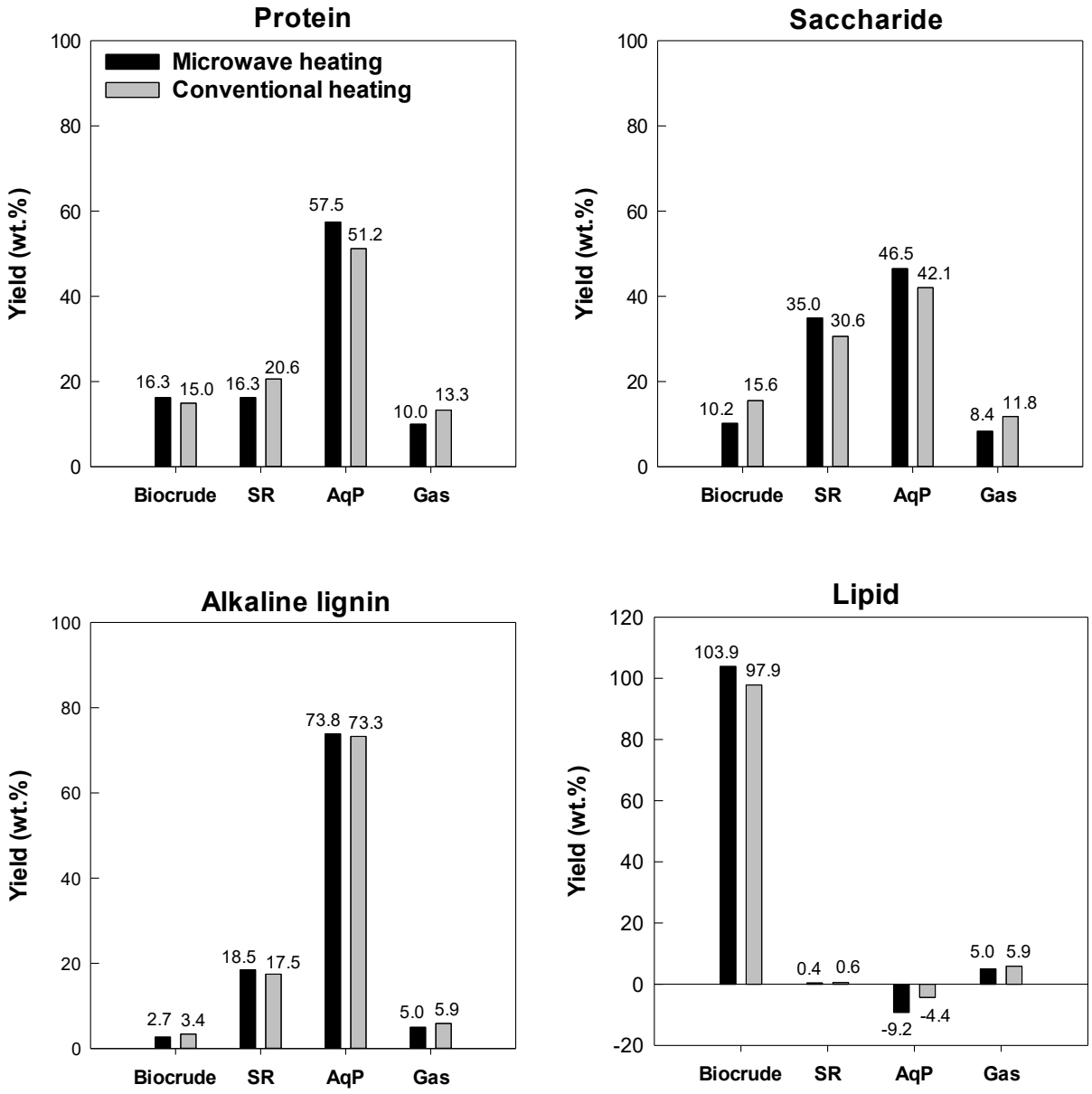

Fig. 9.1 The product yield (wt.%) from hydrothermal liquefaction of individual protein, saccharide, lignin and lipid under microwave and conventional heating.

Table 9.1 The chemical composition (peak area %) of biocrudes from hydrothermal liquefaction of individual biomass model component.

	Protein		Saccharide		Lignin		Lipid	
	MW	Con	MW	Con	MW	Con	MW	Con
acid	-	3.0	-	0.9	1.1	-	1.7	2.3±1.7
alcohol	1.2	2.0	1.4±0.1	-	3.3	-	1.2	-
aldehyde	-	-	49.3±5.8	67.3±6.9	-	0.7	-	-
amide	5.6±1.6	4.3±0.2	-	1.0	-	-	-	-

	Protein		Saccharide		Lignin		Lipid	
	MW	Con	MW	Con	MW	Con	MW	Con
amine	6.1±2.1	7.1±2.0	-	3.7±1.8	1.1	1.4	-	-
DKP	64.3±1.7	62.4±0.9	-	-	-	-	-	-
ester	3.7±2.2	7.4±1.3	8.0±2.8	3.8±0.9	6.2	12.0	83.3	85.0±4.7
furan	-	-	13.3±1.5	9.7	-	-	-	-
hydrocarbon	1.5	1.8	10.1±4.2	10.9±7.5	16.6	0.6	9.9	5.3±3.9
ketone	8.9±1.3	12.2±4.0	8.7±1.5	6.0±2.2	14.6	15.9	1.0	4.0±1.3
phenol	3.7±2.1	2.0	5.9±3.6	1.3±0.9	55.7	66.3	0.7	1.5±0.7
others	2.1	1.5±0.1	3.2±2.1	1.2±0.3	-	3.2	2.2	2.4

9.4.2 Influence of heating method on binary mixtures

There were six binary mixtures (50/50 by mass), including protein-saccharide, protein-lignin, protein-lipid, saccharide-lignin, saccharide-lipid and lignin-lipid. The effect of heating method on the product yield from HTL of these six binary mixtures were presented in Fig. 9.2. MW-HTL of protein-saccharide mixture exhibited a relatively low biocrude yield and high SR yield than conventional HTL, along with comparable AqP and gas yield. This indicted that MW irradiation was not favourable for biocrude formation from HTL of protein-saccharide mixture. Similar influence of heating method on HTL of protein-lignin mixture was observed, in which MW-HTL resulted in less biocrude but more SR formation than conventional HTL. Since saccharide and lignin can be considered as carbohydrate, it is rational to believe that HTL of protein-carbohydrate mixture under MW irradiation can generate less biocrude but more solid residue than conventional heating. This was likely due to MW irradiation induced more intensive repolymerisation of decomposition intermediates than conventional heating. The chemical composition of biocrude obtained from HTL of binary mixtures were presented in Table 9.2. As for the binary mixture of protein and saccharide, using different heating methods did not alter the chemical composition of resulting biocrude, in which nitrogen containing DKP was the primary chemical group. DKP was also the major component for the biocrude obtained from HTL of protein-lignin mixture, regardless of heating method.

Comparable AqP and gas yield were observed for MW-HTL and conventional HTL of saccharide-lignin mixture as shown in Fig. 9.2. However, MW-HTL of saccharide-lignin mixture led to a lower biocrude yield (5.7 wt.%) than conventional HTL (9.9 wt.%), as evidenced by a

much more SR formation under MW irradiation (39.3 wt.% vs. 32.1 wt.%). Using different heating methods led to slightly different biocrude chemical composition as shown in Table 9.2. MW-HTL has less phenol but more ketone than conventional HTL, indicating MW irradiation enhanced the transformation of phenolic compounds into ketone. In terms of HTL of saccharide-lipid mixture, a slightly lower biocrude yield along with higher SR yield were once again observed for MW-HTL as compared to conventional HTL. Ester was the dominant chemical group in biocrude from saccharide-lipid, and MW-HTL and conventional HTL had comparable percent of ester (~72%). It is worthwhile to mention that 5-10% of aldehyde (mainly furfural) was observed for saccharide-lipid biocrude, but it was absent in the biocrude from HTL of saccharide-protein. The absence of aldehyde was likely due to the readily happened Maillard reaction between furfural and DKP (from protein degradation), but the interaction between furfural and ester (from lipid hydrolysis) was much less intensive.

As for HTL of protein-lipid mixture, a higher biocrude yield (56.6 wt.%) but lower SR (22.8 wt.%) and gas yield (5.0 wt.%) were observed for MW-HTL compared to that of conventional heating. These suggested that MW irradiation favoured the biocrude formation from protein-lipid mixture at the expense of char and gas formation. Amide formation from ester and DKP reaction has been widely reported for HTL of protein-lipid under conventional heating (Chiaberge et al., 2013), and MW-HTL of protein-lipid resulted in slightly higher amide and ester content in biocrude than conventional HTL in this study. A much higher biocrude yield (53.0 wt.% vs. 41.7 wt.%) was also observed from MW-HTL of lignin-lipid mixture, as evidenced by its lower SR yield (19.4 wt.% vs. 29.2 wt.%) than conventional HTL. The chemical composition of lignin-lipid biocrude was not influenced by the heating method as shown in Table 9.2.

9.4.3 Influence of heating method on ternary and quaternary mixtures

In comparison with conventional HTL, lower biocrude yields were observed for MW-HTL of ternary mixtures as shown in Fig. 9.3. MW irradiation led to a lower biocrude yield for protein-saccharide-lipid mixture (49.3 wt.%) and saccharide-lignin-lipid mixture (34.7 wt.%) than that of 55.2 wt.% and 44.2 wt.% for conventional HTL respectively. It is notable that both these two ternary mixtures contained saccharide and lipid, in which MW-HTL of saccharide-lipid binary mixture was proved to produce less biocrude but more SR in section 9.4.2. Thus, the addition of either protein or lignin into saccharide-lipid mixture did not change its response to different heating

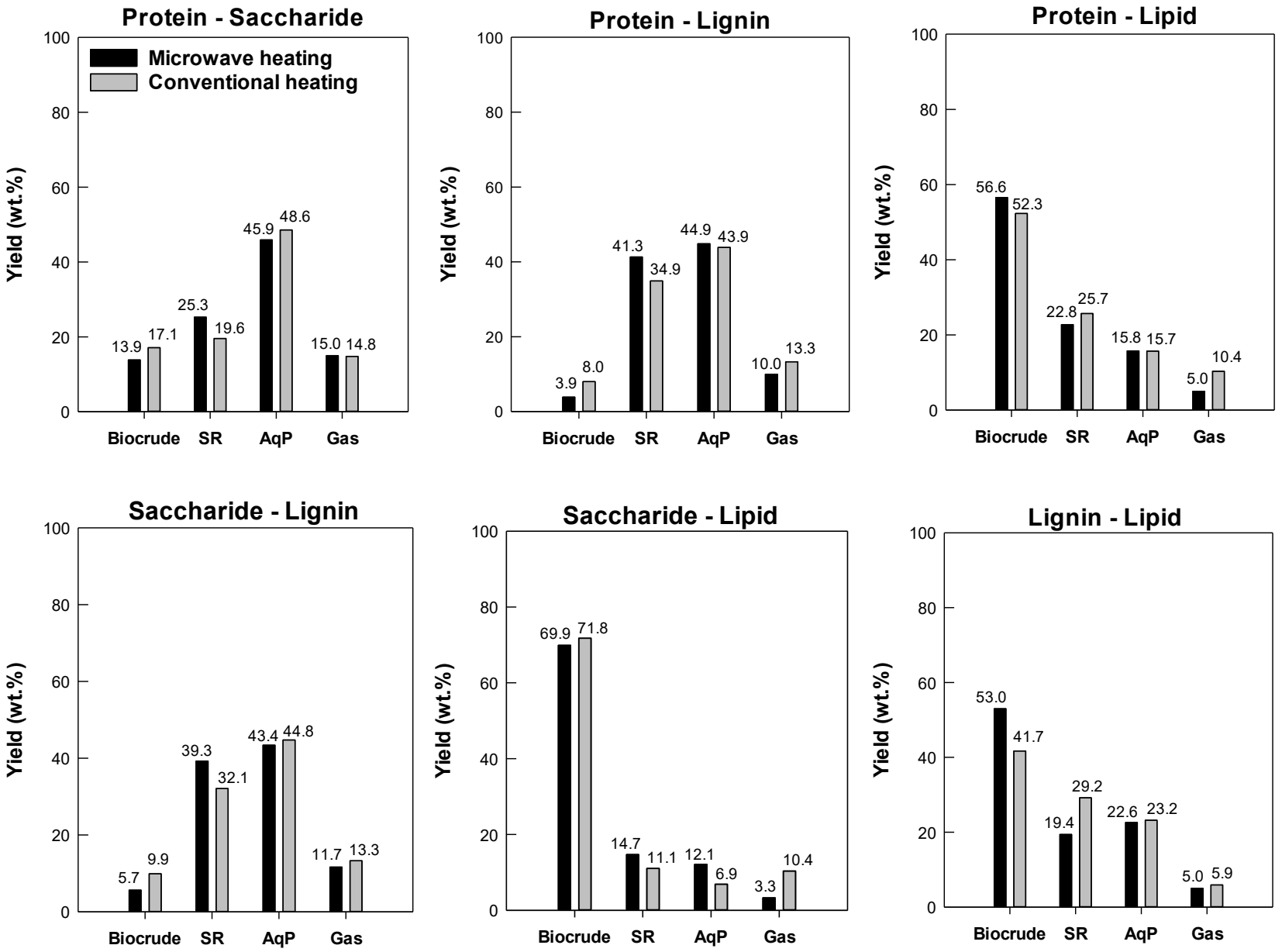
Protein - Saccharide
Microwave heating
Conventional heating
Yield (wt.%)
100
80
60
40
20
0
13.9
17.1
25.3
19.6
45.9
48.6
15.0
14.8
Biocrude
SR
AqP
Gas
Protein - Lignin
3.9
8.0
41.3
34.9
44.9
43.9
10.0
13.3
Protein - Lipid
56.6
52.3
22.8
25.7
15.8
15.7
5.0
10.4
Saccharide - Lignin
5.7
9.9
39.3
32.1
43.4
44.8
11.7
13.3
Saccharide - Lipid
69.9
71.8
14.7
11.1
12.1
6.9
3.3
10.4
Lignin - Lipid
53.0
41.7
19.4
29.2
22.6
23.2
5.0
5.9

Fig. 9.2 The product yield (wt.%) from hydrothermal liquefaction of binary mixtures of protein, saccharide, lignin and lipid under microwave and conventional heating.

methods during biocrude formation. The biocrude chemical composition for HTL of ternary mixtures were presented in Table 9.3, and the influence of heating method was negligible for either protein-saccharide-lipid or saccharide-lignin-lipid. Due to the presence of lipid in both these two ternary mixtures, ester was the major component for the obtained biocrudes.

As for HTL of protein-lignin-lipid ternary mixture, a lower biocrude yield (23.0 wt.%) and a higher SR yield of 33.9 wt.% was observed for MW-HTL compared to that of 26.1 wt.% and 31.3 wt.% for conventional HTL respectively. This was not expected according to the results from HTL of protein-lipid and lignin-lipid in section 9.4.2, in which MW irradiation was demonstrated to promote biocrude formation and diminish SR formation. This unexpected observation from protein-lignin-lipid was mainly because both protein-lipid interaction and lignin-lipid interaction happened less readily compared to protein-lignin interaction, that has been proven to cause lower biocrude yield but higher SR yield. Although heating method exhibited certain degree of influence on the product distribution for protein-lignin-lipid, comparable biocrude chemical compositions were observed for MW-HTL and conventional HTL. In terms of HTL of protein-saccharide-lignin ternary mixture, MW irradiation had a lower biocrude yield but higher SR yield than conventional heating, and this was in agreement with previous observations from HTL of either protein-saccharide, protein-lignin or saccharide-lignin. The biocrude chemical composition from HTL of protein-saccharide-lignin was not affected by heating method, in which DKP (~60%) and phenol (~20%) was the primary and secondary chemical group respectively.

MW effect on product yield from HTL of quaternary mixture was presented in Fig. 9.4, and it can be observed that MW-HTL and conventional HTL had comparable biocrude yield (32.5 wt.% vs. 33.7 wt.%) and gas yield (10.0 wt.% vs. 8.9 wt.%). However, more SR formation along with a lower AqP yield were observed for MW-HTL of quaternary mixture compared to conventional HTL. This can be either attributed to the suppression of feedstock decomposition into AqP products under MW irradiation or the enhanced repolymerization of water-soluble products to form more SR under MW irradiation. The chemical composition of obtained biocrude was independent to the heating method used, and ester accounted for the largest proportion of GC-MS detectable biocrude as shown in Table 9.3.

Table 9.2 The chemical composition (peak area %) of biocrudes from hydrothermal liquefaction of binary mixtures.

	Protein-saccharide		Protein-lignin		Protein-lipid		Saccharide-lignin		Saccharide-lipid		Lignin-lipid	
	MW	Con	MW	Con	MW	Con	MW	Con	MW	Con	MW	Con
acid	1.2	-	2.1	2.3±1.3	1.7±1.1	1.9±0.6	-	-	1.4±0.4	5.7±0.2	-	1.5±0.4
alcohol	1.4	-	-	-	0.5	-	-	-	1.1±0.3	-	-	-
aldehyde	-	-	-	-	-	-	1.3±0.3	1.2±0.2	10.9±0.5	6.6±0.2	1.2	-
amide	-	-	-	2.2±0.9	21.0±4.2	16.8±0.9	1.0	2.8	-	-	-	-
amine	14.4±0.8	8.9±4.3	3.9±1.5	3.3±2.2	1.3±0.8	-	1.6±0.1	2.1±1.1	1.2	-	1.5±0.5	-
DKP	64.0±1.9	63.9±3.9	61.7±6.5	63.4±3.1	3.8±0.4	4.8±0.3	-	-	-	-	-	-
ester	2.1±0.9	1.9±0.2	-	3.7±0.5	69.7±2.7	63.8±0.9	3.7±2.1	1.1	74.7±7.2	71.1±6.7	70.6±3.9	74.2±4.4
furan	-	-	-	2.7±0.4	-	-	-	-	-	-	-	-
hydrocarbon	7.2	10.0±1.1	0.7±0.1	-	0.5	3.4±0.1	7.3±1.4	7.9±1.6	2.2±1.6	10.4±5.5	3.5±1.3	7.5±3.7
ketone	6.3±2.2	5.4±1.7	5.0±1.5	6.5±2.8	1.3	3.4±0.5	17.6±2.2	24.8±1.4	4.9±2.2	1.5	5.9±1.3	2.6±0.2
phenol	4.3±3.1	7.8±3.4	24.8±5.1	15.7±2.0	0.6	0.9	67.1±1.3	58.8±4.4	2.2±1.6	4.0±2.8	11.3±4.8	12.6±2.1
others	6.6	2.7	2.9±2.2	0.7	-	3.1±0.1	-	3.8	1.7±0.4	1.8	6.6±2.8	3.3

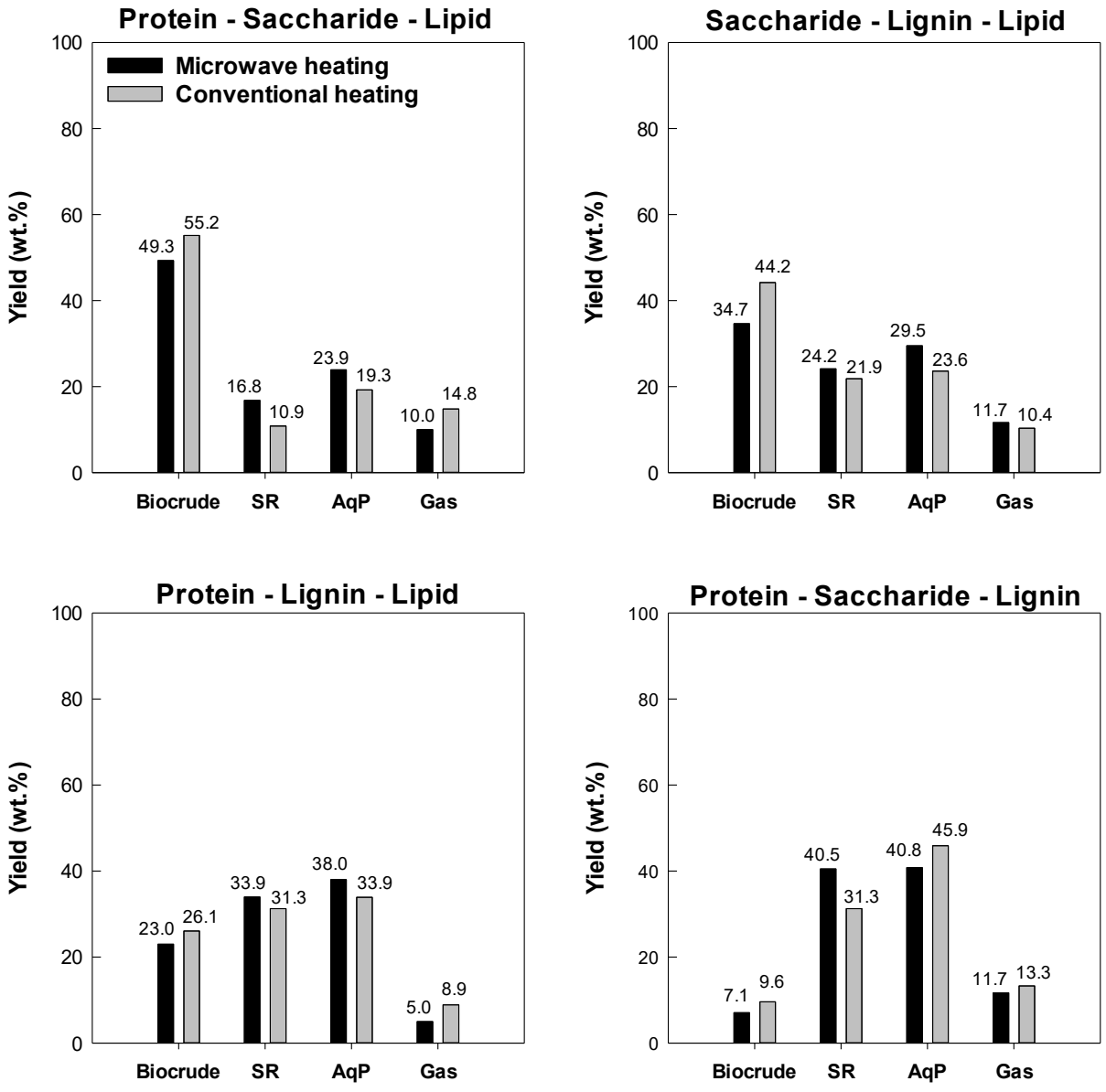

Fig. 9.3 The product yield (wt.%) from hydrothermal liquefaction of ternary mixtures of protein, saccharide, lignin and lipid under microwave and conventional heating.

Table 9.3 The chemical composition (peak area %) of biocrudes from hydrothermal liquefaction of binary and ternary mixtures.

	Protein-saccharide-lignin		Protein-saccharide-lipid		Protein-lignin-lipid		Saccharide-lignin-lipid		Protein-saccharide-lignin-lipid	
	MW	Con	MW	Con	MW	Con	MW	Con	MW	Con
acid	-	-	0.7	0.9	1.0	1.5±0.1	0.6±0.2	1.9	0.6	1.8
alcohol	-	-	-	-	-	-	-	-	1.7	-
aldehyde	-	1.2	-	-	-	-	2.4	1.1±0.3	0.8	-
amide	2.3±0.1		3.1±2.2	1.7±0.2	17.5±3.5	18.3±0.3	0.5	-	4.0±2.5	1.8±0.1
amine	6.4±2.6	4.8±1.3	1.7	2.7±0.9	4.0±0.3	4.9±0.1	0.8	-	1.9	1.2±0.1
DKP	60.9±0.2	57.1±1.0	3.3±0.3	5.8±2.4	1.6±0.3	3.8±0.4	-	-	4.0±0.7	3.7±0.9
ester	-	1.6±0.3	75.2±3.4	69.9±1.5	69.8±4.8	61.2	79.1±1.8	74.0±2.3	76.4±4.3	74.1±4.2
furan	-	-	-	4.0	-	-	-	-	-	-
hydrocarbon	2.5±0.4	7.2±0.1	7.0±3.6	8.2±0.5	1.6±0.2	5.2±0.8	5.2±0.1	14.7±0.9	3.3±1.9	7.7±0.6
ketone	2.2±1.2	4.9±0.1	3.4±1.9	2.4±0.8	1.2±0.6	1.6	1.4	-	0.6±0.2	2.2
phenol	20.9±0.3	19.1±2.1	3.0±2.0	1.3±0.4	2.6±0.3	2.2±0.3	9.6±2.7	6.9±1.9	7.2±0.6	7.0±3.0
others	4.7±3.2	4.7±2.1	2.6±2.2	3.2±1.3	1.2±0.1	2.1±0.5	3.0±0.4	1.4±0.1	1.3±0.1	1.6±0.4

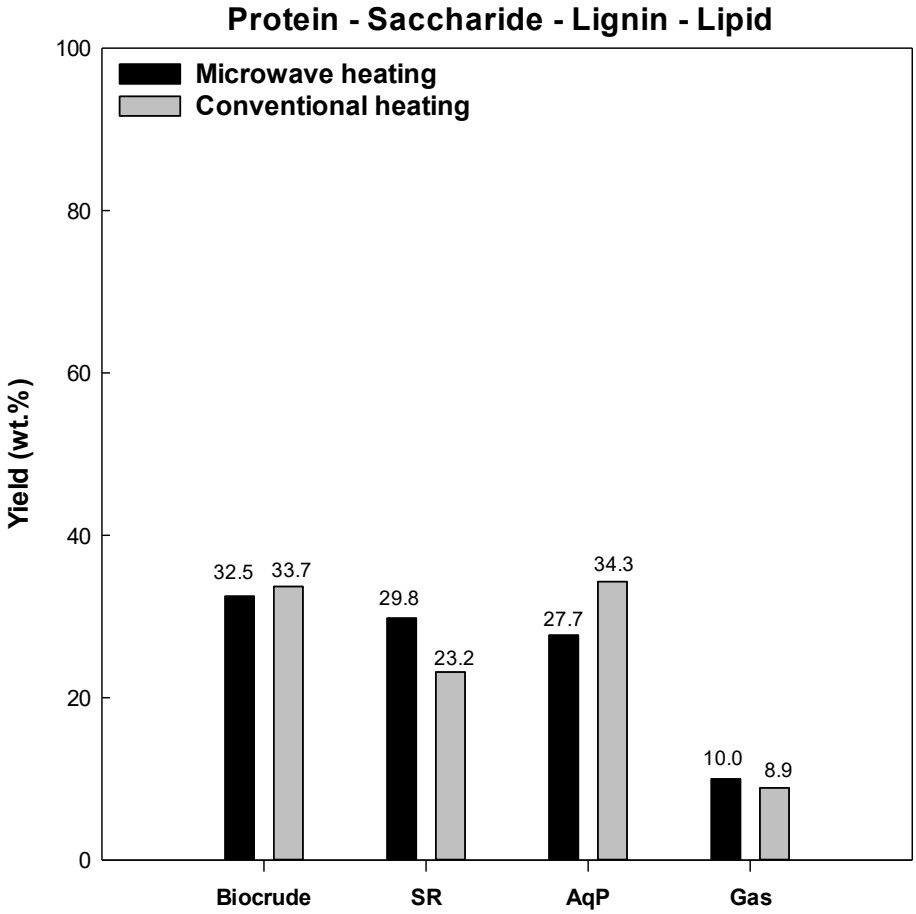

Fig. 9.4 The product yield (wt.%) from hydrothermal liquefaction of quaternary mixtures of protein, saccharide, lignin and lipid under microwave and conventional heating.

9.4.4 Influence of heating method on actual feedstocks

The influence of heating method on HTL of actual feedstocks was also investigated, and the used actual feedstocks included food processing waste (spent coffee ground, SCG), lignocellulosic biomass (maple sawdust), and low-lipid microalgae (*Chlorella sp.*) as shown in Table 9.4. It is worthwhile to mention that the data of HTL of SCG were adapted from Section 8.4.3.1. The detailed biochemical compositions of studied feedstocks have been presented in section 6.4.1.

As seen in Table 9.4, MW-HTL of SCG generated a slightly higher biocrude yield (27.8 wt.%) than conventional HTL (25.7 wt.%). This might be caused by a fairly high percent of lipid (9.5%) in SCG along with a protein content of 14.2%, in which MW-HTL of protein-lipid binary mixture

produced more biocrude than conventional HTL as proved in Section 9.4.2. The chemical composition of biocrude obtained from HTL of actual feedstocks were presented in Table 9.5. The chemical composition of SCG biocrude was comparable between MW-HTL and conventional HTL, and ester was the primary chemical in the biocrudes. These were consistent with the observations from HTL of model quinary mixture, in which SCG also contained protein (15%), lipid (10%), saccharide (50%) and lignin (25%).

In terms of lignocellulosic biomass (sawdust), MW-HTL of sawdust generated slightly less biocrude than conventional HTL, and this can be attributed to the high contents of saccharide (66.0%) and lignin (23.2%) in sawdust, in which MW-HTL of saccharide-lignin binary mixture produced less biocrude than conventional HTL as presented in Section 9.4.2. Although MW-HTL of saccharide-lignin mixture tended to produce more SR *via* intermediates repolymerization, comparable SR yields were observed for sawdust. For both MW-HTL and conventional HTL, the obtained sawdust biocrudes were featured with the aldehyde and phenolic compounds. It was noticed that MW-HTL of sawdust exhibited a higher content of aldehyde (50.1%) than conventional HTL (43.8%), and this was different with HTL of saccharide. Biocrude from MW-HTL of saccharide was proved to have less aldehyde than that of conventional HTL in Section 9.4.1. This observed difference illustrated the varied performance of MW irradiation in HTL of sawdust and saccharide in regards of biocrude chemical composition.

In the MW-HTL of low-lipid microalgae (*Chlorella sp.*), a much higher biocrude yield (28.9 wt.%) was observed than that of 22.8 wt.% in conventional HTL, indicating that MW irradiation promoted the biocrude formation from HTL of *Chlorella sp.* microalgae. The *Chlorella sp.* microalgae used was mainly composed of protein (63.2%) and carbohydrate (~23.6%). It is interesting to note that MW-HTL of protein-carbohydrate model mixture was proved to generate less biocrude than conventional HTL, which was opposite to the result obtained from HTL of *Chlorella sp.* microalgae. Since the lipid content in *Chlorella sp.*was extremely low (0.9%), a high biocrude yield under MW irradiation was unlikely due to the protein-lipid interaction even though it generated more biocrude under MW irradiation than conventional heating. The reason for the higher biocrude yield from MW-HTL of low-lipid microalgae (*Chlorella sp.*) remains uncovered. Using different heating methods did not substantially change the chemical composition of

Chlorella sp. biocrudes, which ester, amide and DKP were evenly distributed and accounted for more than 60%.

Table 9.4 The product yield (wt.%) from hydrothermal liquefaction of spent coffee ground, *Chlorella sp.* and sawdust under microwave and conventional heating.

Feedstock	Heating method	Biocrude	SR	AqP	Gas
Spent coffee grounds	MW heating	27.8±0.6	28.5±0.5	33.7±0.1	10.0±0.0
	Conventional heating	25.7±0.7	27.1±0.9	33.9±1.4	13.3±1.5
Sawdust	MW heating	23.7±1.2	30.0±1.0	34.6±1.9	11.7±1.7
	Conventional heating	25.2±0.2	31.1±0.7	30.5±0.6	13.3±1.5
Chlorella sp.	MW heating	28.9±0.9	8.1±0.6	54.7±1.4	8.3±1.7
	Conventional heating	22.8±0.8	8.5±0.0	55.4±0.7	13.3±0.5

Note: MW = microwave; SR = solid residue; AqP = aqueous phase.

Table 9.5 The chemical composition (peak area %) of biocrudes from hydrothermal liquefaction of actual feedstocks.

	Spent coffee grounds		Sawdust		*Chlorella sp.*	
	MW	Con	MW	Con	MW	Con
acid	3.6±0.4	3.1±0.4	-	-	1.5	4.3
alcohol	2.8±1.1	2.1±0.2	-	-	-	-
aldehyde	-	-	50.1±1.7	43.8±1.8	-	-
amide	0.9	1.1	-	-	20.2±3.6	20.2±3.6
amine	11.7±0.2	11.7±0.6	-	-	1.8±0.6	6.5±0.1
DKP	6.0±1.6	5.1±0.5	-	-	16.5±0.5	22.5±0.9
ester	56.4±4.2	58.2±4.1	-	-	25.7±1.7	19.9±1.2
furan	-	1.7±0.1	-	-	-	-
hydrocarbon	4.1±0.2	4.2±0.7	8.3±4.6	6.8±0.7	16.4±2.5	12.9±0.3
ketone	5.9±3.4	1.9±1.1	14.4±0.1	16.9	5.8±0.5	6.7±0.3
phenol	7.9±0.7	11.3±2.3	25.2±2.5	28.6±1.5	12.9±2.3	8.5±0.3
others	-	-	2.0±0.3	4.0±0.9	-	1.5

9.4.5 Mixture design analysis

A statistical method, mixture design without augment points was utilized in this chapter. This method has been proved to be an adequate method for studying synergistic effect (SE) and antagonistic effect (AE) on product yield in Chapter 4. The influence of heating method on the SE and AE was evaluated *via* analysis of variance from mixture design as presented in Table 9.2.

MW-HTL and conventional HTL performed in a similar manner for protein-lipid mixture, as both had SE on SR yield. A comparable performance of MW irradiation and conventional heating was also observed in HTL of saccharide-lignin and lignin-lipid. As for HTL of saccharide-lipid, both MW irradiation and conventional heating resulted in SE on biocrude yield and AE on SR yield. For the protein-lignin interaction, MW irradiation and conventional heating had comparable SE on SR yield and AE on AqP yield even though MW irradiation led an AE on biocrude yield. Different performance of MW-HTL and conventional HTL was only observed in mixture of protein and saccharide, in which MW irradiation had a SE on gas yield but conventional heating had an AE on SR yield. Overall, MW irradiation and conventional heating had no significant impact on the SE/AE of product yield, indicating using these two heating methods did not substantially alter the model components' interaction under HTL conditions.

Table 9.6 Analysis of variance (ANOVA) p-values for hydrothermal liquefaction of biomass model components under microwave heating and conventional heating. Synergism and antagonism were shown as (+) and (-) in bold respectively.

	Microwave-assisted HTL				Conventional HTL			
Source	Biocrude	SR	AqP	Gas	Biocrude	SR	AqP	Gas
Protein-lipid	0.063	**0.000 (+)**	0.269	0.260	0.066	**0.003 (+)**	0.386	0.910
Saccharide-lignin	0.393	**0.000 (+)**	**0.000 (-)**	**0.009 (+)**	0.871	**0.007 (+)**	**0.004 (-)**	**0.025 (+)**
Lignin-lipid	**0.044 (-)**	**0.001 (+)**	0.356	0.617	**0.001 (-)**	**0.000 (+)**	0.055	0.523
Saccharide-lipid	**0.003 (+)**	**0.015 (-)**	0.185	0.663	**0.000 (+)**	**0.001 (-)**	**0.001 (-)**	0.163
Protein-lignin	**0.012 (-)**	**0.000 (+)**	**0.000 (-)**	0.595	0.118	**0.000 (+)**	**0.000 (-)**	0.112
Protein-saccharide	0.484	0.419	0.075	**0.010 (+)**	0.145	**0.002 (-)**	0.466	0.124

Note: HTL = hydrothermal liquefaction; SR = solid residue; AqP = aqueous phase.

9.5 Conclusions

Hydrothermal liquefaction (HTL) of individual, binary, ternary and quaternary mixtures of protein, saccharide, lipid and lignin were carried out under microwave (MW) irradiation at 270 °C for 20 min with a heating rate of 10 °C/min and a feedstock concentration of 8.3 wt.% in this chapter. Parallel experiments using conventional heating were conducted to explore the influence of heating method on the HTL product yield/quality.

In comparison with conventional heating, MW irradiation led to a lower biocrude yield from saccharide, comparable biocrude yield from protein and lignin, and higher biocrude yield from lipid. As for biocrude chemical composition, heating method exhibited negligible influence on protein and lipid biocrude, but slightly changed the aldehyde and phenol content for saccharide and lignin biocrude respectively. HTL of saccharide-containing binary mixtures (saccharide-protein, saccharide-lignin, saccharide-lipid) under MW irradiation generated less biocrude but more solid residue (SR) than conventional heating. This was likely due to that MW irradiation induced more intensive repolymerisation of intermediates decomposed from saccharide to form more SR rather than biocrude compared to the conventional heating. MW-HTL of protein-lipid and lignin-lipid resulted in a higher biocrude yield but a lower SR yield than conventional HTL. Among the six binary mixtures studied, only the biocrudes from saccharide-lignin and protein-lipid showed marginal difference in chemical composition when using different heating methods.

MW-HTL and conventional HTL of actual feedstocks were also carried out. In terms of the heating method's influence on biocrude yield, HTL of spent coffee grounds and sawdust was in the same trend as HTL of model components, but not for the low-lipid microalgae (*Chlorella sp.*). Two heating methods resulted in the biocrudes with comparable chemical composition for spent coffee grounds and *Chlorella sp.* while the sawdust biocrude from MW-HTL contained more aldehyde than that from conventional HTL. The mixture design analysis on the product yield found that two heating methods did not substantially affect the interactions among the model components under HTL conditions.

Chapter 10: Overall Conclusions and Future Work

10.1 Overall conclusions

Hydrothermal liquefaction (HTL) is a promising thermochemical conversion technique for the production of crude bio-oil. In this thesis, research was conducted to investigate the influence of bio-crude recovery procedures on the quantity/quality of biocrude, develop quantitative models for the predication of product yields, explore interactions among constituents of biomass through using representative biomass model components, study the co-liquefaction effect in HTL of mixed feedstocks, and evaluate the feasibility of microwave-assisted HTL. The specific conclusions to original research objectives are summarized as follows:

i) Biocrude recovery methods such as solvent extraction, Soxhlet extraction and microwave-assisted extraction had no significant effect on the yield and physicochemical properties of biocrude. However, solvents used (hereby hexane, acetone, DCM and THF) to extract biocrude did significantly affect the quantity/quality of the biocrude. Using dichloromethane as an extraction solvent followed by filtration was determined to be a favourable biocrude recovery method.

ii) Two kinds of mathematical models were developed to predict the yields of products in HTL. One is to predict the yields of biocrude and solid residue as a function of biomass model components (cellulose, hemicellulose, lignin, protein and lipid). The model also included interactive terms representing interactions among five biomass components. This model exhibited good predictability (high R^2_{adj}) and was verified by actual feedstocks such as spent coffee grounds and microalgae. The other is a more advanced prediction model, taking both biomass components (saccharide, lignin protein and lipid) and process variables (temperature, time and mass ratio of water/feedstock) as model inputs. The model predictability was further validated by actual feedstock, spent coffee grounds under different HTL conditions. The advanced models performed well on either the optimization of HTL process variables when the biochemical composition of feedstock was given, or the optimization of biochemical composition at a given HTL condition. These models are extremely useful for assessing the potential of various kinds of biomass.

iii) The yield and chemical composition of biocrude were highly associated with feedstock's biochemical composition. The contribution of individual biomass components to the yield of HTL biocrude was determined to be in the order of lipid >> protein > cellulose >

hemicellulose ≥ lignin. Both hemicellulose and cellulose biocrude was featured by aldehyde, and phenol was the most abundant chemical for lignin biocrude. Protein biocrude mainly consisted of nitrogenous compounds, such as diketopiperazine. Lipid biocrude had a high amount of fatty acids and esters. Studies on the interaction between biomass model components discovered Maillard reactions between protein and carbohydrates and amide formation from protein and lipid interaction. The interactions among biomass model components were also affected by process variables. Within the experimental range, relatively mild HTL conditions eliminated alkaline lignin-lipid interaction and protein-lipid interaction, and thus enhanced biocrude formation.

iv) Investigation on hydrothermal co-liquefaction of different feedstocks revealed the existence of statistically significant co-liquefaction (CE), either synergistic effect or antagonistic effect. The feedstock mixing ratio and processing temperature were found to be influential for the co-liquefaction effect, and the temperature effect was dependent on the level of mixing ratio in the co-liquefaction of spent coffee grounds/sawdust and *Chlorella. sp.*/sawdust as shown in chapter 7. When the feedstock combination was considered as an experimental factor, it exhibited much more impact on the CE compared to those of temperature and mixing ratio. Spent coffee grounds/*Chlorella. sp.* was a favourable combination and co-liquefying them at 320 °C with a mixing ratio of 50:50 (by mass) led to the most desirable CE (net increment of 6.3 wt.%) on biocrude yield. The principle component analysis suggested that if there was a positive CE on biocrude yield, then a negative CE was likely to be observed for solid residue yield, *vice versa*. Acknowledge of co-liquefaction effect is valuable for making a full use of all kinds of biomass, optimizing feedstock combination and improving biocrude yield.

v) Microwave-assisted HTL of spent coffee grounds was proved to be technically feasible, in which a biocrude yield of 30.1 wt.% was obtained at an optimal heating rate of 13.5 °C/min, temperature of 270 °C, feedstock concentration of 8.3 wt.% for 20 min. In comparison with conventional heating, microwave irradiation had comparable product yield/quality in the case of HTL of spent coffee grounds. Regarding HTL of biomass model components, MW irradiation led to a lower biocrude yield from saccharide, comparable biocrude yield from protein and lignin, and higher biocrude yield from lipid than conventional heating. As for biocrude chemical composition, heating method exhibited negligible influence on protein

and lipid biocrude, but slightly changed the chemical composition of saccharide and lignin biocrude which were rich in aldehyde and phenolics respectively. It was also found that using different heating methods did not substantially alter the interactions between biomass model components under HTL conditions.

10.2 Future work

i) Although the attempt has been made to predict HTL product yield as functions of the composition of feedstock and HTL processing variables, the ash content of biomass was not taken into consideration. Future quantitative prediction models should include the mineral content in biomass which could play an important role in HTL product distribution. The developed models allow for satisfactory predictions on the product yield for several feedstocks as shown in chapter 4 and 5, but more research efforts are required to further verify these models' predictability using a broad spectrum of biomass. More importantly, whether the developed models can predict the product yield from co-liquefaction of different types of biomass remains unexplored, it therefore would be interesting to examine the predictability of developed models in co-liquefaction.

ii) Biocrude is usually considered to be the most valuable product from HTL of biomass, and its physicochemical properties such as higher heating value and viscosity have been widely investigated. However, the oxidative stability and storage stability of HTL biocrude have not been explored yet in this research field, even though they are important parameters for the assessment of biocrude's overall quality. More research efforts are also required to further explore the utilization of solid residue (hydrochar) and aqueous phase from HTL of biomass. For instance, the potential of using hydrochar as catalyst support, soil amendments, or as activated carbon for carbon dioxide capture; the nutrient-rich aqueous phase might be a good medium for growing some plants or a good source of valuable organic acids and phenolics.

iii) Both hydrothermal co-liquefaction and microwave-assisted HTL are emerging and promising topics and deserve more research efforts. Future research could focus on the kinetics study on co-liquefaction and microwave-assisted HTL of biomass to better understand co-liquefaction effect and microwave effect on product distribution.

iv) Subcritical water is claimed to be a green and renewable solvent, however, a large amount of organic solvent is still being used to recover biocrude in the downstream processing. This hinders the overall sustainability and economic viability of biocrude production, a solvent-free

HTL technique should be developed to produce ‘flowable and above-water’ biocrude from biomass.

References

Aguilar-Reynosa, A., Romaní, A., Ma. Rodríguez-Jasso, R., Aguilar, C.N., Garrote, G., Ruiz, H.A., 2017. Microwave heating processing as alternative of pretreatment in second-generation biorefinery: An overview. Energy Convers. Manag. 136, 50–65. https://doi.org/10.1016/j.enconman.2017.01.004

Aida, T.M., Sato, Y., Watanabe, M., Tajima, K., Nonaka, T., Hattori, H., Arai, K., 2007. Dehydration of d-glucose in high temperature water at pressures up to 80MPa. J. Supercrit. Fluids 40, 381–388. https://doi.org/10.1016/j.supflu.2006.07.027

Aida, T.M., Shiraishi, N., Kubo, M., Watanabe, M., Smith, R.L., 2010. Reaction kinetics of d-xylose in sub- and supercritical water. J. Supercrit. Fluids 55, 208–216. https://doi.org/10.1016/j.supflu.2010.08.013

Akhtar, J., Amin, N.A.S., 2011. A review on process conditions for optimum bio-oil yield in hydrothermal liquefaction of biomass. Renew. Sustain. Energy Rev. 15, 1615–1624. https://doi.org/10.1016/j.rser.2010.11.054

Alenezi, R., Leeke, G.A., Santos, R.C.D., Khan, A.R., 2009. Hydrolysis kinetics of sunflower oil under subcritical water conditions. Chem. Eng. Res. Des. 87, 867–873. https://doi.org/10.1016/j.cherd.2008.12.009

Anastas, P.T., Warner, J.C., 2000. Green chemistry: theory and practice. Oxford University Press.

Azwanida, N., 2015. A Review on the Extraction Methods Use in Medicinal Plants, Principle, Strength and Limitation. Med. Aromat. Plants 04. https://doi.org/10.4172/2167-0412.1000196

Barbier, J., Charon, N., Dupassieux, N., Loppinet-Serani, A., Mahé, L., Ponthus, J., Courtiade, M., Ducrozet, A., Quoineaud, A.-A., Cansell, F., 2012. Hydrothermal conversion of lignin compounds. A detailed study of fragmentation and condensation reaction pathways. Biomass Bioenergy 46, 479–491. https://doi.org/10.1016/j.biombioe.2012.07.011

Biller, P., Johannsen, I., dos Passos, J.S., Ottosen, L.D.M., 2018. Primary sewage sludge filtration using biomass filter aids and subsequent hydrothermal co-liquefaction. Water Res. 130, 58–68. https://doi.org/10.1016/j.watres.2017.11.048

Biller, P., Madsen, R.B., Klemmer, M., Becker, J., Iversen, B.B., Glasius, M., 2016. Effect of hydrothermal liquefaction aqueous phase recycling on bio-crude yields and composition. Bioresour. Technol. 220, 190–199. https://doi.org/10.1016/j.biortech.2016.08.053

Biller, P., Ross, A.B., 2011. Potential yields and properties of oil from the hydrothermal liquefaction of microalgae with different biochemical content. Bioresour. Technol. 102, 215–225. https://doi.org/10.1016/j.biortech.2010.06.028

Bobleter, O., 1994. Hydrothermal degradation of polymers derived from plants. Prog. Polym. Sci. 19, 797–841. https://doi.org/10.1016/0079-6700(94)90033-7

Brand, S., Hardi, F., Kim, J., Suh, D.J., 2014. Effect of heating rate on biomass liquefaction: Differences between subcritical water and supercritical ethanol. Energy 68, 420–427. https://doi.org/10.1016/j.energy.2014.02.086

Brilman, D.W.F., Drabik, N., Wądrzyk, M., 2017. Hydrothermal co-liquefaction of microalgae, wood, and sugar beet pulp. Biomass Convers. Biorefinery 7, 445–454. https://doi.org/10.1007/s13399-017-0241-2

Brown, T.M., Duan, P., Savage, P.E., 2010. Hydrothermal Liquefaction and Gasification of Nannochloropsis sp. Energy Fuels 24, 3639–3646. https://doi.org/10.1021/ef100203u

Bundhoo, Z.M.A., 2018. Microwave-assisted conversion of biomass and waste materials to biofuels. Renew. Sustain. Energy Rev. 82, 1149–1177. https://doi.org/10.1016/j.rser.2017.09.066

Cantero, D.A., Bermejo, M.D., Cocero, M.J., 2013. Kinetic analysis of cellulose depolymerization reactions in near critical water. J. Supercrit. Fluids 75, 48–57. https://doi.org/10.1016/j.supflu.2012.12.013

Chen, C.-Y., Zhao, X.-Q., Yen, H.-W., Ho, S.-H., Cheng, C.-L., Lee, D.-J., Bai, F.-W., Chang, J.-S., 2013. Microalgae-based carbohydrates for biofuel production. Biochem. Eng. J., Biorefineries, Biomaterials, and bio-based functional chemicals 78, 1–10. https://doi.org/10.1016/j.bej.2013.03.006

Chen, Jinyang, Zhang, C., Li, M., Chen, Jingmin, Wang, Y., Zhou, F., 2018. Microwave-enhanced sub-critical hydrolysis of rice straw to produce reducing sugar catalyzed by ionic liquid. J. Mater. Cycles Waste Manag. 20, 1364–1370. https://doi.org/10.1007/s10163-017-0628-y

Chen, W.-T., Zhang, Y., Zhang, J., Schideman, L., Yu, G., Zhang, P., Minarick, M., 2014a. Co-liquefaction of swine manure and mixed-culture algal biomass from a wastewater treatment system to produce bio-crude oil. Appl. Energy 128, 209–216. https://doi.org/10.1016/j.apenergy.2014.04.068

Chen, W.-T., Zhang, Y., Zhang, J., Yu, G., Schideman, L.C., Zhang, P., Minarick, M., 2014b. Hydrothermal liquefaction of mixed-culture algal biomass from wastewater treatment system into bio-crude oil. Bioresour. Technol. 152, 130–139. https://doi.org/10.1016/j.biortech.2013.10.111

Cheng, S., D'cruz, I., Wang, M., Leitch, M., Xu, C. (Charles), 2010. Highly Efficient Liquefaction of Woody Biomass in Hot-Compressed Alcohol−Water Co-solvents. Energy Fuels 24, 4659–4667. https://doi.org/10.1021/ef901218w

Chiaberge, S., Leonardis, I., Fiorani, T., Bianchi, G., Cesti, P., Bosetti, A., Crucianelli, M., Reale, S., De Angelis, F., 2013. Amides in Bio-oil by Hydrothermal Liquefaction of Organic Wastes: A Mass Spectrometric Study of the Thermochemical Reaction Products of Binary Mixtures of Amino Acids and Fatty Acids. Energy Fuels 27, 5287–5297. https://doi.org/10.1021/ef4009983

Croce, A., Battistel, E., Chiaberge, S., Spera, S., De Angelis, F., Reale, S., 2017. A Model Study to Unravel the Complexity of Bio-Oil from Organic Wastes. ChemSusChem 10, 171–181. https://doi.org/10.1002/cssc.201601258

Deguchi, S., Tsujii, K., Horikoshi, K., 2006. Cooking cellulose in hot and compressed water. Chem. Commun. 3293. https://doi.org/10.1039/b605812d

Demirbas, A., 2009. Biorefineries: Current activities and future developments. Energy Convers. Manag. 50, 2782–2801. https://doi.org/10.1016/j.enconman.2009.06.035

Déniel, M., Haarlemmer, G., Roubaud, A., Weiss-Hortala, E., Fages, J., 2017a. Hydrothermal liquefaction of blackcurrant pomace and model molecules: understanding of reaction mechanisms. Sustain. Energy Fuels 1, 555–582. https://doi.org/10.1039/C6SE00065G

Déniel, M., Haarlemmer, G., Roubaud, A., Weiss-Hortala, E., Fages, J., 2017b. Modelling and Predictive Study of Hydrothermal Liquefaction: Application to Food Processing Residues. Waste Biomass Valorization 8, 2087–2107. https://doi.org/10.1007/s12649-016-9726-7

Déniel, M., Haarlemmer, G., Roubaud, A., Weiss-Hortala, E., Fages, J., 2016. Energy valorisation of food processing residues and model compounds by hydrothermal liquefaction. Renew. Sustain. Energy Rev. 54, 1632–1652. https://doi.org/10.1016/j.rser.2015.10.017

Domínguez, A., Menéndez, J.A., Inguanzo, M., Pis, J.J., 2005. Investigations into the characteristics of oils produced from microwave pyrolysis of sewage sludge. Fuel Process. Technol. 86, 1007–1020. https://doi.org/10.1016/j.fuproc.2004.11.009

Dong, Q., Xiong, Y., 2014. Kinetics study on conventional and microwave pyrolysis of moso bamboo. Bioresour. Technol. 171, 127–131. https://doi.org/10.1016/j.biortech.2014.08.063

Elaigwu, S.E., Greenway, G.M., 2016a. Chemical, structural and energy properties of hydrochars from microwave-assisted hydrothermal carbonization of glucose. Int. J. Ind. Chem. 7, 449–456. https://doi.org/10.1007/s40090-016-0081-0

Elaigwu, S.E., Greenway, G.M., 2016b. Microwave-assisted and conventional hydrothermal carbonization of lignocellulosic waste material: Comparison of the chemical and structural properties of the hydrochars. J. Anal. Appl. Pyrolysis 118, 1–8. https://doi.org/10.1016/j.jaap.2015.12.013

Elliott, D.C., 2007. Historical Developments in Hydroprocessing Bio-oils [WWW Document]. https://doi.org/10.1021/ef070044u

Elliott, D.C., Biller, P., Ross, A.B., Schmidt, A.J., Jones, S.B., 2015. Hydrothermal liquefaction of biomass: Developments from batch to continuous process. Bioresour. Technol. 178, 147–156. https://doi.org/10.1016/j.biortech.2014.09.132

Eskicioglu, C., Kennedy, K.J., Droste, R.L., 2007a. Enhancement of Batch Waste Activated Sludge Digestion by Microwave Pretreatment. Water Environ. Res. Alex. 79, 2304–17.

Eskicioglu, C., Terzian, N., Kennedy, K.J., Droste, R.L., Hamoda, M., 2007b. Athermal microwave effects for enhancing digestibility of waste activated sludge. Water Res. 41, 2457–2466. https://doi.org/10.1016/j.watres.2007.03.008

Feng, H., Zhang, B., He, Z., Wang, S., Salih, O., Wang, Q., 2018. Study on co-liquefaction of Spirulina and Spartina alterniflora in ethanol-water co-solvent for bio-oil. Energy 155, 1093–1101. https://doi.org/10.1016/j.energy.2018.02.146

Gai, C., Li, Y., Peng, N., Fan, A., Liu, Z., 2015a. Co-liquefaction of microalgae and lignocellulosic biomass in subcritical water. Bioresour. Technol. 185, 240–245. https://doi.org/10.1016/j.biortech.2015.03.015

Gai, C., Zhang, Y., Chen, W.-T., Zhang, P., Dong, Y., 2015b. An investigation of reaction pathways of hydrothermal liquefaction using Chlorella pyrenoidosa and Spirulina platensis. Energy Convers. Manag. 96, 330–339. https://doi.org/10.1016/j.enconman.2015.02.056

Galadima, A., Muraza, O., 2018. Hydrothermal liquefaction of algae and bio-oil upgrading into liquid fuels: Role of heterogeneous catalysts. Renew. Sustain. Energy Rev. 81, 1037–1048. https://doi.org/10.1016/j.rser.2017.07.034

Gan, J., Yuan, W., 2013. Operating condition optimization of corncob hydrothermal conversion for bio-oil production. Appl. Energy 103, 350–357. https://doi.org/10.1016/j.apenergy.2012.09.053

Gao, Y., Chen, H., Wang, J., Shi, T., Yang, H., Wang, X., 2011. Characterization of products from hydrothermal liquefaction and carbonation of biomass model compounds and real biomass. J. Fuel Chem. Technol. 39, 893–900.

Garrote, G., Dominguez, H., Parajo, J.C., 1999. Hydrothermal processing of lignocellulosic materials. Eur. J. Wood Wood Prod. 57, 191–202.

Gollakota, A., Savage, P.E., 2018. Hydrothermal Liquefaction of Model Food Waste Biomolecules and Ternary Mixtures under Isothermal and Fast Conditions. ACS Sustain. Chem. Eng. 6, 9018–9027. https://doi.org/10.1021/acssuschemeng.8b01368

Gollakota, A.R.K., Kishore, N., Gu, S., 2018. A review on hydrothermal liquefaction of biomass. Renew. Sustain. Energy Rev. 81, 1378–1392. https://doi.org/10.1016/j.rser.2017.05.178

Goyal, H.B., Seal, D., Saxena, R.C., 2008. Bio-fuels from thermochemical conversion of renewable resources: A review. Renew. Sustain. Energy Rev. 12, 504–517. https://doi.org/10.1016/j.rser.2006.07.014

Gronnow, M.J., Budarin, V.L., Mašek, O., Crombie, K.N., Brownsort, P.A., Shuttleworth, P.S., Hurst, P.R., Clark, J.H., 2012. Torrefaction/biochar production by microwave and conventional slow pyrolysis – comparison of energy properties. GCB Bioenergy 5, 144–152. https://doi.org/10.1111/gcbb.12021

Guo, J., Zhuang, Y., Chen, L., Liu, J., Li, D., Ye, N., 2012. Process optimization for microwave-assisted direct liquefaction of Sargassum polycystum C.Agardh using response surface methodology. Bioresour. Technol. 120, 19–25. https://doi.org/10.1016/j.biortech.2012.06.013

Hardi, F., Mäkelä, M., Yoshikawa, K., 2017. Non-catalytic hydrothermal liquefaction of pine sawdust using experimental design: Material balances and products analysis. Appl. Energy 204, 1026–1034. https://doi.org/10.1016/j.apenergy.2017.04.033

Hietala, D.C., Faeth, J.L., Savage, P.E., 2016. A quantitative kinetic model for the fast and isothermal hydrothermal liquefaction of Nannochloropsis sp. Bioresour. Technol. 214, 102–111. https://doi.org/10.1016/j.biortech.2016.04.067

Hietala, D.C., Koss, C.K., Narwani, A., Lashaway, A.R., Godwin, C.M., Cardinale, B.J., Savage, P.E., 2017. Influence of biodiversity, biochemical composition, and species identity on the quality of biomass and biocrude oil produced via hydrothermal liquefaction. Algal Res. 26, 203–214. https://doi.org/10.1016/j.algal.2017.07.020

Holliday, R.L., King, J.W., List, G.R., 1997. Hydrolysis of Vegetable Oils in Sub- and Supercritical Water. Ind. Eng. Chem. Res. 36, 932–935. https://doi.org/10.1021/ie960668f

Hong, S.M., Park, J.K., Lee, Y.O., 2004. Mechanisms of microwave irradiation involved in the destruction of fecal coliforms from biosolids. Water Res. 38, 1615–1625. https://doi.org/10.1016/j.watres.2003.12.011

Hoz, A. de la, Díaz-Ortiz, Á., Moreno, A., 2005. Microwaves in organic synthesis. Thermal and non-thermal microwave effects. Chem. Soc. Rev. 34, 164–178. https://doi.org/10.1039/B411438H

Hu, Y., Feng, S., Bassi, A., Xu, C. (Charles), 2018. Improvement in bio-crude yield and quality through co-liquefaction of algal biomass and sawdust in ethanol-water mixed solvent and recycling of the aqueous by-product as a reaction medium. Energy Convers. Manag. 171, 618–625. https://doi.org/10.1016/j.enconman.2018.06.023

Hu, Y., Feng, S., Yuan, Z., Xu, C. (Charles), Bassi, A., 2017. Investigation of aqueous phase recycling for improving bio-crude oil yield in hydrothermal liquefaction of algae. Bioresour. Technol. 239, 151–159. https://doi.org/10.1016/j.biortech.2017.05.033

Huang, H., Yuan, X., 2015. Recent progress in the direct liquefaction of typical biomass. Prog. Energy Combust. Sci. 49, 59–80. https://doi.org/10.1016/j.pecs.2015.01.003

Huang, Y.-F., Chiueh, P.-T., Kuan, W.-H., Lo, S.-L., 2016. Microwave pyrolysis of lignocellulosic biomass: Heating performance and reaction kinetics. Energy 100, 137–144. https://doi.org/10.1016/j.energy.2016.01.088

Huang, Y.-F., Chiueh, P.-T., Kuan, W.-H., Lo, S.-L., 2013. Microwave pyrolysis of rice straw: Products, mechanism, and kinetics. Bioresour. Technol. 142, 620–624. https://doi.org/10.1016/j.biortech.2013.05.093

Huber, G.W., Iborra, S., Corma, A., 2006. Synthesis of Transportation Fuels from Biomass: Chemistry, Catalysts, and Engineering. Chem. Rev. 106, 4044–4098. https://doi.org/10.1021/cr068360d

Jarvis, J.M., Billing, J.M., Hallen, R.T., Schmidt, A.J., Schaub, T.M., 2017. Hydrothermal Liquefaction Biocrude Compositions Compared to Petroleum Crude and Shale Oil. Energy Fuels 31, 2896–2906. https://doi.org/10.1021/acs.energyfuels.6b03022

Jasiūnas, L., Pedersen, T.H., Toor, S.S., Rosendahl, L.A., 2017. Biocrude production via supercritical hydrothermal co-liquefaction of spent mushroom compost and aspen wood sawdust. Renew. Energy 111, 392–398. https://doi.org/10.1016/j.renene.2017.04.019

Jaya Shankar Tumuluru, Christopher T Wright, Richard D Boardman, Timothy Kremer, 2012. Proximate and Ultimate Compositional Changes in Corn Stover during Torrrefaction using Thermogravimetric Analyzer and Microwaves. American Society of Agricultural and Biological Engineers, pp. 337–398. https://doi.org/10.13031/2013.41777

Jensen, C.U., Rodriguez Guerrero, J.K., Karatzos, S., Olofsson, G., Iversen, S.B., 2017. Fundamentals of Hydrofaction^{TM}: Renewable crude oil from woody biomass. Biomass Convers. Biorefinery 7, 495–509. https://doi.org/10.1007/s13399-017-0248-8

Jin, B., Duan, P., Xu, Y., Wang, F., Fan, Y., 2013. Co-liquefaction of micro- and macroalgae in subcritical water. Bioresour. Technol. 149, 103–110. https://doi.org/10.1016/j.biortech.2013.09.045

Jones, C.S., Mayfield, S.P., 2012. Algae biofuels: versatility for the future of bioenergy. Curr. Opin. Biotechnol., Energy biotechnology • Environmental biotechnology 23, 346–351. https://doi.org/10.1016/j.copbio.2011.10.013

Kamio, E., Takahashi, S., Noda, H., Fukuhara, C., Okamura, T., 2008. Effect of heating rate on liquefaction of cellulose by hot compressed water. Chem. Eng. J. 137, 328–338. https://doi.org/10.1016/j.cej.2007.05.007

Kang, S., Li, X., Fan, J., Chang, J., 2013. Hydrothermal conversion of lignin: A review. Renew. Sustain. Energy Rev. 27, 546–558. https://doi.org/10.1016/j.rser.2013.07.013

King, J., Holliday, R., List, G., 1999. Hydrolysis of soybean oil. in a subcritical water flow reactor. Green Chem. 1, 261–264.

King, J.W., Holliday, R.L., List, G.R., 1999. Hydrolysis of soybean oil. Green Chem. 1, 261–264. https://doi.org/10.1039/a908861j

Klingler, D., Berg, J., Vogel, H., 2007. Hydrothermal reactions of alanine and glycine in sub- and supercritical water. J. Supercrit. Fluids 43, 112–119. https://doi.org/10.1016/j.supflu.2007.04.008

Koley, S., Khadase, M.S., Mathimani, T., Raheman, H., Mallick, N., 2018. Catalytic and non-catalytic hydrothermal processing of Scenedesmus obliquus biomass for bio-crude production – A sustainable energy perspective. Energy Convers. Manag. 163, 111–121. https://doi.org/10.1016/j.enconman.2018.02.052

Lahijani, P., Zainal, Z.A., Mohamed, A.R., Mohammadi, M., 2014. Microwave-enhanced CO2 gasification of oil palm shell char. Bioresour. Technol. 158, 193–200. https://doi.org/10.1016/j.biortech.2014.02.015

Lee, J.H., Hwang, H., Moon, J., Choi, J.W., 2016. Characterization of hydrothermal liquefaction products from coconut shell in the presence of selected transition metal chlorides. J. Anal. Appl. Pyrolysis 122, 415–421. https://doi.org/10.1016/j.jaap.2016.11.005

Leng, L., Li, Jun, Yuan, X., Li, Jingjing, Han, P., Hong, Y., Wei, F., Zhou, W., 2018. Beneficial synergistic effect on bio-oil production from co-liquefaction of sewage sludge and lignocellulosic biomass. Bioresour. Technol. 251, 49–56. https://doi.org/10.1016/j.biortech.2017.12.018

Leow, S., Witter, J.R., Vardon, D.R., Sharma, B.K., Guest, J.S., Strathmann, T.J., 2015. Prediction of microalgae hydrothermal liquefaction products from feedstock biochemical composition. Green Chem. 17, 3584–3599. https://doi.org/10.1039/C5GC00574D

Li, C., Aston, J.E., Lacey, J.A., Thompson, V.S., Thompson, D.N., 2016. Impact of feedstock quality and variation on biochemical and thermochemical conversion. Renew. Sustain. Energy Rev. 65, 525–536. https://doi.org/10.1016/j.rser.2016.06.063

Li, Q., Liu, D., Hou, X., Wu, P., Song, L., Yan, Z., 2016. Hydro-liquefaction of microcrystalline cellulose, xylan and industrial lignin in different supercritical solvents. Bioresour. Technol. 219, 281–288. https://doi.org/10.1016/j.biortech.2016.07.048

Li, Y., Leow, S., Fedders, A.C., Sharma, B.K., Guest, J.S., Strathmann, T.J., 2017. Quantitative multiphase model for hydrothermal liquefaction of algal biomass. Green Chem. 19, 1163–1174. https://doi.org/10.1039/C6GC03294J

Liu, J., Zhuang, Y., Li, Y., Chen, L., Guo, J., Li, D., Ye, N., 2013. Optimizing the conditions for the microwave-assisted direct liquefaction of Ulva prolifera for bio-oil production using response surface methodology. Energy 60, 69–76. https://doi.org/10.1016/j.energy.2013.07.060

López Barreiro, D., Beck, M., Hornung, U., Ronsse, F., Kruse, A., Prins, W., 2015. Suitability of hydrothermal liquefaction as a conversion route to produce biofuels from macroalgae. Algal Res. 11, 234–241. https://doi.org/10.1016/j.algal.2015.06.023

López Barreiro, D., Prins, W., Ronsse, F., Brilman, W., 2013. Hydrothermal liquefaction (HTL) of microalgae for biofuel production: State of the art review and future prospects. Biomass Bioenergy, 20th European Biomass Conference 53, 113–127. https://doi.org/10.1016/j.biombioe.2012.12.029

Lorente, A., Remón, J., Budarin, V.L., Sánchez-Verdú, P., Moreno, A., Clark, J.H., 2019. Analysis and optimisation of a novel "bio-brewery" approach: Production of bio-fuels and bio-chemicals by microwave-assisted, hydrothermal liquefaction of brewers' spent grains. Energy Convers. Manag. 185, 410–430. https://doi.org/10.1016/j.enconman.2019.01.111

Lu, J., Liu, Z., Zhang, Y., Li, B., Lu, Q., Ma, Y., Shen, R., Zhu, Z., 2017. Improved production and quality of biocrude oil from low-lipid high-ash macroalgae Enteromorpha prolifera via addition of crude glycerol. J. Clean. Prod., Special Volume on Improving natural resource management and human health to ensure sustainable societal development based upon insights gained from working within 'Big Data Environments' 142, 749–757. https://doi.org/10.1016/j.jclepro.2016.08.048

Lu, J., Liu, Z., Zhang, Y., Savage, P.E., 2018. Synergistic and antagonistic interactions during hydrothermal liquefaction of soybean oil, soy protein, cellulose, xylose, and lignin. ACS Sustain. Chem. Eng. https://doi.org/10.1021/acssuschemeng.8b03156

Lü, X., Saka, S., 2012. New insights on monosaccharides' isomerization, dehydration and fragmentation in hot-compressed water. J. Supercrit. Fluids 61, 146–156. https://doi.org/10.1016/j.supflu.2011.09.005

Madsen, R.B., Bernberg, R.Z.K., Biller, P., Becker, J., Iversen, B.B., Glasius, M., 2017a. Hydrothermal co-liquefaction of biomasses – quantitative analysis of bio-crude and aqueous phase composition. Sustain. Energy Fuels 1, 789–805. https://doi.org/10.1039/C7SE00104E

Madsen, R.B., Zhang, H., Biller, P., Goldstein, A.H., Glasius, M., 2017b. Characterizing Semivolatile Organic Compounds of Biocrude from Hydrothermal Liquefaction of Biomass. Energy Fuels 31, 4122–4134. https://doi.org/10.1021/acs.energyfuels.7b00160

Meetani, M.A., Zahid, O.K., Michael Conlon, J., 2010. Investigation of the pyrolysis products of methionine-enkephalin-Arg-Gly-Leu using liquid chromatography–tandem mass spectrometry. J. Mass Spectrom. 45, 1320–1331. https://doi.org/10.1002/jms.1845

Mohamed, B.A., Kim, C.S., Ellis, N., Bi, X., 2016. Microwave-assisted catalytic pyrolysis of switchgrass for improving bio-oil and biochar properties. Bioresour. Technol. 201, 121–132. https://doi.org/10.1016/j.biortech.2015.10.096

Mok, W.S., Antal Jr, M.J., Varhegyi, G., 1992. Productive and parasitic pathways in dilute acid-catalyzed hydrolysis of cellulose. Ind. Eng. Chem. Res. 31, 94–100.

Mok, W.S.L., Antal Jr, M.J., 1992. Uncatalyzed solvolysis of whole biomass hemicellulose by hot compressed liquid water. Ind. Eng. Chem. Res. 31, 1157–1161.

Montgomery, D.C., 2017. Design and Analysis of Experiments, 9th ed. John Wiley & Sons.

Naik, S.N., Goud, V.V., Rout, P.K., Dalai, A.K., 2010. Production of first and second generation biofuels: A comprehensive review. Renew. Sustain. Energy Rev. 14, 578–597. https://doi.org/10.1016/j.rser.2009.10.003

Nazari, L., Yuan, Z., Ray, M.B., Xu, C. (Charles), 2017. Co-conversion of waste activated sludge and sawdust through hydrothermal liquefaction: Optimization of reaction parameters using response surface methodology. Appl. Energy 203, 1–10. https://doi.org/10.1016/j.apenergy.2017.06.009

Nazari, L., Yuan, Z., Souzanchi, S., Ray, M.B., Xu, C. (Charles), 2015. Hydrothermal liquefaction of woody biomass in hot-compressed water: Catalyst screening and comprehensive characterization of bio-crude oils. Fuel 162, 74–83. https://doi.org/10.1016/j.fuel.2015.08.055

Nie, Y., Bi, X., 2018a. Life-cycle assessment of transportation biofuels from hydrothermal liquefaction of forest residues in British Columbia. Biotechnol. Biofuels 11. https://doi.org/10.1186/s13068-018-1019-x

Nie, Y., Bi, X.T., 2018b. Techno-economic assessment of transportation biofuels from hydrothermal liquefaction of forest residues in British Columbia. Energy 153, 464–475. https://doi.org/10.1016/j.energy.2018.04.057

Nigam, P.S., Singh, A., 2011. Production of liquid biofuels from renewable resources. Prog. Energy Combust. Sci. 37, 52–68. https://doi.org/10.1016/j.pecs.2010.01.003

Pavlovič, I., Knez, Ž., Škerget, M., 2013. Hydrothermal Reactions of Agricultural and Food Processing Wastes in Sub- and Supercritical Water: A Review of Fundamentals, Mechanisms, and State of Research [WWW Document]. https://doi.org/10.1021/jf401008a

Pedersen, T.H., Jasiūnas, L., Casamassima, L., Singh, S., Jensen, T., Rosendahl, L.A., 2015. Synergetic hydrothermal co-liquefaction of crude glycerol and aspen wood. Energy Convers. Manag. 106, 886–891. https://doi.org/10.1016/j.enconman.2015.10.017

Pedersen, T.H., Rosendahl, L.A., 2015. Production of fuel range oxygenates by supercritical hydrothermal liquefaction of lignocellulosic model systems. Biomass Bioenergy 83, 206–215. https://doi.org/10.1016/j.biombioe.2015.09.014

Peterson, A.A., Lachance, R.P., Tester, J.W., 2010. Kinetic Evidence of the Maillard Reaction in Hydrothermal Biomass Processing: Glucose−Glycine Interactions in High-Temperature, High-Pressure Water. Ind. Eng. Chem. Res. 49, 2107–2117. https://doi.org/10.1021/ie9014809

Peterson, A.A., Vogel, F., Lachance, R.P., Fröling, M., Antal, Jr., M.J., Tester, J.W., 2008. Thermochemical biofuel production in hydrothermal media: A review of sub- and supercritical water technologies. Energy Environ. Sci. 1, 32. https://doi.org/10.1039/b810100k

Pino-Jelcic, S.A., Hong, S.M., Park, J.K., 2006. Enhanced Anaerobic Biodegradability and Inactivation of Fecal Coliforms and Salmonella spp. in Wastewater Sludge by Using Microwaves. Water Environ. Res. 78, 209–216. https://doi.org/10.2175/106143005X90498

Pragya, N., Pandey, K.K., Sahoo, P.K., 2013. A review on harvesting, oil extraction and biofuels production technologies from microalgae. Renew. Sustain. Energy Rev. 24, 159–171. https://doi.org/10.1016/j.rser.2013.03.034

Putten, R.-J. van, Waal, J.C. van der, Jong, E. de, Rasrendra, C.B., Heeres, H.J., Vries, J.G. de, 2013. Hydroxymethylfurfural, A Versatile Platform Chemical Made from Renewable Resources [WWW Document]. https://doi.org/10.1021/cr300182k

Remón, J., Randall, J., Budarin, V.L., Clark, J.H., 2019. Production of bio-fuels and chemicals by microwave-assisted, catalytic, hydrothermal liquefaction (MAC-HTL) of a mixture of pine and spruce biomass. Green Chem. 21, 284–299. https://doi.org/10.1039/C8GC03244K

Ren, S., Lei, H., Wang, L., Yadavalli, G., Liu, Y., Julson, J., 2014. The integrated process of microwave torrefaction and pyrolysis of corn stover for biofuel production. J. Anal. Appl. Pyrolysis 108, 248–253. https://doi.org/10.1016/j.jaap.2014.04.008

Robinson, J., Dodds, C., Stavrinides, A., Kingman, S., Katrib, J., Wu, Z., Medrano, J., Overend, R., 2015. Microwave Pyrolysis of Biomass: Control of Process Parameters for High Pyrolysis Oil Yields and Enhanced Oil Quality. Energy Fuels 29, 1701–1709. https://doi.org/10.1021/ef502403x

Ross, A.B., Biller, P., Kubacki, M.L., Li, H., Lea-Langton, A., Jones, J.M., 2010. Hydrothermal processing of microalgae using alkali and organic acids. Fuel 89, 2234–2243. https://doi.org/10.1016/j.fuel.2010.01.025

Saba, A., Lopez, B., Lynam, J.G., Reza, M.T., 2018. Hydrothermal Liquefaction of Loblolly Pine: Effects of Various Wastes on Produced Biocrude. ACS Omega 3, 3051–3059. https://doi.org/10.1021/acsomega.8b00045

Sasaki, M., Fang, Z., Fukushima, Y., Adschiri, T., Arai, K., 2000. Dissolution and Hydrolysis of Cellulose in Subcritical and Supercritical Water. Ind. Eng. Chem. Res. 39, 2883–2890. https://doi.org/10.1021/ie990690j

Sato, N., Quitain, A.T., Kang, K., Daimon, H., Fujie, K., 2004. Reaction Kinetics of Amino Acid Decomposition in High-Temperature and High-Pressure Water. Ind. Eng. Chem. Res. 43, 3217–3222. https://doi.org/10.1021/ie020733n

Shahir, S.A., Masjuki, H.H., Kalam, M.A., Imran, A., Fattah, I.M.R., Sanjid, A., 2014. Feasibility of diesel–biodiesel–ethanol/bioethanol blend as existing CI engine fuel: An assessment of properties, material compatibility, safety and combustion. Renew. Sustain. Energy Rev. 32, 379–395. https://doi.org/10.1016/j.rser.2014.01.029

Sheehan, J.D., Savage, P.E., 2017. Modeling the effects of microalga biochemical content on the kinetics and biocrude yields from hydrothermal liquefaction. Bioresour. Technol. 239, 144–150. https://doi.org/10.1016/j.biortech.2017.05.013

Sheng, L., Wang, X., Yang, X., 2018. Prediction model of biocrude yield and nitrogen heterocyclic compounds analysis by hydrothermal liquefaction of microalgae with model compounds. Bioresour. Technol. 247, 14–20. https://doi.org/10.1016/j.biortech.2017.08.011

Shin, H.-Y., Ryu, J.-H., Park, S.-Y., Bae, S.-Y., 2012. Thermal stability of fatty acids in subcritical water. J. Anal. Appl. Pyrolysis 98, 250–253. https://doi.org/10.1016/j.jaap.2012.08.003

Simoneit, B.R.T., Rushdi, A.I., bin Abas, M.R., Didyk, B.M., 2003. Alkyl Amides and Nitriles as Novel Tracers for Biomass Burning. Environ. Sci. Technol. 37, 16–21. https://doi.org/10.1021/es020811y

Singh, A., Nair, G.R., Liplap, P., Gariepy, Y., Orsat, V., Raghavan, V., 2014. Effect of Dielectric Properties of a Solvent-Water Mixture Used in Microwave-Assisted Extraction of Antioxidants from Potato Peels. Antioxidants 3, 99–113. https://doi.org/10.3390/antiox3010099

Sintamarean, I.M., Pedersen, T.H., Zhao, X., Kruse, A., Rosendahl, L.A., 2017. Application of Algae as Cosubstrate To Enhance the Processability of Willow Wood for Continuous Hydrothermal Liquefaction. Ind. Eng. Chem. Res. 56, 4562–4571. https://doi.org/10.1021/acs.iecr.7b00327

Smallwood, I., 2012. Handbook of Organic Solvent Properties. Butterworth-Heinemann.

Song, W., Wang, S., Guo, Y., Xu, D., 2017. Bio-oil production from hydrothermal liquefaction of waste Cyanophyta biomass: Influence of process variables and their interactions on the product distributions. Int. J. Hydrog. Energy 42, 20361–20374. https://doi.org/10.1016/j.ijhydene.2017.06.010

Tekin, K., Karagöz, S., Bektaş, S., 2014. A review of hydrothermal biomass processing. Renew. Sustain. Energy Rev. 40, 673–687. https://doi.org/10.1016/j.rser.2014.07.216

Teri, G., Luo, L., Savage, P.E., 2014. Hydrothermal Treatment of Protein, Polysaccharide, and Lipids Alone and in Mixtures. Energy Fuels 28, 7501–7509. https://doi.org/10.1021/ef501760d

Toor, S.S., Reddy, H., Deng, S., Hoffmann, J., Spangsmark, D., Madsen, L.B., Holm-Nielsen, J.B., Rosendahl, L.A., 2013. Hydrothermal liquefaction of Spirulina and Nannochloropsis salina under subcritical and supercritical water conditions. Bioresour. Technol. 131, 413–419. https://doi.org/10.1016/j.biortech.2012.12.144

Toor, S.S., Rosendahl, L., Rudolf, A., 2011. Hydrothermal liquefaction of biomass: A review of subcritical water technologies. Energy 36, 2328–2342. https://doi.org/10.1016/j.energy.2011.03.013

Torri, C., Garcia Alba, L., Samorì, C., Fabbri, D., Brilman, D.W.F. (Wim), 2012. Hydrothermal Treatment (HTT) of Microalgae: Detailed Molecular Characterization of HTT Oil in View of HTT Mechanism Elucidation. Energy Fuels 26, 658–671. https://doi.org/10.1021/ef201417e

Valdez, P.J., Dickinson, J.G., Savage, P.E., 2011. Characterization of Product Fractions from Hydrothermal Liquefaction of *Nannochloropsis* sp. and the Influence of Solvents. Energy Fuels 25, 3235–3243. https://doi.org/10.1021/ef2004046

Valdez, P.J., Tocco, V.J., Savage, P.E., 2014. A general kinetic model for the hydrothermal liquefaction of microalgae. Bioresour. Technol. 163, 123–127. https://doi.org/10.1016/j.biortech.2014.04.013

Vo, T.K., Lee, O.K., Lee, E.Y., Kim, C.H., Seo, J.-W., Kim, J., Kim, S.-S., 2016. Kinetics study of the hydrothermal liquefaction of the microalga Aurantiochytrium sp. KRS101. Chem. Eng. J. 306, 763–771. https://doi.org/10.1016/j.cej.2016.07.104

Vogel, A.I., Tatchell, A.R., Furnis, B.S., Hannaford, A.J., Smith, P.W.G., 1996. Vogel's Textbook of Practical Organic Chemistry, 5 edition. ed. Pearson, Harlow.

Wahyudiono, Sasaki, M., Goto, M., 2008. Recovery of phenolic compounds through the decomposition of lignin in near and supercritical water. Chem. Eng. Process. Process Intensif. 47, 1609–1619. https://doi.org/10.1016/j.cep.2007.09.001

Wang, Y., Wang, H., Lin, H., Zheng, Y., Zhao, J., Pelletier, A., Li, K., 2013. Effects of solvents and catalysts in liquefaction of pinewood sawdust for the production of bio-oils. Biomass Bioenergy 59, 158–167. https://doi.org/10.1016/j.biombioe.2013.10.022

Wu, X., Liang, J., Wu, Y., Hu, H., Huang, S., Wu, K., 2017. Co-liquefaction of microalgae and polypropylene in sub-/super-critical water. RSC Adv 7, 13768–13776. https://doi.org/10.1039/C7RA01030C

Xiao, N., Luo, H., Wei, W., Tang, Z., Hu, B., Kong, L., Sun, Y., 2015. Microwave-assisted gasification of rice straw pyrolytic biochar promoted by alkali and alkaline earth metals. J. Anal. Appl. Pyrolysis 112, 173–179. https://doi.org/10.1016/j.jaap.2015.02.001

Xiu, S., Shahbazi, A., Shirley, V., Mims, M.R., Wallace, C.W., 2010. Effectiveness and mechanisms of crude glycerol on the biofuel production from swine manure through hydrothermal pyrolysis. J. Anal. Appl. Pyrolysis 87, 194–198. https://doi.org/10.1016/j.jaap.2009.12.002

Xiu, S., Shahbazi, A., Shirley, V.B., Wang, L., 2011a. Swine manure/Crude glycerol co-liquefaction: Physical properties and chemical analysis of bio-oil product. Bioresour. Technol. 102, 1928–1932. https://doi.org/10.1016/j.biortech.2010.08.026

Xiu, S., Shahbazi, A., Wallace, C.W., Wang, L., Cheng, D., 2011b. Enhanced bio-oil production from swine manure co-liquefaction with crude glycerol. Energy Convers. Manag. 52, 1004–1009. https://doi.org/10.1016/j.enconman.2010.08.028

Xu, C., Lad, N., 2008. Production of Heavy Oils with High Caloric Values by Direct Liquefaction of Woody Biomass in Sub/Near-critical Water. Energy Fuels 22, 635–642. https://doi.org/10.1021/ef700424k

Xu, Y., Yu, H., Hu, X., Wei, X., Cui, Z., 2014. Bio-oil Production from Algae via Thermochemical Catalytic Liquefaction. Energy Sources Part Recovery Util. Environ. Eff. 36, 38–44. https://doi.org/10.1080/15567036.2012.682199

Yang, J., Astatkie, T., He, Q.S., 2016a. A comparative study on the effect of unsaturation degree of camelina and canola oils on the optimization of bio-diesel production. Energy Rep. 2, 211–217. https://doi.org/10.1016/j.egyr.2016.08.003

Yang, J., Caldwell, C., Corscadden, K., He, Q.S., Li, J., 2016b. An evaluation of biodiesel production from Camelina sativa grown in Nova Scotia. Ind. Crops Prod. 81, 162–168. https://doi.org/10.1016/j.indcrop.2015.11.073

Yang, J., He, Q. (Sophia), Corscadden, K., Niu, H., 2018a. The impact of downstream processing methods on the yield and physiochemical properties of hydrothermal liquefaction bio-oil. Fuel Process. Technol. https://doi.org/10.1016/j.fuproc.2018.07.006

Yang, J., He, Q. (Sophia), Corscadden, K., Niu, H., Lin, J., Astatkie, T., 2019a. Advanced models for the prediction of product yield in hydrothermal liquefaction via a mixture design of biomass model components coupled with process variables. Appl. Energy 233–234, 906–915. https://doi.org/10.1016/j.apenergy.2018.10.035

Yang, J., He, Q. (Sophia), Niu, H., Corscadden, K., Astatkie, T., 2018b. Hydrothermal liquefaction of biomass model components for product yield prediction and reaction pathways exploration. Appl. Energy 228, 1618–1628. https://doi.org/10.1016/j.apenergy.2018.06.142

Yang, J., (Sophia) He, Q., Yang, L., 2019b. A review on hydrothermal co-liquefaction of biomass. Appl. Energy 250, 926–945. https://doi.org/10.1016/j.apenergy.2019.05.033

Yang, L., He, Q. (Sophia), Havard, P., Corscadden, K., Xu, C. (Charles), Wang, X., 2017. Co-liquefaction of spent coffee grounds and lignocellulosic feedstocks. Bioresour. Technol. 237, 108–121. https://doi.org/10.1016/j.biortech.2017.02.087

Yang, L., Li, Y., Savage, P.E., 2014. Hydrolytic Cleavage of C–O Linkages in Lignin Model Compounds Catalyzed by Water-Tolerant Lewis Acids. Ind. Eng. Chem. Res. 53, 2633–2639. https://doi.org/10.1021/ie403545n

Yang, L., Mahmood, N., Corscadden, K., Xu, C. (Charles), He, Q. (Sophia), 2016a. Production of crude bio-oil via direct liquefaction of spent K-Cups. Biomass Bioenergy 95, 354–363. https://doi.org/10.1016/j.biombioe.2016.07.006

Yang, L., Nazari, L., Yuan, Z., Corscadden, K., Xu, C. (Charles), He, Q. (Sophia), 2016b. Hydrothermal liquefaction of spent coffee grounds in water medium for bio-oil production. Biomass Bioenergy 86, 191–198. https://doi.org/10.1016/j.biombioe.2016.02.005

Yang, L., Si, B., Tan, X., Chu, H., Zhou, X., Zhang, Yuanhui, Zhang, Yalei, Zhao, F., 2018. Integrated anaerobic digestion and algae cultivation for energy recovery and nutrient supply from post-hydrothermal liquefaction wastewater. Bioresour. Technol. 266, 349–356. https://doi.org/10.1016/j.biortech.2018.06.083

Yang, W., Li, X., Li, Z., Tong, C., Feng, L., 2015a. Understanding low-lipid algae hydrothermal liquefaction characteristics and pathways through hydrothermal liquefaction of algal major components: Crude polysaccharides, crude proteins and their binary mixtures. Bioresour. Technol. 196, 99–108. https://doi.org/10.1016/j.biortech.2015.07.020

Yang, W., Li, X., Li, Z., Tong, C., Feng, L., 2015b. Understanding low-lipid algae hydrothermal liquefaction characteristics and pathways through hydrothermal liquefaction of algal major components: Crude polysaccharides, crude proteins and their binary mixtures. Bioresour. Technol. 196, 99–108. https://doi.org/10.1016/j.biortech.2015.07.020

Ye, Z., Xiu, S., Shahbazi, A., Zhu, S., 2012. Co-liquefaction of swine manure and crude glycerol to bio-oil: Model compound studies and reaction pathways. Bioresour. Technol. 104, 783–787. https://doi.org/10.1016/j.biortech.2011.09.126

Yin, C., 2012. Microwave-assisted pyrolysis of biomass for liquid biofuels production. Bioresour. Technol. 120, 273–284. https://doi.org/10.1016/j.biortech.2012.06.016

Yin, S., Dolan, R., Harris, M., Tan, Z., 2010. Subcritical hydrothermal liquefaction of cattle manure to bio-oil: Effects of conversion parameters on bio-oil yield and characterization of bio-oil. Bioresour. Technol. 101, 3657–3664. https://doi.org/10.1016/j.biortech.2009.12.058

Yin, S., Tan, Z., 2012. Hydrothermal liquefaction of cellulose to bio-oil under acidic, neutral and alkaline conditions. Appl. Energy 92, 234–239. https://doi.org/10.1016/j.apenergy.2011.10.041

Yong, T.L.-K., Matsumura, Y., 2013. Kinetic Analysis of Lignin Hydrothermal Conversion in Sub- and Supercritical Water. Ind. Eng. Chem. Res. 52, 5626–5639. https://doi.org/10.1021/ie400600x

Yu, J., Biller, P., Mamahkel, A., Klemmer, M., Becker, J., Glasius, M., Iversen, B.B., 2017. Catalytic hydrotreatment of bio-crude produced from the hydrothermal liquefaction of aspen wood: a catalyst screening and parameter optimization study. Sustain. Energy Fuels 1, 832–841. https://doi.org/10.1039/C7SE00090A

Yuan, Z., Cheng, S., Leitch, M., Xu, C. (Charles), 2010. Hydrolytic degradation of alkaline lignin in hot-compressed water and ethanol. Bioresour. Technol. 101, 9308–9313. https://doi.org/10.1016/j.biortech.2010.06.140

Zhai, Y., Chen, Z., Chen, H., Xu, B., Li, P., Qing, R., Li, C., Zeng, G., 2015. Co-liquefaction of sewage sludge and oil-tea-cake in supercritical methanol: yield of bio-oil, immobilization and risk assessment of heavy metals. Environ. Technol. 36, 2770–2777. https://doi.org/10.1080/09593330.2015.1049210

Zhang, B., Keitz, M. von, Valentas, K., 2008. Thermal Effects on Hydrothermal Biomass Liquefaction. Appl. Biochem. Biotechnol. 147, 143–150. https://doi.org/10.1007/s12010-008-8131-5

Zhang, B., Lin, Q., Zhang, Q., Wu, K., Pu, W., Yang, M., Wu, Y., 2017. Catalytic hydrothermal liquefaction of Euglena sp. microalgae over zeolite catalysts for the production of bio-oil. RSC Adv 7, 8944–8951. https://doi.org/10.1039/C6RA28747F

Zhang, B., von Keitz, M., Valentas, K., 2009. Thermochemical liquefaction of high-diversity grassland perennials. J. Anal. Appl. Pyrolysis 84, 18–24. https://doi.org/10.1016/j.jaap.2008.09.005

Zhang, C., Tang, X., Sheng, L., Yang, X., 2016. Enhancing the performance of Co-hydrothermal liquefaction for mixed algae strains by the Maillard reaction. Green Chem. 18, 2542–2553.

Zhang, J., Chen, W.-T., Zhang, P., Luo, Z., Zhang, Y., 2013. Hydrothermal liquefaction of Chlorella pyrenoidosa in sub- and supercritical ethanol with heterogeneous catalysts. Bioresour. Technol. 133, 389–397. https://doi.org/10.1016/j.biortech.2013.01.076

Zhang, L., Champagne, P., (Charles) Xu, C., 2011. Bio-crude production from secondary pulp/paper-mill sludge and waste newspaper via co-liquefaction in hot-compressed water. Energy 36, 2142–2150. https://doi.org/10.1016/j.energy.2010.05.029

Zhou, D., Zhang, L., Zhang, S., Fu, H., Chen, J., 2010. Hydrothermal Liquefaction of Macroalgae Enteromorpha prolifera to Bio-oil. Energy Fuels 24, 4054–4061. https://doi.org/10.1021/ef100151h

Zhu, Z., Rosendahl, L., Toor, S.S., Chen, G., 2018. Optimizing the conditions for hydrothermal liquefaction of barley straw for bio-crude oil production using response surface methodology. Sci. Total Environ. 630, 560–569. https://doi.org/10.1016/j.scitotenv.2018.02.194

Zhu, Z., Rosendahl, L., Toor, S.S., Yu, D., Chen, G., 2015. Hydrothermal liquefaction of barley straw to bio-crude oil: Effects of reaction temperature and aqueous phase recirculation. Appl. Energy 137, 183–192. https://doi.org/10.1016/j.apenergy.2014.10.005

Zou, S., Wu, Y., Yang, M., Li, C., Tong, J., 2010. Bio-oil production from sub- and supercritical water liquefaction of microalgae Dunaliella tertiolecta and related properties. Energy Env. Sci 3, 1073–1078. https://doi.org/10.1039/C002550J